

Universidade Nova de Lisboa

Faculdade de Ciências Médicas

The Role of Complex Chromosome Translocations in Leukemia

Luís Miguel Ramos Vieira

Doutoramento em Ciências da Vida

Especialidade de Biologia Molecular e Celular

2011

The Role of Complex Chromosome Translocations in Leukemia

Universidade Nova de Lisboa

Faculdade de Ciências Médicas

The Role of Complex Chromosome Translocations in Leukemia

Luís Miguel Ramos Vieira

Licenciado em Biologia pela Faculdade de Ciências da Universidade de Lisboa

**Dissertação Apresentada para Obtenção do
Grau de Doutor em Ciências da Vida
Especialidade de Biologia Molecular e Celular**

Professora Orientadora: Doutora Maria Gomes da Silva

2011

Para os meus pais

In this dissertation parts of text were transcribed from the following publications and manuscript:

1. Vieira L, Marques B, Cavaleiro C, Ambrósio AP, Jorge M, Neto A, Costa JM, Júnior EC, Boavida MG (2005) Molecular cytogenetic characterization of rearrangements involving 12p in leukemia. *Cancer Genet Cytogenet* **157**: 134-139.

My contribution to this publication included selection of cosmid, bacterial artificial chromosome (BAC) and yeast artificial chromosome (YAC) clones, growth of clone colonies, preparation of DNA and labeling of clones for fluorescence *in situ* hybridization (FISH) analysis. I also performed reverse transcription-polymerase chain reaction (RT-PCR) studies and sequencing analysis of *ETV6-RUNX1* fusion transcripts.

2. Vieira L, Sousa AC, Matos P, Marques B, Alaiz H, Ribeiro MJ, Braga P, da Silva MG, Jordan P (2006) Three-way translocation involves *MLL*, *MLLT3* and a novel cell cycle control gene, *FLJ10374*, in the pathogenesis of acute myeloid leukemia with t(9;11;19)(p22;q23;p13.3). *Genes Chromosomes Cancer* **45**: 455-469.

I have contributed to this publication through the identification of the *CCDC94-MLL* genomic fusion by long distance inverse-polymerase chain reaction (LDI-PCR), detection of truncated *CCDC94* transcripts by 3' rapid amplification of cDNA ends (RACE), analysis of *CCDC94* expression in leukemic cell lines and normal human tissues by RT-PCR, amplification and cloning of full-length *CCDC94* cDNA in expression vectors, evaluation of *CCDC94* suppression by RT-PCR in short interfering RNA (siRNA)-treated cells and computational sequence analysis, including design of primers and siRNA oligos, selection of restriction enzymes for LDI-PCR experiments, analysis of DNA, RNA and protein sequences, as well as selection of *MLLT3* and *CCDC94* clones for use as FISH probes.

3. Vieira L, Vaz A, Ambrósio AP, Nogueira M, Marques B, Silva E, Matos P, Pereira AM, Jordan P, da Silva MG. Three-way translocation (X;20;16)(p11;q13;q23) in essential thrombocythemia implicates *NFATC2* in dysregulation of GM-CSF expression and megakaryocyte proliferation (submitted).

My contribution to this manuscript included delimitation of a chromosome 20q deletion by polymerase chain reaction (PCR) analysis of short tandem repeat polymorphisms, preparation of genomic DNA for whole-genome array study, analysis of array data, 5' RACE analysis of *NFATC2* transcripts, 3' RACE analysis of *WWOX* transcripts, analysis of *NFATC2* expression in normal human tissues by RT-PCR, detection of a transcribed single nucleotide polymorphism in *NFATC2* by PCR, RT-PCR and sequencing analysis, mutational analysis of *JAK2* and *NFATC2*, evaluation of *NFATC2* suppression in siRNA-treated cells by real-time quantitative PCR (Q-PCR), analysis of *NFATC2* expression in patients and controls by Q-PCR, analysis of Q-PCR data in cell lines and human samples, and computational sequence analysis including design of primers and siRNA oligo, selection of YAC, BAC and P1-derived artificial chromosome (PAC) clones for FISH studies, as well as analysis of DNA, RNA and protein sequences.

I also wrote the manuscripts and prepared all figures and tables.

Acknowledgments

I wish to acknowledge primarily Prof. Maria Gomes da Silva for accepting to be my thesis supervisor. Prof. M. Gomes da Silva provided the best moments in my career by believing in this project from the first minute and allowing it to become a reality. I also wish to acknowledge for her excellent discussions of experimental results and scientific contributions to this thesis, as well as for continuous motivation and sincere friendship for the last 6 years.

I also wish to acknowledge all the researchers and clinicians who were co-authors of the publications included in this dissertation. Above all, I am sincerely indebted to Prof. Maria Guida Boavida for accepting me as her student at the Departamento de Genética (INSA) in October 1993 and for an inestimable teaching of the world of cancer genetics. I am also deeply grateful to Dr. Paula Ambrósio for priceless karyotype studies and to Dr. Bárbara Marques for notable FISH experiments. In addition, I am also truly grateful to Prof. Peter Jordan for providing outstanding scientific support. Finally, I wish to sincerely thank Elizabeth Silva for performing most of the molecular diagnostics of leukemia while I was committed to research work.

At the institutional level I must thank Instituto Nacional de Saúde Dr. Ricardo Jorge for providing all the necessary laboratory facilities that made this thesis possible. This would not also been achieved without relevant financial support from Liga Portuguesa Contra o Cancro, Fundação para a Ciência e a Tecnologia and Associação Portuguesa Contra a Leucemia.

My final acknowledgment is addressed to my wife Célia, to whom I am grateful for unrestricted love, companionship and endless support throughout the last 14 years.

Preface

My interest in genetics began when I was a Biology student at Faculdade de Ciências da Universidade de Lisboa in the early 90's. During the last 2 years of my graduation I worked as a volunteer at the Departamento de Biologia Vegetal in the genetics of microorganisms. When I graduated in 1993 my genetics teacher Prof. Graça Fialho recommended that I should pursue my professional interests in genetics at the Departamento de Genética of the Instituto Nacional de Saúde Dr. Ricardo Jorge (DG-INSA). At that time, Prof. Maria Guida Boavida, who was in charge of DG-INSA, was looking for a graduate student to initiate the molecular diagnosis of leukemias in the laboratory. Luckily, I was accepted for that assignment and together with my colleagues Paula Ambrósio and Bárbara Marques we constituted a small team developing conventional cytogenetics, fluorescence *in situ* hybridization and molecular techniques to interpret and report chromosomal abnormalities in leukemia patients. With time, however, I gradually become interested in pursuing a more research directed activity towards the characterization of novel chromosomal abnormalities in leukemia.

I started this endeavour with a comprehensive retrospective analysis of leukemia karyotype registries at the DG-INSA and Laboratório de Hematologia of the Instituto Português de Oncologia de Francisco Gentil (LH-IPOFG) in Lisbon, under the guidance of Prof. Maria Guida Boavida and Prof. Maria Gomes da Silva, respectively. The purpose was to select samples carrying reciprocal chromosome translocations undescribed in the literature and potentially use them to pursue molecular investigation of novel breakpoint locations and associated fusion genes. After a first scrutiny, I subsequently focused my interest in translocations in which one of the breakpoint locations was already known to constitute a recurrent target site. Moreover, only cytogenetic records which were obtained at the time of initial diagnosis were considered. Both approaches increased the likelihood of identifying novel leukemogenic fusion genes. The final output of the review comprised a total of 5 different translocations, including 2 collected from DG-INSA database and 3 obtained from the LH-IPOFG database.

Incidentally, preliminary studies disclosed that at least one additional chromosome was involved in 4 out of the 5 selected translocations, thus revealing an unexpected complex nature. A fundamental question then rose to my mind: Is the role of extra breakpoint locations involved in complex translocations merely accessory or is it also relevant to the proliferation and survival of the leukemic clone? I then addressed Prof. Maria Gomes da Silva in 2005 with a tentative idea for a PhD project under her supervision involving the role of complex

chromosome translocations in leukemogenesis. This project soon became a reality and 6 years later all I can say is that I have made the right choice.

Abstract

Tumourigenesis is a multistep process which results from the accumulation of successive genetic mutations in a normal cell. In leukemia for instance, recurrent translocations play a part in this process by generating fusion genes which lead to the production of hybrid proteins with an oncogenic role. However, a minor subset of chromosomal translocations referred to as complex or variant involves extra breakpoints at variable genome locations in addition to those implicated in the formation of fusion genes. We aimed to describe in this work the role, if any, of genes located at extra breakpoint locations or which are affected by breakpoint-adjacent deletions through the study of 5 leukemia patients.

Two of the patients presented with *ETV6*(12p13)-*RUNX1*(21q22) and *MLL*(11q23)-*MLLT3*(9p22) fusion genes as a result of a t(12;21;5) and a t(9;11;19), respectively. Detailed molecular characterization of the extra breakpoint at chromosome 19 in the latter case revealed that a novel ubiquitously expressed gene, *CCDC94*, with a potential role in cell cycle regulation, was disrupted by the breakpoint. We demonstrated using *in vitro* cellular assays that this gene codifies for a nuclear protein which negatively regulates cell cycle progression. These data shows that extra breakpoint locations of complex translocations may result in haplo-insufficiency of critical proliferation genes, thereby cooperating with the generation of hybrid proteins to provide unrestrained cell proliferation.

In the other 3 patients there were breakpoint-associated deletions which precluded the formation of putative fusion genes. In a case with a t(12;6;15) we characterized a deletion at 12p13 which eliminated *ETV6* and 8 other genes including *CDKN1B*. These findings indicate that concomitant loss of *ETV6* and *CDKN1B*, which encodes a cyclin-dependent kinase inhibitor responsible for blocking entry of cells into the G1 phase of the cell cycle, acted cooperatively to promote leukemogenic proliferation. The same notion applied to a case with a dic(9;12) in which 2 genes encoding hematopoietic transcription factors - *ETV6* and *PAX5* (9p13)- were deleted as a result of breakpoint-adjacent deletions. Similarly, we found that 2 transcription factor genes involved in the regulation of cytokine expression, *NFATC2* (20q13) and *MAF* (16q23), were involved in deletions contiguous to the breakpoints in a patient with a t(X;20;16). *In vitro* suppression of *NFATC2* mRNA or inhibition of *NFATC2* protein activity enhanced cell proliferation as a result of an increase in the production of a myeloid-lineage stimulating hematopoietic cytokine, GM-CSF. These results suggest that haplo-insufficiency of *NFATC2* and *MAF* genes had a cooperative effect in inducing cell proliferation as a result of a dysregulation of cytokine production.

Two main conclusions may be drawn from our studies: (i) In complex translocations associated with the production of fusion genes, additional breakpoints may cooperate in tumorigenesis by targeting genes that control cell proliferation; (ii) In complex translocations associated with small breakpoint-adjacent deletions, at least 2 genes with similar or complementary functions need to be deregulated to promote tumorigenesis.

Résumé

La tumorigenèse est un processus qui se déroule en de plusieurs étapes et qui résulte de l'accumulation de mutations génétiques continues dans une cellule normal. Par exemple, dans la leucémie, les translocations récurrentes ont un rôle dans ce processus pour former des gènes de fusion qui conduisent à la production de protéines hybrides avec une fonction oncogénique. Cependant, il existe une petite minorité de translocations chromosomiques, appelées de complexes ou variantes, qui impliquent des points de rupture additionnels dans d'autres localisations génomiques au delà des impliqués dans la formation des gènes de fusion. L'objectif de cet étude était celui de déterminer le rôle, s'il existe, des gènes localisés dans les points de rupture additionnels et/ou associés avec délétions contigues aux points de rupture, dans l'étude de 5 patients avec de la leucémie.

Deux de ces patients étudiés ont révélé la présence des gènes de fusion *ETV6*(12p13)-*RUNX1*(21q22) et *MLL*(11q23)-*MLLT3*(9p22) comme résultat de t(12;21;5) et t(9;11;19), respectivement. Dans ce dernier cas, la caractérisation détaillée du local de rupture additionnel dans le chromosome 19 a révélé qu'un nouveau gène, *CCDC94*, exprès ubiquitairement et avec un rôle potentiel dans la régulation du cycle cellulaire, était interrompu par le point de rupture. Par des essais cellulaires *in vitro* on a démontré que *CCDC94* codifie une protéine nucléaire qui règle négativement la progression du cycle cellulaire. Ces résultats montrent que les points de rupture additionnels présents dans des translocations complexes peuvent entraîner dans la haplo-insuffisance de gènes essentiels impliqués dans la prolifération, en coopérant de cette façon avec la formation de protéines de fusion pour provoquer une prolifération cellulaire incontrôlée.

Les 3 autres patients étudiés ont révélé des délétions associées avec les points de rupture qui n'ont pas conduit à la formation de gènes de fusion. Dans le cas avec t(12;6;15) on a caractérisé une délétion dans la bande 12p13 qui a résulté dans l'élimination du gène *ETV6* et encore les 8 autres gènes en comprenant *CDKN1B*. Ces résultats indiquent que la perte simultanée de *ETV6* et de *CDKN1B*, qui codifie une protéine responsable par le blocage de l'entrée de cellules en phase G1 du cycle cellulaire, a une action de coopération dans la promotion de la leucémogénèse. On applique la même notion dans un cas avec dic(9;12) dans lequel 2 gènes qui codifient pour des facteurs de transcription, étaient éliminés comme résultat de délétions contigues aux points de rupture. De même on a constaté que 2 gènes, *NFATC2* (20q13) et *MAF* (16q23), tous 2 impliqués dans la régulation de l'expression des cytokines hématopoïétiques, étaient incluses dans les régions délétionées adjacentes aux points de rupture dans un patient avec t(X;20;16). La suppression de l'expression du gène

NFATC2, ou l'inhibition de l'activité de la respective protéine ont augmenté la prolifération cellulaire *in vitro* dû à la plus grande production de la cytokine GM-CSF. Ces résultats suggèrent que la haplo-insuffisance des 2 gènes a eu un effet coopératif dans l'induction de la prolifération cellulaire par la dérégulation de l'expression des cytokines hématopoïétiques.

De ces études 2 conclusions principales peuvent être tirées: (i) Les points de rupture additionnels, qui se produisent dans les translocations complexes associées avec la formation de gènes de fusion, peuvent avoir pour conséquence la dérégulation des gènes contrôleurs de la prolifération cellulaire; (ii) dans des translocations complexes caractérisées par délétions associées aux points de rupture, il aura besoin d'éliminer au moins 2 gènes avec des fonctions similaires ou complémentaires, pour promouvoir coopérativement la tumorigenèse.

Resumo

A tumorigénese é um processo de transformação celular que se desenrola tipicamente em várias etapas. Os diferentes níveis de evolução tumoral resultam da acumulação sucessiva de mutações genéticas numa célula normal que lhe conferem uma vantagem selectiva no respectivo meio tecidual. As mutações podem manifestar-se sob a forma de alterações nucleotídicas pontuais ao nível da sequência de DNA, levando a uma desregulação da função proteica ou à formação de proteínas não-funcionais, ou através de alterações cromossómicas numéricas ou estruturais. Na leucemia, por exemplo, os genes híbridos que resultam de translocações cromossómicas desempenham um importante papel no processo tumorigénico. Estes genes são transcritos sob a forma de um RNA mensageiro de fusão, o qual é traduzido numa proteína híbrida com função oncogénica.

Frequentemente, os subtipos de doença leucémica estão associados com translocações cromossómicas que envolvem 2 pontos de quebra recorrentes e específicos. É disto exemplo a leucemia mielóide crónica, em que uma translocação recíproca entre os cromossomas 9 e 22 conduz à formação de um gene de fusão *BCR-ABL1*. Em diferentes subtipos de doença, existe também uma pequena proporção de casos que apresenta translocações cromossómicas complexas, que envolvem um ou mais pontos de quebra adicionais em outras localizações genómicas além das que estão implicadas na formação dos genes de fusão. Por vezes, os pontos de quebra estão também associados a deleções extensas de material genético que se pensa terem uma função importante na tumorigénese. No entanto, o papel destas regiões genómicas no desenvolvimento tumoral não tem sido um motivo recorrente de estudo. Neste contexto, o objectivo desta dissertação foi o de determinar o potencial papel tumorigénico de alterações génicas adicionais ocorridas nos pontos de quebra de translocações cromossómicas complexas.

Para a prossecução do objectivo proposto, foram estudados 5 rearranjos cromossómicos distintos associados com diferentes tipos de doença hematológica maligna, nomeadamente a leucemia linfoblástica aguda de células B (2 casos), leucemia mielóide aguda, neoplasma mieloproliferativo e síndrome mielodisplásico/neoplasma mieloproliferativo, não classificável. O mapeamento dos pontos de quebra foi efectuado utilizando a hibridação fluorescente *in situ* e diferentes metodologias de biologia molecular, tendo como base a informação inicial da análise citogenética. Em casos seleccionados, o papel dos novos genes candidatos foi avaliado *in vitro* utilizando modelos de linhas celulares, nomeadamente no que respeita às funções de controlo da proliferação celular e de regulação transcricional.

De entre os 5 casos estudados, quatro deles evidenciaram translocações complexas envolvendo 3 cromossomas, nomeadamente $t(12;21;5)(p13;q22;q13)$, $t(12;6;15)(p13;p24\sim25;q22)$, $t(9;11;19)(p22;q23;p13)$ e $t(X;20;16)(p11;q13;q23)$. No caso remanescente, foi observada uma translocação dicêntrica $dic(9;12)(p11;p11)$ acompanhada de deleções extensas em ambos os pontos de quebra. Nos casos com $t(12;21;5)$ e $t(9;11;19)$ as translocações estavam associadas com a presença de genes de fusão recorrentes, nomeadamente *ETV6(12p13)-RUNX1(21q22)* e *MLL(11q23)-MLLT3(9p22)*, indicando que se tratavam de rearranjos complexos das translocações $t(12;21)$ e $t(9;11)$ associadas com a leucemia linfoblástica aguda de células B e a leucemia mielóide aguda, respectivamente.

O papel dos pontos de quebra adicionais foi estudado em detalhe no caso com $t(9;11;19)$. Através da metodologia de *long distance inverse-polymerase chain reaction*, foram identificados os pontos de quebra na sequência de DNA dos 3 cromossomas envolvidos na translocação. Além dos pontos de quebra nos genes *MLL* e *MLLT3*, foi observado que o local de quebra no cromossoma 19 interrompeu a sequência de um novo gene, designado *CCDC94*, conduzindo à sua haplo-insuficiência nas células com $t(9;11;19)$. Através de ensaios de *reverse transcription-polymerase chain reaction* verificámos que o gene *CCDC94* é expresso ubiquitariamente em tecidos humanos normais. A análise informática da sequência prevista da proteína *CCDC94* indicou uma elevada identidade de aminoácidos com a proteína *cwf16*, envolvida na regulação do ciclo celular da levedura *Schizosaccharomyces pombe*. Através da clonagem do DNA complementar de *CCDC94* em vectores de expressão, e após a transfecção destes em culturas de linhas celulares *in vitro*, observámos que este gene codifica uma proteína de localização exclusivamente nuclear. A expressão ectópica da proteína *CCDC94* diminuiu a progressão do ciclo celular e a proliferação das células em cultura. Inversamente, a supressão do transcrito do gene *CCDC94* através de interferência de RNA conduziu a um aumento significativo da proliferação celular, confirmando que *CCDC94* regula negativamente a proliferação e a progressão do ciclo celular. Estes resultados mostram que os pontos de quebra adicionais, presentes em translocações cromossómicas complexas em leucemia, podem resultar na haplo-insuficiência de genes controladores dos mecanismos proliferativos, cooperando desta forma com a acção das proteínas de fusão para proporcionar ao clone leucémico uma proliferação celular descontrolada.

Nos restantes 3 casos estudados não foram identificados genes de fusão. Ao invés, todos aqueles apresentaram deleções de extensão variável associadas com os pontos de quebra cromossómicos. No caso com $t(12;6;15)$, identificámos uma deleção de 1.2 megabases de DNA na banda 12p13 que resultou na eliminação de 9 genes incluindo *ETV6* e *CDKN1B*. O gene *ETV6* codifica um factor de transcrição que é essencial para a formação das diferentes

linhagens hematopoiéticas na medula óssea, enquanto *CDKN1B* é traduzido numa proteína responsável por bloquear a entrada das células na fase G1 do ciclo celular e, conseqüentemente, por travar a proliferação celular. Neste contexto, os resultados obtidos indicam que a perda simultânea de *ETV6* e de *CDKN1B*, através de uma translocação cromossómica complexa, constituiu uma acção cooperativa na leucemogénese. A mesma noção pode aplicar-se ao caso com *dic(9;12)*, no qual pelo menos 2 genes que codificam para factores de transcrição importantes na linhagem hematopoiética, *PAX5* no cromossoma 9 e *ETV6* no cromossoma 12, estavam delecionados como resultado do rearranjo cromossómico. Dado que o factor de transcrição *PAX5* regula negativamente a expressão do gene *FLT3*, que desempenha uma função pró-proliferativa, é expectável que a haplo-insuficiência de *PAX5* no caso com *dic(9;12)* terá tido como consequência uma elevação dos níveis de expressão de *FLT3*, contribuindo deste modo para uma proliferação celular aumentada.

A *t(X;20;16)* foi identificada num doente com trombocitémia essencial (TE), uma doença que está intimamente relacionada com alterações de vias intracelulares reguladas por citocinas. Neste caso, através da utilização de um *array* genómico, identificámos a presença de pequenas delecções associadas com os pontos de quebra nos cromossomas 16 e 20. No cromossoma 16 apenas um gene, *MAF*, estava delecionado, enquanto no cromossoma 20 a delecção tinha abrangido 3 genes. Dos genes delecionados, dois deles, *NFATC2* (20q13) e *MAF* (16q23), codificam proteínas que operam como reguladores transcricionais de citocinas hematopoiéticas. Dado que *NFATC2* se localiza numa região que constitui um alvo frequente de delecções em neoplasmas mieloproliferativos, incluindo a trombocitémia essencial, efectuámos um estudo detalhado do papel deste gene na proliferação megacariocítica e na regulação da expressão de uma citocina hematopoiética (*GM-CSF*), implicada na maturação das diferentes linhagens mielóides.

Utilizando um modelo de linha celular de trombocitémia essencial, verificámos que a supressão do transcrito do gene *NFATC2 in vitro*, por interferência de RNA, estava associada com um aumento da proliferação celular. Em concordância, o bloqueio da activação da proteína *NFATC2* através de um inibidor específico da sua interacção com a calcineurina, conduziu a um aumento da proliferação celular *in vitro*. Utilizando a PCR quantitativa em tempo real, detectou-se um aumento da produção do RNA de *GM-CSF* em ambos os ensaios celulares, indicando que o factor de transcrição *NFATC2* pode regular negativamente a expressão de *GM-CSF* em células de trombocitémia essencial. No geral, estes resultados mostram que a redução dos níveis fisiológicos do transcrito *NFATC2*, ou a redução da respectiva actividade proteica, estão relacionados com a proliferação de megacariocitos através do aumento da produção de *GM-CSF*. De acordo com estes resultados, verificámos que

as células dos doentes com TE apresentam níveis mais baixos do transcrito *NFATC2* do que a população normal. Dado que o factor de transcrição MAF desempenha igualmente um papel como regular transcricional de citocinas, é plausível que a haplo-insuficiência dos genes *NFATC2* e *MAF*, resultante do rearranjo cromossómico complexo t(X;20;16), teve um efeito cooperativo importante na patogénese da trombocitémia essencial através da alteração do padrão normal de expressão das citocinas hematopoiéticas.

Em síntese, efectuámos nesta dissertação um estudo citogenético de 4 translocações cromossómicas complexas incluindo t(12;21;5), t(12;6;15), t(9;11;19) e t(X;20;16), e de uma translocação dicêntrica dic(9;12), associadas com diferentes neoplasmas hematológicos. Em casos seleccionados efectuámos também um estudo molecular detalhado das regiões dos pontos de quebra. Esta análise permitiu-nos identificar 2 genes, *CCDC94* no cromossoma 19 e *NFATC2* no cromossoma 20, cuja haplo-insuficiência pode promover o aumento da proliferação celular das células leucémicas. A partir destes estudos podem ser retiradas 2 noções principais: (i) Os pontos de quebra adicionais, que ocorrem em translocações complexas associadas com a formação de genes de fusão, podem ter como consequência a desregulação de genes controladores da proliferação celular (e.g., *CCDC94*); (ii) As translocações complexas caracterizadas pela ausência de genes de fusão recorrentes poderão estar preferencialmente associadas com a presença de deleções, envolvendo um ou mais genes, nos pontos de quebra; nestas situações, serão necessários pelo menos 2 genes com funções celulares semelhantes (e.g., *NFATC2* e *MAF*) ou complementares (e.g., *ETV6* e *CDKN1B*) para, quando deleccionados, promoverem de forma cooperativa a leucemogénese. Nestes termos, o modelo de alterações genéticas sequenciais que caracteriza o desenvolvimento do cancro pode ser substituído por um modelo em que vários genes-alvo são simultaneamente desregulados pela formação de uma translocação cromossómica complexa, evitando deste modo a necessidade de ocorrência de alterações genéticas subsequentes.

Table of Contents

Table Index	xxiv
Figure Index	xxv
Abbreviations	xxvii
1. General Introduction	1
1.1. The Philadelphia Chromosome as a Paradigm of Cancer Genetics	3
1.2. Recurrent Chromosome Translocations in Acute Myeloid Leukemia	5
1.2.1. Translocation (8;21)(q22;q22)	6
1.2.2. Inversion (16)(p13q22)/Translocation (16;16)(p13;q22)	6
1.2.3. Translocation (15;17)(q22;q21)	7
1.3. Generation of Fusion Genes by Alternative Chromosomal Rearrangements	8
1.3.1. Complex Translocations	8
1.3.2. Submicroscopic Insertions	10
1.4. Biological Characteristics of Complex Translocations	11
1.4.1. Incidence in Chronic Myeloid Leukemia and Acute Myeloid Leukemia	11
1.4.2. Relevance for Pathogenesis	13
1.4.3. Genome Distribution of Additional Breakpoint Locations	14
1.4.4. Stepwise Formation of Translocations	16
1.4.5. Breakpoint-adjacent Deletions	18
1.4.6. Molecular Mechanisms of Chromosomal Rearrangement	21
1.5. The Neutral Versus the Alternative Hypothesis	22
2. Aims	25
3. Results	29
3.1. Molecular Cytogenetic Characterization of Rearrangements Involving 12p in Leukemia	31
3.1.1. Abstract	32
3.1.2. Introduction	32
3.1.3. Cases Summary	33
3.1.4. Materials and Methods	34
3.1.4.1. Cytogenetic and Fluorescence in Situ Hybridization Analyses of Chromosome Rearrangements	34
3.1.4.2. Molecular Analysis of <i>ETV6-RUNX1</i> Fusion Transcripts	35
3.1.4.3. Mutational Analysis of <i>ETV6</i>	35
3.1.5. Results	35
3.1.5.1. Hidden <i>ETV6-RUNX1</i> Fusion as a Result of a Complex t(12;21;5)(p13;q22;q13) in B-cell Acute Lymphoblastic Leukemia	35
3.1.5.2. Interstitial Deletion at 12p13 as a Consequence of a 3-way t(12;6;15)(p13;p24~25;q22) in a Patient with Myelodysplastic Syndrome/Myeloproliferative Neoplasm, Unclassifiable	38
3.1.5.3. Deletion of <i>ETV6</i> at 12p13 and of <i>PAX5</i> at 9p13 as a Result of dic(9;12)(p11;p11) in B-cell Acute Lymphoblastic Leukemia	40
3.1.6. Discussion	41

3.2. Three-way Translocation Involves *MLL*, *MLLT3* and a Novel Cell Cycle Control Gene, *CCDC94*, in the Pathogenesis of Acute Myeloid Leukemia with t(9;11;19)(p22;q23;p13) _ 43

3.2.1. Abstract	44
3.2.2. Introduction	44
3.2.3. Case Summary	46
3.2.4. Materials and Methods	46
3.2.4.1. Cytogenetic and Fluorescence <i>in Situ</i> Hybridization Analyses of Chromosome Rearrangements	46
3.2.4.2. Molecular Analysis and Cloning of <i>MLL-MLLT3</i> Fusion Transcripts	46
3.2.4.3. Cloning of Genomic Fusions on the der(11) and der(19) Chromosomes	47
3.2.4.4. Detection of Truncated <i>CCDC94</i> Transcripts	48
3.2.4.5. Detection of <i>CCDC94</i> mRNA Expression in Cell Lines and Normal Tissues	48
3.2.4.6. Subcellular Localization of <i>CCDC94</i> Protein	49
3.2.4.7. Effect of <i>CCDC94</i> Expression on Cell Cycle Progression and Cell Survival	50
3.2.4.8. Effect of <i>CCDC94</i> mRNA Suppression on Cell Proliferation	50
3.2.4.9. Computational Sequence Analysis	51
3.2.5. Results	51
3.2.5.1. Translocation t(9;11;19) Is a 3-Way Complex of t(9;11) that Rearranges <i>MLL</i> with <i>MLLT3</i> and Results in an <i>MLL</i> Exon 5- <i>MLLT3</i> Exon 6 Fusion Transcript	51
3.2.5.2. A Novel Gene at 19p13.3, <i>CCDC94</i> , Is Disrupted by Fusion to the 3' End of <i>MLL</i>	53
3.2.5.3. The <i>CCDC94</i> Gene Is Ubiquitously Expressed in Human Cells	58
3.2.5.4. <i>CCDC94</i> Is a Nuclear Protein with a Role in Cell Cycle Progression	60
3.2.6. Discussion	65

3.3. Three-way Translocation (X;20;16)(p11;q13;q23) in Essential Thrombocythemia Implicates *NFATC2* in Disregulation of GM-CSF Expression and Megakaryocyte Proliferation 69

3.3.1. Abstract	70
3.3.2. Introduction	70
3.3.3. Case Summary	72
3.3.4. Materials and Methods	72
3.3.4.1. Collection and Preparation of Samples	72
3.3.4.2. Cytogenetic and Fluorescence <i>in Situ</i> Hybridization Analyses of Chromosome Rearrangements	73
3.3.4.3. Delimitation of the 20q Deletion Boundaries Using Microsatellite Polymorphisms	74
3.3.4.4. Analysis of Chromosome Rearrangements by Whole-genome Array	75
3.3.4.5. Rapid Amplification of cDNA Ends	75
3.3.4.6. Expression Analysis of <i>NFATC2</i> in Normal Human Tissues	76
3.3.4.7. Detection of a Transcribed Single Nucleotide Polymorphism in the <i>NFATC2</i> Gene	77
3.3.4.8. Mutational Analysis of <i>JAK2</i> and <i>NFATC2</i> Genes	78
3.3.4.9. Inhibition of the Calcineurin/NFAT Signaling Pathway	79
3.3.4.10. <i>In Vitro</i> Suppression of <i>NFATC2</i> Using a Short Interfering RNA	80
3.3.4.11. Quantification of <i>GM-CSF</i> RNA Expression in SET-2 Cells	80
3.3.4.12. Quantification of <i>NFATC2</i> RNA Levels in Patients with Essential Thrombocythemia and Controls	81
3.3.5. Results	82
3.3.5.1. Detection of Submicroscopic Interstitial Deletions at 20q13.13 and 16q23.1 in a Patient with Essential Thrombocythemia	82
3.3.5.2. The <i>WWOX</i> Gene is Not Rearranged in the Patient with t(X;20;16)	88

3.3.5.3. <i>NFATC2</i> is Ubiquitously Expressed in Normal Human Cells and Both Alleles are Present in Peripheral Blood Leukocytes of Patients with Essential Thrombocythemia _____	90
3.3.5.4. The <i>NFATC2</i> gene is not Mutated in Patients with Essential Thrombocythemia _____	91
3.3.5.5. <i>NFATC2</i> Expression is Diminished in Granulocytes of Patients with Essential Thrombocythemia _____	92
3.3.5.6. Inhibition of NFAT Activation <i>in Vitro</i> is Associated with Megakaryocytic Proliferation _	93
3.3.5.7. Suppression of <i>NFATC2</i> RNA Promotes Cell Proliferation <i>in Vitro</i> _____	95
3.3.5.8. Reduced <i>NFATC2</i> Expression or Inhibition of <i>NFATC2</i> Activity Increases <i>GM-CSF</i> Expression in SET-2 Cells _____	96
3.3.6. Discussion _____	99
4. Conclusions and Future Perspectives _____	103
5. References _____	115

Table Index

<i>Table I. Proportion of complex translocations among Philadelphia-positive CML patients originating from different countries.</i>	12
<i>Table II. Summary of chromosome bands involved in 3- or 4-way complex rearrangements of t(8;21), t(15;17) and inv(16) reported in the literature.</i>	16
<i>Table III. Summary of clinical features, G-banded karyotype, FISH analysis and ETV6 status in the 3 patients.</i>	33
<i>Table IV. Designation of primers and corresponding sequences used in this study.</i>	47
<i>Table V. Designation of siRNA oligos and corresponding sequences used in this study.</i>	50
<i>Table VI. Localization of clones used as FISH probes and corresponding STS markers and primer sequences.</i>	73
<i>Table VII. STS markers used for delimitation of the 20q deletion.</i>	75
<i>Table VIII. Primers used for 3' and 5' RACE analyses.</i>	76
<i>Table IX. Primers used for detection of the rs6013193 SNP in NFATC2 genomic DNA.</i>	77
<i>Table X. Primers used for detection of a transcribed SNP (rs6013193) in exon 4 of NFATC2.</i>	78
<i>Table XI. Primers used for amplification of NFATC2 exons and corresponding flanking exon/intron boundaries.</i>	79
<i>Table XII. Primers and probe used for analysis of GM-CSF expression by Q-PCR.</i>	81

Figure Index

Figure 1. Diagrammatic representation of the t(9;22) and its molecular consequences in CML. _____	4
Figure 2. Schematic representation of a standard t(9;22) and a complex t(9;22;11) in CML. _____	9
Figure 3. Formation of a complex translocation by stepwise rearrangements involving chromosomes 9, 22 and 11. _____	17
Figure 4. Analysis of chromosome rearrangements by FISH on a bone marrow metaphase cell with t(12;21;5). _____	36
Figure 5. Detection of ETV6-RUNX1 fusion by FISH, RT-PCR and direct sequencing analyses. _____	37
Figure 6. Analysis of chromosome rearrangements by FISH on bone marrow cells with t(12;6;15). _____	38
Figure 7. Diagrammatic representation of human chromosome 12 and of an enlarged 12p13 region targeted by the translocation breakpoints in the t(12;6;15)(p13;p24~25;q22). _____	39
Figure 8. Analysis of chromosome rearrangements by FISH on bone marrow metaphases with dic(9;12)(p11;p11). _____	40
Figure 9. Analysis of chromosome rearrangements by FISH in a bone marrow cell with t(9;11;19). _____	52
Figure 10. Detection of the MLL-MLLT3 fusion by FISH, RT-PCR and direct sequencing analyses. _____	53
Figure 11. LDI-PCR analyses of the genomic breakpoint junctions on der(11) and der(19). _____	54
Figure 12. Genomic sequence fusions originated at the der(19) and der(11) breakpoints. _____	56
Figure 13. Analysis of CCDC94 transcripts by 3' RACE and direct sequencing. _____	57
Figure 14. Analysis of CCDC94 rearrangement by FISH in a metaphase with t(9;11;19). _____	58
Figure 15. Expression profile of the CCDC94 gene in human cells. _____	59
Figure 16. Sequence alignment between the human CCDC94 protein and the cwf16 protein of <i>S. pombe</i> . _____	61
Figure 17. Domain composition, expression and intracellular localization of the human CCDC94 protein. _____	62
Figure 18. Effect of CCDC94 expression on G1- to S-phase cell cycle progression and on survival of NIH-3T3 cells. _____	63
Figure 19. Suppression of CCDC94 transcripts in NIH-3T3 cells. _____	64
Figure 20. Effect of CCDC94 suppression on G1- to S-phase cell cycle progression of NIH-3T3 cells. _____	65
Figure 21. Results of cytogenetics and FISH analyses on bone marrow cells with t(X;20;16). _____	83
Figure 22. Results of capillary electrophoresis analysis of heterozygous polymorphisms located at 20q13.13. _____	84
Figure 23. Schematic representation of human chromosome 20 and of an enlarged 20q13.13 region targeted by the breakpoints of a complex t(X;20;16). _____	85
Figure 24. Results of whole-genome array analysis of chromosome region 20q13.13. _____	86
Figure 25. Results of whole-genome array analysis of chromosome region 16q23.1-16q23.2 _____	87
Figure 26. Results of 3' RACE analysis of WWOX transcripts. _____	89
Figure 27. Expression of NFATC2 in normal human tissues. _____	90
Figure 28. Expression of NFATC2 in hematopoietic cells. _____	91
Figure 29. Analysis of JAK2V617F mutation in the patient with t(X;20;16). _____	92
Figure 30. Comparison of NFATC2 mRNA expression in granulocytes of ET patients and normal individuals. _____	93
Figure 31. Inhibition of NFAT activation in SET-2 cells. _____	94
Figure 32. Suppression of NFATC2 transcripts in SET-2 cells. _____	95
Figure 33. Effect of NFATC2 suppression in proliferation of SET-2 cells. _____	96
Figure 34. Partial suppression of NFATC2 mRNA promotes GM-CSF expression in SET-2 cells. _____	97
Figure 35. Inhibition of NFAT activity promotes GM-CSF expression in SET-2 cells. _____	98

Abbreviations

6-FAM	6-carboxyfluorescein
ALL	acute lymphoblastic leukemia
AML	acute myeloid leukemia
APL	acute promyelocytic leukemia
AS-PCR	allele specific-polymerase chain reaction
ATRA	all-trans retinoic acid
AUAP	abridged universal amplification primer
BAC	bacterial artificial chromosome
bcr	breakpoint cluster region
BCR1	breakpoint cluster region 1
BCR2	breakpoint cluster region 2
BLAST	basic local alignment search tool
bp	base pairs
BrdU	bromodeoxyuridine
CAD	chromosome abnormality database
CBF	core binding factor
CC	coiled-coil
CDS	common deleted segment
CG	cytosine-guanine
ChAS	chromosome analysis suite
CML	chronic myeloid leukemia
CS	calf serum
DAPI	4',6-diamidino-2-phenylindole
DLBCL	diffuse large B-cell lymphoma
DMSO	dimethyl sulfoxide
DNAt2	DNA topoisomerase II
dNTP	desoxyribonucleotide triphosphate
EDTA	ethylenediamine tetraacetic acid
ET	essential thrombocythemia
Ets	erythroblastosis virus, E26-E twenty six
FISH	fluorescence <i>in situ</i> hybridization
FITC	fluorescein isothiocyanate
G1-phase	gap1 phase

GFP	green fluorescent protein
hr	hours
IM	imatinib mesylate
ISH	<i>in situ</i> hybridization
IVIC	Instituto Venezolano de Investigaciones Científicas
kb	kilobase
kDa	kiloDalton
LDI-PCR	long distance inverse-polymerase chain reaction
LTR	long terminal repeat
Mb	megabase
MDS	myelodysplastic syndrome
MDS/MPN, U	myelodysplastic syndrome/myeloproliferative neoplasm, unclassifiable
μM	micromolar
min	minutes
mm	millimeter
MPN	myeloproliferative neoplasm
NCBI	national center for biotechnology information
NES	nuclear export signal
ng	nanogram
NHEJ	non-homologous end joining
NLS	nuclear localization signal
OS	Okhiro syndrome
PAC	P1-derived artificial chromosome
PCR	polymerase chain reaction
PMF	primary myelofibrosis
PV	polycythemia vera
Q-PCR	quantitative-polymerase chain reaction
RACE	rapid amplification of cDNA ends
RT-PCR	reverse transcription-polymerase chain reaction
SARs	scaffold-associated regions
SDS	sodium dodecyl sulphate
SDS-PAGE	sodium dodecyl sulphate-polyacrilamide gel electrophoresis
sec	seconds
siControl	short interfering RNA control
siRNA	short interfering RNA

SNP	single nucleotide polymorphism
S-phase	synthesis phase
STR	short tandem repeat
STS	sequence tagged site
t-ALL	therapy-related acute lymphoblastic leukemia
t-AML	therapy-related acute myeloid leukemia
TAMRA	tetramethyl-6-carboxyrhodamine
TE	Tris EDTA
Tris	(hydroxymethyl)aminomethane
TRITC	tetramethylrhodamine isothiocyanate
U	units
UKCCG	United Kingdom cancer cytogenetics group
vol	volume
WCP	whole chromosome painting
wt	weight
YAC	yeast artificial chromosome

In this thesis italic capital letters will be used for designating genes whereas non-italic capital letters will be utilized for designating proteins. Official gene symbols and names will be predominantly used throughout this thesis.

1. GENERAL INTRODUCTION

1.1. THE PHILADELPHIA CHROMOSOME AS A PARADIGM OF CANCER GENETICS

Physical integrity of the eukaryotic chromosome complement is crucial for normal cell physiology and homeostasis. The notion that chromosome abnormalities could play a role in the formation of tumours began to develop with the work of 2 German pathologists at the nineteenth-twentieth century transition. David von Hansemann initially speculated that chromosome aberrations and mitotic abnormalities were associated with the formation and progression of tumours, whereas Theodor Boveri later proposed that the alteration in the number of chromosomes in a normal somatic cell might have a role in the initiation of cancer (von Hansemann, 1890; Boveri, 1914). However, scientific evidence to corroborate these hypotheses waited almost 50 years for the development of new cytogenetic techniques which improved the overall quality of metaphase chromosome preparations.

Taking advantage of technical improvements in tissue culture procedures, Peter Nowell and David Hungerford firstly identified a characteristic small chromosome in the neoplastic bone marrow metaphase cells of patients with chronic myeloid leukemia (CML) (Nowell & Hungerford, 1960; Nowell & Hungerford, 1961). This somatic chromosome abnormality was designated as the Philadelphia chromosome, in accordance to the location of its discovery (Tough *et al.*, 1961). Using fluorescence analysis with quinacrine mustard, Caspersson *et al.* (1970) initially established that the Philadelphia chromosome was a chromosome 22 with a deletion at the long arm, i.e., a 22q- chromosome. Later, it was revealed by the combined use of quinacrine mustard fluorescence and Giemsa staining that the end of the long arm of one chromosome 9 contained an extra material from another chromosome, most probably chromosome 22 (Rowley, 1973a). These results established that the Philadelphia chromosome was a derivative chromosome 22 [der(22)] resulting from a reciprocal translocation between one homologue of each pair of chromosomes 9 and 22.

The development of DNA hybridization probes to detect genomic rearrangements allowed the identification of the sequences disrupted at the breakpoints. It was shown that the DNA sequence of the breakpoint cluster region (*BCR*) gene at chromosome band 22q11, and of the human homologue of the transforming sequence of Abelson murine leukemia virus gene, the *c-abl* oncogene 1, non-receptor tyrosine kinase (*ABL1*) gene at chromosome band 9q34, were interrupted by the translocation breakpoints (de Klein *et al.*, 1982; Heisterkamp *et al.*, 1983; Groffen *et al.*, 1984; Heisterkamp *et al.*, 1985). Since both genes are oriented from 5' to 3' in the centromere to telomere direction, the translocation produces a 5'*BCR*-3'*ABL1* fusion gene on the 22q- chromosome and a reciprocal 5'*ABL1*-3'*BCR* hybrid gene on the 9q+ chromosome (**Fig. 1**).

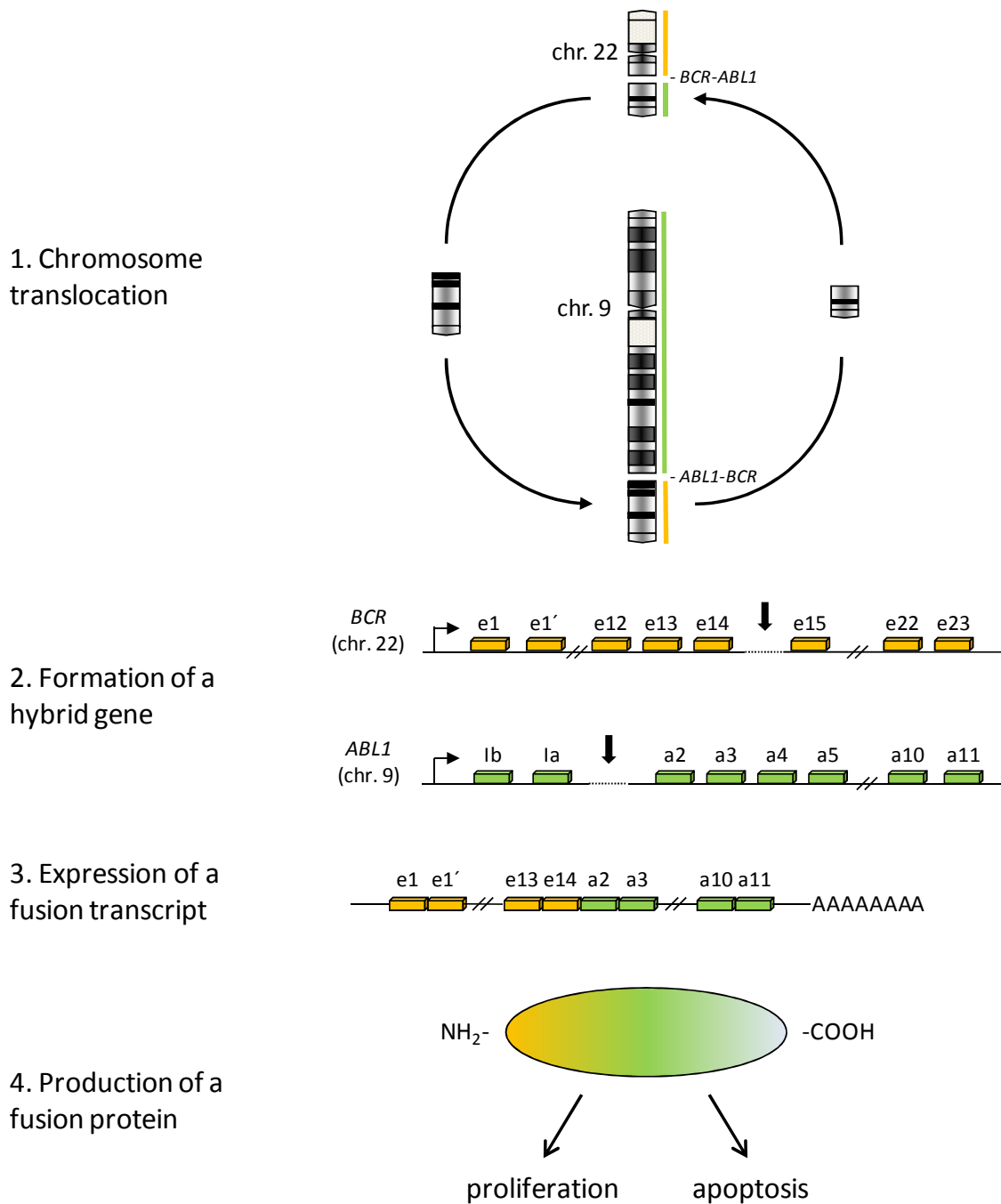


Figure 1. Diagrammatic representation of the t(9;22) and its molecular consequences in CML.

The reciprocal exchange of material between one homologue of each pair of chromosomes 9 and 22 leads to the formation of a *BCR-ABL1* hybrid gene on the derivative chromosome 22 and of an *ABL1-BCR* hybrid gene on the derivative chromosome 9. For simplicity only the *BCR-ABL1* fusion transcript is shown in detail. Transcription of the *BCR-ABL1* hybrid gene originates an in-frame fusion mRNA which is translated into a fusion protein. The fusion protein interferes with normal intracellular signaling pathways resulting in increased proliferation and blockage of apoptosis of CML cells. Arrows pointing downwards indicate the breakpoint positions within the *BCR* and *ABL1* genes. The example shown here represents the formation of a common e14a2 *BCR-ABL1* fusion transcript, however, other transcript configurations (e.g., e13a2 or, rarely, e13a3 or e14a3) are also possible depending on the intron in which the breakpoints occur. Each green or orange box represents an *ABL1* or *BCR* exon, respectively. Exons are not shown to scale. Designations of exons are shown above each box. The stretch of adenosine (A) nucleotides represents the poly-A tail of mature *BCR-ABL1* mRNA.

Molecular studies have shown that the *BCR-ABL1* fusion gene is transcribed in all Philadelphia chromosome-positive patients whereas the reciprocal fusion mRNA is present in only 60% of *BCR-ABL1*-positive cases (Shtivelman *et al.*, 1985; Melo *et al.*, 1993). The product of the *BCR-ABL1* fusion gene is a novel 210 KiloDalton (KDa) hybrid protein which displays increased tyrosine kinase activity (Konopka *et al.*, 1984; Lugo *et al.*, 1990). The oncogenic activity of BCR-ABL1 involves the activation of various cellular signaling pathways that promote proliferation and block apoptosis of CML cells (reviewed in Sawyers, 1997). Moreover, a myeloproliferative disorder resembling the chronic phase of human CML is produced in mice which have been transplanted with bone marrow hematopoietic stem cells infected with *BCR-ABL1* encoding-retroviruses (Daley *et al.*, 1990; Kelliher *et al.*, 1990). These data showed that the *BCR-ABL1* fusion gene is a critical leukemogenic lesion in CML.

An inhibitor of ABL1 tyrosine kinase activity, imatinib mesylate (IM), was successfully developed to block BCR-ABL1 kinase activity in CML cells (Druker *et al.*, 1996). IM induces major cytogenetic remissions (i.e., between 0-35% of metaphases with the Ph chromosome) in almost 90% of cases and is thus the preferred first-line treatment approach for CML patients in chronic phase (O'Brien *et al.*, 2003). Improvement of the genetic characterization of cancers by application of the binomial Philadelphia chromosome-IM is fundamental to achieve therapeutic success in other tumour types in the future (Sherbenou & Druker, 2007).

1.2. RECURRENT CHROMOSOME TRANSLOCATIONS IN ACUTE MYELOID LEUKEMIA

In contrast to CML, leukemic cells from patients diagnosed with acute myeloid leukemia (AML) display extensive karyotypic heterogeneity. Among the various types of chromosomal rearrangements which can be observed in AML patients, four of these comprise approximately 50% of cases overall (reviewed in Rowley, 2001). These include $t(8;21)(q22;q22)$, $inv(16)(p13q22)$ or $t(16;16)(p13;q22)$, $t(15;17)(q22;q21)$ and $t(9;11)(p22;q23)$. Each of these rearrangements generates a fusion gene which leads to the production of an oncogenic hybrid protein responsible for inducing a differentiation and/or maturation arrest at an early developmental stage of myeloid cells. In this section we will briefly review the main molecular and functional features of $t(8;21)$, $inv(16)/t(16;16)$ and $t(15;17)$. The $t(9;11)$ will be dealt in further detail in chapter 3 (section 3.2).

1.2.1. TRANSLOCATION (8;21)(q22;q22)

The t(8;21)(q22;q22) was the only recurrent chromosome translocation in human leukemia to be discovered before the t(9;22) (Rowley, 1973b). Its presence is associated with a high frequency of Auer rods in the leukemic cells, significant neutrophil maturation and prominent eosinophilia in the bone marrow (Bitter *et al.*, 1987). The molecular consequence of the rearrangement is a fusion of the 5' part of the *runt*-related transcription factor 1 (*RUNX1*, formerly known as *AML1* or *CBFA2*) gene from 21q22 to 3' sequences of the *runt*-related transcription factor 1, translocated to 1 (*RUNX1T1*, previously known as *ETO*) gene at chromosome 8q22 (Miyoshi *et al.*, 1991; Erickson *et al.*, 1992; Nisson *et al.*, 1992; Miyoshi *et al.*, 1993). Since *RUNX1T1* is not expressed in hematopoietic cells, the putative reciprocal 5'*RUNX1T1*-3'*RUNX1* fusion transcripts have not been identified (Nucifora & Rowley, 1995).

The *RUNX1* gene encodes the alpha subunit of the heterodimeric core binding factor (CBF) complex which drives transcription of several hematopoietic lineage specific genes (Ogawa *et al.*, 1993; reviewed in Downing, 1999). Differentiation arrest in t(8;21)-positive cells likely results from an impaired transcriptional activity of the *RUNX1-RUNX1T1* hybrid protein at CBF sites within gene promoters (reviewed in Downing, 1999). Recently, corticosteroids and dihydrofolate reductase inhibitors have been shown to modulate the activity of the *RUNX1-RUNX1T1* fusion protein *in vitro* and to induce differentiation of *RUNX1-RUNX1T1* positive cells whilst inhibiting cell proliferation, suggesting that those compounds may be useful as therapeutic agents for treating AML patients with t(8;21) in the future (Corsello *et al.*, 2009).

1.2.2. INVERSION (16)(p13q22)/TRANSLOCATION (16;16)(p13;q22)

A pericentric inversion of chromosome 16, inv(16)(p13q22) or, less frequently, an alternative configuration in the form of a translocation between both homologues, t(16;16)(p13;q22), are characteristically associated to AML with bone marrow and peripheral blood eosinophilia (de la Chapelle & Lahtinen, 1983; Le Beau *et al.*, 1983; Liu *et al.*, 1995). As a result of either rearrangement, the core binding factor, beta subunit (*CBFB*) gene located at 16q22 fuses to the myosin, heavy chain 11, smooth muscle (*MYH11*) gene at 16p13, giving rise to a *CBFB-MYH11* fusion gene at 16q22 (Liu *et al.*, 1993b; van der Reijden *et al.*, 1993). The putative reciprocal *MYH11-CBFB* fusion transcript was not identified, either because of the existence of deletions adjacent to the 16p13 breakpoint in some inv(16)-positive patients or

because of a lack of activity of the *MYH11* promoter in hematopoietic cells (reviewed in Liu *et al.*, 1995).

The *CBFB* gene codes for the non-DNA binding subunit of the CBF complex whereas *MYH11* codes for a smooth muscle form of myosin heavy chain. As in the case of RUNX1-RUNX1T1, the CBFB-MYH11 fusion protein acts by repressing gene transcription. A new heterodimerization domain generated at the junctional region of the protein moieties is capable of sequestering RUNX1 with much higher affinity compared with normal interaction between CBFB and RUNX1, thereby impairing its DNA-binding function (Huang *et al.*, 2004). Furthermore, a repression domain encoded by the C-terminal region of MYH11 is capable of association with the mSin3A co-repressor, further contributing to transcriptional inactivation mediated by the CBFB-MYH11 chimeric protein (Durst *et al.*, 2003). In view of the similarities between the mode of action of the CBFB-MYH11 and RUNX1-RUNX1T1 hybrid proteins, it is possible that corticosteroids or dihydrofolate reductase enzyme inhibitors may also be effective in inducing maturation of leukemic myeloid cells with *CBFB-MYH11* rearrangement.

1.2.3. TRANSLOCATION (15;17)(q22;q21)

Rowley *et al.* (1977) initially proposed that a chromosomal insertion was responsible for the presence of chromosome 17 material at the long arm of chromosome 15 in a patient with acute promyelocytic leukemia (APL). However, subsequent reports of other APL patients clearly showed that the rearrangement involved a reciprocal translocation between chromosomes 15 and 17 instead of an insertion (Scheres *et al.*, 1978; Testa *et al.*, 1978). As a consequence of the t(15;17), a fusion occurs between the retinoic acid receptor, alpha (*RARA*) gene at chromosome 17q21 and the promyelocytic leukemia (*PML*) gene at chromosome 15q22 (de Thé *et al.*, 1990). The resultant fusion on the der(15) chromosome generates an in-frame *PML-RARA* fusion transcript which can be detected in all patients with the translocation (de Thé *et al.*, 1990; Kakizuka *et al.*, 1991). In contrast, the reciprocal *RARA-PML* fusion gene on the der(17) chromosome is expressed in only 67-78% of the *PML-RARA*-positive APL patients (Alcalay *et al.*, 1992; Borrow *et al.*, 1992), thus reflecting its minor role as a critical leukemogenic lesion.

The PML protein associates with subnuclear bodies which are involved in the regulation of transcription (reviewed in Zhong *et al.*, 2000) whereas RARA belongs to the superfamily of vitamin D3, steroid and thyroid hormone nuclear receptors (Giguere *et al.*, 1987; Petkovich *et al.*, 1987; Evans, 1988). Both the wild-type RARA protein and the PML-RARA fusion protein can

bind to promoter response elements in the DNA sequences of target genes (reviewed in Lin *et al.*, 2001). However, the transactivation potential of the PML-RARA hybrid protein is weaker than that of the native RARA protein (de Thé *et al.*, 1991), indicating that repression of transcriptional activity is also responsible for a maturation arrest in APL. However, in contrast to AML patients with t(8;21) or inv(16), patients with t(15;17) can be successfully treated with arsenic trioxide or all-trans retinoic acid (ATRA) (Huang *et al.*, 1988; Chen *et al.*, 1996). For instance, the interaction between PML-RARA, co-repressors and histone deacetylases is lost under pharmacological concentrations of ATRA, thus allowing relaxation of the chromatin and restart of RARA target gene transcription, and ultimately leading to normal myeloid terminal maturation (Lin *et al.*, 2001).

1.3. GENERATION OF FUSION GENES BY ALTERNATIVE CHROMOSOMAL REARRANGEMENTS

In a minority of newly-diagnosed leukemia patients, one or more extra chromosomes may also intervene in the rearrangement between the 2 chromosomes involved in the standard translocation, leading to the formation of complex chromosomal rearrangements. In other rare patients, gene fusion may also occur by mechanisms other than standard or complex translocations. In this section we will review alternative chromosomal rearrangements associated with CML and its pathognomonic *BCR-ABL1* fusion as an example of the cytogenetic portfolio associated with the formation of fusion genes in leukemia.

1.3.1. COMPLEX TRANSLOCATIONS

It was early observed in some CML patients that rearrangement of chromosomes 9 and 22 could also implicate rearrangements of additional chromosome bands without compromising the formation of the Philadelphia chromosome (Hayata *et al.*, 1973; Gahrton *et al.*, 1974; Hayata *et al.*, 1975; Sonta & Sandberg, 1977; Pasquali *et al.*, 1979; Sandberg, 1980). These alternative rearrangements were originally subdivided into separate cytogenetic classes designated as “complex” and “unusual” translocations (Sonta & Sandberg, 1977). An example of a complex translocation is illustrated in **Fig. 2**. This hypothetical rearrangement involves a breakpoint at 11q21 in addition to the recurrent breakpoints at bands 9q34 and 22q11. As in

the case of a standard t(9;22), the terminal region of the long arm of chromosome 9 containing the 3' part of *ABL1* is translocated to chromosome band 22q11 where it fuses to 5' *BCR*. In turn, the 3' *BCR* sequence along with the remaining region of the long arm of chromosome 22 is translocated to chromosome band 11q21 whereas the translocated segment of chromosome 11q is joined to the 5' *ABL1* sequence at the 9q34 breakpoint. As expected, the reciprocal 5' *ABL1*-3' *BCR* fusion gene is not generated because the 3' side of *BCR* is relocated to chromosome 11 instead of chromosome 9.

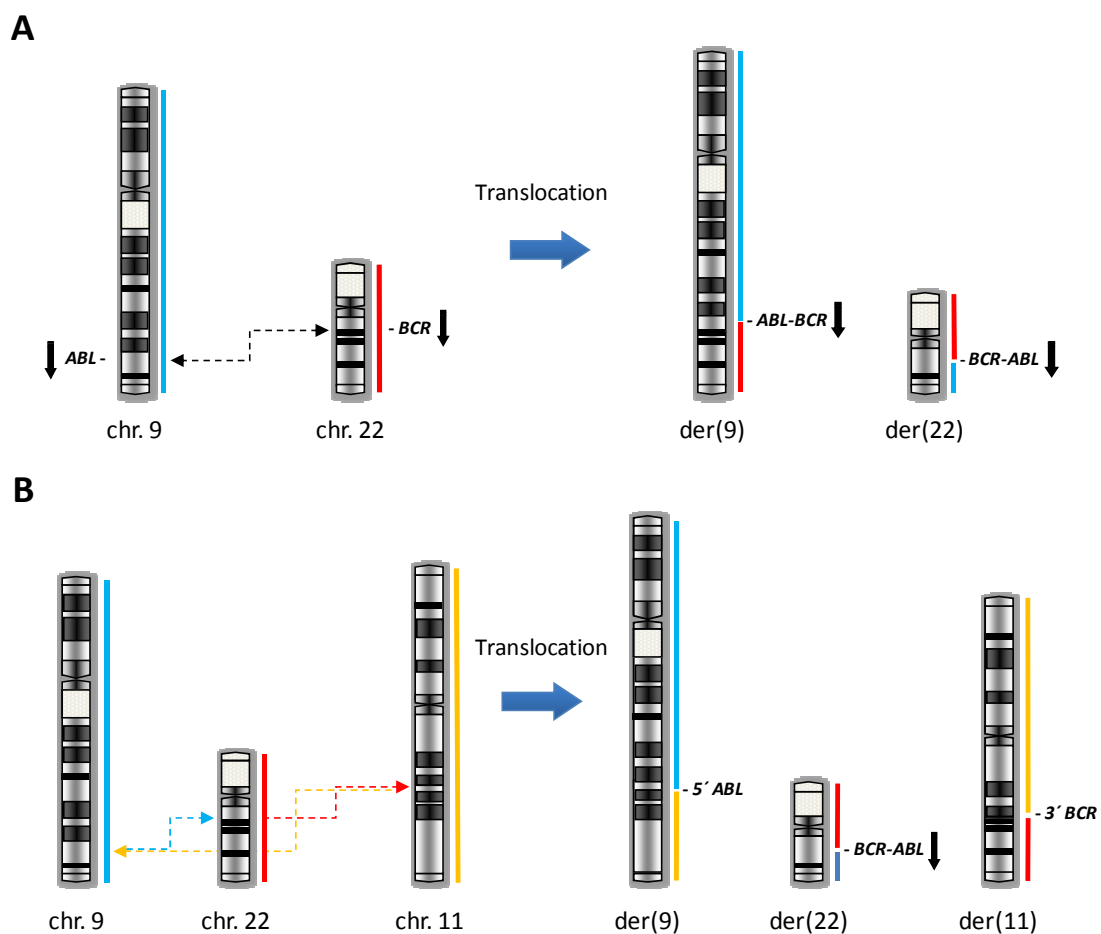


Figure 2. Schematic representation of a standard t(9;22) and a complex t(9;22;11) in CML.

(A) A standard t(9;22)(q34;q11) is formed as a result of breakpoints at chromosomes 9 (band 9q34) and 22 (band 22q11) followed by rejoining of the partial segments of the long arm of each chromosome to the opposite partner. As a consequence, a *BCR-ABL1* fusion gene is formed at the der(22), the Philadelphia chromosome, whereas a reciprocal *ABL1-BCR* hybrid gene is generated at the der(9). **(B)** In contrast to the standard translocation, a complex t(9;22;11)(q34;q11;q21) involves an extra breakpoint at band 11q21. In this single-step rearrangement, the terminal part of chromosome 9 joins the chromosome 22 to produce a *BCR-ABL1* fusion gene. Simultaneously, the terminal part of chromosome 22 moves to the long arm of chromosome 11 whereas the translocated segment of this chromosome fuses to the 9q34 region. Consequently, no reciprocal *ABL1-BCR* fusion is produced. Dashed lines with arrows are used to indicate the movement of material between each of the chromosomes involved in the rearrangement. Vertical blue, red and orange lines correspond to chromosome 9, 22 and 11 sequences, respectively. Vertical arrows adjacent to the *BCR* and *ABL1* genes indicate the direction of gene transcription.

In contrast to complex rearrangements, unusual or “variant” translocations referred to those cases in which only the Philadelphia chromosome and a rearranged chromosome other than the der(9), were detectable by conventional cytogenetic techniques (reviewed in Huret, 1990). These observations initially suggested that the Philadelphia chromosome could be originated by a translocation involving band 22q11 and other genomic regions besides chromosome band 9q34. However, a comparative study of complex and variant translocations suggested that the differences observed between them derived mostly from the inability of chromosome banding techniques to distinguish between the translocated region of chromosome 9 and that of the extra chromosome involved in the translocation, because of their similar size and microscopic appearance (Pasquali *et al.*, 1979). Indeed, it was subsequently demonstrated using higher resolution cytogenetic techniques such as reverse banding, or *in situ* hybridization (ISH), that in variant translocations a fusion had also occurred between the terminal part of chromosome 9q and the 22q11 region, or between the *ABL1* and *BCR* genes (Hagemeijer *et al.*, 1984; Bartram *et al.*, 1985; Morris & Fitzgerald, 1987; Morris *et al.*, 1988), indicating that these rearrangements are actually complex translocations in most if not in all patients (Fitzgerald & Morris, 1991).

1.3.2. SUBMICROSCOPIC INSERTIONS

A *BCR* rearrangement or juxtaposition between the *BCR* and *ABL1* genes was initially demonstrated in some CML patients with a normal karyotype (Kurzrock *et al.*, 1986; Fitzgerald *et al.*, 1987; Ohyashiki *et al.*, 1988). The formation of the *BCR-ABL1* fusion gene in these “Philadelphia-negative” CML patients was shown to result mostly from submicroscopic insertions of the 3' part of the *ABL1* gene into *BCR* at 22q11, or of 5' *BCR* into *ABL1* at 9q34, without apparent reciprocal transfer of genetic material to the other chromosome (Morris *et al.*, 1986; Dreazen *et al.*, 1987; Rassool *et al.*, 1990; Nishigaki *et al.*, 1992; Hagemeijer *et al.*, 1993; Lazaridou *et al.*, 1994; Nacheva *et al.*, 1994; Abeliovich *et al.*, 1995; Vieira *et al.*, 1999). Similarly, submicroscopic insertions also explained the existence of *RUNX1-RUNX1T1*-positive or *PML-RARA*-positive AML cases without t(8;21) or t(15;17), respectively (Hiorns *et al.*, 1994; Grimwade *et al.*, 1997; Grimwade *et al.*, 2000; Gamberdinger *et al.*, 2003).

In CML the *BCR-ABL1* fusion gene can be detected in over 50% of Philadelphia-negative patients using fluorescence *in situ* hybridization (FISH) and/or molecular techniques (Melo, 1997). Hematological parameters, clinical course and response to treatment of Philadelphia-negative *BCR-ABL1*-positive patients are similar to those observed in patients presenting with

the Philadelphia chromosome (van der Plas *et al.*, 1991). In this context, the designation “Philadelphia-negative CML” should be eliminated to avoid misinterpretation with rare patients whose disease is otherwise clinically and hematologically classified as CML but who do not present the *BCR-ABL1* fusion gene (Melo, 1997). The same notion should be applied to AML patients lacking the presence of t(8;21), inv(16)/t(16;16) or t(15;17) who show the presence of the correspondent fusion gene counterpart.

1.4. BIOLOGICAL CHARACTERISTICS OF COMPLEX TRANSLOCATIONS

The existence of complex translocations raises some questions concerning their biological characteristics: (i) What is the frequency of complex translocations among leukemia patients? (ii) Do complex translocations grant any modification of disease characteristics compared to the counterpart standard translocation? (iii) Are extra breakpoints evenly distributed throughout the genome or is there any clustering? (iv) Do complex translocations succeed to a single breakage and joining event as in the case of standard translocations or do they occur by consecutive events? And (iv) the molecular features mediating inter-chromosomal recombination in complex translocations are also shared by their 2-way equivalents? Again, we will use CML and AML as model disorders for answering these questions. These examples have been chosen due to the high number of available literature reports and not because of an intention to indicate the existence of a particular pattern of karyotypic variability that distinguishes CML or AML from other types of hematopoietic neoplasms.

1.4.1. INCIDENCE IN CHRONIC MYELOID LEUKEMIA AND ACUTE MYELOID LEUKEMIA

De Braekeleer (1987) calculated, on the basis of a retrospective analysis of 4061 patients for whom cytogenetic data was available, that the overall proportion of CML cases with a complex translocation was 4.3%. The author also noticed that the percentage of patients with a complex translocation varied according to the geographic origin of the patient. As an example, complex translocations comprised 9.01% of United Kingdom patients whereas the corresponding percentage in Italy was only 3.62% (De Braekeleer, 1987). To overcome the risks of literature bias, Fisher *et al.* (2005) conducted a retrospective analysis of an independent

series of patients belonging to the Wessex Regional Genetics Laboratory in England. The authors observed that 9.3% of the 428 registered CML cases showed a complex translocation, which is in close agreement with data from De Braekeleer (1987). Representative examples of the proportion of complex translocations observed in various countries are shown in **Table I** for comparison.

Table I. Proportion of complex translocations among Philadelphia-positive CML patients originating from different countries.

Total number of Ph-positive cases	Number of cases with complex translocations	Percentage	Geographic origin	Reference
119 (a)	20 (b)	16.8%	United Kingdom	Potter <i>et al.</i> (1981)
103	3	2.9%	Japan	Oshimura <i>et al.</i> (1982)
180	14	7.8%	South Africa	Bernstein <i>et al.</i> (1984)
126 (c)	18	14.0%	United States	Przepiorka & Thomas (1988)
105	6	5.7%	Italy	Zaccaria <i>et al.</i> (1989)
166	7	4.2%	Germany	Hild & Fonatsch (1990)
111	8	7.2%	France	Morel <i>et al.</i> (2003)

Only series exceeding 100 patients are presented. Results are listed in chronological order. (a) Includes 16 patients studied after disease transformation; (b) includes 2 cases presenting with del(22)(q11); (c) karyotype analysis was performed in the accelerated or blastic crisis phase of disease.

Similarly to the t(9;22), the incidence of complex rearrangements of t(8;21) in AML patients also appears to differ according to the country of origin. As an example, a study on French, Belgian and German patients with t(8;21) reported that complex rearrangements involving one or more extra chromosome bands in addition to 8q22 and 21q22 were found in 3.4% of cases whereas the corresponding percentage among Japanese and North-american patients was of 15.2% and 8.6%, respectively (Groupe Français de Cytogénétique Hématologique, 1990; Maseki *et al.*, 1993; Gallego *et al.*, 1994). Moreover, Fisher *et al.* (2005) determined that 6.3% of t(8;21)-positive cases registered at the United Kingdom Cancer Cytogenetics Group (UKCCG) karyotype database in acute leukemia presented the translocation in a complex configuration.

Complex rearrangements of t(15;17) are apparently less frequent than those of t(9;22) or t(8;21). A retrospective review study of *PML-RARA*-positive European APL cases lacking the archetypal t(15;17) estimated that the proportion of patients with complex translocations is of approximately 2% (Grimwade *et al.*, 2000). In agreement with these data, Fisher *et al.* (2005) identified 2.6% of patients with complex translocations among APL cases with rearrangements of chromosomes 15q22 and 17q21 registered at the UKCCG database. In the case of

inv(16)/t(16;16) the presence of complex rearrangements is also well documented. However, assessment of the corresponding proportion has not been estimated because of the very low number of reported cases (reviewed in Martinez-Climent *et al.*, 1999; Li *et al.*, 2001; Ohsaka *et al.*, 2008). This may in part be related to the fact that inv(16) is present in a lower proportion (6%) of AML patients compared to those presenting with either t(15;17) (14%) or t(8;21) (18%) (reviewed in Rowley, 2001).

1.4.2. RELEVANCE FOR PATHOGENESIS

Following a review of over 400 CML patients with complex translocations described in the literature, Mitelman (1993) ascertained that all chromosomes except the Y chromosome had already been reported as translocation partners of chromosomes 9 and 22. Although some degree of breakpoint clustering was noticeable, the majority of breakpoint locations differed widely among patients (Mitelman, 1993), underscoring the notion that those additional genomic lesions do not induce important biological changes in *BCR-ABL1*-positive CML cells. This view is also supported by various clinical-cytogenetic studies which have demonstrated that clinical features, hematologic parameters, prognosis and/or survival did not differ between patients presenting with a standard t(9;22) or with a complex rearrangement (Hayata *et al.*, 1975; Sonta & Sandberg, 1977; Sandberg, 1980; De Braekeleer, 1987).

However, not all studies reached the same conclusions. In one of the first reports covering a large series of patients, Potter *et al.* (1981) determined that the duration of the chronic phase of the disease was significantly shorter for patients younger than 60 years-old who presented with non-standard rearrangements than for those who did not. In agreement with these data, individual CML and AML cases with complex translocations have been associated with an aggressive disease phenotype and/or a diminished survival (Martin *et al.*, 1997; De Weer *et al.*, 2008).

One possible explanation for the contradictory data may be related to the specific chromosomal regions which are targeted by additional breakpoints. According to the hypothesis put forward by O'Brien *et al.* (1997), it is possible that the similar overall survival between patients with complex translocations and those with a standard t(9;22) results from the inclusion of patients with different complex abnormalities in the same group, where some aberrations confer a worse prognosis and others do not, and therefore compensate each other on the whole.

1.4.3. GENOME DISTRIBUTION OF ADDITIONAL BREAKPOINT LOCATIONS

At least 50 AML patients with 3-way (Lindgren & Rowley, 1977; Kondo *et al.*, 1978; Fitzgerald *et al.*, 1983; Oguma *et al.*, 1983; Slater *et al.*, 1983; Ayraud *et al.*, 1985; Testa *et al.*, 1985; Tagushi *et al.*, 1986; Berger *et al.*, 1987; Minamihisamatsu & Ishihara, 1988; Uchida *et al.*, 1988; Groupe Français de Cytogénétique Hématologique, 1990; Hurwitz *et al.*, 1992; Sundareshan *et al.*, 1992; Downing *et al.*, 1993; Maseki *et al.*, 1993; Gallego *et al.*, 1994; Starza *et al.*, 1997; Wong *et al.*, 1998; Harrison *et al.*, 1999; Shinagawa *et al.*, 1999; Xue *et al.*, 2001; Ishida *et al.*, 2002; Miyagi *et al.*, 2002; Gamerdinger *et al.*, 2003; Mathew *et al.*, 2003; Farra *et al.*, 2004; Ahmad *et al.*, 2008; Kawakami *et al.*, 2008; Udayakumar *et al.*, 2008; Vundinti *et al.*, 2008; Tirado *et al.*, 2009) or 4-way complex (de Greef *et al.*, 1995; Vieira *et al.*, 2001) rearrangements of t(8;21) have been reported between 1977 and 2009. Complex translocations in these patients have been shown to involve additional breakpoints at all chromosomes except chromosomes 21, 22 and Y (**Table II**). The most frequently involved included chromosomes 1 and 17 (8 breakpoints each), chromosome 15 (5 breakpoints), chromosome 12 (4 breakpoints) and chromosome 11 (3 breakpoints). Among a total of 40 different breakpoint locations, nine were involved at least twice. These included bands 17q23 (4 cases), 1p36 (3 cases) and 1q23, 5q31, 8p23, 11p15, 12q13, 15q21 and 20q13 (2 cases each). Notably, bands 1p36 and 17q23 comprise altogether 18% of all alternative breakpoint locations in our review of AML patients with complex rearrangements of t(8;21).

To our knowledge, 3-way or 4-way complex rearrangements of t(15;17) have been reported in at least 26 AML patients between 1980 and 2000 (Bernstein *et al.*, 1980; Misawa *et al.*, 1986; Berger *et al.*, 1987; Bjerrum *et al.*, 1987; Huret *et al.*, 1987; Osella *et al.*, 1991; Chen *et al.*, 1994; McKinney *et al.*, 1994; Calabrese *et al.*, 1996; Galieni *et al.*, 1996; Grimwade *et al.*, 1996; Saitoh *et al.*, 1998; Yamamoto *et al.*, 1998; Wan *et al.*, 1999; Grimwade *et al.*, 2000). Among 14 different extra chromosomes involved in complex translocations, eight were implicated at least twice including chromosome 2 (4 cases), chromosomes 1, 3 and 5 (3 cases each), and chromosomes 4, 11 and 19 (2 cases each). Among a total of 23 different breakpoint locations, bands 3p21, 4q21, 11q13 and 19p13 were reported in 2 cases each.

Between 1983 and 2008 3-way complex rearrangements of inv(16)/t(16;16) have been reported in 12 AML patients at least (de la Chapelle & Lahtinen, 1983; Bhambhani *et al.*, 1986; Bernard *et al.*, 1989; Thompson *et al.*, 1991; Yip *et al.*, 1991; Berger *et al.*, 1993; Dierlamm *et al.*, 1998; Martinez-Climent *et al.*, 1999; Li *et al.*, 2001; Ohsaka *et al.*, 2008), comprising a total of 11 different additional breakpoint locations. Interestingly, involvement of chromosomes 1

or 3 was found in 3 patients each, embracing half of all reported cases. Only one chromosomal band, 1p32, was a target of rearrangement in 2 patients.

In contrast to the examples described above, and as previously mentioned, hundreds of complex rearrangements of t(9;22) have been reported in the literature (De Braekeleer, 1987; Mitelman, 1993; Fisher *et al.*, 2005). In a review of complex translocations in CML patients, De Braekeleer (1987) initially showed that a total of 28 chromosome bands were statistically over-represented ($P < 0.001$) among 117 different breakpoint locations reported in the literature. The top 9 breakpoint hotspots included bands 2q11, 3p21, 6p21, 11q13, 12p13, 14q32, 17p13, 17q12 and 17q25 (De Braekeleer, 1987). A non-random occurrence of breaks at these and other regions was also observed at the chromosome abnormality database (CAD) of the United Kingdom (Fisher *et al.*, 2005), indicating that the classification of breakpoint hotspots was not influenced by literature bias. The number of observed breaks for bands 11q13, 14q32 and 17q1, for example, was calculated as 4-5 times higher than expected if breakpoints occurred randomly in the genome (Fisher *et al.*, 2005). Moreover, the location of breakpoint hotspots determined at the CAD was also found to coincide largely with the genome distribution of cytosine-guanine (CG)-rich regions (Fisher *et al.*, 2005). These CG-rich regions of genomic DNA are particularly found at CpG islands located within promoter regions of genes, within genes themselves as well as at repetitive sequences such as the Alu (see section 1.4.6.).

Taken together, available cytogenetic data in CML and AML patients with complex translocations suggests that additional breakpoints are not randomly distributed in the genome. This evidence highlights the possibility that alterations at other genomic regions in addition to the recurrent breakpoint locations could also be of importance in tumour development.

Table II. Summary of chromosome bands involved in 3- or 4-way complex rearrangements of t(8;21), t(15;17) and inv(16) reported in the literature.

Chromosome arm	t(8;21)	t(15;17)	inv(16)
1p	1p36 (3); 1p13; 1p35	1p32; 1p36	1p32 (2)
1q	1q23 (2); 1q32	1q23	1q32
2p	2p25	2p24; 2p21	-
2q	2q*	2q21; 2q2?1	-
3p	-	3p21 (2); 3p12	-
3q	3q27	-	3q21; 3q22;3q26
4q	4q35	4q21 (2)	-
5q	5q31 (2)	5q13; 5q14; 5q35	5q33
6p	6p21	6p21	-
6q	6q21	-	-
7p	-	7p22	-
7q	7q32	7q22	-
8p	8p23 (2)	-	-
8q	-	8q22	8q24
9p	-	-	9p23
9q	9q34	-	-
10p	10p15	-	-
11p	11p15 (2); 11p13	-	-
11q	-	11q13 (2)	11q14
12p	12p12-13; 12p13	-	-
12q	12q13 (2)	-	12q24
13p	-	13p13	-
13q	13q12; 13q14	-	-
14q	14q11; 14q24	-	-
15q	15q21 (2); 15q15; 15q?21q?26; 15q26	-	-
16q	16q*	-	-
17p	17p23; 17p13; 17p11	-	-
17q	17q23 (4); 17q21	-	-
18q	18q23	-	18q12
19p	19p13	19p13 (2)	-
19q	19q13	-	-
20p	-	20p13	-
20q	20q13 (2)	-	-
21q	-	21q22	-
Xp	Xp22	-	-
Xq	-	Xq13	-

This review excludes cases with more complex chromosome rearrangements involving translocations in association with deletions or insertions. The total number of breakpoints does not tally with the number of patients with complex rearrangements of t(8;21) and t(15;17) because some of these rearrangements involve more than one additional breakpoint location. Breakpoints are grouped according to chromosome arm. Numbers in parenthesis indicate number of cases with involvement of a particular chromosome band; *, unspecified breakpoint location.

1.4.4. STEPWISE FORMATION OF TRANSLOCATIONS

The simultaneous identification of at least 2 abnormal cellular clones in the same CML patient, one presenting with a t(9;22) and the other(s) showing a complex rearrangement of the standard translocation, was initially considered as clear-cut evidence that complex translocations arised through sequential events (Lessard & Le Pris , 1982; Hogge *et al.*, 1984;

Pederson, 1984). However, in the vast majority of cases with a complex rearrangement only a single abnormal clone is detected by cytogenetic analysis. In these cases, it is not certain that a complex translocation may have resulted from a secondary rearrangement which followed the formation of the t(9;22). The easiest technical way to demonstrate that a stepwise rearrangement had occurred is by means of the identification of reminiscent material from chromosome 22 on the der(9) chromosome, thus reflecting the occurrence of a secondary 9q breakpoint telomeric to the one involved in t(9;22) (**Fig. 3**). In this situation, the integrity of the reciprocal *ABL1-BCR* fusion gene is not likely to be affected by the secondary translocation.

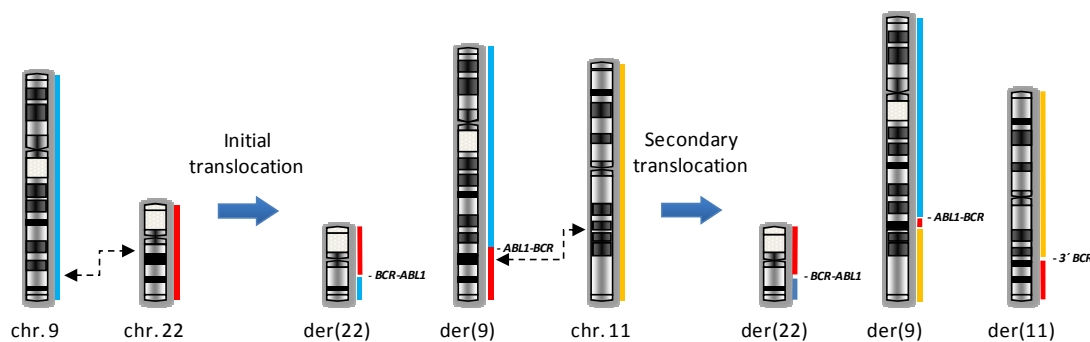


Figure 3. Formation of a complex translocation by stepwise rearrangements involving chromosomes 9, 22 and 11. In this hypothetical example a complex translocation is generated following the formation of a secondary translocation between the der(9) chromosome which resulted from a t(9;22) and an additional chromosome (e.g., chromosome 11). Because the 9q breakpoint occurs at a position telomeric to the original breakpoint in the *ABL1* gene, material derived from chromosome 22 is detectable on the der(9) chromosome in addition to chromosome 11. In contrast to the single-step rearrangement which lacks an *ABL1-BCR* hybrid gene, the integrity of the fusion gene during a stepwise rearrangement is likely to be maintained. Dashed lines with arrows indicate the exchange of material between chromosomes at each of the corresponding breakpoints. The blue, red and orange vertical lines represent chromosome 9, 22 and 11 sequences, respectively.

The introduction of isotopic ISH and, later, of FISH as technical adjuncts to conventional cytogenetics, has tremendously improved the analysis and interpretation of the mechanisms of translocation at a single cell level. Initial studies used radioactive-labeled probes for *BCR* and the platelet-derived growth factor beta polypeptide (*PDGFB*) gene, which lies distally to *BCR* at chromosome band 22q13.1, to identify the presence of chromosome 22 sequences on the der(9) chromosome (Ohyashiki *et al.*, 1987; Abe *et al.*, 1989; Zaccaria *et al.*, 1989; Calabrese *et al.*, 1992). Using whole chromosome painting (WCP) fluorescent probes for chromosomes 9 and 22 as an alternative approach, Calabrese *et al.* (1994) later demonstrated that complex translocations in 9 out of 10 CML patients investigated resulted from a secondary translocation which occurred after the appearance of the t(9;22). Moreover, using *BCR*- and *ABL1*-gene

specific fluorescent probes (Arnoldus *et al.*, 1990; Tkachuk *et al.*, 1990; Dewald *et al.*, 1993), it was shown that stepwise rearrangements were also potentially involved in the generation of *BCR-ABL1*-positive CML cases with an apparently normal karyotype (Morris *et al.*, 1990; Morris *et al.*, 1991). However, is the observation of chromosome 22 material on the der(9) chromosome sufficient evidence to prove the existence of sequential translocations?

Fitzgerald & Morris (1991) proposed that a single breakage and reunion event could explain that in some complex translocations material from chromosome 22 is observed on both the der(9) chromosome and the additional chromosome involved in the translocation. This “concerted genomic rearrangement” illustrates how 4 or more breakpoints occurring simultaneously, including 2 breakpoints at the 22q11 region, may generate a 3-way complex translocation by incorrect rejoining of the broken ends (Fitzgerald & Morris, 1991). The same model can explain the occurrence of submicroscopic insertions of 3′ *ABL1* sequences into chromosome 22 in CML patients with a normal karyotype as an alternative to 2 consecutive translocations (Morris *et al.*, 1990; Fitzgerald & Morris, 1991). A significant advantage of the “concerted genomic rearrangement” model is that it avoids the need for a chromosomal damaging agent to target the same chromosome 22 region twice on different occasions, as required by the alternative stepwise model of formation of complex translocations.

1.4.5. BREAKPOINT-ADJACENT DELETIONS

The consequences of a standard reciprocal translocation in a leukemic cell may extend far more than the formation of fusion genes. In CML for instance, approximately 10-15% of patients with a standard t(9;22) display large genomic deletions on the der(9) chromosome which encompass the *ABL1/BCR* junction and that may extend centromeric or telomeric to the *ABL1* breakpoint (Sinclair *et al.*, 2000; Lee *et al.*, 2006; Kreil *et al.*, 2007). In these patients, deletions are present in all metaphase cells with a t(9;22) and are equally frequent at diagnosis and following disease progression (Huntly *et al.*, 2001). These observations strongly suggest that deletions occur at the time of generation of the t(9;22) (Huntly *et al.*, 2001) and are, therefore, a relevant feature of the CML clone during the chronic phase of the disease.

An immediate consequence of deletions at the der(9) chromosome is the loss of *ABL1-BCR* fusion gene expression (Huntly *et al.*, 2002). However, lack of *ABL1-BCR* expression was also demonstrated in CML patients without genomic deletions, indicating that transcription of the fusion gene may be regulated by other mechanisms (Huntly *et al.*, 2002). Consistent with these observations, the loss of *ABL1-BCR* expression was not found to be associated with a

poorer patient prognosis (Huntly *et al.*, 2002). In contrast, the presence of the deletion itself severely affected the survival of patients comparatively to those without deletions (Sinclair *et al.*, 2000; Huntly *et al.*, 2001; Huntly *et al.*, 2002; Lee *et al.*, 2003; Lee *et al.*, 2006). Furthermore, the prognostic significance of the deletion was also shown to be independent of the age, sex, percentage of peripheral blood blasts and platelet count (Sinclair *et al.*, 2000), indicating that it constitutes a strong prognostic factor in t(9;22)-positive CML. Taken together, these data is consistent with a model of disease in which rapid progression may be due to loss of one or more critical genes mapping along the deleted regions at the der(9) chromosome. Ultimately, this model may be adapted to every malignancy associated with a recurrent reciprocal chromosomal rearrangement and/or fusion gene formation, thus providing a biological basis for disease heterogeneity (Huntly *et al.*, 2003).

Deletions at the der(9) chromosome have been found to occur more frequently in CML patients with complex rearrangements than in those with a classic translocation (Sinclair *et al.*, 2000). In a study of 253 CML patients, deletions were present in 39% of cases with complex translocations as compared to only 12% of those with the standard t(9;22) (Huntly *et al.*, 2001). Moreover, genomic deletions have also been observed at the extra breakpoint locations involved in complex rearrangements (Albano *et al.*, 2003), therefore increasing the complexity of molecular defects associated with complex translocations. FISH mapping has been used as an attempt to identify potential disease-related genes lying within the deleted regions (Albano *et al.*, 2003; Anelli *et al.*, 2004). As an example, the tumour necrosis factor receptor superfamily member 21 (*TNFRSF21*) gene was included in the deleted region at 6p12 in one CML patient presenting with a complex t(6;9;22)(p12;q34;q11) (Albano *et al.*, 2003). *TNFRSF21* is a member of a subgroup of the tumor necrosis factor receptor superfamily known as the death receptors. These receptors are characterized by the presence of a cytoplasmic domain (death domain) which triggers apoptosis when stimulated by a cognate ligand. In mammalian cells ectopic expression of *TNFRSF21* stimulates apoptosis (Pan *et al.*, 1998). In this context, it is possible that haplo-insufficiency of *TNFRSF21* may reduce its apoptotic effect, thus contributing to increased survival of *BCR-ABL1*-positive cells.

The breakpoint positions of the interstitial deletions detected at the der(9) breakpoint in t(9;22)-positive cells are highly heterogeneous in different patients (Sinclair *et al.*, 2000). The consequence of this phenomenon is that deletions may vary extensively in length and eliminate different sets of genes located at the long arm of chromosome 9. Whether a single gene or 2 or more genes contribute to the overall worse prognosis conferred by deletions in CML patients remains to be solved. A similar scenario may also apply to the Philadelphia-negative chronic myeloproliferative neoplasms (MPN) characterized cytogenetically by the

presence of interstitial deletions of the long arm of chromosome 20 [del(20q)]. Among MPN patients a del(20q) has been found to occur in 8.4% of polycythemia vera (PV), 7.1% of primary myelofibrosis (PMF) and 0.2% of essential thrombocythemia (ET) patients at diagnosis or during the course of the disease (Bench *et al.*, 1998a). Deletions typically extend from band 20q11.2 to band 20q13.1 (small deletions) or from band 20q11.2 to band 20q13.3 (large deletions), respectively (Nacheva *et al.*, 1995). As in the case of CML patients with der(9) deletions, the locations of the centromeric and telomeric breakpoints of the del(20q) are highly heterogeneous in different MPN patients (reviewed in Bench *et al.*, 2001).

Several studies attempted to define the smallest common deleted segment (CDS) in different patients with myeloid disorders and del(20q), using southern blot complemented with restriction fragment length polymorphism analysis (Hollings, 1994), FISH and/or polymerase chain reaction (PCR) analysis of microsatellite markers (Roulston *et al.*, 1993; Asimakopoulos *et al.*, 1994; Bench *et al.*, 1998b; Wang *et al.*, 1998a; Bench *et al.*, 2000; Wang *et al.*, 2000; MacGrogan *et al.*, 2001; Douet-Gilbert *et al.*, 2008), real-time quantitative PCR (Q-PCR) (Schaub *et al.*, 2009) and genome-wide high-resolution single nucleotide polymorphism (SNP) array analysis (Huh *et al.*, 2010). Until recently a 2.7 megabase (Mb) CDS at 20q11.2-q13 prevailed as the smallest single common region of deletion in MPN patients with del(20q) (Bench *et al.*, 2000). A candidate imprinted gene located within the CDS and expressed in CD34+ cells, *L3MBTL*, was identified and found not to be mutated in MPN patients with or without a del(20q) (Li *et al.*, 2004). A more recent study has shown that a second CDS spanning 1.8 Mb at 20q13.12 can also be defined in patients with different myeloid disorders and a del(20q) (Huh *et al.*, 2010). However, no candidate gene in this region has yet been identified. Altogether, available data suggest that the notion of a common deleted region as a site which contains a putative tumour suppressor gene may not apply to the recurrent del(20q) in MPN patients.

In MPN patients the occurrence of a del(20q) was found to be significantly associated with the presence of a somatic activating mutation in the Janus kinase 2 (*JAK2*) gene located at chromosome 9p24, *JAK2V617F* (Baxter *et al.*, 2005; James *et al.*, 2005; Jones *et al.*, 2005; Kralovics *et al.*, 2005), indicating that these genetic alterations are likely to cooperate in MPN pathogenesis (Campbell *et al.*, 2006). *JAK2* is a cytoplasmic tyrosine kinase protein which associates with the intracytoplasmic portion of several membrane cytokine receptors including those for erythropoietin, thrombopoietin, interleukin-3 or granulocyte macrophage-colony stimulating factor (GM-CSF) (Parganas *et al.*, 1998). These receptors as well as those for interleukin-5, prolactin, leptin and growth hormone signal exclusively through *JAK2* to promote hematopoietic cell development and proliferation (reviewed in Murray, 2007). Ligand-receptor

coupling leads to JAK2 phosphorylation, which in turn phosphorylates back the receptor and activates various downstream signaling pathways involved in cell proliferation and survival (reviewed in Delhommeau *et al.*, 2006).

The *JAK2V617F* mutation confers constitutive activity of the tyrosine kinase domain of JAK2 in a cytokine-independent or hypersensitive way (James *et al.*, 2005). Hypersensitivity to cytokines suggests that physiological mechanisms of cytokine production and regulation in clonal MPN cells may also be affected. For instance, up-regulation of serum levels of colony stimulating factor-1 has been found in patients with classic MPN (Gilbert *et al.*, 1989) whereas overproduction of interleukin-8 and interleukin-11 was found in PV patients (Hermouet *et al.*, 2002). Moreover, plasma levels of tissue inhibitor of metalloproteinase, macrophage inflammatory protein-1 β and insulin-like growth factor binding factor-2 are elevated in PMF patients (Ho *et al.*, 2007). However, the mechanisms involved and the protein factors responsible for their up-regulation remain to be determined.

1.4.6. MOLECULAR MECHANISMS OF CHROMOSOMAL REARRANGEMENT

The breakage and reunion of chromosome segments through translocation or other mechanisms have had a major role in the shaping of the eukaryote genome during evolution (Kazazian, 2004). In humans such processes have been largely mediated by a class of mobile DNA sequences called non-long terminal repeat (LTR) retrotransposons. These DNA sequences have the capability to integrate into new locations within the genome following transcription to RNA and subsequent reverse transcription to DNA (Kazazian, 2004). One common type of non-LTR retrotransposon is the Alu element which constitutes roughly 11% of the human genome sequence (Kazazian, 2004). Interestingly, it was earlier determined that either the *BCR* or the *ABL1* gene have an approximately 39% homology to Alu sequences (Chisoe *et al.*, 1995), suggesting that these DNA elements might be implicated in the recombination mechanism between chromosomes 9 and 22. This hypothesis had obtained previous support from a study of a CML patient in which Alu sequences were found to overlap the breakpoints at both genes (de Klein *et al.*, 1986). However, in later studies comprising a total of 23 patients, no significant clustering of breakpoints at Alu sequences was observed in *ABL1* and/or in *BCR* (Sowerby *et al.*, 1993; Chisoe *et al.*, 1995; Zhang *et al.*, 1995). In acute leukemias Alu sequences were found to be present at the breakpoints of chromosomal rearrangements involving the myeloid/lymphoid or mixed-lineage leukemia (*MLL*) gene at chromosome band 11q23 (Megonigal *et al.*, 1997).

If complex translocations arise preferentially through a single concerted breakage and reunion mechanism as proposed by Fitzgerald & Morris (1991), and if Alu sequences may be found at the breakpoints of the *ABL1* and *BCR* genes, then these specific DNA sequences are also likely to be present at the breakpoint location on the additional chromosome(s) involved in the translocation. In this context, a chromosome 11 breakpoint was analyzed in 2 different CML patients presenting with a complex $t(9;22;11)(q34;q11;q13)$. Although breakpoints in both patients were located 100-250 kilobases (kb) apart within band 11q13, Alu sequences were found in very close proximity to the breakpoints in each case (Koduru *et al.*, 1993; Morris *et al.*, 1996). Involvement of Alu sequences in complex rearrangements was further stressed in 2 other CML patients in whom an Alu element mapped near or at the breakpoint site directly in the partner chromosome sequence fused to 3' *BCR* (Jefferis *et al.*, 1998). In an additional patient with an extra rearrangement of band 22q11.2, the breakpoint was found to occur at the immunoglobulin lambda locus (*IGL@*) gene (Benjes *et al.*, 1999). However, it was not possible to identify potential recombination sequences recurrently involved in the somatic rearrangement of immunoglobulin genes in lymphoid cells, at the breakpoint regions of *IGL@* or of 3' *BCR* (Benjes *et al.*, 1999).

More recent bioinformatics data showed that Alu sequences are significantly under-represented within the 5 kb major breakpoint region of *BCR* and within a common 25 kb breakpoint region of *ABL1* (Jefferis *et al.*, 2001). In turn, several different types of interspersed repeat elements are present at a higher frequency than expected at the junction sequences of both genes (Matarucchi *et al.*, 2008). However, no specific type of DNA repeat sequence was yet found to be recurrently present at breakpoint positions within *BCR* or *ABL1*. Taken together, the presence of similar sequence features such as Alu(s) at the 9q34 and 22q11 breakpoints, as well as at the extra breakpoints implicated in complex translocations, raises the possibility that a common pathogenetic mechanism underlies the formation of both standard and complex rearrangements. In this setting it can be anticipated that additional breakpoints may also target genes whose disruption contributes to transformation of hematopoietic cells.

1.5. THE NEUTRAL VERSUS THE ALTERNATIVE HYPOTHESIS

A putative pathogenetic role of the additional breakpoints involved in complex translocations can be addressed at least by 2 opposing views, herein tentatively classified as

the “neutral hypothesis” and the “alternative hypothesis”. The neutral hypothesis supports the notion that extra breakpoints play no part in disease development, in addition to the role provided by the recurrent breakpoints of the standard translocation. This hypothesis stems from the observation that the nature of the extra chromosomes involved in complex rearrangements, as well as the localization of their respective breakpoints, is highly heterogeneous (Mitelman, 1993). In other words, no recognizable pattern of complex chromosome rearrangement exists that can be considered pathognomonic. Consequently, it is unlikely that physical disruption of genes located at such a variety of chromosome locations, or changes in their expression levels, may be equally relevant in the natural history of disease.

In contrast, the alternative hypothesis proposes that extra breakpoints may provide a further biological advantage to leukemic cells by affecting genes important for normal cell growth and differentiation. This hypothesis is supported by 2 lines of evidence obtained from the analysis of complex chromosome translocations in CML. First, the location of extra breakpoints is not randomly distributed throughout the genome (De Braekeleer, 1987). Secondly, as previously mentioned, the location of extra breakpoints largely coincides with the genome distribution of CG-rich regions (Fisher *et al.*, 2005), suggesting that additional breakpoints may target specific genes. Data supporting the alternative hypothesis was provided by the recent molecular characterization of breakpoints of a 4-way translocation involving extra breaks at chromosomes 3 and 17 in a CML patient at blast crisis. In this case, sequences from chromosome 17 juxtaposed to the 5' side of the *EVI1* oncogene at chromosome band 3q26 resulting in an increase in the expression levels of this gene (De Weer *et al.*, 2008). This case shows compelling evidence that complex translocations in CML may simultaneously target tumour-related genes in addition to the *BCR* and *ABL1* genes.

The alternative hypothesis constituted the basis for the present dissertation. Although abundant studies have been made available in the literature which describes the presence of complex chromosomal translocations in leukemia, only a few cases have been studied in the light of the involvement of the extra chromosomal regions (Koduru *et al.*, 1993; Morris *et al.*, 1996; Jeffs *et al.*, 1998; De Weer *et al.*, 2008). This is mostly due to the fact that the mapping and cloning of additional breakpoint locations is time-consuming and requires the use of several different techniques. As a consequence, a significant lack of experimental data exists to support the notion that additional breakpoints in complex translocations target important genes for maintenance of normal cell homeostasis. In summary, evidence obtained from detailed molecular analysis of breakpoints in complex translocations may aid in the identification of potential novel tumour-associated genes.

2. AIMS

The primary aim of this work was to address the contributing role of genes located at extra breakpoints of complex chromosome translocations for the pathogenesis of hematopoietic neoplasms. According to this main goal, five secondary objectives were proposed:

- (i) To localize and describe the genes located at the breakpoint regions involved in the chromosomal rearrangements of 5 patients with hematopoietic neoplasms, including:
 - A t(5;12)(q13;p13) in B-cell acute lymphoblastic leukemia (ALL);
 - A t(12;15)(p13;q22) in myelodysplastic syndrome/myeloproliferative neoplasm, unclassifiable (MDS/MPN, U);
 - A dic(9;12)(p11;p11) in B-cell ALL;
 - A t(9;11;19)(p22;q23;p13) in AML;
 - A t(X;20)(p11;q13) in ET;
- (ii) To detect putative fusion genes and characterize hybrid transcripts involved in complex translocations;
- (iii) To perform mutational analysis of candidate genes located at the breakpoint regions;
- (iv) To determine the expression profile of novel potentially pathogenic genes in normal and leukemic cells;
- (v) To assess a role of the protein product of these genes in *in vitro* cell proliferation and/or survival assays.

A similar methodological approach was conducted in the 5 cases. Initially, adequate DNA probes for mapping of chromosome breakpoints were selected from available databases and labeled with fluorophores for FISH analysis. The localization of novel breakpoint regions was performed by “chromosome-walking”. In 2 cases, detailed localization of breakpoint regions was performed by long distance inverse-polymerase chain reaction (LDI-PCR) or by PCR analysis of polymorphic markers complemented with a whole-genome array study, respectively.

Putative fusion transcripts generated by chromosomal translocations were identified using different technical approaches based on reverse transcription-polymerase chain reaction (RT-PCR) and characterized by sequencing analysis. In addition, candidate genes at breakpoint regions were analyzed using PCR and direct sequencing for the presence of nucleotide mutations.

The expression profile of 2 genes located at newly-identified breakpoint positions was studied by RT-PCR in normal cells and/or in leukemic cell lines originating from different hematopoietic lineages. Finally, the role of these disease-candidate genes in proliferation, apoptosis or transcription regulation was evaluated using cell line models *in vitro*. To these purposes, we suppressed the transcripts of interest using RNA interference and/or inactivated the protein function with a specific inhibitory drug. In one case we also ectopically expressed the protein of interest in cell line cultures. At the end, a comprehensive approach was utilized to relate molecular changes at each of the breakpoint locations with a differential role of complex translocations in leukemogenesis.

3. RESULTS

3.1. MOLECULAR CYTOGENETIC CHARACTERIZATION OF REARRANGEMENTS INVOLVING 12p IN LEUKEMIA

Published in: Vieira L, Marques B, Cavaleiro C, Ambrósio AP, Jorge M, Neto A, Costa JM, Júnior EC, Boavida MG (2005) Molecular cytogenetic characterization of rearrangements involving 12p in leukemia. *Cancer Genet Cytogenet* **157**: 134-139.

We wish to acknowledge Dr. Peter Marynen (University of Leuven & Flanders Interuniversity Institute for Biotechnology, Belgium) for providing *ETV6* cosmid clones, Dr. Mariano Rocchi (University of Bari, Italy) for providing BAC clones 467M14 and 328C17, Dr. Joana Diamond (Centro de Investigação em Patobiologia Molecular, Instituto Português de Oncologia de Francisco Gentil) for providing a sample from patient 1, and Dr. Dezsö David (Departamento de Genética, Instituto Nacional de Saúde Dr. Ricardo Jorge) for helpful comments on the manuscript.

This work was supported by a grant from Núcleo Regional do Sul – Liga Portuguesa Contra o Cancro.

3.1.1. ABSTRACT

Translocations involving the short arm of chromosome 12 are frequent events among patients with various hematological malignancies. In approximately half of the patients, FISH analysis has shown that the breakpoints are clustered within the Ets variant 6 (*ETV6*, also known as *TEL*) gene at 12p13, leading to its fusion with a variety of partner genes on different chromosomes. The remaining patients have breakpoints centromeric or telomeric to *ETV6* or, less frequently, interstitial 12p13 deletions, which invariably involve this gene. In most cases reported, 12p translocations were found associated with other structural and/or numerical abnormalities as part of a complex karyotype. Initially, using conventional cytogenetic analysis we characterized the chromosomal breakpoints of 3 leukemia patients presenting with a t(5;12)(q13;p13), dic(9;12)(p11;p11) and a t(12;15)(p13;q22), respectively, as the sole structural abnormalities in the karyotype. These rearrangements were further investigated using FISH and molecular studies. The cases with t(5;12) and t(12;15) revealed cryptic 3-way translocations, undetected on conventional cytogenetic analysis. One of the cases presented an *ETV6* rearrangement with an unsuspected fusion with the *RUNX1* gene at 21q22. In the other patient, an interstitial 12p deletion was found which included *ETV6* and 8 other genes. In the patient with dic(9;12) both the *ETV6* and the paired box 5 (*PAX5*) gene at 9p13 were deleted, indicating that dic(9;12) in B-cell ALL does not always conduct to a *PAX5-ETV6* fusion gene. This study illustrates the chromosomal and molecular heterogeneity of rearrangements underlying 12p chromosome translocations in leukemia.

3.1.2. INTRODUCTION

Aberrations of the short arm of chromosome 12 consisting mainly of balanced or unbalanced translocations, insertions and deletions are frequently implicated in both lymphoid and myeloid hematological malignancies (Mitelman, 2004). The *ETV6* gene, a member of the *Ets* family of transcriptional regulators, was initially found as a target gene at the 12p13 region by way of its fusion to the platelet-derived growth factor receptor, beta polypeptide (*PDGFRB*) gene in 3 patients with chronic myelomonocytic leukemia and t(5;12)(q33;p13) (Golub *et al.*, 1994). Since this first report, several different chromosomal rearrangements involving *ETV6* in a wide spectrum of hematological malignancies have been described (Berger *et al.*, 1997; Sato *et al.*, 1997; Tosi *et al.*, 1998; Wlodarska *et al.*, 1998; Otero *et al.*, 2001). To date, at least 20 different partner genes involved in *ETV6* translocations have been identified including *MDS2*

(1p36), *ARNT* (1q21), *ARG* (1q25), *MDS/EVI1* (3q26), *FGFR3* (4p16), *BTL* (4q11-q12), *ACSB2* (5q31), *PDGFRB* (5q33), *STL* (6q23), *MNX1* (7q36), *PAX5* (9p13), *JAK2* (9p24), *SYK* (9q22), *ABL1* (9q34), *CDX2* (13q12), *TTL* (13q14), *TRKC* (15q25), *PER1* (17p12-13), *RUNX1* (21q22) and *MN1* (22q11) (reviewed in Odero *et al.*, 2001; Yagasaki *et al.*, 2001; Odero *et al.*, 2002; Penas *et al.*, 2003; Qiao *et al.*, 2003). In particular, the *ETV6-RUNX1* fusion gene generated by a t(12;21)(p13;q22), was found to be the most common fusion gene in childhood precursor B-cell ALL, accounting for approximately 25% of the cases (Golub *et al.*, 1995; Romana *et al.*, 1995).

FISH analysis has shown that *ETV6* rearrangements occur in approximately half of the patients with 12p13 balanced translocations (Sato *et al.*, 1997; Odero *et al.*, 2001) while, in the remaining cases, breakpoints can be found telomeric or centromeric to *ETV6* (Sato *et al.*, 1997). In a few other cases, apparently balanced 12p translocations were found to harbour interstitial deletions at 12p13, which included *ETV6* and the cyclin-dependent kinase inhibitor 1B (*CDKN1B*) gene (Wlodarska *et al.*, 1996). However, 12p13 rearrangements are frequently found as part of a complex karyotype in which several additional structural and/or numerical abnormalities were present (Wlodarska *et al.*, 1996; Berger *et al.*, 1997; Sato *et al.*, 1997; Tosi *et al.*, 1998; Wlodarska *et al.*, 1998; Odero *et al.*, 2001). In this report, we used FISH to characterize the 12p breakpoints in 3 leukemia patients with cytogenetic evidence of a t(5;12)(q13;p13), t(12;15)(p13;q22) and dic(9;12)(p11;p11), and to assess the involvement of *ETV6* in each rearrangement. We also used molecular approaches in the cases with t(5;12) and t(12;15) to characterize alterations of *ETV6*.

3.1.3. CASES SUMMARY

Two patients with B-cell ALL and one with MDS/MPN, U presenting with 12p structural rearrangements were included in this study (**Table III**).

Table III. Summary of clinical features, G-banded karyotype, FISH analysis and *ETV6* status in the 3 patients.

Patient	Sex/age (years)	Diagnosis	G-banded karyotype/Revised karyotype (FISH)	<i>ETV6</i> status
1	M/6	B-cell ALL	47,XY,+21,t(5;12)(q13;p13)[11]/46,XY[1] 47,XY,+21,t(12;21;5)(p13;q22;q13)[11]/46,XY[1]	rearranged
2	M/82	MDS/MPN, U	47,XY,+8,t(12;15)(p13;q22)[30] 47,XY,+8,t(12;6;15)(p13;p24~25;q22) [30]	deleted
3	M/9	B-cell ALL	45,XY,dic(9;12)(p11;p11)[17]/46,XY[3]	deleted

Abbreviations: B-ALL, B-cell acute lymphoblastic leukemia; M, male; MDS/MPN, U, myelodysplastic syndrome/myeloproliferative neoplasm, unclassifiable.

3.1.4. MATERIALS AND METHODS

3.1.4.1. CYTOGENETIC AND FLUORESCENCE IN SITU HYBRIDIZATION ANALYSES OF CHROMOSOME REARRANGEMENTS

Cytogenetic analysis was performed on bone marrow samples collected at diagnosis and cultured following standard protocols. A G-banded karyotype was produced according to the International System for Human Cytogenetic Nomenclature (ISCN, 1995). Cell suspensions prepared for cytogenetic analysis were used for characterization of translocation breakpoints by FISH. A total of 15 RPC111 library-bacterial artificial chromosome (BAC) probes were chosen to cover an almost contiguous 3 Mb region at 12p13 including *ETV6*. These are ordered as follows (<http://www.ncbi.nlm.nih.gov/mapview/>): centromere – 688K16 – 377D9 – 392P7 – 59H1 – 180M15 – 253I19 – 267J23 – 525I3 – 418C2 – 96B19 – 434C1 – 407P10 – 711K1 – 289M22 – 291B21 - telomere. Additionally, 12p and 6p subtelomeric BAC probes 467M14 and 328C17, respectively, were used (kindly supplied by Dr. Mariano Rocchi, University of Bari, Italy). The *ETV6* gene was analysed using a yeast artificial chromosome (YAC) probe (YAC 964C10) and 6 LL12NCO1-cosmid library clones including 179A6 (exon 1A), 50F4 (exon 2), 175F2 (intron 2), 2G8 (intron 1B-exon 4), 184C4 (introns 3-5) and 148B6 (exon 8 and 3' region), kindly provided by Dr. Peter Marynen (University of Leuven & Flanders, Interuniversity Institute for Biotechnology, Belgium) (Baens *et al.*, 1996). Chromosome 12 was also identified by means of a centromeric probe (pBR12) whereas a heterochromatic region probe (pHUR198) was used for chromosome 9. Additionally, two YAC probes (764A6 and 742H2) were used for the 9p13-p21 region, the latter covering the *PAX5* gene.

DNA was extracted from YAC, BAC and cosmid clones using conventional procedures and labelled by nick-translation with digoxigenin-11-dUTP according to standard protocols or biotin-14-dATP (BioNick Labeling System, Invitrogen). Furthermore, labeled WCP probes for chromosomes 5, 6, 12, 15 and 21 (Cambio), as well as the LSI *TEL/AML1* ES dual color translocation probe (Vysis), were utilized. Hybridization of the probes, post-hybridization washes and detection of signals were performed as described (Matos *et al.*, 2000).

3.1.4.2. MOLECULAR ANALYSIS OF *ETV6-RUNX1* FUSION TRANSCRIPTS

Analysis of *ETV6-RUNX1* fusion transcripts in patient 1 was carried out by RT-PCR as described (van Dongen *et al.*, 1999) using a bone marrow sample obtained at diagnosis. The amplified fragments were purified using the Concert Rapid Gel Extraction System (Genomed) and sequenced using the ABI Prism 3100 Genetic Analyzer (Applied Biosystems). Sequences were compared to *ETV6* and *RUNX1* mRNA sequences (GenBank accession number U11732.1 and D43969.1, respectively).

3.1.4.3. MUTATIONAL ANALYSIS OF *ETV6*

Screening of *ETV6* mutations was carried out in patient 2. Genomic DNA was extracted from a bone marrow sample using a salting-out procedure followed by standard phenol-chloroform purification and ethanol precipitation. Amplification of *ETV6* exons was performed according to Stegmaier *et al.* (1996) with minor adjustments. Products were sequenced as described above.

3.1.5. RESULTS

3.1.5.1. HIDDEN *ETV6-RUNX1* FUSION AS A RESULT OF A COMPLEX t(12;21;5)(p13;q22;q13) IN B-CELL ACUTE LYMPHOBLASTIC LEUKEMIA

Cytogenetic analysis of bone marrow cells from patient 1 revealed an apparently reciprocal translocation t(5;12)(q13;p13) on the majority of metaphases analysed. In order to localize the 12p13 breakpoint, FISH was performed with a BAC clone which covers a region from intron 2 to the 3' end of *ETV6* (RPC11-418C2) and 2 others localized distal (RPC11-434C1 and -96B19) and proximal (RPC11-525I3 and -267J23) to it. Results showed that BAC 418C2 overlapped the 12p13 breakpoint, indicating that the *ETV6* sequence was rearranged (results not shown). It was also noticed that the hybridization signal on the der(12) was weaker than on the partner chromosome, suggesting that the breakpoint occurred closer to the 3' end of the gene. Subsequent analysis with *ETV6* cosmids 148B6 and 184C4 showed that 148B6 hybridized on the der(12) while 184C4 hybridized on the partner chromosome, revealing that the breakpoint was localized between exons 5 and 8 of *ETV6* (results not shown).

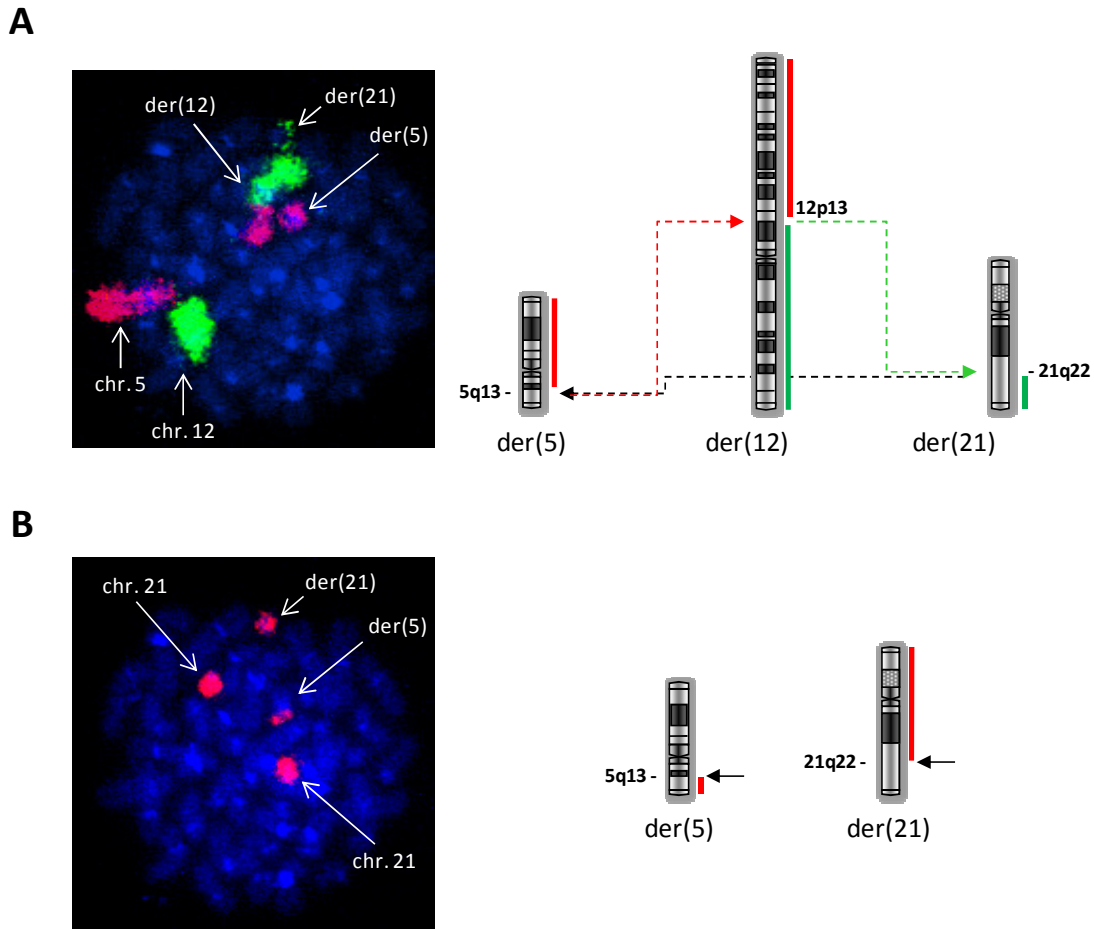


Figure 4. Analysis of chromosome rearrangements by FISH on a bone marrow metaphase cell with $t(12;21;5)$. (A) Left: Hybridization of a metaphase cell with WCP probe for chromosome 5 (red signal) and WCP probe for chromosome 12 (green signal). Right: Corresponding diagrammatic representation of derivative chromosomes showing a 3-way $t(12;21;5)$. Dashed lines are used to indicate the movement of material between each of the chromosomes involved in the rearrangement. Vertical red and green lines on the right side of chromosomes show the location of chromosome 5 and chromosome 12 materials respectively, after formation of the translocation. (B) Left: Hybridization of the same metaphase cell shown in (A) with WCP probe for chromosome 21 (red signal). Right: Corresponding diagrammatic representation of der(5) and der(21) chromosomes showing the location of FISH signals.

Unexpectedly, all probes used that mapped distally to the breakpoint on der(12) were localized on a small G-group chromosome instead of on chromosome 5. Using WCP probes, a 3-way rearrangement was observed, with chromosome 5q material on the short arm of chromosome 12, the terminal part of chromosome 12p on the long arm of chromosome 21, and the remaining part of chromosome 21q on chromosome 5q (Fig. 4). The involvement of chromosomes 12 and 21 in the translocation was highly suggestive that an *ETV6-RUNX1* fusion gene was present. To confirm this hypothesis, FISH and RT-PCR studies were conducted to detect gene fusion in the patient's cells. Hybridization with the *TEL/AML1* translocation probe in metaphase cells showed a co-localization of *ETV6* and *RUNX1* signals on chromosome band

21q22 (**Fig. 5A**). Accordingly, RT-PCR followed by sequencing analysis showed 2 types of fusion transcripts consisting of an in-frame joining between exon 5 of *ETV6* and exon 2 (or exon 3) of *RUNX1* (**Fig. 5B and C**).

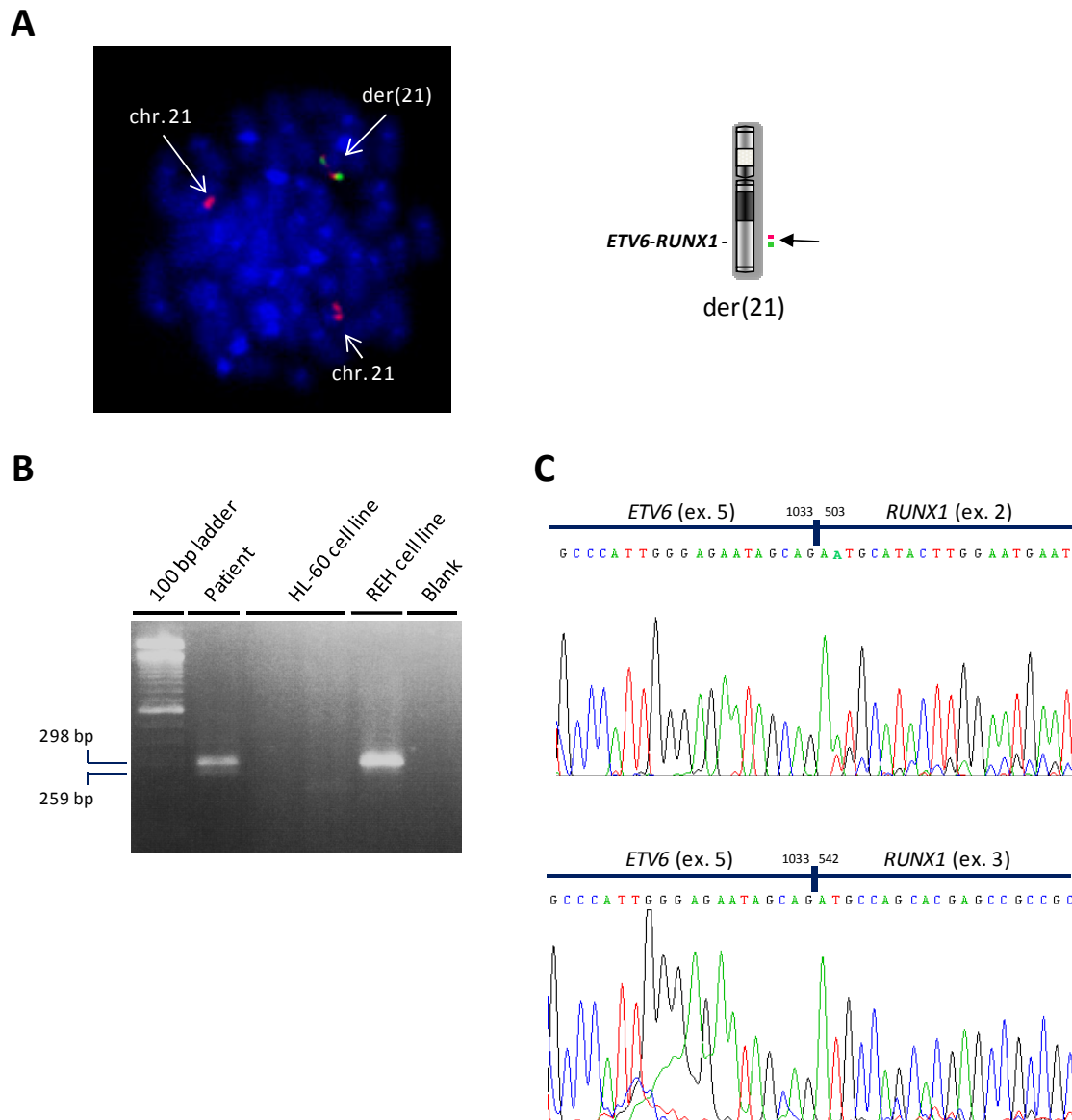


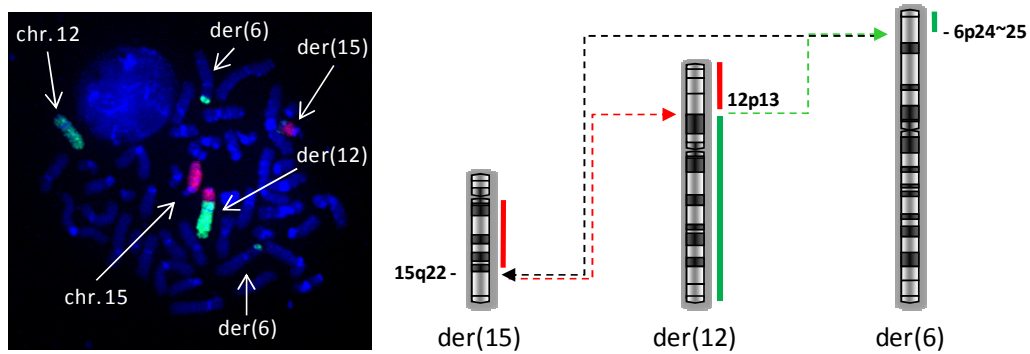
Figure 5. Detection of *ETV6-RUNX1* fusion by FISH, RT-PCR and direct sequencing analyses.

(A) Left: Hybridization of a metaphase cell with the *TEL/AML1* probes. An *ETV6* signal (green) co-localizes with a *RUNX1* signal (red) on the der(21) chromosome. The native *ETV6* signal on normal chromosome 12p13 is not visible on this metaphase. Right: Schematic representation of FISH results on the der(21) chromosome. Horizontal arrow indicates the approximate location of translocation breakpoint. **(B)** Ethidium bromide-stained agarose gel (2%) electrophoresis of RT-PCR products. Two different *ETV6-RUNX1* fusion products of 298 basepairs (bp) and 259 bp (less intense) were detected in the patient cDNA sample. HL-60 is an *ETV6-RUNX1*-negative cell line whereas REH is an *ETV6-RUNX1*-positive cell line (van Dongen *et al.*, 1999). The blank control contains water instead of template cDNA. **(C)** Partial electropherograms obtained by direct sequencing of amplification products detected in the patient sample. The upper sequence corresponds to the 298 bp band and shows a fusion of *ETV6* exon 5 to *RUNX1* exon 2. The lower sequence corresponds to the 259 bp band and shows an alternatively-spliced variant *ETV6-RUNX1* fusion transcript which lacks *RUNX1* exon 2. The numbers above the nucleotide sequences indicate the most 3' nucleotide of *ETV6* and the most 5' nucleotide of *RUNX1* according to the corresponding mRNA sequences (GenBank accession number U11732.1 and D43969.1, respectively).

3.1.5.2. INTERSTITIAL DELETION AT 12p13 AS A CONSEQUENCE OF A 3-WAY $t(12;6;15)(p13;p24\sim25;q22)$ IN A PATIENT WITH MYELOYDYSPLASTIC SYNDROME/MYELOPROLIFERATIVE NEOPLASM, UNCLASSIFIABLE

A seemingly balanced translocation $t(12;15)(p13;q22)$ was found in all metaphases analysed in patient 2. However, FISH with WCP and subtelomeric probes disclosed that the terminal region of the short arm of chromosome 12 was present on the short arm of chromosome 6, band 6p24~25, instead of on chromosome 15. In turn, the 6p terminal region was joined to the long arm of chromosome 15 while the 15q22-qter region moved to chromosome 12 (**Fig. 6A and B**). These results revealed that the translocation was definitely a 3-way rearrangement involving chromosomes 6, 12 and 15.

A



B

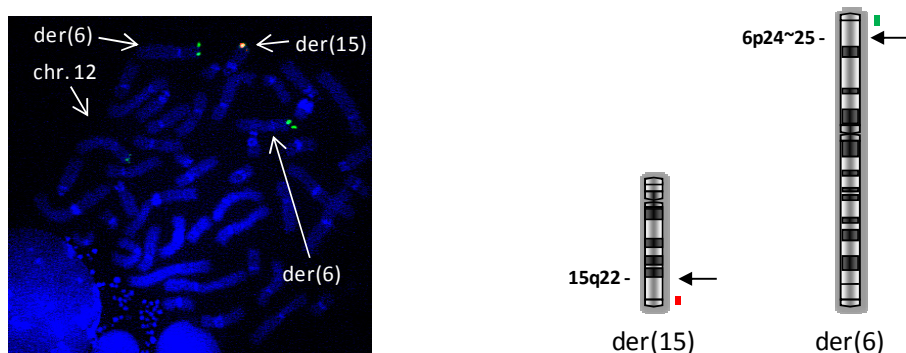


Figure 6. Analysis of chromosome rearrangements by FISH on bone marrow cells with $t(12;6;15)$.

(A) Left: Hybridization with WCP probe for chromosome 12 (green signal) and WCP probe for chromosome 15 (red signal). Right: Corresponding diagrammatic representation of derivative chromosomes demonstrating the presence of a 3-way translocation involving chromosomes 6, 12 and 15. Dashed lines are used to indicate the movement of material between each of the chromosomes involved in the rearrangement. Vertical red and green lines at the right side of the chromosomes show the location of chromosome 15 and chromosome 12 materials, respectively, after formation of the translocation. **(B)** Left: Hybridization with subtelomeric BAC clones 467M14 (green signal) and 328C17 (red signal) for 12p and 6p, respectively, confirming a $t(12;6;15)$. Right: Corresponding diagrammatic representation of derivative chromosomes showing the location of FISH signals.

Additionally, FISH studies showed that the translocated 12p13-12pter chromosomal region was present at both chromosomes 6. This finding indicated that mitotic recombination had occurred between the normal and rearranged chromosomes 6 or, alternatively, that the rearranged chromosome 6 was duplicated whereas the normal homologue was lost. Subsequent FISH studies were meant to verify if *ETV6* had been disrupted by the translocation breakpoints as in the case of patient 1. Hybridization with YAC 964C10, which covers a large genomic region (~1.5 Mb) at band 12p13, including the *ETV6* gene, revealed a strong signal on normal chromosome 12 but no signal on the der(12) (results not shown). However, a weak signal was observed on both der(6), suggesting that a breakpoint had occurred telomeric to *ETV6* at band 12p13. To confirm this hypothesis, metaphase cells were subsequently hybridized with each of the 6 *ETV6* cosmids. Results unequivocally showed that signals were only present on the normal chromosome 12 confirming that one copy of *ETV6* was deleted as a result of the translocation. To test if the remaining copy of the *ETV6* gene had been rendered non-functional as a result of nucleotide mutations, the entire *ETV6* coding sequence was screened by PCR and direct sequencing analysis. However, nucleotide alterations were not detected in the non-rearranged *ETV6* allele (data not shown), suggesting that the contribution of *ETV6* to leukemogenesis was accomplished through a haplo-insufficiency mechanism.

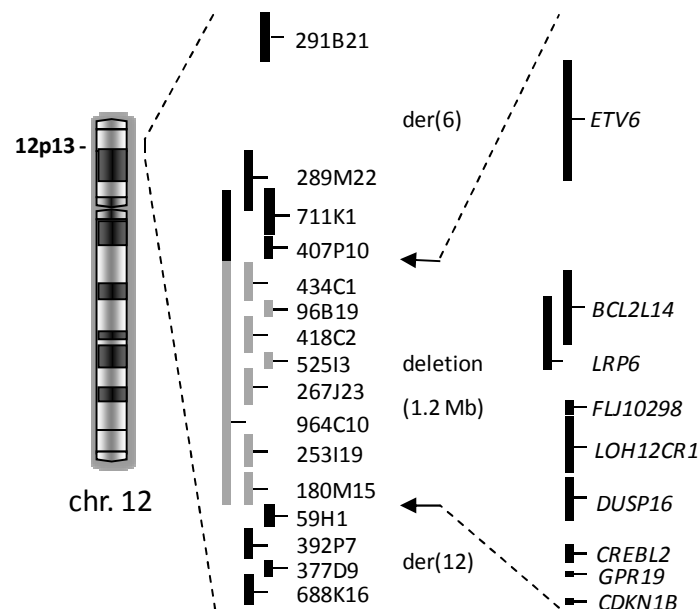


Figure 7. Diagrammatic representation of human chromosome 12 and of an enlarged 12p13 region targeted by the translocation breakpoints in the $t(12;6;15)(p13;p24\sim25;q22)$.

The breakpoints were associated with an interstitial deletion of 1.2 Mb which comprised *ETV6* and 8 other genes located centromeric to it. The distal and proximal breakpoints were positioned between probe 434C1 and 407P10, and probe 180M15 and 59H1, respectively. Probes used in breakpoint mapping are shown as black (non-deleted) or grey (deleted) vertical lines at the right side of the chromosome. The approximate location of deleted genes is shown on the right side of the figure.

To further localize the 12p13 breakpoints, FISH was conducted using a panel of 15 closely-spaced BAC probes. Results showed that 7 consecutive probes (from 434C1 to 180M15, including both of these) hybridized on normal chromosome 12 only. In contrast, distal and proximal positioned probes hybridized on der(6) and on der(12), respectively, in addition to normal chromosome 12, thus confirming translocation $t(12;6;15)(p13;p24\sim25;q22)$. In conclusion, FISH results in metaphase cells with $t(12;6;15)$ established the presence of a cryptic interstitial deletion at band 12p13 with an approximate length of 1.2 Mb comprising at least 9 known genes, ordered from telomere to centromere as follows: *ETV6*, *BCL2L14*, *LRP6*, *FLJ10298*, *LOH12CR1*, *DUSP16*, *CREBL2*, *GPR19* and *CDKN1B* (Fig. 7).

3.1.5.3. DELETION OF *ETV6* AT 12p13 AND OF *PAX5* AT 9p13 AS A RESULT OF $dic(9;12)(p11;p11)$ IN B-CELL ACUTE LYMPHOBLASTIC LEUKEMIA

Cytogenetic studies complemented with FISH analysis using a centromeric probe for chromosome 12 and a heterochromatic region probe for chromosome 9, showed a dicentric fusion $dic(9;12)(p11;p11)$ in the majority of cells analysed in patient 3 (Fig. 8A). Because this patient was a 9 year-old boy with B-cell ALL, FISH analysis was performed with the *TEL/AML1* translocation probe to exclude a cryptic *ETV6-RUNX1* fusion as seen in patient 1 (results not shown).

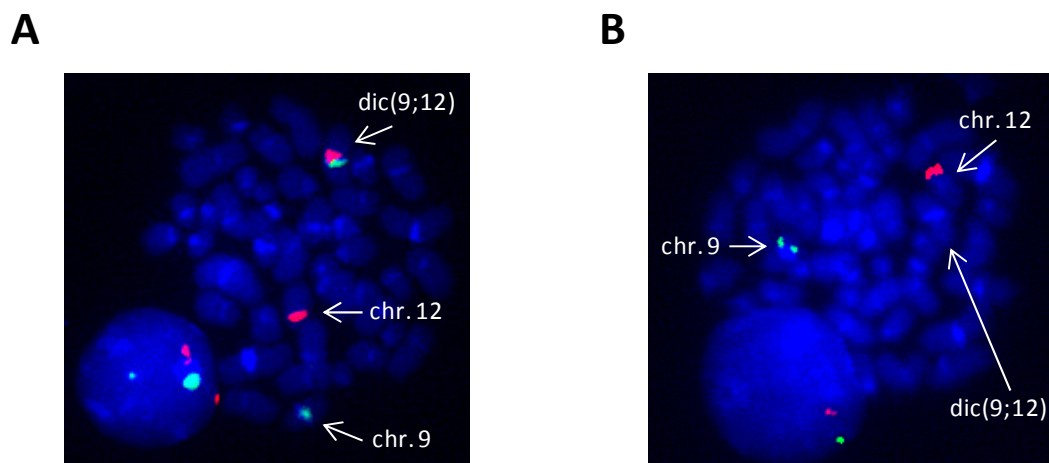


Figure 8. Analysis of chromosome rearrangements by FISH on bone marrow metaphases with $dic(9;12)(p11;p11)$. (A) Hybridization with a heterochromatic region probe for chromosome 9 (green) and a centromeric probe for chromosome 12 (red), showing the presence of a $dic(9;12)$ (B) Hybridization with YAC probe 964C10 (red) and 742H2 (green) covering *ETV6* (12p13) and *PAX5* (9p13), respectively. Signals are only observed on the normal chromosomes 9 and 12, indicating that *ETV6* and *PAX5* are deleted in the rearranged chromosomes.

Subsequent FISH studies with *ETV6* cosmids showed signals on the normal chromosome 12 only, indicating that *ETV6* was deleted on the rearranged chromosome homologue. Identical results were obtained using BAC probes 267J23 and 688K16, both of which map centromeric to *ETV6* at band 12p13. Hybridization with YAC probes 764A6 and 742H2 was performed to confirm absence of the 9p13 region including the *PAX5* gene. In both experiments, hybridization signals were present on the normal chromosome 9 only (**Fig. 8B**). In summary, at least the 12p13-12pter and the 9p13-pter regions including the *ETV6* and the *PAX5* genes, respectively, were lost as a result of dic(9;12).

3.1.6. DISCUSSION

Heterogeneity of breakpoint locations has been reported in patients with hematological malignant disorders and 12p13 translocations (Sato *et al.*, 1997; La Starza *et al.*, 1999; Odero *et al.*, 2001; Odero *et al.*, 2003). In approximately half of the patients, the breakpoints occur in the *ETV6* gene (Sato *et al.*, 1997; Odero *et al.*, 2001) and lead to gene fusion with different partner genes on various chromosomes (reviewed in Odero *et al.*, 2001; Yagasaki *et al.*, 2001; Odero *et al.*, 2002; Penas *et al.*, 2003; Qiao *et al.*, 2003). In the remaining cases, the breakpoints at 12p13 occur either telomeric or centromeric to *ETV6*, suggesting that other genes lying in the vicinity of *ETV6* could also play a role in malignant transformation. In agreement with these data, molecular cytogenetic analysis of apparently balanced 12p translocations has uncovered the presence of interstitial deletions at 12p13, which included several other genes in addition to *ETV6* (Wlodarska *et al.*, 1996; La Starza *et al.*, 1999). This was also the case of our patient 2 in whom an apparently balanced chromosomal translocation between chromosomes 12 and 15 masked the presence of a 1.2-Mb interstitial deletion at 12p13, which included *ETV6* and 8 other genes lying centromeric to it. The length and chromosomal position of the interstitial deletion detected in our patient matched the location of a commonly deleted segment at 12p13 which has been defined in patients with different hematological malignancies presenting with cytogenetically visible deletions (Wlodarska *et al.*, 1996). Whether *ETV6* is likely to be the main target gene in these patients and in ours remains to be determined. However, the complexity of chromosome rearrangements detected in our patient, including additional breakpoints at chromosomes 6 and 15, as well as a duplication of the der(6), suggests that leukemogenesis resulted from several gene changes at the involved chromosomes rather than from deletion of one allele of the *ETV6* gene only. In agreement with this hypothesis, we have not detected the presence of nucleotide mutations in the non-

rearranged *ETV6* allele, suggesting that *ETV6* was haplo-insufficient but otherwise functional in cells with t(12;6;15).

On the other hand, patients presenting with cytogenetically balanced translocations involving breakpoints in *ETV6* and in a partner chromosome other than chromosome 21, may hide an *ETV6-RUNX1* fusion as we found in our patient 1. In this case, gene fusion resulted from a 3-way translocation involving chromosomes 5, 12 and 21. These 3-way rearrangements of t(12;21) are apparently rare among the universe of *ETV6-RUNX1*-positive patients (Berger *et al.*, 1997; Wiemels *et al.*, 2000; Mathew *et al.*, 2001). However, the t(12;21) is not easily detected by conventional cytogenetic analysis because of the similar length and cytogenetic appearance of the terminal regions of chromosomes 12 and 21 involved in the translocation. Thus, it is possible that complex translocations involving an extra chromosome in addition to chromosomes 12 and 21 may be easily mistaken for a 2-way translocation involving chromosome 12 and a different partner chromosome. Thus, in view of the present results and of the knowledge that the *ETV6-RUNX1* fusion gene is usually associated with a better outcome in children with B-cell ALL, detection of the molecular rearrangement by FISH or RT-PCR should be recurrently performed in B-cell ALL patients presenting with cytogenetic evidence of 12p13 rearrangement other than the classical t(12;21)(p13;q22).

The *PAX5* gene, a transcription factor which encodes the B-cell-specific activator protein, is a partner gene of *ETV6* in ALL with t(9;12)(q11;p13) (Cazzaniga *et al.*, 2001). Recently, *PAX5-ETV6* fusion was described as the molecular counterpart of the dicentric translocation dic(9;12)(p11-13;p11-12), a recurrent abnormality which accounts for close to 1% of ALL in children (Strehl *et al.*, 2003). In the later study, it was proposed that the translocations dic(9;12)(p11-13;p11-12) with *ETV6* and *PAX5* rearrangement should be referred to as dic(9;12)(p13;p13) since these genes are localized at 12p13 and 9p13, respectively. However, in our patient 3, both genes were deleted, excluding the presence of a *PAX5-ETV6* rearrangement. Since the dic(9;12)(p11;p11) was the sole chromosomal abnormality in the karyotype of the patient, we hypothesize that the hemizygous presence of one or both of these genes may also be relevant in leukemogenesis. In particular, since *PAX5* is essential to initiate and maintain the B lymphoid transcription program during early B-cell development (Mikkola *et al.*, 2002), when it is expressed from one allele only (Nutt *et al.*, 1999), deletion of *PAX5* as a result of the dicentric fusion in our case may result in loss of function and, consequently, in a blockage of B-cell lineage commitment. Taken together, the present study illustrates the heterogeneity of chromosomal and molecular rearrangements underlying 12p translocations in leukemia patients.

3.2. THREE-WAY TRANSLOCATION INVOLVES *MLL*, *MLLT3* AND A NOVEL CELL CYCLE CONTROL GENE, *CCDC94*, IN THE PATHOGENESIS OF ACUTE MYELOID LEUKEMIA WITH t(9;11;19)(p22;q23;p13)

Published in: Vieira L, Sousa AC, Matos P, Marques B, Alaiz H, Ribeiro MJ, Braga P, da Silva MG, Jordan P (2006) Three-way translocation involves *MLL*, *MLLT3* and a novel cell cycle control gene, *FLJ10374*, in the pathogenesis of acute myeloid leukemia with t(9;11;19)(p22;q23;p13.3). *Genes Chromosomes Cancer* **45**: 455-469.

We are grateful to Dr. Joana Diamond and Dr. Margarida Jorge (Instituto Português de Oncologia de Francisco Gentil) for providing patient samples, Dr. Mariano Rocchi (University of Bari, Italy) for providing BAC clone RP11-336O12, and Dr. Ana P. Ambrósio and Dr. Ana L. Silva (Departamento de Genética, Instituto Nacional de Saúde Dr. Ricardo Jorge) for expert laboratory assistance.

This work was supported by a grant from Núcleo Regional do Sul-Liga Portuguesa Contra o Cancro and Fundação para a Ciência e a Tecnologia-Programa de Financiamento Plurianual do Centro de Investigação em Genética Molecular Humana.

3.2.1. ABSTRACT

The *MLL* gene at 11q23 undergoes chromosomal translocation with a large number of partner genes in both ALL and AML. We report a novel t(9;11;19)(p22;q23;p13.3) disrupting *MLL* in an infant AML patient. The 5' end of *MLL* fused to chromosome 9 sequences on the der(11), whereas the 3' end was translocated to chromosome 19. We developed LDI-PCR assays to investigate the localization of the breakpoints on der(11) and der(19). We found that intron 5 of *MLL* was fused to intron 5 of the myeloid/lymphoid or mixed-lineage, translocated to 3 (*MLLT3*, previously known as *AF9*) gene at the der(11) genomic breakpoint, resulting in a novel in-frame *MLL* exon 5-*MLLT3* exon 6 fusion transcript. On the der(19), a novel gene annotated as coiled-coil domain containing 94 (*CCDC94*, formerly known as *FLJ10374*) was disrupted by the breakpoint. Using RT-PCR analysis, we showed that *CCDC94* is ubiquitously expressed in human cells. Expression of the *CCDC94* protein in different cell lines revealed that it localized exclusively to the nucleus. In serum-starved NIH-3T3 cells the expression of *CCDC94* decreased the rate of G1- to S-phase transition of the cell cycle, whereas the suppression of *CCDC94* through short interfering RNA (siRNA) oligos increased cell proliferation. These results indicate that *CCDC94* negatively regulates cell cycle progression and proliferation. Thus, a single chromosomal rearrangement resulting in formation of the *MLL-MLLT3* fusion gene and haplo-insufficiency of *CCDC94* may have cooperated to promote leukemogenesis in the AML patient with t(9;11;19).

3.2.2. INTRODUCTION

Translocations of chromosome 11q23 are observed in 5-10% of patients with de novo AML and ALL. Notably, 11q23 translocations are present in over 50% of children under one year of age with ALL and AML (Sorensen *et al.*, 1994; Martinez-Climent *et al.*, 1995). In addition, approximately 30% of cancer patients who develop therapy-related acute leukemia (t-AML or t-ALL) or therapy-related myelodysplastic syndrome also show 11q23 balanced chromosome aberrations, particularly after treatment with DNA topoisomerase II (DNAt2)-inhibitors (Bloomfield *et al.*, 2002). The *MLL* gene was originally found to be the target gene disrupted at 11q23 in leukemia patients with t(4;11) and t(11;19) (Ziemin-Van Der Poel *et al.*, 1991; Djabali *et al.*, 1992; Gu *et al.*, 1992; Tkachuk *et al.*, 1992). The *MLL* gene shows 3 regions of sequence similarity to the trithorax gene, a known transcriptional regulator in *Drosophila*

melanogaster. Like trithorax, *MLL* positively maintains the expression of various homeobox genes during development (Ayton & Cleary, 2001).

The t(9;11)(p22;q23) is the most common translocation involving 11q23 in de novo AML and t-AML and results in fusion of the *MLL* to the *MLLT3* gene (Iida *et al.*, 1993; Nakamura *et al.*, 1993). In the t(9;11) and other 11q23 translocations, the *MLL* breakpoints are clustered within an 8.3-kb *Bam*HI breakpoint cluster region (bcr), which includes the genomic sequence beginning at the 3' side of exon 5 and extending to the 5' side of exon 11 (Gu *et al.*, 1992). In contrast, two major breakpoint cluster regions, known as BCR1 (or site A) and BCR2 (or site B), have been recognized in *MLLT3*. BCR1 includes the 3' region of intron 4 and BCR2 encompasses introns 7-8 of *MLLT3* (Iida *et al.*, 1993; Nakamura *et al.*, 1993; Negrini *et al.*, 1993; Yamamoto *et al.*, 1994; Super *et al.*, 1997; Atlas *et al.*, 1998; Odero *et al.*, 2000; Strissel *et al.*, 2000; Langer *et al.*, 2003). Despite the heterogeneity of the genomic breakpoints, the RNA junctions in t(9;11)-positive patients show in-frame *MLL-MLLT3* fusion transcripts consisting of a variable *MLL* bcr exon fused to the exons 5, 8, or 9 of *MLLT3* (Iida *et al.*, 1993; Nakamura *et al.*, 1993; Yamamoto *et al.*, 1994; Super *et al.*, 1997; Atlas *et al.*, 1998; Odero *et al.*, 2000). Structural elements like DNAt2 cleavage sites and scaffold-associated regions (SARs) have been found at the breakpoints in *MLL* and *MLLT3*, indicating that illegitimate recombination events mediated by specific DNA elements are likely to contribute to the fusion of these genes (Felix *et al.*, 1995; Strissel *et al.*, 2000).

Like *MLL*-associated acute leukemias, most other hematopoietic malignancies are characterized by reciprocal chromosome translocations. Routine cytogenetic analysis has shown that, in addition to both recurrent breakpoints, these translocations can involve further breaks in one or more chromosomes. In particular, 3-way or more translocations were found to account for 9.3%, 6.3%, and 2.6% of complex t(9;22), t(8;21), and t(15;17), respectively (Fisher *et al.*, 2005). Nevertheless, little is known about the contribution of additional breakpoints to the process of leukemogenesis. In this article, we describe an infant AML patient whose leukemic cells harbored a complex t(9;11) presenting as a novel 3-way t(9;11;19)(p22;q23;p13.3). We found that this rearrangement led to the formation of a variant *MLL-MLLT3* fusion transcript. Furthermore, the extra breakpoint at 19p13.3 disrupted *CCDC94*, a previously uncharacterized gene that negatively regulates cell cycle progression and proliferation. We propose that the concomitant formation of the *MLL-MLLT3* fusion gene and disruption of *CCDC94* mutually promoted leukemogenesis in this patient with t(9;11;19).

3.2.3. CASE SUMMARY

An 11-month-old girl was admitted to the hospital with a 4-day history of fever, cough, and paleness. Peripheral blood counts revealed anemia (hemoglobin 6.9 g/dL) and normal numbers of white blood cells and platelets. Hepatomegaly was present. The morphologic examination of the bone marrow aspirate suggested AML. Immunophenotypic studies showed the presence of 54% blasts positive for CD33, CD15, CD4, HLA-DR and CD45, of which 50% and 25% were positive for CD117 and CD11b, respectively. The blasts were CD13 negative. A diagnosis of AML-M4 was made.

3.2.4. MATERIALS AND METHODS

3.2.4.1. CYTOGENETIC AND FLUORESCENCE *IN SITU* HYBRIDIZATION ANALYSES OF CHROMOSOME REARRANGEMENTS

A bone marrow sample collected at diagnosis was used for routine cytogenetic analysis. G-banded metaphase chromosomes of bone marrow cells were prepared following standard techniques, and the karyotype was established according to ISCN (1995) guidelines. Fixed cells prepared for cytogenetics were used for FISH analysis of chromosome rearrangements, as described previously (Vieira *et al.*, 2005). Hybridization experiments were performed with WCP probes for chromosomes 9, 11, and 19 (Cambio), the *MLL* gene probe (Q-Biogene) and BAC clones RP11-336O12 (GenBank accession number AL513498; kindly provided by Dr. Mariano Rocchi, University of Bari, Italy) and CTB-144D21 (GenBank accession number AC008616, obtained from Research Genetics).

3.2.4.2. MOLECULAR ANALYSIS AND CLONING OF *MLL-MLLT3* FUSION TRANSCRIPTS

A bone marrow sample obtained at disease relapse following a sex-mismatched bone marrow transplantation was used for the molecular analysis and characterization of chromosome rearrangements. The technique of cDNA panhandle PCR was used, with minor modifications, to identify *MLL*-containing transcripts originating on der(11) (Megonigal *et al.*, 2000). Amplification products were cloned using the TOPO TA Cloning Kit (Invitrogen) according to the manufacturer's instructions. Transformants were screened by whole-cell PCR for the presence of *MLL*-containing sequences. Positive clones were sequenced using Big-Dye

technology and the ABI Prism 3100 Genetic Analyzer (Applied Biosystems). For direct analysis of *MLL-MLL3* fusion transcripts, three micrograms of total RNA were reverse transcribed to cDNA using Ready-to-go You-prime First Strand Beads (Amersham Biosciences) and random hexamers (Invitrogen) as primers. One-tenth of the cDNA (4 μ l) was subsequently amplified by PCR with *MLL*-ex5s and *MLL3*-ex8as primers (**Table IV**). PCR products were analyzed on 2% agarose gels stained with ethidium bromide.

Table IV. Designation of primers and corresponding sequences used in this study.

Primer name	Sequence 5' → 3'	Technique
<i>MLL</i> -ex5s	TCCTCCACGAAAGCCCGTCGAG	RT-PCR
<i>MLL3</i> -ex8as	CTTGTCACATTCCACATTCTT	RT-PCR
<i>MLL3</i> -ex6	CTGCGACTTCGGCTGCCTCCTCTA	LDI-PCR
<i>MLL3</i> -int6	TTGGAAGGAAAGGGGTTGCCTGTG	LDI-PCR
<i>MLL</i> -ex6	GATACTTGGGCGGGAGCCACTTTT	LDI-PCR
<i>MLL</i> -int6	TGTTTCTCTGCCATTTCTCAGGGATGT	LDI-PCR
<i>MLL</i> -int5	GTTTCTGTTTCTTTATTATTAAC	LDI-PCR
<i>MLL</i> -int6.1	CCAGGTACTIONCAGGAGGCT	LDI-PCR
<i>CCDC94</i> -ex5s	ACGTGGACTTCGAGGCTATG	RACE, RT-PCR
<i>CCDC94</i> -ex6s	AAGCCAGAAAGCGAAGACTG	RACE
<i>CCDC94</i> -ex8as	GTCCAGGTATGCACCCAGTT	RT-PCR
<i>CCDC94</i> -NTER	ATGTGCGAGCGAAAAGTATTAAAC	Cloning
<i>CCDC94</i> -CTER	CCTGGGAGGGCTCAGTTGCT	Cloning
ms <i>CCDC94</i> _s	AGCTTCTGGAGGAGGAGGAG	RT-PCR mouse cells
ms <i>CCDC94</i> _as	TGCCAACTGTGCTTTACTGC	RT-PCR mouse cells

3.2.4.3. CLONING OF GENOMIC FUSIONS ON THE der(11) AND der(19) CHROMOSOMES

The technique of LDI-PCR, described by Willis *et al.* (1997), was adapted with minor modifications to clone the *MLL* breakpoints on der(11) and der(19). For identification of the fusion point between *MLL* and *MLL3* genomic sequences on the der(11), suitable *DraI* restriction sites in introns 5 and 6 of *MLL3* were identified using the genomic sequence of the chromosome 9 BAC RP11-336O12 (GenBank accession number AL513498) as template. Amplification of circular DNA was performed with *MLL3*-ex6 and *MLL3*-int6 primers, which yield a 2103 bp fragment from a non-rearranged *MLL3* locus. To localize the fusion point of 3' *MLL* on the der(19), *PstI* restriction sites within the *MLL* gene were identified using the genomic sequence of the chromosome 11 BAC RP11-770J1 (GenBank accession number AP001267) as template. Amplification was performed with *MLL*-ex6 and *MLL*-int6 primers, which produce a 1305 bp fragment from a non-rearranged *MLL* gene. Because of the presence

of adenosine and thymine tracts more than 14 nucleotides long within the LDI-PCR products, sequencing of the latter was performed with *MLL-int5* and *MLL-int6.1* primers. PCR products were run on 0.8% agarose gels stained with ethidium bromide, cloned, and sequenced as indicated above.

3.2.4.4. DETECTION OF TRUNCATED *CCDC94* TRANSCRIPTS

The rapid amplification of cDNA ends (RACE) methodology was used for detection of the truncated *CCDC94* mRNA in the patient's bone marrow cells. One microgram of total RNA was converted into cDNA using the 3' RACE System (Invitrogen) according to the manufacturer's instructions. The *CCDC94* cDNA was amplified by nested PCR using the primers provided by the manufacturer in conjunction with *CCDC94-ex5s* primer on the first round and *CCDC94-ex6s* primer on the second round. PCR products were analyzed on an ethidium bromide-stained 2.5% agarose gel, cloned and sequenced as described beyond.

3.2.4.5. DETECTION OF *CCDC94* MRNA EXPRESSION IN CELL LINES AND NORMAL TISSUES

Expression of the *CCDC94* gene was evaluated by RT-PCR using cDNA samples obtained from 16 different normal human tissues and cells (Human Multiple Tissue cDNA Panels I and II, Clontech) as well as from 6 hematopoietic (697, NB4, LAMA-84, TOM-1, Kasumi-1, and REH) and 6 non-hematopoietic (SW480, HCT116, HeLa, HEK-293, HT29, and RH-30) cell lines. Samples were amplified using primers *CCDC94-ex5s* and *CCDC94-ex8as*. To check for the integrity of RNA and efficient cDNA synthesis in each cell line, a partial sequence of the ubiquitously expressed *ABL1* transcript was amplified using primers described in Cross *et al.* (1993). Amplification of the *G3PDH* transcript was performed with primers included in the Human Multiple Tissue cDNA Panels and used as a normalizer of *CCDC94* expression in normal tissues. Amplifications were carried out using standard reaction conditions and cycling parameters. Reaction products were electrophoresed on ethidium bromide-stained 2% agarose gels.

3.2.4.6. SUBCELLULAR LOCALIZATION OF CCDC94 PROTEIN

A full-length *CCDC94* cDNA was amplified from total RNA obtained from the HT29 colon cell line by RT-PCR using primers *CCDC94*-NTER and *CCDC94*-CTER. A 983 bp fragment of *CCDC94* beginning at the ATG codon in exon 1 and ending 11 bp distally to the stop codon in exon 8 was amplified and subcloned into the pcDNA3.1/NT-GFP-TOPO expression vector (Invitrogen) according to the manufacturer's instructions. Additionally, a FLAG-tagged *CCDC94* cDNA was made by digestion of the GFP-*CCDC94* construct with *KpnI* and *XbaI* and subsequent ligation into the pFLAG-CMV-2 expression vector (Sigma) using the Rapid DNA Ligation Kit (Roche Applied Science). Both constructs were sequenced to confirm authenticity of the sequence and conservation of the reading frame at the cloning sites.

Transfection experiments were independently conducted in 3 different cell lines from distinct cellular origins (NIH-3T3 mouse fibroblasts, DLD1 human colon carcinoma cells, and HeLa human cervix carcinoma cells) to access localization of the tagged *CCDC94* protein. Cells were maintained in culture using Dulbecco's Modified Essential Medium supplemented with 10% (v/v) of either new born calf serum (CS) for NIH-3T3 or fetal CS for DLD1 and HeLa cell lines (Invitrogen). Initially, approximately 4×10^5 cultured cells were seeded on 6 glass coverslips placed within 35 mm-diameter culture dishes. Two micrograms of plasmid constructs were transfected 24 hr later using Lipofectamine 2000 (Invitrogen) according to the manufacturer's instructions. Cells were incubated for an additional 18 hr period before harvesting. Immunofluorescence analysis including fixation and permeabilization of cells, incubation of antibodies for detection of green fluorescent protein (GFP) expression, and imaging were performed as described (Matos & Jordan, 2005). The *CCDC94* protein expression in cells transfected with FLAG-tagged *CCDC94* cDNA was detected using a primary mouse anti-FLAG M2 antibody (Sigma) followed by a secondary goat anti-mouse fluorescein isothiocyanate (FITC) antibody (Jackson ImmunoResearch). The actin cytoskeleton and nuclear morphology were visualized using phalloidin-tetramethylrhodamine isothiocyanate (TRITC) (Sigma) and 4',6-diamidino-2-phenylindole (DAPI) (Sigma), respectively, in cells transfected with either tag. Expression of the transfected plasmid constructs was also evaluated by sodium dodecyl sulphate-polyacrilamide gel electrophoresis (SDS-PAGE) and Western blotting as previously described (Matos *et al.*, 2003) using monoclonal anti-FLAG M2 antibody (Sigma) or polyclonal rabbit anti-GFP ab290 antibody (Abcam).

3.2.4.7. EFFECT OF *CCDC94* EXPRESSION ON CELL CYCLE PROGRESSION AND CELL SURVIVAL

CS-starved NIH-3T3 mouse fibroblasts were used as a model system for evaluating the effect of *CCDC94* protein expression on cell survival and on the transition from the gap1 phase (G1-phase) to the synthesis phase (S-phase) of the cell cycle, as described (Matos & Jordan, 2005). The statistical significance of the results was accessed using the two-tailed Student *t* test.

3.2.4.8. EFFECT OF *CCDC94* MRNA SUPPRESSION ON CELL PROLIFERATION

Two different 21-mer chemically synthesized siRNA oligos (*msCCDC94_1* and *msCCDC94_2*) obtained from MWG (Ebersberg, Germany) were designed using the mouse *CCDC94* cDNA sequence (GenBank accession number NM_028381) as template (**Table V**). Additionally, a siRNA specific for the mRNA of the non-endogenous GFP was used as a control. Transfection of each of the siRNA oligos (100 pmoles) was independently performed in CS-starved NIH-3T3 cells placed on coverslips within 35 mm-diameter culture dishes. Cells were incubated in the presence of bromodeoxyuridine (BrdU) for 24 hr, and then the coverslips removed and analyzed as described previously (Matos & Jordan, 2005). Total RNA was extracted from the remaining cells and converted to cDNA, as described above, following a previous incubation with Dnase I Rnase-free enzyme (Ambion). Amplification of cDNA was carried out using *msCCDC94_s* and *msCCDC94_as* primers for *CCDC94* and *ABL1* primers as a control, as described above. Amplification products were run on ethidium bromide-stained 2% agarose gels. The level of *CCDC94* transcript knock-down was documented by densitometric analysis of amplified products.

Table V. Designation of siRNA oligos and corresponding sequences used in this study.

siRNA name	Sequence 5' → 3'
<i>msCCDC94_1</i>	UCUCCGAUUCUACAUAATT
<i>msCCDC94_2</i>	AGCACAGUUGGCAGGCUUATT
GFP	GGCUACGUCCAGGAGCGCACCTT

3.2.4.9. COMPUTATIONAL SEQUENCE ANALYSIS

Resources available at the National Center for Biotechnology Information (NCBI) Web site (<http://www.ncbi.nlm.nih.gov>) including Evidence Viewer, Map Viewer, or basic local alignment search tool (BLAST), were used for obtaining the RNA sequence from *CCDC94*, for selection of BAC probes for chromosomes 9 and 19, and for analysis of cDNA panhandle PCR and LDI-PCR sequencing data, respectively. The Webcutter 2.0 software (<http://rna.lundberg.gu.se/cutter2>) was used to select appropriate restriction enzymes for the LDI-PCR assays. Primers for LDI-PCR and *CCDC94* transcript analyses were designed using Primer3 software available at http://frodo.wi.mit.edu/cgi-bin/primer3/primer3_www.cgi (Rozen & Skaletsky, 2000). Alignment of protein sequences was conducted using the BLASTP 2.2.24+ program (Altschul *et al.*, 1997) with a compositional score matrix adjustment (Altschul *et al.*, 2005). Prediction of localization sites of *CCDC94* protein in the cells and potential motifs was performed with the PSORT WWW server (<http://psort.ims.u-tokyo.ac.jp>). The siRNA oligos were designed with software available at MWG Web site (http://www.mwg-biotech.com/html/s_synthetic_acids/s_rna.shtml). Densitometric analysis of agarose gels was performed with ImageJ software from the National Institutes of Health (<http://rsb.info.nih.gov/ij>).

3.2.5. RESULTS

3.2.5.1. TRANSLOCATION t(9;11;19) IS A 3-WAY COMPLEX OF t(9;11) THAT REARRANGES *MLL* WITH *MLLT3* AND RESULTS IN AN *MLL* EXON 5-*MLLT3* EXON 6 FUSION TRANSCRIPT

In karyotype analysis combined with WCP of the patient's bone marrow cells at diagnosis, all metaphases analysed showed a single rearrangement involving chromosomes 9, 11, and 19: 46,XX,t(9;11;19)(p22;q23;p13.3)[15] (**Fig. 9**). The breakpoint at 11q23 prompted the use of FISH to search for an *MLL* gene rearrangement. Metaphase cells hybridized with the *MLL* probe showed signals on the normal chromosome 11 and on der(11) and der(19), revealing that the breakpoint disrupted the *MLL* gene (results not shown). Thus, the 3' end of *MLL* was translocated to chromosome 19 while the 5' end of the gene remained on chromosome 11 and was fused to sequences from chromosome 9. These results suggested that the t(9;11;19) was a complex rearrangement of t(9;11)(p22;q23) that had fused the *MLL* with the *MLLT3* gene from 9p22 (Iida *et al.*, 1993; Nakamura *et al.*, 1993). The *MLL-MLLT3*

fusion gene was indeed confirmed by 2-color FISH in metaphases with a t(9;11;19) using the *MLL* probe and the BAC probe RP11-336O12 covering the *MLLT3* gene (Fig. 10A).

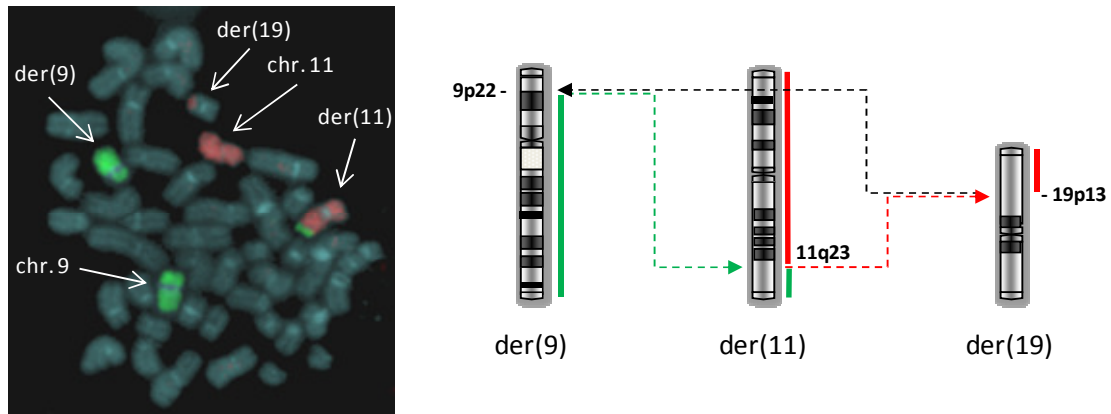


Figure 9. Analysis of chromosome rearrangements by FISH in a bone marrow cell with t(9;11;19).

Left: Hybridization with WCP probes for chromosomes 9 (green) and 11 (red) showing a der(9), a der(11), and a der(19), resulting from a 3-way complex t(9;11;19)(p22;q23;p13.3). Right: Corresponding diagrammatic representation of derivative chromosomes. Dashed lines are used to indicate the movement of material between each of the chromosomes involved in the rearrangement. Vertical green and red lines at the right side of chromosomes show the location of chromosome 9 and chromosome 11 materials, respectively, after formation of the translocation.

Because of the heterogeneous fusion sites in the *MLL-MLLT3* hybrid genes and of the possibility of alternative splicing events (Iida *et al.*, 1993; Nakamura *et al.*, 1993; Yamamoto *et al.*, 1994), a cDNA panhandle PCR technique was used to identify fusion transcripts involving the 5' side of *MLL* (Megonigal *et al.*, 2000). After nested PCR, this assay yielded several discrete amplification products that were subsequently cloned and sequenced (results not shown). A BLAST analysis of the cloned sequences revealed *MLL*-derived transcripts, one corresponding to a fusion of *MLL* exon 5 to the *MLLT3* gene. RT-PCR with gene-specific primers was then performed which resulted in the amplification of a 532-bp product, the sequencing of which confirmed the presence of an *MLL-MLLT3* fusion transcript that consisted of an in-frame fusion between exon 5 of *MLL* and exon 6 of *MLLT3* (Fig. 10B and C).

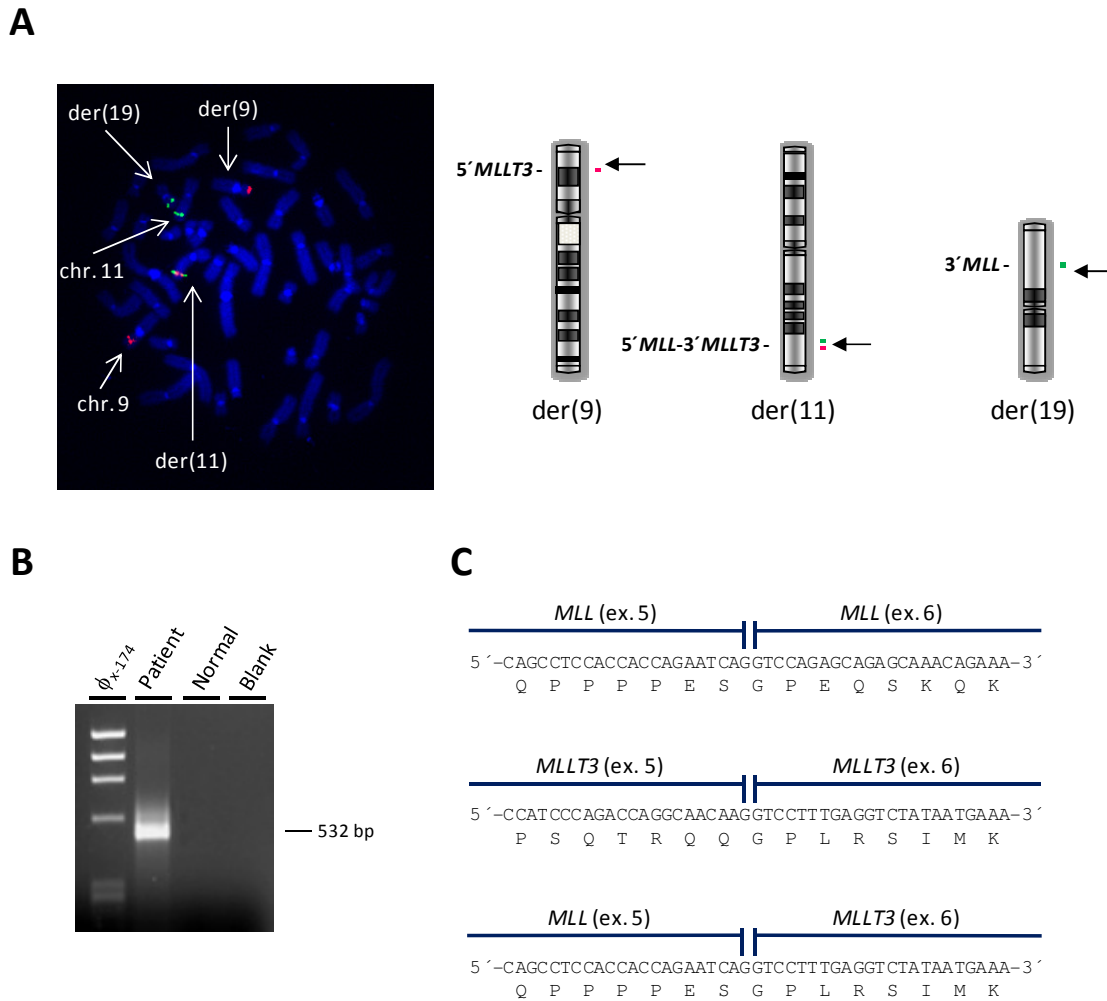


Figure 10. Detection of the *MLL-MLLT3* fusion by FISH, RT-PCR and direct sequencing analyses.

(A) Left: Hybridization with the *MLL* gene probe (green) and the BAC probe RP11-336O12 (red) covering the *MLLT3* gene at 9p22. Signals from the *MLL* probe were present on the normal chromosome 11, der(11), and der(19) whereas signals from probe RP11-336O12 were observed on the der(9) and der(11) in addition to the normal chromosome 9. The der(11) showed a co-localization of green and red signals corresponding to the *MLL-MLLT3* fusion gene. Right: Schematic representation of corresponding derivative chromosomes and location of hybridization signals. **(B)** Agarose gel electrophoresis analysis of RT-PCR products for detection of *MLL-MLLT3* fusion transcripts. A 532 bp amplification product was present in the patient cDNA sample. No amplification products were detected in a cDNA sample from a normal individual and in the blank (no cDNA) control. **(C)** Partial mRNA sequences of normal *MLL* exon 5-exon 6 and *MLLT3* exon 5-exon 6 junctions, and corresponding *MLL-MLLT3* fusion in the patient. Capital letters below the mRNA sequences indicate the corresponding aminoacid residues.

3.2.5.2. A NOVEL GENE AT 19p13.3, *CCDC94*, IS DISRUPTED BY FUSION TO THE 3' END OF *MLL*

LDI-PCR has been previously used to amplify immunoglobulin heavy joining group (*IGHJ@*) translocations in B-cell malignancies in order to identify the fusion partner gene sequence (Willis *et al.*, 1997). Briefly, genomic DNA was digested with an appropriate

restriction enzyme, re-ligated to form monomeric circles, and amplified using primers annealing to a known *IGHJ@* sequence in the circularized molecules. In the present work, an LDI-PCR assay was designed to identify the *MLL-MLLT3* genomic fusion sequence at the *MLL* bcr in the der(11).

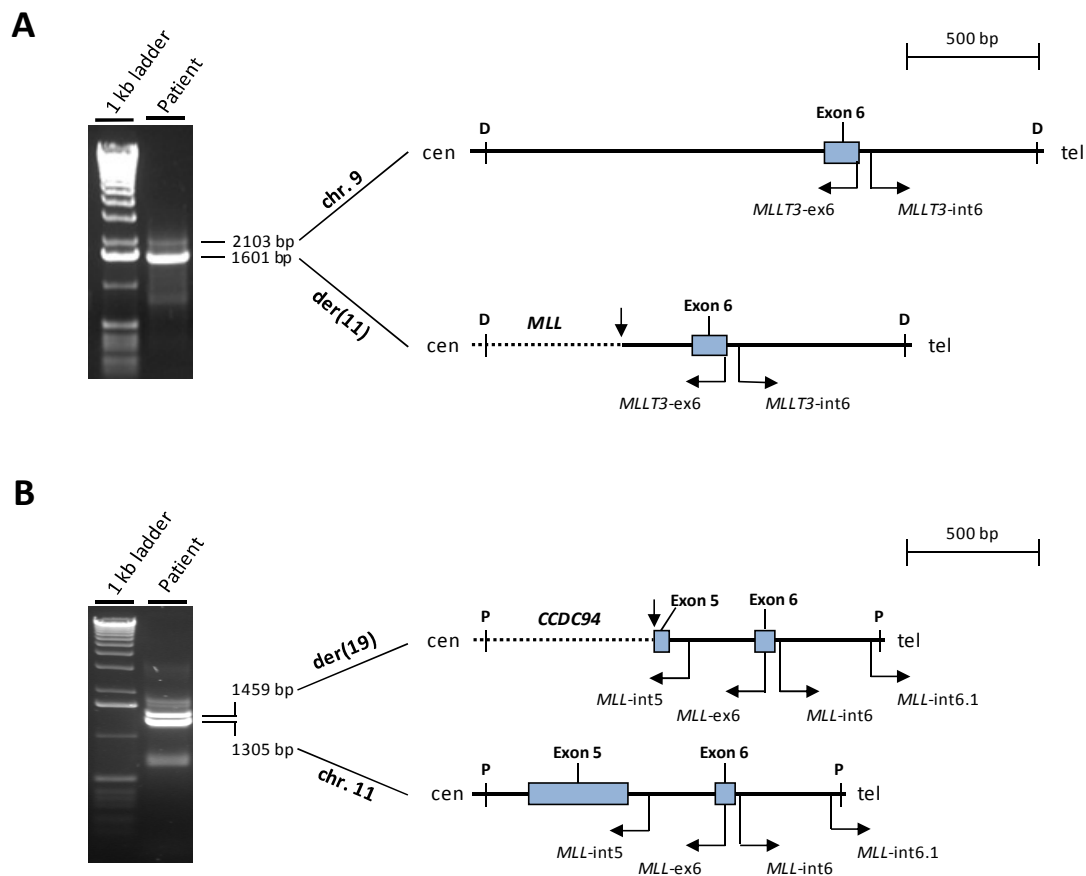


Figure 11. LDI-PCR analyses of the genomic breakpoint junctions on der(11) and der(19).

(A) Left: Detection of normal and rearranged *MLLT3* alleles by agarose gel electrophoresis analysis of LDI-PCR products. Bands of 2103 and 1601 bp, corresponding to the non-rearranged and rearranged *MLLT3* alleles on the normal chromosome 9 and der(11), respectively, were observed. The molecular weight marker is 1 kb ladder (Invitrogen). Right: Corresponding diagrammatic representation of genomic fragments amplified by LDI-PCR. The horizontal arrows indicate the position and orientation of the primers used in the LDI-PCR assay. The vertical arrow shows the localization of the genomic junction of *MLL* and *MLLT3* on the der(11). The *MLLT3* genomic sequence is represented by a solid line whereas the *MLL* sequence is shown by a dotted line. D, *DraI* restriction site; cen, centromere; tel, telomere. **(B)** Left: Detection of normal and rearranged *MLL* alleles by agarose gel electrophoresis analysis of LDI-PCR products. Bands of 1459 and 1305 bp, corresponding to the rearranged and non-rearranged *MLL* alleles on der(19) and normal chromosome 11, respectively, were observed. The molecular weight marker is 1 kb ladder (Invitrogen). Right: Corresponding diagrammatic representation of genomic fragments amplified by LDI-PCR. The horizontal arrows indicate the position and orientation of the primers used in the LDI-PCR assay and sequencing analysis. The vertical arrow shows the localization of the genomic junction of *CCDC94* and *MLL* on the der(19). The *MLL* genomic sequence is represented by a solid line whereas the *CCDC94* sequence is shown by a dotted line. P, *PstI* restriction site; cen, centromere; tel, telomere.

After *DraI* digestion and subsequent ligation, DNA was amplified with primers located in exon 6 and in the proximal 5' side of intron 6 of *MLLT3*. Agarose gel electrophoresis analysis of PCR products showed a 2103 bp band corresponding to the normal *MLLT3* allele derived from the non-rearranged chromosome 9 and an extra band of 1601 bp (**Fig. 11A**). Sequencing analysis of the latter band showed a fusion of intron 5 of *MLL* with intron 5 of *MLLT3* which was expected because of the results of RT-PCR analysis.

The definition of the *MLL* intronic sequence flanking the der(11) breakpoint subsequently allowed the design of another LDI-PCR assay to identify the 19p13.3 sequence fused to the 3' portion of *MLL*. A band of 1305 bp which corresponded to the germline *MLL* allele and an additional band of 1459 bp were observed on the gel after amplification of *PstI* digested-DNA with primers located in exon 6 and in the proximal 5' side of intron 6 of *MLL* (**Fig. 11B**). Sequencing analysis of the latter PCR product showed that a 641 bp unknown sequence was fused to *MLL*. Database searches identified this sequence as part of intron 6 of the *CCDC94* gene which maps to the 19p13.3 chromosomal region.

The *MLL* breakpoint on the der(11) was at nucleotide position 367, 368, or 369 in intron 5 (GenBank accession number U04737), whereas the *MLLT3* breakpoint on the der(11) was after either nucleotide 31868, 31869, or 31870 in intron 5 (GenBank accession number AL513498). The repetition of 2 and 5 thymine nucleotides at the breakpoints of *MLL* and *MLLT3*, respectively, precluded exact assignment of the breakpoint locations (**Fig. 12**). The *MLL* breakpoint on the der(19) was at nucleotide position 206 or 207 in exon 5 (GenBank accession number U04737), and the *CCDC94* breakpoint was either after nucleotide 58267 or 58268 in intron 6 (GenBank accession number AC008616). Again, these breakpoints could not be precisely defined because of the 2 thymine nucleotides at the breakpoints of both genes.

Depending on the exact breakpoint positions, there were 161-164 nucleotides from the same *MLL* sequence on der(11) and der(19). This observation is compatible with the occurrence of 2 breaks occurring in each strand of *MLL* separated by 161-164 bases that originated single-stranded configuration overhangs. Subsequently, the double-stranded configuration would have been restored by polymerization of the sequence between both breaks in a template-dependent manner, therefore originating a duplicated sequence from *MLL* on both derivative chromosomes. We detected short homologous sequences at the breakpoint junctions of *MLL* and *MLLT3*, and of *CCDC94* and *MLL*, suggesting that the non-homologous end joining (NHEJ) pathway of double strand break repair was involved in fusion of 5' *MLL* to *MLLT3* and of *CCDC94* to 3' *MLL* (Felix *et al.*, 1995).

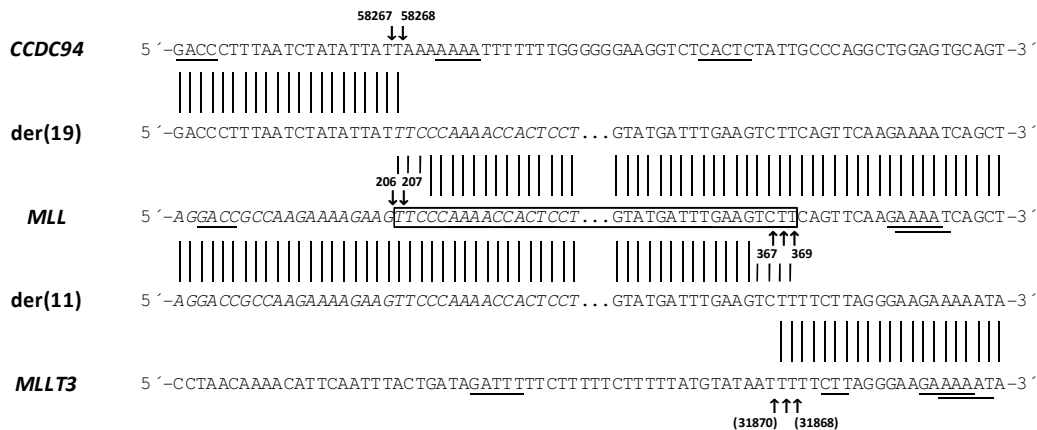


Figure 12. Genomic sequence fusions originated at the der(19) and der(11) breakpoints.

Partial genomic sequences of the antisense strand of *CCDC94* (reverse of GenBank accession number AC008616), *MLL* (GenBank accession number U04737), and *MLLT3* (reverse complement of GenBank accession number AL513498), and of the corresponding junction sequences on the der(19) and der(11). Numbers between brackets indicate nucleotide positions in the original GenBank sequence. Vertical solid lines indicates homology between *CCDC94*, *MLL*, or *MLLT3*, and the corresponding derivative chromosomes. A box represents a duplicated *MLL* sequence between nucleotide positions 206 or 207 in exon 5 and nucleotide positions 367, 368 or 369 in intron 5. An arrow pointing downwards indicates localization of possible breakpoints in *CCDC94* and *MLL*, whereas an arrow pointing upwards indicates localization of possible breakpoints in *MLL* and *MLLT3*. The *MLL* exon 5 sequence is shown in italics. Microhomologies of 3-5 bp between *MLL* and *MLLT3* and between *CCDC94* and *MLL* are underlined.

In theory a truncated *CCDC94* protein could be expressed on the der(9) as a result of the fusion of the translocated *CCDC94* allele to chromosome 9 sequences. To test this hypothesis, a 3' RACE analysis was performed to identify the rearranged *CCDC94* transcript. After nested PCR, two major bands of 827 bp and 297 bp were amplified (**Fig. 13**). Sequencing analysis showed that the upper band corresponded to the non-rearranged *CCDC94* transcript originating from the normal chromosome 19 whereas the lower one consisted in the fusion of exon 6 of *CCDC94* to the antisense strand of the *MLLT3* gene. This fusion transcript comprised 112 nucleotides from the antisense strand of *MLLT3* corresponding to positions 43009-43120 in BAC RP11-336O12 (GenBank accession number AL513498) and contained a poly-A signal (AAUAAA) resulting in the addition of a poly-A tail 18 nucleotides downstream. Because there was no stop codon within this sequence to end protein synthesis, the hybrid protein cannot detach from the ribosome, thus rendering the truncated *CCDC94* transcript non-functional. The transcribed sequence from the *MLLT3* antisense strand on the der(9) started at position 43009 while the genomic breakpoint of *MLLT3* on the der(11) was at the more telomeric positions 31870, 31869, or 31868 (GenBank accession number AL513498). A detailed inspection of the genomic sequence surrounding position 43009 from *MLLT3* revealed the presence of an AG dinucleotide at positions 43007-43008, suggesting that a cryptic splice site

was used to add the additional 112 nucleotides from chromosome 9 to the *CCDC94* truncated transcript.

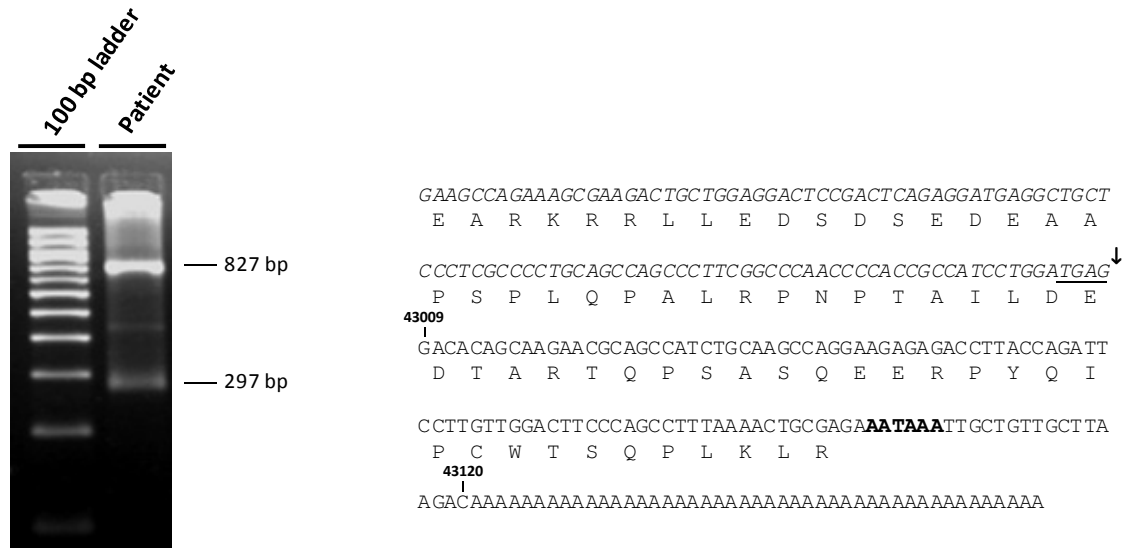


Figure 13. Analysis of *CCDC94* transcripts by 3' RACE and direct sequencing.

Left: Agarose gel electrophoresis analysis of PCR products obtained by RACE. Bands of 827 bp and 297 bp were amplified corresponding to the non-rearranged and rearranged *CCDC94* transcripts, respectively. Right: Partial sequence of the *CCDC94* rearranged transcript. The *CCDC94* exon 6 sequence is shown in italics whereas the remaining sequence corresponds to the antisense strand of *MLL3* between nucleotide positions 43009 and 43120 (GenBank accession number AL513498), followed by a poly-A tail. The arrow indicates the fusion point (position 43009) of *MLL3* to *CCDC94*. The poly-A signal (AATAAA) is shown in boldface. The four base sequence TGAG (underlined) at the end of *CCDC94* exon 6 sequence is also present on the antisense strand of *MLL3* between positions 43005 and 43008 immediately before the fusion point (not shown on this sequence). Capital letters below the mRNA sequence indicate the corresponding amino acid residues.

Confirmation that the 19p13.3 breakpoint interrupted the *CCDC94* gene was obtained by FISH following hybridization of the patient's metaphase cells with the BAC probe CTB-144D21, which contains the genomic sequence from exon 2 to the 3' end of *CCDC94* (Fig. 14). Interestingly, the breakpoint was only approximately 90 kb telomeric of the *SH3GL1* gene, another known partner gene of *MLL* in the t(11;19)(q23;p13.3) (So *et al.*, 1997), suggesting preferential breakage at this chromosomal region in *MLL*-associated leukemias.

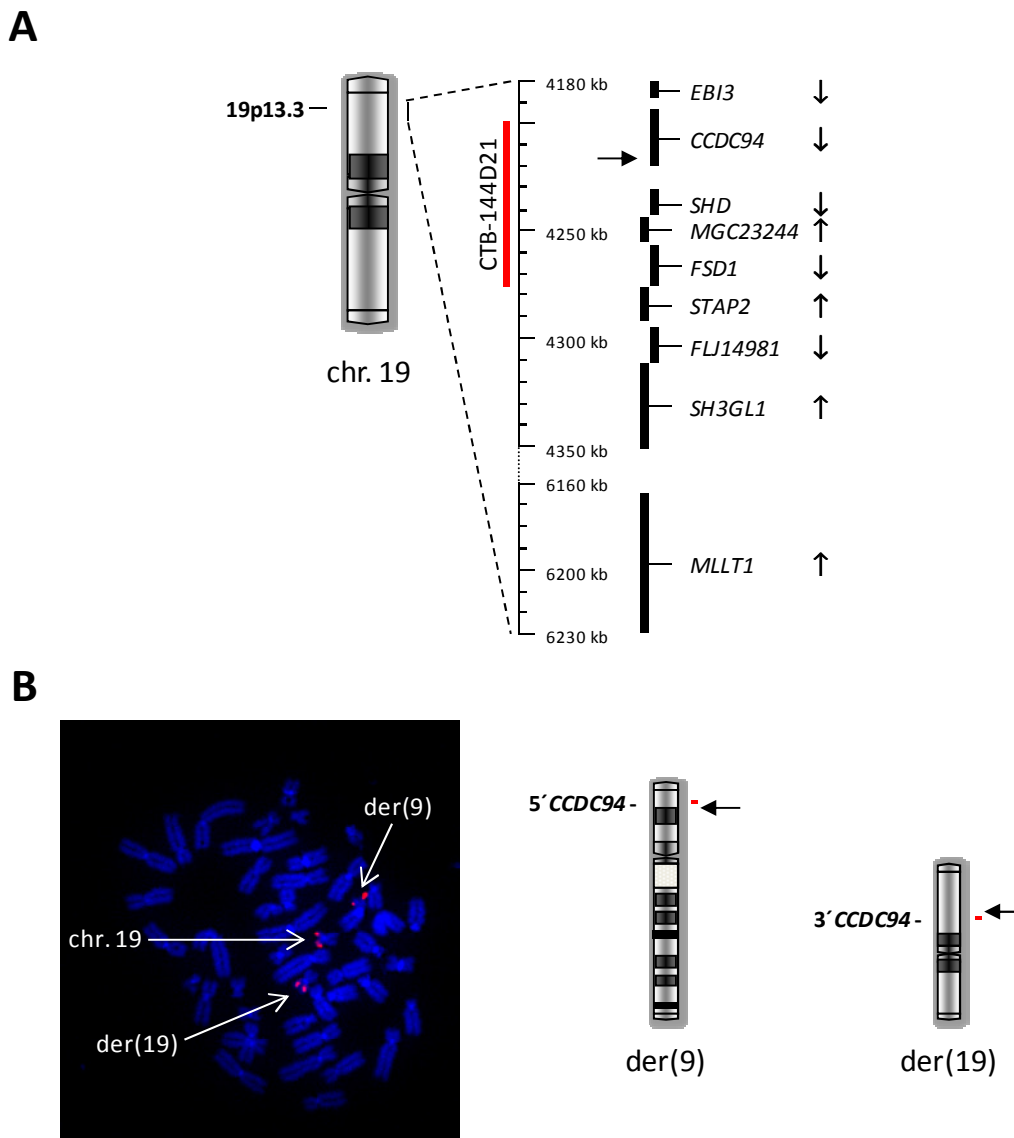


Figure 14. Analysis of *CCDC94* rearrangement by FISH in a metaphase with t(9;11;19).

(A) Representation of human chromosome 19 and of a partial 19p13.3 segment indicating the localization and orientation (vertical arrows) of *CCDC94* and 8 other known genes in this region. *SH3GL1* and *MLLT1* are 2 *MLL* partner genes involved in t(11;19)(q23;p13.3). The location of BAC CTB-144D21 covering the *CCDC94* gene at chromosome band 19p13.3 is shown as a red vertical line. The horizontal arrow indicates the approximate location of the chromosomal breakpoint in the t(9;11;19). A scale is shown in kb starting from the telomere of the short arm. (B) Left: Hybridization of a metaphase cell with t(9;11;19) using BAC CTB-144D21. Right: Corresponding schematic representation of the location of hybridization signals on the derivative chromosomes. In addition to the normal chromosome 19, signals were also present on the der(9) and der(19), confirming the presence of a breakpoint within the *CCDC94* gene.

3.2.5.3. THE *CCDC94* GENE IS UBIQUITOUSLY EXPRESSED IN HUMAN CELLS

To date, there are no experimental data on the *CCDC94* gene except for its mRNA sequence and corresponding annotation (GenBank accession number NM_018074). According

to the human genome reference sequence database, the coding sequence of *CCDC94* is distributed over 8 exons in a region of approximately 27 kb. RT-PCR and sequence analysis of the complete *CCDC94* coding sequence in 2 cell lines (SW480 and HT29) using primers at the initial ATG codon and at the 3' side of the stop codon yielded an expected PCR product of 983 bp, thus confirming the predicted exon/intron structure of the gene (results not shown).

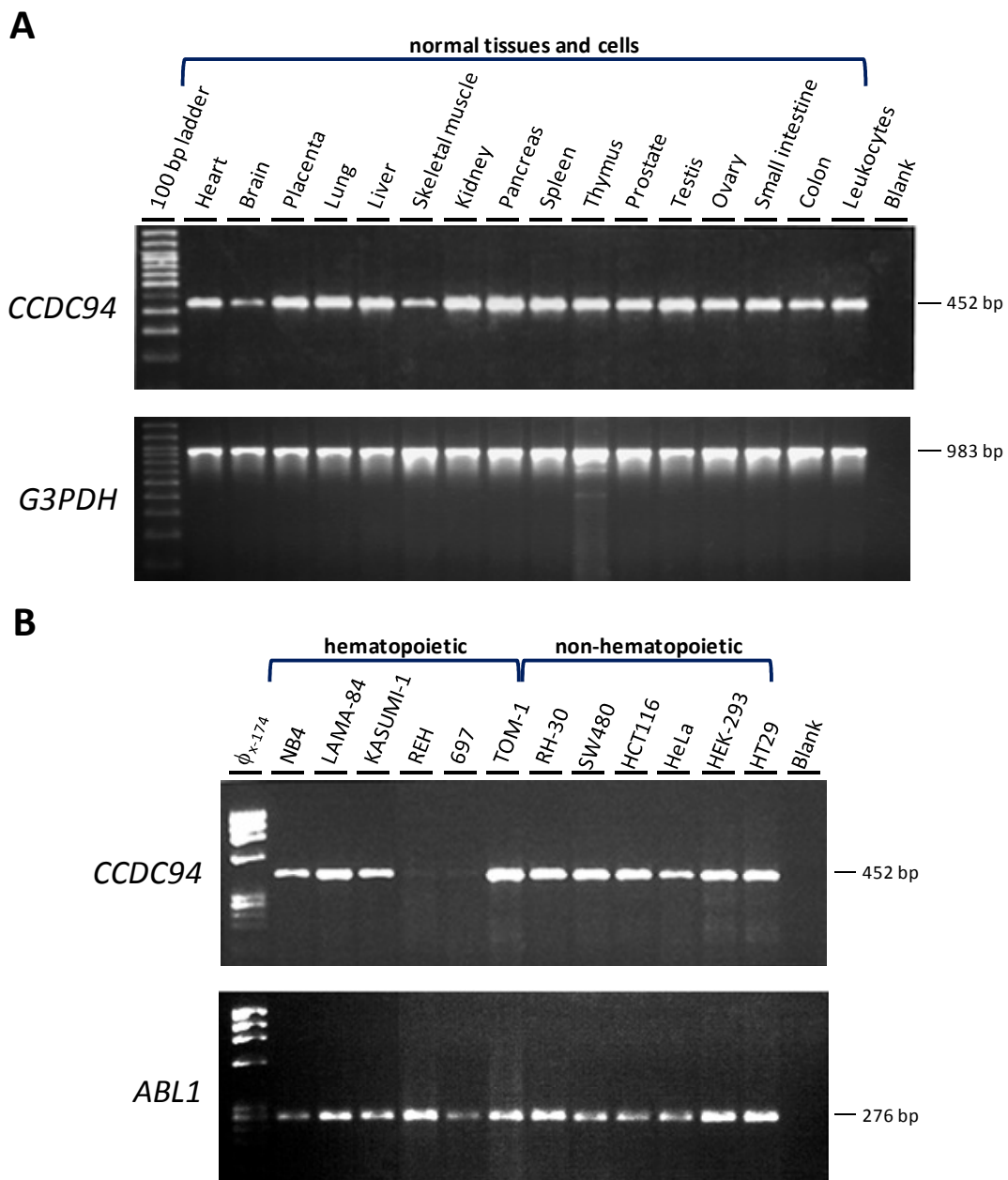


Figure 15. Expression profile of the *CCDC94* gene in human cells.

(A) Agarose gel electrophoresis analysis of *CCDC94* expression and *G3PDH* control expression in 16 different normal human tissues and cells. **(B)** Agarose gel electrophoresis analysis of *CCDC94* expression and *ABL1* control expression in 12 different tumour cell lines. The *CCDC94* gene was expressed in all cDNA samples tested, although at apparently low levels in REH and 697 lymphoid cell lines. Sizes of PCR products are shown at the right of the gel images.

RT-PCR was also used to assess the expression of *CCDC94* in 16 different normal human tissues and cells as well as in 12 tumour cell lines of a variety of origins. The results showed that the *CCDC94* transcript was amplified in every normal sample, indicating that the gene is ubiquitously expressed in human cells (**Fig. 15A**). In cell lines, the expression levels of *CCDC94* were more similar among those of non-hematopoietic origin than between those of hematopoietic origin (**Fig. 15B**). In particular, expression of *CCDC94* was significantly lower in 2 (REH and 697) out of 3 B-cell lymphoblastic leukemia cell lines comparing to those of myeloid lineage (NB4, LAMA-84 and Kasumi-1), indicating that this gene may have a more pronounced role in myeloid lineage cells.

3.2.5.4. CCDC94 IS A NUCLEAR PROTEIN WITH A ROLE IN CELL CYCLE PROGRESSION

According to the GenBank database, *CCDC94* has an open reading frame of 972 nucleotides which encode a 323-aminoacid protein. Protein homology searches revealed that *CCDC94* belongs to the conserved DUF572 family of eukaryotic proteins of unknown function. However, similarity searches followed by BLAST alignment showed that *CCDC94* is highly similar to the 270-aminoacid cell cycle control protein *cbf1* of the yeast *Schizosaccharomyces pombe*. The similarity region includes aminoacids 1-192 of *CCDC94* and aminoacids 1-204 of *cbf1*, of which approximately half (99 residues) are identical (**Fig. 16**). Using the Psort II computer program, the complete *CCDC94* hypothetical protein sequence (GenBank accession numbers AAH19096, AAH00561 and NP_060544) was searched for functional motifs. We found that *CCDC94* contains 2 coiled-coil (CC) domains in the middle region of the protein and 2 regions at aminoacid positions 203-206 and 238-246 whose corresponding residues, RKRR and PKPKRKVEV respectively, matched the consensus nuclear localization signal (NLS) (**Fig. 17A**). Furthermore, *CCDC94* contains proline at a frequency of 8%, which is above the average rate of 4.1% in human proteins, suggesting a possible role as a transcriptional activator (Nakamura *et al.*, 1993).

With these data in mind, the entire coding sequence of *CCDC94* was cloned in 2 expression vectors which were used to transfect 3 cell lines (HeLa, NIH-3T3 and DLD1) in order to determine its intracellular localization and its potential role in the cell cycle. The transcription of the *CCDC94* mRNA originates a protein with a calculated molecular mass of 37 kDa. To confirm the expression of the *CCDC94* protein, Western blot analysis was performed with HeLa cell lysates using anti-GFP (**Fig. 17B**) and anti-FLAG (results not shown) antibodies.

For every cell line/construct combination tested, the epitope-tagged CCDC94 protein localized to the nucleus and was absent from the cytoplasm (**Fig. 17C**).

A

```

CCDC94: 1  MSERKVLNKYYPPDFDPSKIP-----K LKLPKDRQYVVRLMAPFNMRCKTCGEYIYK GKK 55
           MSERKVLNKY•PPD+DPS••P•••••K•+•P•••+••VRLM•PF+MRC•TCGEYIYK GKK
cwf16: 1  MSERKVLNKYIPPDYDPSIRPPK KKKKFQGPNGGKLTVR LMTPF SMRCHTCGEYIYK GKK 60

CCDC94: 56  FNARKETVQNEVYLG LPIFRFYIKCTRCLAEITFKTDPENTDYTM EHGATRNFQ--AEKL 113
           FNARKE••••E•Y••+•I•RFYI+CTRC•AEITF•TDP++•DY••E•GA+RN++•••EK•
cwf16: 61  FNARKEKT-GEKYFS IDILRFYIRCTRCAA EITFITDPKHADYAAESGASR NYEPWHEKR 119

CCDC94: 114  LEEEEKRVQKEREDE ELN NPMKVLENR TKDSKLEMEVLENLQ ELKDLNQRQA HVDFE --- 170
           L+E•E+••••ER•D••••+•M+•LE•+T•D+K•+M++•+•L•EL++•+•R++•V++•••
cwf16: 120  LQEYEENELAERN DIPEEDEM EKLEQK TLDTKR QMQISDALDELREKSARR SRVNIDDAI 179

CCDC94: 171  AMLRQH---RLSEEE RRRQQQE EDEQE TAALLEEARKRR LLEDSDSEDEAAPS LQPALR 227
           A+L++•••••+•EEE•++++•EE+E••••A•••••+••••+••••••••L•••+•
cwf16: 180  ALLKEDAYGSIEEEE SKKRKF EEEEEIDREAKSLFSSQDGEI IRR LNAETTVEKELPKPID 239

CCDC94: 228  PNP TAILDEAPKPKR KVEVWEQSVGSLGSRPPL SRLVVVKKAKAD PDCSNGQPQAAP TPG 287
           •••••+•••••+•••••+•••••+•••••+•••••+•••••+•••••+•••••+•••••
cwf16: 240  LVSEKLATS NIPNFQPPKYAKR KMEKKV LV----- 270

CCDC94: 288  APQNRKEANPTPLTP GASSLSQLGAYLDSDD SNGSN 323
           ••••••••••••••••••••••••••••••••••••••••••••••••••••••••••
cwf16: -----

```

B

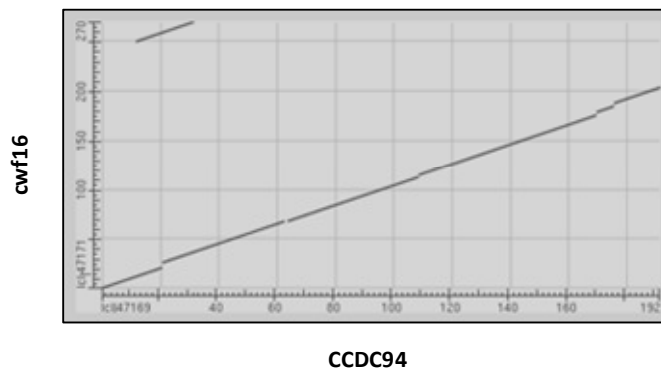


Figure 16. Sequence alignment between the human CCDC94 protein and the cwf16 protein of *S. pombe*. (A) Aminoacid sequence alignment between CCDC94 (GenBank accession number NP_060544) and cwf16 (GenBank accession number Q9P7C5) using BLAST analysis with compositional score matrix adjustment (Altschul *et al.*, 2005). The intervening sequence represents aminoacid identity (letter) and aminoacid similarity (plus sign) between CCDC94 and cwf16. Black dots indicate dissimilar aminoacids. Numbers indicate aminoacid positions. Horizontal bars in CCDC94 and cwf16 represent sequence gaps. (B) Dot matrix view of CCDC94 and cwf16 alignment. Lines in the graph indicate regions of aminoacid similarity between proteins. The region between positions 1 and 192 of CCDC94 is highly similar to the region comprised between aminoacids 1 and 204 of cwf16. A smaller region of CCDC94 between aminoacids 13 and 32 is also similar to aminoacids 251 to 270 of cwf16. X- and Y-axis represent CCDC94 and cwf16 aminoacid sequences, respectively.

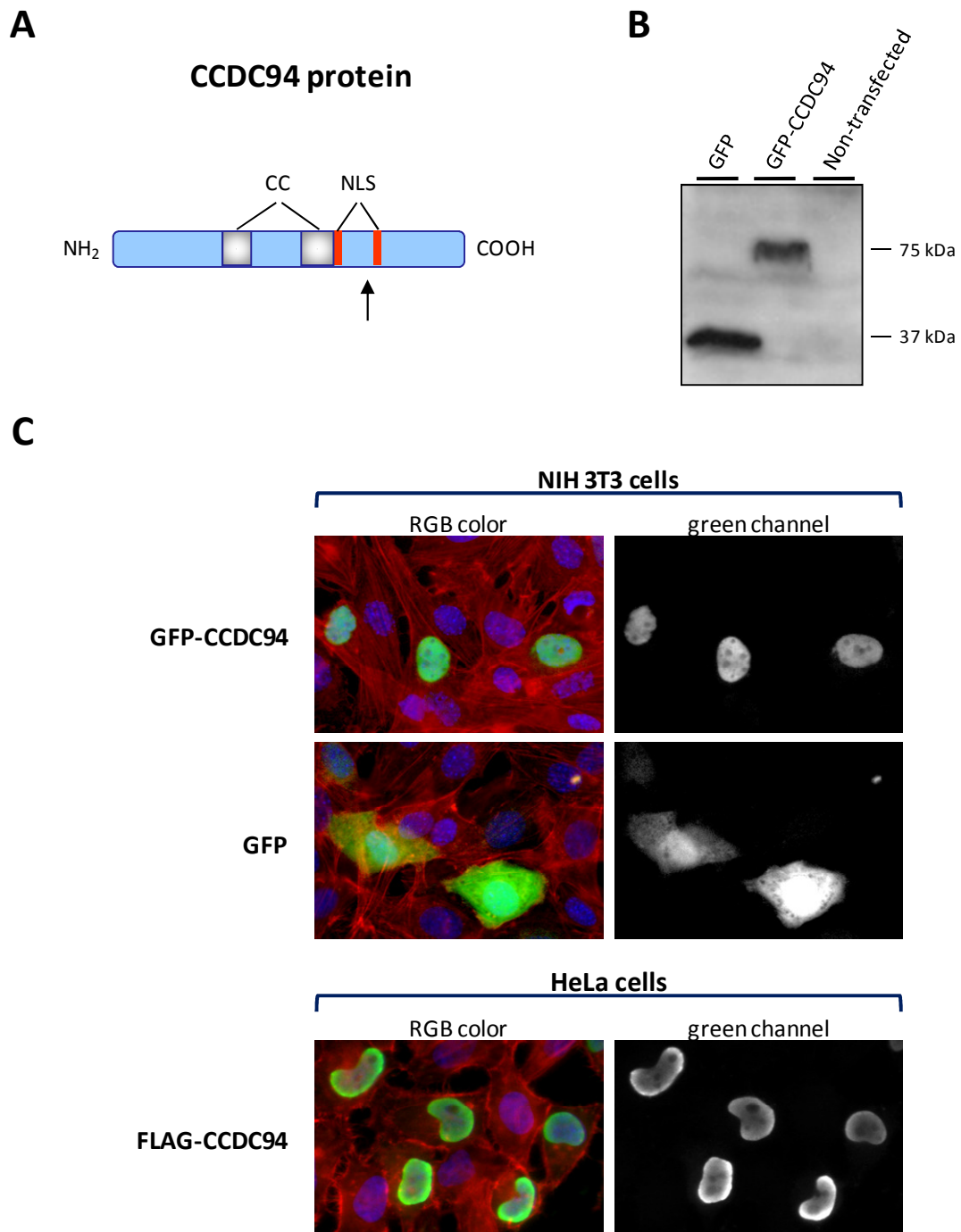


Figure 17. Domain composition, expression and intracellular localization of the human CCDC94 protein.

(A) Diagrammatic representation of the putative 323-aminoacid CCDC94 protein containing 2 CC domains and 2 NLS. The arrow underneath the protein outline indicates the approximate location of the *CCDC94* breakpoint in t(9;11;19) in respect to its corresponding coding sequence. The breakpoint was immediately upstream of the sequence coding for the most C-terminal NLS. **(B)** Western-blot results of GFP- and GFP-CCDC94-transfected HeLa cell lysates probed with rabbit anti-GFP ab290 antibody. Approximate sizes of protein bands are shown alongside the gel image. **(C)** Left panels: Red-green-blue (RGB) images corresponding to immunofluorescence analyses of NIH-3T3 cells transfected with GFP- and GFP-CCDC94, and of HeLa cells transfected with FLAG-CCDC94. Right panels: Corresponding grey images of the green channel. For either cell type the CCDC94 protein was exclusively found in the nucleus. In NIH-3T3 cells, GFP alone and GFP-CCDC94 were detected using the same antibodies as for Western blot. Detection of the CCDC94 protein in cells transfected with FLAG-tagged cDNA was performed using a primary mouse anti-FLAG M2 antibody followed by secondary goat anti-mouse FITC antibody. The actin cytoskeleton and nuclear shape were visualized using phalloidin-TRITC and DAPI, respectively, in cells transfected with either tag.

CS-starved mouse fibroblasts are a well-characterized cell model system to study cell cycle progression, as previously described (Matos & Jordan, 2005). These cells significantly decrease the rate of the G1- to S-phase transition of the cell cycle when the CS concentration in culture medium is reduced from 10% to 1%. Thus, to evaluate a potential role of the *CCDC94* protein in the G1- to S-phase progression, NIH-3T3 cells were starved in 1% CS, after which the percentage of BrdU incorporation into replicated DNA was compared between cells transfected with the *CCDC94* cDNA or the expression vector alone.

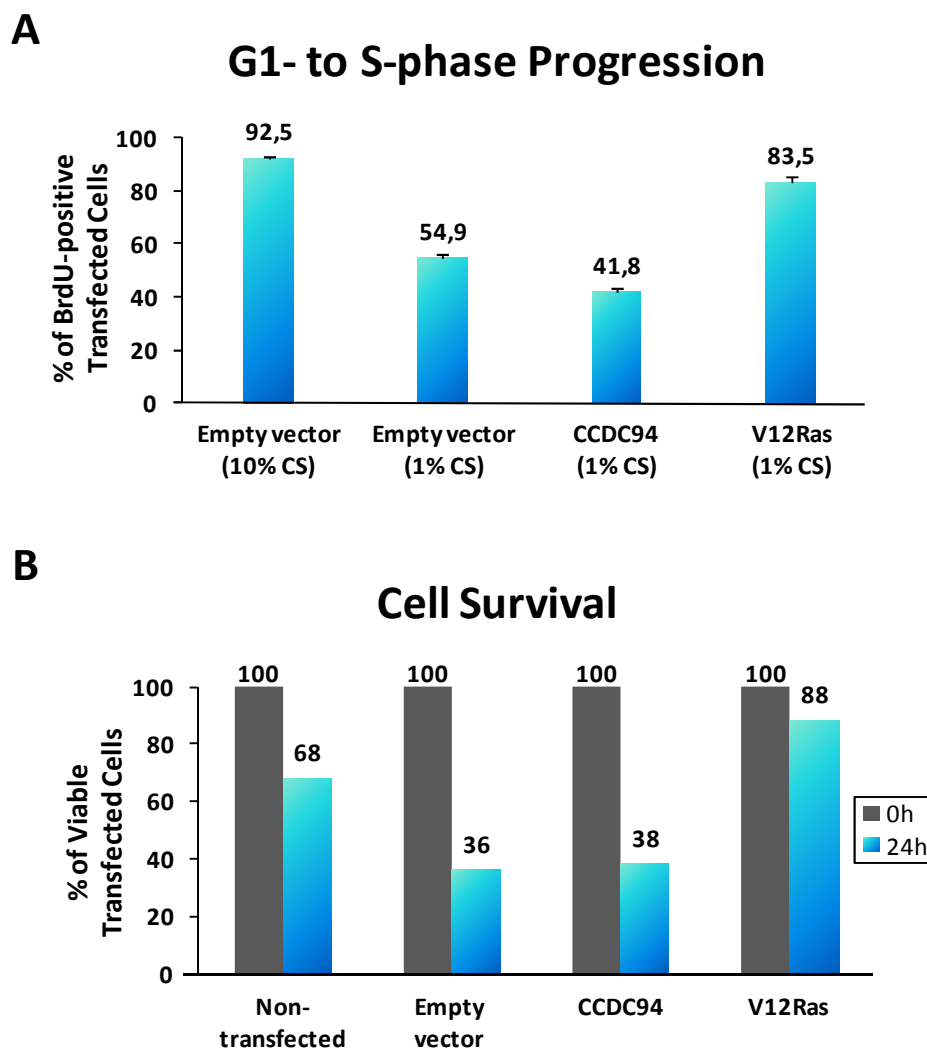


Figure 18. Effect of *CCDC94* expression on G1- to S-phase cell cycle progression and on survival of NIH-3T3 cells. (A) Results of the G1- to S-phase cell cycle progression assays. *CCDC94* induced a decreased rate of G1- to S-phase transition in serum-starved fibroblasts compared to the empty vector. The percentage of BrdU incorporation in serum-starved NIH-3T3 cells transfected with the highly oncogenic *H-RAS* gene (*V12Ras*) is also shown for comparison. Bars represent the average values of 2 independent experiments. Vertical lines on top of the bars indicate standard deviation. (B) Results of the cell survival assay. *CCDC94* had no relevant positive effect on NIH-3T3 cell survival after 24 hr of starvation in a serum-free medium compared to the empty vector. The percentage of viable NIH-3T3 transfected cells with oncogenic *V12Ras* is shown for comparison.

Incorporation of BrdU was observed in 54.9% of the cells [total cells counted (n)=305] transfected with the GFP vector alone, whereas it was restored in 83.5% of the cells (n =332) transfected with oncogenic *H-RAS* cDNA used as a control (**Fig. 18A**). In contrast, only 41.8% of cells (n =281) expressing the CCDC94 protein were BrdU-positive. Thus, the expression of the CCDC94 protein further inhibited the rate of G1- to S-phase transition in a statistically significant manner (P =0.013). However, the expression of CCDC94 had apparently no effect on cell viability, because after 24 hr of starvation in CS-free medium, 36% of cells (n =121) transfected with the empty vector were alive as compared to 38% of cells (n =116) containing the CCDC94 protein (**Fig. 18B**).

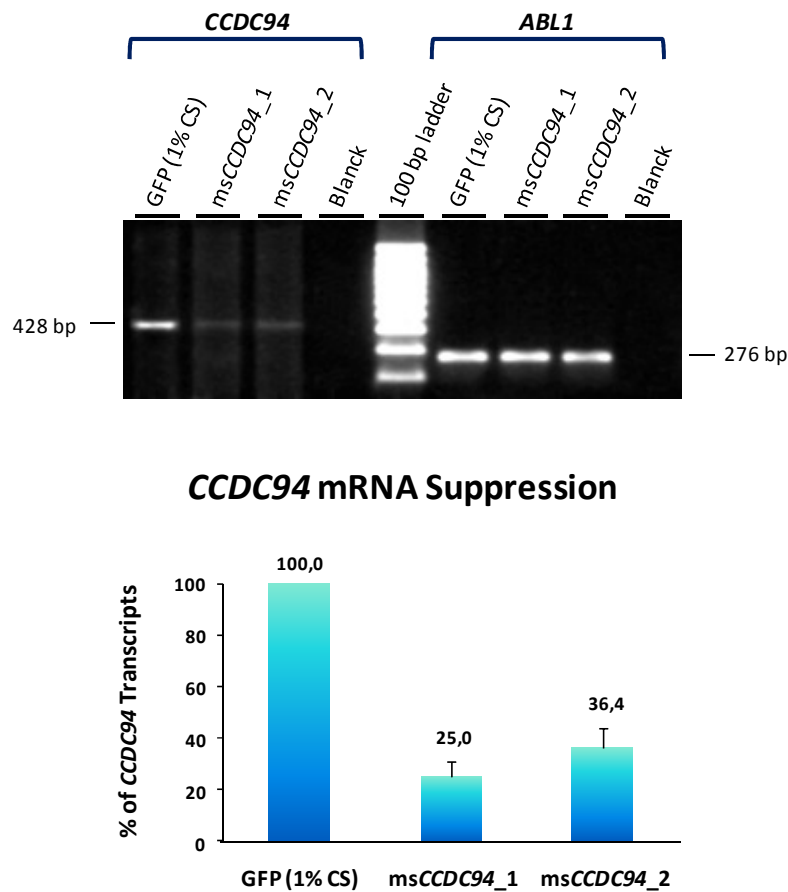


Figure 19. Suppression of *CCDC94* transcripts in NIH-3T3 cells.

Upper panel: Agarose gel electrophoresis analysis of *CCDC94* and *ABL1* RT-PCR products amplified from serum-starved NIH-3T3 cells transfected with siRNA oligos. Corresponding sizes of amplification products are shown on each side of the gel image. Lower panel: Graphical representation of densitometric analysis of the RT-PCR products. The *ABL1* amplicon was used as a loading normalizer, and the values of *CCDC94* expression were plotted as a percentage of the cells transfected with GFP siRNA. Bars represent the average values of 2 independent experiments. Vertical lines on top of the bars indicate standard deviation.

To confirm the role of *CCDC94* in cell cycle regulation, RNA interference was performed to knock down endogenous *CCDC94* expression in NIH-3T3 cells. Following 24 hr of siRNA transfection, *CCDC94* transcript levels assessed by densitometric analysis of semi-quantitative RT-PCR results showed successful suppression down to 25% and 36.4% with siRNA oligos *msCCDC94_1* and *msCCDC94_2*, respectively, compared to the control GFP siRNA (**Fig. 19**). Under these conditions, incorporation of BrdU, which dropped to 46.7% ($n=467$) in cells transfected with GFP siRNA, was rescued to 77% ($n=607$) and 75.6% ($n=599$) with *msCCDC94_1* and *msCCDC94_2*, respectively (**Fig. 20**). These data show that a reduction in *CCDC94* expression stimulates cell cycle progression and proliferation.

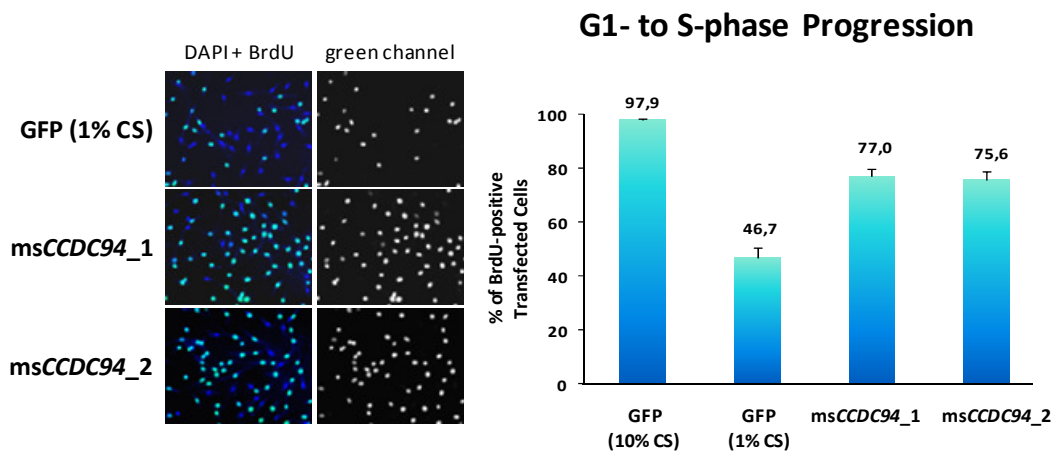


Figure 20. Effect of *CCDC94* suppression on G1- to S-phase cell cycle progression of NIH-3T3 cells.

Transfection with either *CCDC94* siRNA resulted in increased numbers of BrdU-positive cells after 24 hr incubation when compared to the control (GFP). Left: Representative immunofluorescence images of serum-starved NIH-3T3 cells transfected with GFP, *msCCDC94_1*, and *msCCDC94_2* siRNAs. Right: Graphical representation of quantitative analysis of cell numbers. The average of 2 independent experiments is shown. Vertical lines indicate standard deviation.

3.2.6. DISCUSSION

We have described an infant patient with AML-M4 whose leukemic cells harbored a $t(9;11;19)(p22;q23;p13.3)$ with involvement of the *MLL* gene at 11q23. The rearrangement resulted in the fusion of *MLL* to the *MLLT3* gene on the der(11), as seen in leukemia patients with a classical $t(9;11)(p22;q23)$ (Iida *et al.*, 1993; Nakamura *et al.*, 1993). However, the presence of an extra chromosome breakpoint at band 19p13.3, where 2 other *MLL* partner genes, *MLLT1* (Tkachuk *et al.*, 1992) and *SH3GL1* (So *et al.*, 1997), are localized, suggested that

MLL could also have rearranged with another gene in the same region. To test this hypothesis, we developed LDI-PCR assays to clone the breakpoints on the der(11) and der(19). Sequence analysis of the amplified *MLL-MLLT3* genomic fusion on the der(11) showed that intron 5 of *MLL* was fused to *MLLT3* intron 5, resulting in an in-frame *MLL* exon 5-*MLLT3* exon 6 fusion transcript. On the der(19), the 3' part of *MLL* was joined to the sequence of a novel gene known as *CCDC94*. This gene runs 5' to 3' from the telomere to centromere on the short arm of chromosome 19 whereas *MLL* lies 5' to 3' from the centromere to telomere on 11q. Thus, no functional fusion gene can be generated between *CCDC94* and *MLL* as a consequence of the translocation because these 2 genes are oriented in opposite directions on the der(19). The same evidence applies to the *MLLT3-CCDC94* fusion on the der(9) that we amplified, because *MLLT3* runs 5' to 3' from the centromere to the telomere of the chromosome 9 short arm. Thus, the chromosome 19 breakpoint in the t(9;11;19) likely resulted in loss of function of one *CCDC94* allele.

MLLT3 contains 2 major breakpoint cluster regions, BCR1, in intron 4, and BCR2, in the region spanning introns 7 and 8 (Strissel *et al.*, 2000). Recently, breakpoints in intron 3 and the centromeric region of intron 4 were reported in rare ALL and t-AML cases (Langer *et al.*, 2003). We could not find another case with a breakpoint in intron 5 and/or with a direct fusion of *MLLT3* exon 6 to *MLL*, as shown in the present patient, in other reports of t(9;11)-positive patients in which the *MLL-MLLT3* fusion had been analyzed at the genomic and/or RNA levels (Iida *et al.*, 1993; Nakamura *et al.*, 1993; Negrini *et al.*, 1993; Yamamoto *et al.*, 1994; Felix *et al.*, 1995; Super *et al.*, 1997; Atlas *et al.*, 1998; Odero *et al.*, 2000; Strissel *et al.*, 2000; Langer *et al.*, 2003; Whitmarsh *et al.*, 2003). Despite its atypical localization, the intron 5 breakpoint region was nevertheless contained within the SAR2 region of *MLLT3* (Strissel *et al.*, 2000). SARs are A/T-rich DNA regions of variable size found mainly in the non-transcribed flanking regions or in transcribed intronic regions of genes. Because of their DNA unwinding properties, SARs facilitate the access of protein factors responsible for regulating transcription, replication, or chromosome condensation to target sequences (Strissel *et al.*, 2000). In *CCDC94*, the breakpoint site is in a 23 bp A/T tract, which may indicate that it is also in a putative SAR. Although there is no published study on SARs in *CCDC94*, the present data indicate that these DNA structural elements may be implicated in the fusion of both *MLLT3* and *CCDC94* to *MLL* in the patient with t(9;11;19).

Sequence analysis of the *MLL* breakpoints on the der(11) and der(19) showed that a duplicated sequence from *MLL* of 161-164 bp was present in both derivative chromosomes. De novo leukemias associated with *MLL* rearrangements often contain duplications or deletions of several hundred base pairs at the involved breakpoints (Super *et al.*, 1997; Raffini *et al.*, 2002).

By contrast, in treatment-related cases in which DNAt2 inhibitors have been implicated, interchromosomal DNA recombination was achieved with the loss of no or only a few bases (Lovett *et al.*, 2001; Whitmarsh *et al.*, 2003). Although there was no evidence to support the involvement of DNAt2 in DNA damage in our case, it is possible that the duplication may have originated from 2 staggered nicks introduced by 2 DNAt2 in the double-stranded *MLL* DNA followed by subsequent template-directed polymerization of the single-stranded overhangs between the staggered nicks. In this context, a large epidemiological study has shown that maternal consumption of specific naturally-occurring DNAt2 inhibitors during pregnancy increases the risk of AML cases with *MLL* rearrangements (Spector *et al.*, 2005). The presence of microhomologies at the breakpoint junctions of *MLL* and *MLLT3* and of *MLL* and *CCDC94* suggests that the NHEJ mechanism of double-strand break repair was involved in the genesis of the translocation (Felix *et al.*, 1995).

In our study expression of the *CCDC94* gene was observed in all cell lines and normal tissue tested, indicating that this gene is ubiquitously expressed in human cells. The *CCDC94* protein contains 2 CC domains, two NLS at the C-terminus, and is rich in proline. These structural motifs are shared by other partner genes participating in *MLL*-associated 11q23 aberrations, including *AF4*, *MLLT3*, and *MLLT1* (Nakamura *et al.*, 1993), which suggests that *CCDC94* may also have similar properties. The fission yeast protein *cwf16* is highly homologous to *CCDC94* and is part of a large multiprotein complex containing Myb-related protein *cdc5*, implicated in pre-mRNA splicing and cell cycle progression (Ohi *et al.*, 2002). Within the complex, the *cwf16* gene is essential, although its exact function has not been determined (Ohi *et al.*, 2002). In agreement with this, the homologous human protein *CCDC94* localized exclusively to the nucleus in every cell line/expression vector combination analyzed in this study. Furthermore, expression of the protein in NIH-3T3 cells specifically resulted in a decrease in the G1- to S-phase transition but did not affect cell survival. When the *CCDC94* transcript was knocked down using siRNA, an increase in cell proliferation was observed. These results suggest that the *CCDC94* protein is a negative regulator of cell cycle progression. In the AML patient with t(9;11;19), one copy of the *CCDC94* gene was rendered non-functional. Thus, haplo-insufficiency of *CCDC94* may have deregulated cell cycle progression of leukemic cells carrying t(9;11;19), therefore facilitating proliferation of the malignant clone. Assessment of the *CCDC94* expression in the patient's bone marrow cells was not performed due to the fact that the sample available for the RNA studies had been obtained at disease relapse and contained a significant proportion (>25%) of donor cells.

As a means to understand the mechanism of *MLL* fusion proteins *in vivo*, knock-in murine models (Corral *et al.*, 1996; Dobson *et al.*, 1999) and retroviral-mediated transduction

assays (Lavau *et al.*, 1997) have been developed for the *MLL-MLLT3* and *MLL-MLLT1* fusions, respectively. Studies using these models confirmed that expression of either fusion protein could promote leukemogenesis in mice. However, they also showed that the latent period for leukemia onset is relatively long (Lavau *et al.*, 1997; Dobson *et al.*, 1999). In another retrovirus-mediated gene transfer experiment, it was demonstrated that only a very small number of myeloid cells expressed significant levels of the MLL fusion proteins 10 weeks after bone marrow transplantation of hematopoietic progenitors transduced with the *MLL-ELL* fusion gene (Lavau *et al.*, 2000). However, high expression was observed when the animals succumbed to AML, between 100 and 200 days after transplantation (Lavau *et al.*, 2000). These results indicate that additional mutations are likely necessary for the leukemic clone carrying an *MLL* translocation to achieve full tumorigenic potential. In particular, short latency leukemias like those associated with the *MLL-MLLT3* fusion suggest that a simultaneous double hit may occur, thus reducing the need for the acquisition of subsequent mutations (Ayton & Cleary, 2001). In the present case, deregulated cell cycle arrest induced by haploinsufficiency of *CCDC94* along with an *MLL* gain of function may have cooperatively promoted leukemogenesis in the AML carrying the t(9;11;19). Interestingly, molecular analysis of another complex translocation involving chromosomes 4, 7, and 11 in a patient with ALL disclosed that in addition to an *MLL-AF4* fusion gene, the 3' portion of the *MLL* gene was fused in-frame with the cyclin-dependent kinase 6 (*CDK6*) gene on chromosome 7 (Raffini *et al.*, 2002). In this case, it is possible that the CDK6-MLL fusion protein may have contributed to leukemogenesis as well. The main role of *CDK6* in cell cycle progression and its frequent alteration in B- and T-cell malignancies by chromosomal translocation (Corcoran *et al.*, 1999; Su *et al.*, 2004) strengthen the idea that disruption of cell cycle control mechanisms is critical for the progression of a malignancy. Whether genetic alterations of the *CCDC94* gene, other than translocations, also occur in other *MLL-MLLT3*-positive patients exhibiting a reciprocal t(9;11) remains to be determined.

In summary, this work provides evidence for a 3-way complex translocation involving *MLL* and *MLLT3* and shows that extra breakpoints may indicate the locations of additional genes relevant to the proliferation of myeloid cells that otherwise might remain unnoticed. One such candidate gene is *CCDC94*.

3.3. THREE-WAY TRANSLOCATION (X;20;16)(p11;q13;q23) IN ESSENTIAL THROMBOCYTHEMIA IMPLICATES *NFATC2* IN DISREGULATION OF GM-CSF EXPRESSION AND MEGAKARYOCYTE PROLIFERATION

Submitted.

Authors: Vieira L, Vaz A, Ambrósio AP, Nogueira M, Marques B, Silva E, Matos P, Pereira AM, Jordan P, da Silva MG

We acknowledge Dr. Jorg Becker (Instituto Gulbenkian de Ciência, Oeiras, Portugal) for whole-genome array processing, Prof. Jürgen Kohlhase (Institut für Humangenetik und Anthropologie, Universität Freiburg, Freiburg, Germany) and Dr. Dezso David (Departamento de Genética, Instituto Nacional de Saúde Dr. Ricardo Jorge) for fruitful discussions, Prof. Mariano Rocchi (Dipartimento di Genetica e Microbiologia, Università di Bari, Italy) for generous gift of RP11-library BAC clones, Dr. Eleonora Paixão (Departamento de Epidemiologia, Instituto Nacional de Saúde Dr. Ricardo Jorge) for statistical analyses and Dr. Sónia Pedro and Dr. Ana Cardoso (Departamento de Genética, Instituto Nacional de Saúde Dr. Ricardo Jorge) for capillary electrophoresis analyses. I also wish to acknowledge the patients for their volunteer participation in this study.

This work was supported by grants from the Fundação para a Ciência e a Tecnologia-Programa Operacional Ciência e Inovação 2010 (POCI/SAU-OBS/59609/2004) and Associação Portuguesa Contra a Leucemia (Bolsa APCL 2007-40.2P.AP/MJ).

3.3.1. ABSTRACT

ET is a chronic MPN essentially characterized by a sustained excessive amount of circulating platelets. Molecular pathogenesis of ET is linked in approximately half of the patients to a defect in intracellular cytokine signaling pathways as a result of *JAK2* and/or *MPL* gene gain-of-function mutations. However, no genetic defects associated with cytokine production and/or regulation has been identified in ET or in other MPN subtypes. Using molecular cytogenetics, PCR and whole-genome array analyses, we uncovered a submicroscopic deletion at 20q13 in a *JAK2V617F*-positive ET patient with an acquired 3-way t(X;20;16) which deleted the nuclear factor of activated T-cells, cytoplasmic, calcineurin-dependent 2 (*NFATC2*, also known as *NFAT1* or *NFATP*) gene. This gene encodes a transcription factor involved in the regulation of hematopoietic cytokines and is located at a genomic region frequently targeted by chromosome 20q deletions in MPN patients. RNA interference-mediated suppression of *NFATC2* mRNA increased the levels of *GM-CSF* mRNA and promoted proliferation of a *JAK2V617F*-positive ET cell line *in vitro*. These effects were also observed upon treatment of cells with a cell-permeable inhibitor of NFATC2, indicating that loss of NFATC2 may promote proliferation of megakaryocytes through an up-regulation of myeloid lineage-specific cytokines. Preliminary studies also showed lower levels of *NFATC2* mRNA by Q-PCR in granulocytes of ET patients. Moreover, because the t(X;20;16) also resulted in the deletion of the transcription factor *MAF* at 16q23, we hypothesize that haplo-insufficiency of *NFATC2* and *MAF* genes concurred to promote abnormal production of cytokines in the ET patient. Taken together, these results indicate that pathogenesis of ET may also be linked to genetic defects of transcription factor genes involved in the regulation of cytokine expression and further suggest that megakaryocyte proliferation may be under the control of the calcineurin-NFAT pathway.

3.3.2. INTRODUCTION

MPNs are a group of clinically and biologically-overlapping disorders characterized by proliferation of terminally-differentiated erythroid, megakaryocytic and/or myeloid cells. ET is a MPN characterized clinically and pathologically by proliferation of enlarged megakaryocytes in the bone marrow and persistent increase of platelet count in the peripheral blood (Michiels & Thiele, 2002). ET also shares with PV and PMF several features including, for instance, non-random chromosome abnormalities, marrow hypercellularity and fibrosis, thrombosis and

hemorrhage, extramedullary hematopoiesis, and a predisposition for transformation to acute leukemia (Spivak, 2004). In particular, the risk of transformation to other myeloid disorder increases from 9.1% in the first decade to 58.5% in the third decade of the disease (Wolanskyj *et al.*, 2006).

The pathogenesis of ET, PV and PMF is closely linked to abnormalities of the cytokine signaling apparatus (Kaushansky, 2006). Earlier works in PV patients have shown that erythroid progenitor cells form endogenous colonies *in vitro* in the absence of erythropoietin (Prchal & Axelrad, 1974) and that the erythroid, granulocyte-macrophage and megakaryocyte progenitors are hypersensitive to interleukin-3 (IL-3) and granulocyte-macrophage colony stimulating factor (GM-CSF) *in vitro* (Dai *et al.*, 1992). In essential thrombocythemia, megakaryocytic progenitor cells display hypersensitivity to recombinant thrombopoietin (TPO) (Axelrad *et al.*, 2000). More recently, investigations of the defects of erythropoietin signaling in MPN patients led to the discovery of a somatic gain-of-function mutation of the *JAK2* gene (James *et al.*, 2005). The *JAK2*V617F mutation was reported to occur in the majority of patients with PV and in approximately half of those with PMF or ET (Baxter *et al.*, 2005; James *et al.*, 2005; Jones *et al.*, 2005; Kralovics *et al.*, 2005). Moreover, gain-of-function mutations in the *MPL* gene encoding the TPO receptor are additionally seen in roughly 5% of patients with PMF and in rare ET patients but not in those with PV (Pardanani *et al.*, 2006; Pikman *et al.*, 2006). Taken together, these data link a cytokine signaling defect in MPN patients to constitutive activation of the JAK-STAT pathway as a result of *JAK2*V617F or other mutations. However, genetic events in MPN patients potentially responsible for abnormalities in the expression and regulation of cytokine genes remain to be determined.

Here we describe the cytogenetic and molecular study of an acquired 3-way complex translocation detected in the bone marrow cells of an ET patient. The rearrangement was associated with 2 submicroscopic deletions at chromosome bands 20q13.13 and 16q23.1-16q23.2. The 20q deletion overlapped 3 genes only, including *NFATC2*, ATPase class II type 9A (*ATP9A*), and SAL-like 4 (*SALL4*). We focused our attention on *NFATC2* because it is expressed at high levels in CD34+ and megakaryocytic cells (Kiani *et al.*, 2004). *NFATC2* belongs to the NFAT-family of transcription factor proteins which reside in the cytosol in an inactive phosphorylated conformation. In response to an elevation in cytosolic Ca²⁺ levels, NFAT proteins are dephosphorylated by calcineurin, a Ca²⁺/calmodulin-dependent phosphatase (Hogan *et al.*, 2003). Dephosphorylation of serine residues in the NH₂-terminal activation domain of NFAT exposes a NLS and masks a nuclear export signal (NES), therefore enabling NFAT proteins to translocate to the nucleus (Okamura *et al.*, 2000). In the nuclear compartment, activated NFAT proteins associate as dimers or cooperate with other

transcription factors such as AP-1 (FOS/JUN) to drive the expression of several cytokines in hematopoietic cells including interleukin-2, IL-3, interleukin-4 and GM-CSF (Cockerill *et al.*, 1993; Luo *et al.*, 1996).

On this basis we simulated a deficient NFATC2 activity in a *JAK2V617F*-positive ET cell line through suppression of the *NFATC2* transcript or inhibition of NFAT-calcineurin protein interaction *in vitro*. Results of both assays showed an up-regulation of *GM-CSF* mRNA levels and an increase in megakaryocyte proliferation. Accordingly, we found that the levels of *NFATC2* mRNA in granulocytes of ET patients were reduced compared to normal individuals. Taken together, these results indicate that haplo-insufficiency of *NFATC2* as a result of del(20q) or other mechanisms may contribute to proliferation of *JAK2V617F*-positive megakaryocytes.

3.3.3. CASE SUMMARY

A 54-year old female patient presented with a 2-year history of epigastric discomfort. Endoscopy scanning revealed hiatus hernia and gastritis. Abdominal ecographic examination showed splenomegaly. Peripheral blood white cell count and leukocyte differential were normal whereas the platelet numbers were elevated ($900 \times 10^9/L$). Bone marrow aspirate smear was normocellular whilst showing markedly increased numbers of megakaryocytes with a hyperlobulated nucleus. Bone marrow biopsy was hypercellular and showed proliferation of enlarged megakaryocytic cells. A diagnosis of ET was established based on the clinical, hematological and molecular findings, including absence of *BCR-ABL1* fusion transcripts and presence of the *JAK2V617F* mutation in the peripheral blood.

3.3.4. MATERIALS AND METHODS

3.3.4.1. COLLECTION AND PREPARATION OF SAMPLES

A prior informed consent was obtained from each patient. Leukocyte genomic DNA was extracted from ethylenediamine tetraacetic acid (EDTA)-collected blood samples using the robotic workstation MagNA Pure LC Instrument (Roche Applied Science). Peripheral blood mononuclear cells were separated using Lymphoprep (Axis-Shield PoC AS) whereas granulocytes were isolated from the lower interface of the Lymphoprep density gradient following standard erythrocyte lysis.

3.3.4.2. CYTOGENETIC AND FLUORESCENCE *IN SITU* HYBRIDIZATION ANALYSES OF CHROMOSOME REARRANGEMENTS

A bone marrow cell karyotype of the patient was established at diagnosis using standard cytogenetic procedures. Analysis of chromosome rearrangements including breakpoint localization was performed using FISH as previously described (Vieira *et al.*, 2005). FISH probes included WCP probes for chromosomes 16, 20 and X (Cambio) and several YAC, BAC and P1 artificial chromosome (PAC) probes mapping to the long arm of chromosome 20 (**Table VI**).

Table VI. Localization of clones used as FISH probes and corresponding STS markers and primer sequences.

Clone name	Clone type	Localization	STS marker	Primer sequence (5'-3')
RP11-17F3	BAC	20q12	D20S108	F:AAGACTGTCCANACATACA R:CAACAAGTCAGAAGTGCAA
RP11-69I10	BAC	20q13.11	ns	na
RP11-169A6	BAC	20q13.12	RH66078	F:ACCTTCAGAAGAGGCTCTTGG R:GGCCTTGCTCAGAAGTTTTG
RP11-314A4	BAC	20q13.12	ns	na
RP11-124D1	BAC	20q13.12	ns	na
RP11-72F10	BAC	20q13.13	D20S109	F:AAACACACATACAAACACACGCAG R:TCATACCCAGTCCTCTCAAACTC
773G6	YAC	20q13.13	D20S869	F:TGCTTTGTGTGACTGACCA
RP5-914P20	PAC			R:TGTCAACAGCCAGGTCCTA
RP5-1009H6	PAC	20q13.13	SHGC-144024	F:CTTCAACTGGTTGTGCTGAAATG R:AATCTTTGTGGCAGAAATGGAAA
957F3	YAC	20q13.13	D20S857	F:GGGCACCCATAGGTCTCT
RP5-994O24	PAC			R:TTTCACAGGGAGTAGGGCT
RP5-1114A1	PAC	20q13.13	SHGC-83700	F: GCTCCTGATACTGGTCTGGAAAA R:GCAAGGCAAAGATACCTAGTCA
RP5-827A12	PAC	20q13.13	D20S185	F:CTAGGGCCTGGCTGGT R:GGGCCTTCATGCTTCA
RP5-1112F19	PAC	20q13.13	GDB-315181	F:TCCAGGTGTGTAAGACAGG R:AAACTCTGGAACCTGGGAG
RP4-756P4	PAC	20q13.13	D20S845	F:AACCAAATCAGAATACACTGGAA R:CTCACAACCTGGCAAGAAA
RP5-831D17	PAC	20q13.13	D20S1083	F:GGTGGTGATGGAGTCTGAAG R:TATTTTCTATCCTTCAAGTACCC
RP4-548G19	PAC	20q13.13	RH94187	F:TCTTGCATGTACGGTAATTTG R:CGACTTACTCTTTTCATGGCC
RP4-698O15	PAC	20q13.13	Z94476	F:CTCCCTCACCTTTGAACCAA R:TGGTGTAGGATGGCTAACAGG
RP5-965N20	PAC	20q13.13	D20S1057	F:TTGGAAATGACAGACCTTATTTAGT
761F3	YAC			R:TTCCAGCACTGAACACTGCT
747E8	YAC			
RP5-911I5	PAC	20q13.13	SHGC-78862	F:CTGGCTTGGCAATTCAAGACTAC R:AAGCTCAGGACAGATGCAGAGAT
RP11-91L1	BAC	20q13.13	D20S854	F:TATTGCAGGTAGGAGTCCC
845F3	YAC	20q13.2		R:CTTGAAGTTGATGGTTGG
931H6	YAC	20q13.2	D20S469	F:AGCTTTCCTAGCCACTCCAT R:AGCAAAGGTTAAAAGCACCC
RP5-981M18	PAC	20q13.2	G01534	F:CACATGGCCTGAAATGAGCA R:TGACATCTTCTGGCTACAG
RP11-195N11	BAC	20q13.2	ns	na

Clones are ordered from centromere to telomere; F, forward; na, not available; ns, not selected; R, reverse.

Correspondence between clone position and genome sequence was obtained using the Map Viewer resource available at the NCBI website (<http://www.ncbi.nlm.nih.gov/mapview/>). YACs were purchased from Fondation Jean Dausset – CEPH (Paris, France) whereas PACs were obtained from BACPAC Resources (Oakland, CA). BACs were kindly supplied by Prof. Mariano Rocchi (Università di Bari, Italy). Authenticity of clone sequences was confirmed by PCR analysis of selected sequence tagged site (STS) markers. Primer sequences were obtained from the UniSTS database available at the NCBI website. Standard reactions mixtures and amplification parameters were utilized.

3.3.4.3. DELIMITATION OF THE 20q DELETION BOUNDARIES USING MICROSATELLITE POLYMORPHISMS

The methanol:acetic acid solution was removed from frozen bone marrow cell culture pellets after centrifugation. Pellets were digested in cell lysis solution [0.1 M NaCl, 0.001 M EDTA, 0.01 M (hydroxymethyl)aminomethane (Tris)-HCl (pH 8.0), 0.5% sodium dodecyl sulphate (SDS) and 0.1 mg/ml proteinase K] at 56 °C for 3 hours in a thermomixer block. Proteins were precipitated by addition of a saturated ammonium acetate solution (11.6 M) followed by centrifugation. The DNA in the supernatant was precipitated with 100% ethanol, dried and resuspended in 15 µl Tris EDTA (TE) buffer.

Six polymorphic STS markers located at 20q13.13 were analysed by PCR (**Table VII**). Primer sequences were obtained from the UniSTS database at www.ncbi.nlm.nih.gov/unists. A 25-µl reaction mixture was prepared with 9.55 µl of reaction mix (from AmpFISTR Profiler Plus PCR Amplification Kit, Applied Biosystems), 2 µM of 6-carboxyfluorescein (6-FAM)-labelled forward primer, 2 µM of non-labelled reverse primer, 0.05 U/µl AmpliTaq Gold DNA polymerase (Applied Biosystems) and 2.5 ng of DNA. Reactions were carried out with an initial denaturation of 11 min at 95 °C followed by 28 cycles of 1 min at 94 °C, 1 min at 54-60 °C and 1 min at 72 °C. A final extension step of 45 min at 60 °C was performed. Each DNA sample was amplified twice on different days. Samples were subsequently analyzed by capillary electrophoresis using the ABI Prism 3130xl Genetic Analyzer (Applied Biosystems). The 400HD ROX molecular weight marker was used as the internal lane size standard (Applied Biosystems). DNA electropherograms and allele areas were obtained using the GeneMapper v3.7 software (Applied Biosystems). Areas of alleles with overlapping stutter peak positions were corrected by subtracting the corresponding percentage of stutter peak calculated from samples with non-overlapping peak positions.

Table VII. STS markers used for delimitation of the 20q deletion.

STS name	UniSTS no.	GenBank accession no.	Repeat motif	Primer sequence (5'-3')	Amplicon size (bp) *	Annealing temperature (°C)
D20S196	80427	Z24373.1	dinucleotide	F: TTGGTGACCCTGAGACAGAGTG R: AACGAACTACCTGTTGATTTGCTCC	145-176	58
D20S869	72669	Z51140.1	dinucleotide	F: TGCTTTGTGTGACTGACCA R: TGTC AACAGCCAGGTCCTA	236-286	58
D20S857	54045	Z52686.1	dinucleotide	F: GGGCACCCATAGGTCTCT R: TTTCACAGGGAGTAGGGCT	204-220	54
D20S185	36005	Z23858.1	dinucleotide	F: CTAGGGCCTGGCTGGT R: GGGCCTTCATGCTTCA	196-214	60
D20S845	2856	Z52436.1	dinucleotide	F : AACCAAATCAGAATACTGGAA R : CTCACAATTGGCAAGAAA	148-156	54
D20S428	149228	L30950.1	tetranucleotide	F: TCTATAAGTTGGGGCTGCAG R: CTGAAAATCCCATCTCCTGA	237	58

* Product sizes correspond to those described at the UniSTS database of STS markers (www.ncbi.nlm.nih.gov/unists) and not necessarily to those obtained in the present study; The forward primer was labelled with 6-FAM at the 5' side. F, forward; n.a., not available; R, reverse.

3.3.4.4. ANALYSIS OF CHROMOSOME REARRANGEMENTS BY WHOLE-GENOME ARRAY

For microarray analysis a granulocyte cell pellet of the patient was digested in cell lysis solution as indicated above. Purification of genomic DNA was obtained by standard phenol-chloroform extraction and ethanol precipitation. DNA was eluted in TE buffer and quantified spectrophotometrically using the Biophotometer (Eppendorf). Approximately 100 ng of DNA were analysed using the cytogenetics whole-genome 2.7M array (Affymetrix) which contains approximately 2.361 million non-polymorphic markers and 400 thousand SNP markers with an average marker spacing of 1000 bp. Results were analyzed using the Chromosome Analysis Suite (ChAS) 1.1 software (Affymetrix). Signal intensity values of the sample were compared to those from a factory-loaded reference file provided by Affymetrix in the software.

3.3.4.5. RAPID AMPLIFICATION OF CDNA ENDS

The 3' RACE system (Invitrogen) and the 5' RACE system v. 2.0 (Invitrogen) were used according to the manufacturer's instructions to detect truncated *WWOX* and *NFATC2* transcripts, respectively. Briefly, for 3' RACE analysis 2 µg of total RNA from mononuclear cells were

converted to cDNA. PCR was performed using abridged universal amplification primer (AUAP) in combination with *WWOX*-ex8F primer (**Table VIII**). A semi-nested PCR was performed using AUAP in conjunction with *WWOX*-ex8F1 primer. Amplified products were electrophoresed on a 2% agarose gel and purified from the gel using the NucleoSpin Extract II (Macherey-Nagel) kit. For 5' RACE analysis approximately 1.0 µg of total RNA from granulocytes was converted to cDNA using a mixture of *NFATC2*-ex7R1, *NFATC2*-ex9R, *NFATC2*-3'A and *NFATC2*-3'B primers in equivalent amounts. An initial amplification reaction was performed using abridged anchor primer in conjunction with *NFATC2*-ex7R1 or *NFATC2*-3'B primer. A second round of amplification was performed using universal amplification primer or AUAP in conjunction with *NFATC2*-ex6R1 (or *NFATC2*-ex6R2) or *NFATC2*-ex9R primer, respectively. Amplification products were analysed in 2% ethidium bromide stained-agarose gels. Products were purified from the gel using the Jetquick Gel Extraction Spin Kit (Genomed) or directly from the PCR mixture using the DNA clean & concentrator-5 kit (Zymo Research). Purified products were sequenced in a 10 µl-reaction mixture containing 200 nM of primer and 0.5-2 µl of BigDye terminator ready reaction mix v1.1 (Applied Biosystems). Sequencing products were analyzed using the ABI Prism 3130xl Genetic Analyzer (Applied Biosystems).

Table VIII. Primers used for 3' and 5' RACE analyses.

Gene	Localization	Primer name	Primer sequence (5'-3')
<i>WWOX</i>	exon 8	<i>WWOX</i> -ex8F	AGTCGCCTCTCTCCAACAAA
<i>WWOX</i>	exon 8	<i>WWOX</i> -ex8F1	AGGTCCAAGCTCTGCAACAT
<i>NFATC2</i>	exon 6	<i>NFATC2</i> -ex6R1	GTAAAGTTCTGCCCCGTGAG
<i>NFATC2</i>	exon 6	<i>NFATC2</i> -ex6R2	AGGCAGCTGTCTGTGTCTTG
<i>NFATC2</i>	exon 7	<i>NFATC2</i> -ex7R1	TGGCTTCCATCTCCAAA
<i>NFATC2</i>	exon 9	<i>NFATC2</i> -ex9R	CTGCTGGTTGGTGGGTGAGT
<i>NFATC2</i>	3' region	<i>NFATC2</i> -3'A	TTTACGTCTGATTTCTGGCAG
<i>NFATC2</i>	3' region	<i>NFATC2</i> -3'B	TCATAATATGTTTTGTATCCAGC

3.3.4.6. EXPRESSION ANALYSIS OF *NFATC2* IN NORMAL HUMAN TISSUES

The expression pattern of *NFATC2* in human tissues was determined using the Human Multiple Tissue cDNA Panels I and II (Clontech). PCR was performed using a Biometra thermocycler in a 25 µl-reaction volume containing 50 mM KCl, 10 mM Tris-HCl (pH 8.3), 1.5 mM MgCl₂, 0.001% (wt/vol) gelatine, 0.2 mM each dNTP, 4.8 ng/µl of each primer (*NFATC2*-ex3FA: 5'-

GGGCCCACTATGAGACAGAA-3' and *NFATC2*-ex7R1: 5'-TGGCTCCATCTCCCAA-3'), 0.03 U/ μ l AmpliTaq DNA Polymerase (Applied Biosystems) and 2.5 μ l of cDNA. Cycling conditions were 5 min at 94 °C, followed by 35 cycles of 1 min at 95 °C, one min at 58 °C and 1 min at 72 °C, ending with 5 min at 72 °C. The *G3PDH* transcript (loading normalizer) was amplified likewise using primers included in the Human Multiple Tissue cDNA Panels I and II (Clontech). Amplification products were run on 2% agarose gels stained with ethidium bromide.

3.3.4.7. DETECTION OF A TRANSCRIBED SINGLE NUCLEOTIDE POLYMORPHISM IN THE *NFATC2* GENE

Genomic DNA samples were screened for the presence of a heterozygous SNP (A/C) in exon 4 of *NFATC2* (SNP database: rs6013193). Approximately 100-250 ng of genomic DNA was amplified essentially as described above using primers designed in the flanking region of the SNP (**Table IX**). Amplification products were purified using the Jetquick PCR Purification Spin Kit (Genomed) or the DNA clean & concentrator-5 kit (Zymo Research). Sequencing reactions were performed basically as described above (see section 3.3.4.4.) using PCR primers as sequencing primers.

Table IX. Primers used for detection of the rs6013193 SNP in *NFATC2* genomic DNA.

Localization	Primer name	Primer sequence (5'-3')	Amplicon size (bp)	Annealing temperature (°C)
Exon 4	<i>NFATC2</i> -ex4F	GCCATCAACAGCTGCTTCCA	358	60
	<i>NFATC2</i> -ex4R	CACACCCCGCACCTTAATGA		

Total RNA was extracted from mononuclear cells using the RNeasy Mini Kit (QIAGEN). Removal of contaminating genomic DNA was performed using in-column DNA digestion with DNase (QIAGEN). One to three micrograms of total RNA were used to prepare cDNA using the Ready-to-go You-Prime first-strand beads (Amersham) and random hexamers (Invitrogen) as synthesis primers. PCR primer pairs were designed based on available GenBank mRNA sequences to amplify a partial transcribed region of *NFATC2* in heterozygous individuals for the exon 4 SNP (**Table X**). PCR was performed essentially as described in section 3.3.4.5. Purification and sequencing of PCR products were performed as described above. PCR primers were used as sequencing primers.

Table X. Primers used for detection of a transcribed SNP (rs6013193) in exon 4 of *NFATC2*.

Localization	Primer name	Primer sequence (5'-3')	Amplicon size (bp)	Annealing temperature (°C)
Exons 3-6	<i>NFATC2</i> -ex3FA	GGGCCCACTATGAGACAGAA	550	56
	<i>NFATC2</i> -ex6R1	GTAAAGTTCTGCCCGTGAG		

3.3.4.8. MUTATIONAL ANALYSIS OF *JAK2* AND *NFATC2* GENES

Peripheral blood samples from 20 ET patients were analyzed for the *JAK2*V617F mutation and screened for genetic alterations in *NFATC2*. Mutational analysis was performed using whole blood leukocytes or separated cell fractions [in the patient with t(X;20;16)]. Genomic DNA was obtained from granulocytes and mononuclear cells by incubation in cell lysis solution as described above followed by standard phenol-chloroform purification and ethanol precipitation. The presence of *JAK2*V617F was analyzed by allele specific-polymerase chain reaction (AS-PCR), PCR-*Bsa*XI digestion, and/or direct sequencing analysis of *JAK2* exon 14 PCR products, essentially as described (Baxter *et al.*, 2005; Arellano-Rodrigo *et al.*, 2006). All exon and flanking intronic sequences of *NFATC2* were amplified using primers described in **Table XI**. The Primer3 software available at http://frodo.wi.mit.edu/cgi-bin/primer3/primer3_www.cgi (Rozen & Skaletsky, 2000) was used for primer design. PCR was performed using a Biometra thermocycler in a 50 µl-reaction volume containing 50 mM KCl, 10 mM Tris-HCl (pH 8.3), 1.5 mM MgCl₂, 0.001% (wt/vol) gelatine, 0.2 mM each dNTP, 3.0 ng/µl each primer, 0.03 U/µl AmpliTaq DNA Polymerase (Applied Biosystems) and 150 ng of genomic DNA. General cycling conditions were 5 min at 94 °C, followed by 35 cycles of 1 min at 95 °C, one min at 58-68 °C and 1 min at 72 °C, ending with 3 min at 72 °C. Due to the high CG content (74.5%) of exon 1, amplification of the corresponding fragment was performed using the ThermalAce polymerase (Invitrogen) essentially as described in the manufacturer's protocol. Amplicons were purified with Jetquick PCR Purification Spin Kit (GenoMed Inc.) and sequenced in both directions as described above. Sequences were aligned to each other using the ClustalW multiple alignment tool (<http://www.ebi.ac.uk/Tools/clustalw2/index.html>) and further inspected manually for nucleotide alterations.

Table XI. Primers used for amplification of *NFATC2* exons and corresponding flanking exon/intron boundaries.

Amplicon	Primer name	Primer sequence (5'-3')	Amplicon size (bp)	Annealing temperature (°C)
exon 1	<i>NFATC2</i> -ex1FA	CCTCCGGAGCAGGAAGCTC	433	68
	<i>NFATC2</i> -ex1RA	AGGACTCCTGTGCCAGTCC		
exon 2	<i>NFATC2</i> -ex2A1F	GATTGCTCTGCACCGGGAGT	591	60 (a)
	<i>NFATC2</i> -ex2A1R	GGCGAGGTTCTGGGGGAATA	743	66 (b)
	<i>NFATC2</i> -ex2B1F	CCTGCGTCTCGCCAATAAC		
	<i>NFATC2</i> -ex2B1R	AGGGTCTCGCAACCAGCAAG		
exon 3	<i>NFATC2</i> -ex3F	GCAACAAACAGTGGGTCAGCA		
	<i>NFATC2</i> -ex3R	GGTTTATTGCACACATGGCTGAT		
exon 4	<i>NFATC2</i> -ex4F	GCCATCAACAGCTGCTTCCA	358	60
	<i>NFATC2</i> -ex4R	CACACCCCGCACCTTAATGA		
exon 5	<i>NFATC2</i> -ex5F	CGGGTACCTCGCCAGAATA	335	60
	<i>NFATC2</i> -ex5R	GCAGCTTTGGGGTGATCTT		
exon 6	<i>NFATC2</i> -ex6F	TGCATGATTCTGGGGGACAG	297	60
	<i>NFATC2</i> -ex6R	GGTGACACAGGTGGGCAGAG		
exon 7	<i>NFATC2</i> -ex7F	AGGGAAACGTGAGGGGGATT	242	60
	<i>NFATC2</i> -ex7R	CGTGCACATATTGACACACACC		
exon 8	<i>NFATC2</i> -ex8F	TCCTGAGCCCTGTGCCTGTA	264	60
	<i>NFATC2</i> -ex8R	CCTGGATGCGCTTAGGGTCT		
exon 9	<i>NFATC2</i> -ex9AF	CCGTAGGCCATGCAGTGAAC	388	60
	<i>NFATC2</i> -ex9AR	GCCTCGCCTGTGATCCAATA	526	64
	<i>NFATC2</i> -ex9BF	CTGCTGGTTGGTGGGTGAGT		
	<i>NFATC2</i> -ex9BR	GGACTCCCAAGGCCATGTTC		
exon 10	<i>NFATC2</i> -ex10F	TTCTCGGATCAAAGATCACAGTCA		
	<i>NFATC2</i> -ex10R	CGGCATGAGTTGGAAGCGTA		
exon 11	<i>NFATC2</i> -ex11F	AGAAGGTGAGGGGCTGTGGA	177	58
	<i>NFATC2</i> -ex11R	CCCTCTCACTTGCCCCATTC		

(a) cycling conditions were 3 min at 98°C, followed by 35 cycles of 30 sec at 98°C, one min at 60°C and 1 min at 72 °C, ending with 10 min at 72 °C; (b) cycling conditions were 4 min at 98°C, followed by 35 cycles of 40 sec at 98°C, one min at 66°C and 1 min at 72 °C, ending with 10 min at 72 °C.

3.3.4.9. INHIBITION OF THE CALCINEURIN/NFAT SIGNALING PATHWAY

The megakaryocytic SET-2 cell line (Uozumi *et al.*, 2000) was purchased from Deutsche Sammlung von Mikroorganismen und Zellkulturen GmbH (Braunschweig, Germany) and maintained in RPMI medium supplemented with 20% fetal bovine serum (Invitrogen). Approximately 5×10^5 cells were seeded in 35 mm diameter-culture dishes and incubated for 24 hr with dimethyl sulfoxide (DMSO)-diluted NFAT inhibitor, cell permeable (Calbiochem) (Noguchi *et al.*, 2004) at concentrations of 1, 5, 10 and 20 μ M or with an equivalent volume of DMSO (control cells). Cell cultures were also independently treated with inhibitor for 2 hr and subsequently stimulated for 15 min with 0.5 μ M ionomycin, calcium salt *Streptomyces globatus* (Calbiochem) to activate the calcineurin/NFAT signaling pathway (Lee, 1993). After incubation

cells were resuspended, transferred to 2.0 ml microtubes, centrifuged and resuspended again in RPMI medium. A 50 μ l cell aliquot was removed and incubated in trypan blue solution (Gibco) for viability analysis. The remaining cells were resuspended in RLT lysis buffer (Qiagen) and processed for total RNA extraction and cDNA synthesis essentially as described in section 3.3.4.6.

3.3.4.10. *IN VITRO* SUPPRESSION OF *NFATC2* USING A SHORT INTERFERING RNA

A specific siRNA oligonucleotide (5'-GCAUAUCCGCACACCUGUATT-3') for *NFATC2* (*siNFATC2*) was designed using the online siMAX-Design software of Eurofins MWG Operon (<http://www.eurofinsdna.com/service-corner/sirna-design.html>). The *siNFATC2* oligo targets transcript variant 1 of *NFATC2* at exon 8 between nucleotides 2164 and 2182 (GenBank accession number NM_012340). Multiple alignment of mRNA sequences from *NFATC1*, *NFATC2*, *NFATC3* and *NFATC4* confirmed that *siNFATC2* would not cross-hybridize with other NFAT-family members. Approximately 5×10^5 SET-2 cells were transfected with Lipofectamine 2000 (Invitrogen) and 400 pmol of *siNFATC2* or siRNA control (*siControl*) for GFP (see table V in section 3.2.4.8). After 24 hr incubation viable cells were split in 2 aliquots and lysed with RLT buffer as described above for RNA analysis or 1x Laemmli sample buffer supplemented with 5 mM $MgCl_2$ and 50 U Benzonase (Sigma) for Western-blot analysis, respectively. Evaluation of the level of suppression of the *NFATC2* transcript was conducted using Q-PCR as described below (section 3.3.4.12). Protein lysates were run on 10% SDS-PAGE gels. *NFATC2* protein was detected with *NFAT-1* antibody (clone 1, BD Biosciences), cyclin E was detected using mouse anti-cyclin E monoclonal antibody (clone HE12, Abcam, Cambridge, United Kingdom) and tubulin was detected using mouse monoclonal anti- α -tubulin antibody (clone B-5-1-2, Sigma). Goat anti-mouse IgG (H+L)-HRP conjugate (Biorad) was used as a secondary antibody. Densitometric analysis of protein blots was performed using the ImageJ software.

3.3.4.11. QUANTIFICATION OF *GM-CSF* RNA EXPRESSION IN SET-2 CELLS

Primers for Q-PCR analysis were designed using the Primer Express 2.0 program (Applied Biosystems) (**Table XII**). Amplification mixture contained 1X TaqMan Universal Master Mix (Applied Biosystems), 0.3 μ M of each *GM-CSF*-306F and *GM-CSF*-381R primers, 0.2 μ M of *GM-*

CSF-339P probe and 5 μ l of cDNA in a final volume of 25 μ l. In addition, expression of the death inducer-oblierator-1 (*DIDO1*) gene was quantified using a TaqMan gene expression assay (Hs00223101_m1, Applied Biosystems) according to the manufacturer's instructions. Amplification of the glucuronidase beta (*GUSB*) transcript was performed for normalization of results with primers and probe described in Beillard *et al.* (2003). The reaction mixture contained 1X TaqMan Universal Master Mix, 1.8 μ M of each primer, 0.6 μ M of probe and 5 μ l of cDNA in a final volume of 25 μ l. Amplifications were carried out using the ABI Prism 7000 Sequence Detection System (Applied Biosystems). Cycling parameters for *DIDO1* and *GUSB* consisted of 50°C-2 min, 95°C-10 sec and 40 cycles of 95°C-15 sec and 60°C-1 min whereas those for *GM-CSF* were of 50°C-2 min, 95°C-10 min, and 40 cycles of 95°C-20 sec, 55°C-20 sec and 60°C-1 min. Two replicates from each sample were included in the assays. Fold-expression variation was determined using the $\Delta\Delta$ Ct method.

Table XII. Primers and probe used for analysis of *GM-CSF* expression by Q-PCR.

Primer name	Sequence (5'-3')	Exon-exon junction	Amplicon size (bp)
<i>GM-CSF</i> -306F	F: GGCCCTTGACCATGATG		
<i>GM-CSF</i> -381R	R: TCTGGGTTGCACAGGAAGTTT	3-4	76
<i>GM-CSF</i> -339P	P: FAM-CAGCACTGCCCTCCAACCCCG-TAMRA		

F, forward primer; R, reverse primer; P, probe.

3.3.4.12. QUANTIFICATION OF *NFATC2* RNA LEVELS IN PATIENTS WITH ESSENTIAL THROMBOCYTHEMIA AND CONTROLS

Quantification of *NFATC2* RNA was conducted in 12 ET patients and 10 healthy individuals using Q-PCR. Normal samples were obtained from anonymized peripheral blood samples collected after informed written consent from individuals tested for genetic conditions not involving the hematopoietic system. Isolation of peripheral blood granulocytes and extraction of total RNA were performed as described above. Spectrophotometric quantification of total RNA was conducted using a NanoDrop (Thermo Scientific). Synthesis of cDNA was carried out according to the standardized Europe Against Cancer protocol (Gabert *et al.*, 2003) using 50 ng of total RNA as template. Complementary DNA samples were diluted to a final volume of 32 μ l using diethyl pyrocarbonate-treated H₂O. *NFATC2* Q-PCR reaction mixture contained 1X of TaqMan Universal Master Mix (Applied Biosystems), 1X TaqMan gene expression assay (Hs00905451_m1, Applied Biosystems) and 5 μ l of cDNA. *ABL1* was used as the endogenous reference gene as described

(Beillard *et al.*, 2003). Samples were amplified in triplicate for each gene using the ABI Prism 7000 Sequence Detection System (Applied Biosystems). PCR efficiency for each gene was evaluated by inclusion in each Q-PCR assay of serial 10-fold dilutions of a cDNA sample. The following cycling parameters were used: Incubation for 2 min at 50 °C, denaturation of 10 min at 95 °C, followed by 40 cycles of 15 seconds at 95 °C and 1 min at 60 °C. Quantification of *NFATC2* gene expression for each sample was performed using the $2^{-\Delta Ct}$ normalized values (Schmittgen & Livak, 2008). Statistical analysis was performed with the SPSS 17.0 for Windows software.

3.3.5. RESULTS

3.3.5.1. DETECTION OF SUBMICROSCOPIC INTERSTITIAL DELETIONS AT 20q13.13 AND 16q23.1 IN A PATIENT WITH ESSENTIAL THROMBOCYTHEMIA

The bone marrow karyotype of a patient with ET showed a single acquired abnormality consisting in an apparently balanced translocation involving bands Xp11.2 and 20q13 (**Fig. 21A**). However, FISH with WCP probes revealed that the 20q13-20qter region was translocated to the long arm of chromosome 16 instead of chromosome X, whereas the chromosome 16q material was translocated to chromosome X (**Fig. 21B**). These findings demonstrated that the translocation was a 3-way rearrangement between chromosomes X, 20 and 16 with breakpoints at Xp11.2, 20q13.13 and approximately 16q23, respectively (**Fig. 21C**).

We next mapped the 20q breakpoint in cells with t(X;20;16) using FISH with several probes mapping between bands 20q12 and 20q13.2. Results revealed that the breakpoint region was overlapped by YAC 957F3 which displayed hybridization signals on the der(20) and der(16) chromosomes (results not shown). To define the breakpoint region more precisely, a set of 10 PAC probes mapping within the region covered by YAC 957F3 was used. In addition to the signals on the normal chromosome 20, two probes (RP5-1009H6 and RP5-994O24) showed signals on the der(20) whereas 4 probes (RP5-831D17, RP4-548G19, RP4-698O15 and RP5-965N20) displayed signals on the der(16) (results not shown). The intervening 4 probes (RP5-1114A1, RP5-827A12, RP5-1112F19 and RP4-756P4) showed no hybridization signals on either the der(20) or der(16) chromosomes, indicating the presence of a small interstitial deletion within band 20q13.13 (**Fig. 21D**). Subsequent interphase FISH studies of peripheral blood samples from an additional 18 ET patients disclosed no deletions of the 20q13.13 region as seen in the patient with t(X;20;16) (results not shown).

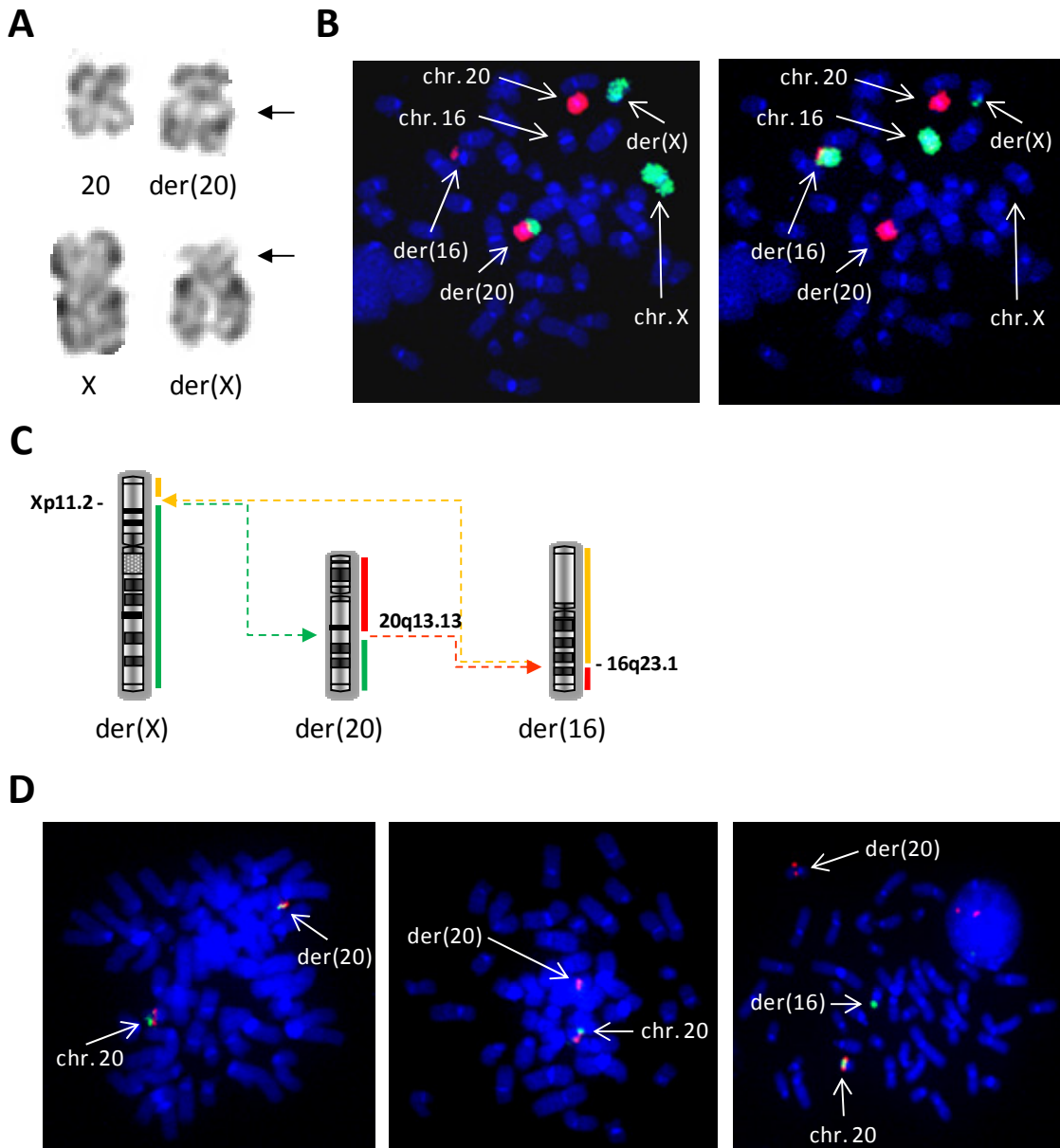


Figure 21. Results of cytogenetics and FISH analyses on bone marrow cells with $t(X;20;16)$.

(A) Partial G-banding karyogram showing normal chromosomes 20 and X, and corresponding derivative chromosomes. Arrows indicate the approximate location of translocation breakpoints. **(B)** Successive hybridization of a metaphase cell with WCP probes for chromosomes X, 20 and 16. Left: Chromosome 20 (red signal) and chromosome X (green signal). Right: chromosome 16 (green signal) and chromosome 20 (red signal). **(C)** Diagrammatic representation of derivative chromosomes involved in the formation of a 3-way $t(X;20;16)$ as evidenced by FISH analyses. Dashed lines are used to indicate the movement of material between each of the chromosomes involved in the rearrangement. Vertical color lines at the right of the chromosomes show the location of chromosome X (green), 20 (red) and 16 (orange) materials after formation of the translocation. **(D)** Delimitation of the breakpoint region at 20q13.13 using FISH. Three different PAC probes mapping to 20q13.13 were used in co-hybridization experiments with the more centromeric RP11-72F10 BAC probe. Left panel: The RP5-994O24 PAC probe (green signal) and the control probe (red signal) showed a co-localization of hybridization signals on the der(20) and normal chromosome 20, indicating that the breakpoint lied telomeric to the PAC probe. Right panel: In addition to the normal chromosome 20, the RP5-831D17 PAC probe (green signal) hybridized on the der(16) whereas the control probe (red signal) hybridized on the der(20), indicating that the breakpoint was localized centromeric to the PAC probe. Middle panel: The intervening RP4-756P4 PAC probe (green signal) displayed a hybridization signal only on the normal chromosome 20, revealing an interstitial deletion of chromosome 20 material.

According to the results of karyotyping, the bone marrow sample of the patient contained approximately one third of normal cells. Thus, it was not possible to determine a loss of heterozygosity by direct comparison between this sample and a normal sample of the patient using STR polymorphisms because both alleles of heterozygous polymorphisms are expected to be detected. In this context, we choose to use allele areas of heterozygous STR polymorphisms determined after capillary electrophoresis of PCR products as a surrogate way to determine which markers were absent as a result of the 20q deletion.

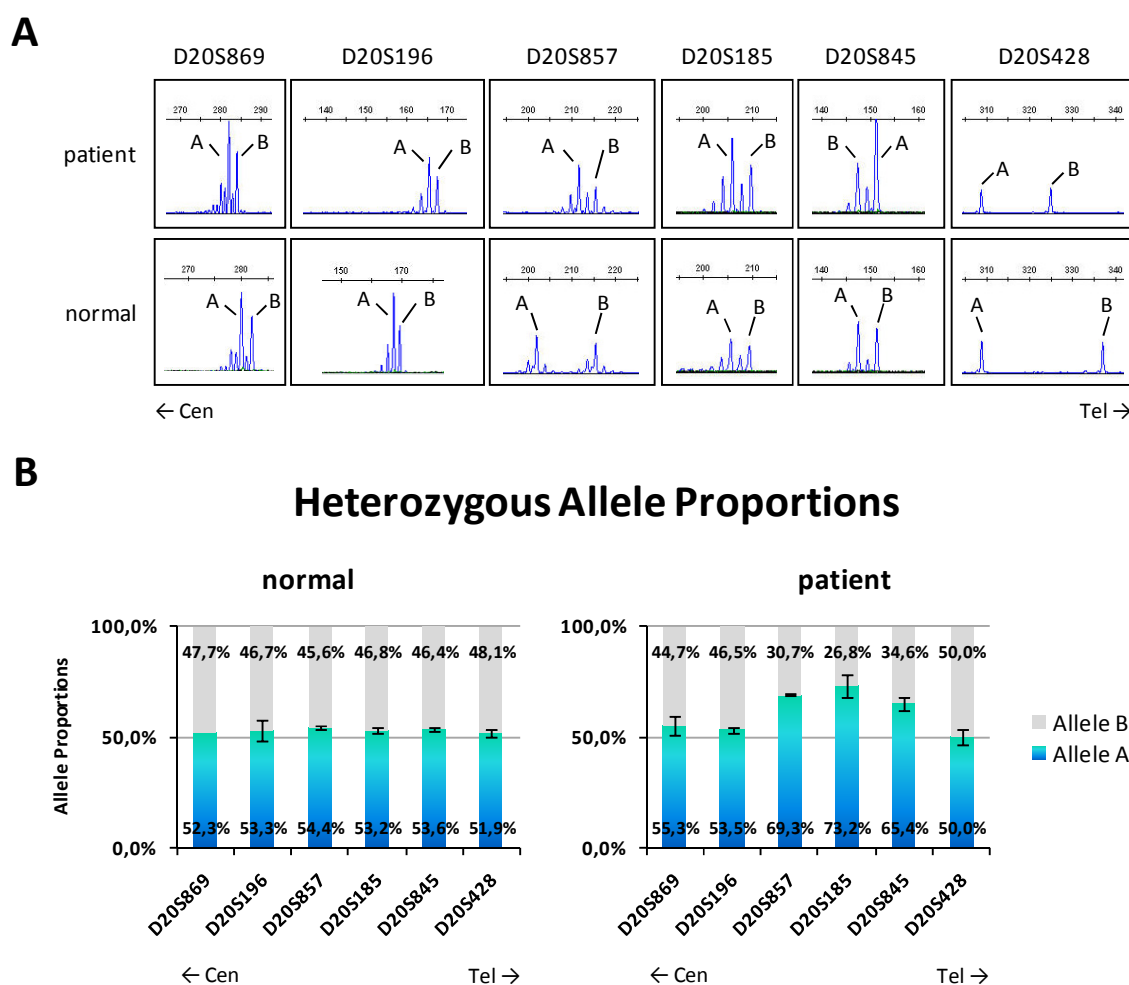


Figure 22. Results of capillary electrophoresis analysis of heterozygous polymorphisms located at 20q13.13.

(A) Partial electropherograms of PCR products corresponding to the amplification of D20S869, D20S196, D20S857, D20S185, D20S845 and D20S428 polymorphisms in the patient with $t(X;20;16)$ and in a control sample. Both individuals were heterozygous for each of the STR polymorphisms. Alleles of heterozygous polymorphisms are represented by letters A and B. The A allele was arbitrarily defined for each polymorphism as the allele peak with higher fluorescence intensity. Scale above allele peaks indicates the size of PCR products in bp. **(B)** Graphical representations of the allele proportions obtained for each of the STR polymorphisms in the normal (left graph) and patient (right graph) samples. A balanced allele proportion was observed in the normal sample for each of the polymorphisms and in the patient sample for polymorphisms D20S869, D20S196 and D20S428. In contrast, an unbalanced allele proportion was detected for polymorphisms D20S857, D20S185 and D20S845 in the patient sample, indicating hemizygous deletion of the region comprised between D20S857 and D20S845. Vertical bars indicate standard deviation obtained from 2 independent experiments. Cen, centromere. Tel, telomere.

If the 2 alleles of a heterozygous polymorphism are present in equivalent amounts in the original template DNA sample and amplify accordingly, then the area of each allele at the end of the amplification reaction should be approximately 50% of the total allele area. Using this theoretical approach we calculated allele proportions obtained in the patient sample with those obtained in a sample from an individual with a normal karyotype, both of which displayed heterozygosity for each polymorphism. The mean allele proportions in the sample with a normal karyotype were of 53.1%:46.9% (range: 51.9-54.4%:45.6-48.1%), thus reflecting a balanced amount of the 2 alleles. A similar allele proportion was obtained in the patient sample for polymorphisms D20S869, D20S196 and D20S428 (mean: 53.0%:47.0%; range: 50.0-55.3%:44.7-50%). In contrast, an unbalanced mean allele proportion of 69.3%:30.7% (range: 65.4-73.2%:26.8-34.6%) was seen for the other 3 polymorphisms in-between (**Fig. 22**).

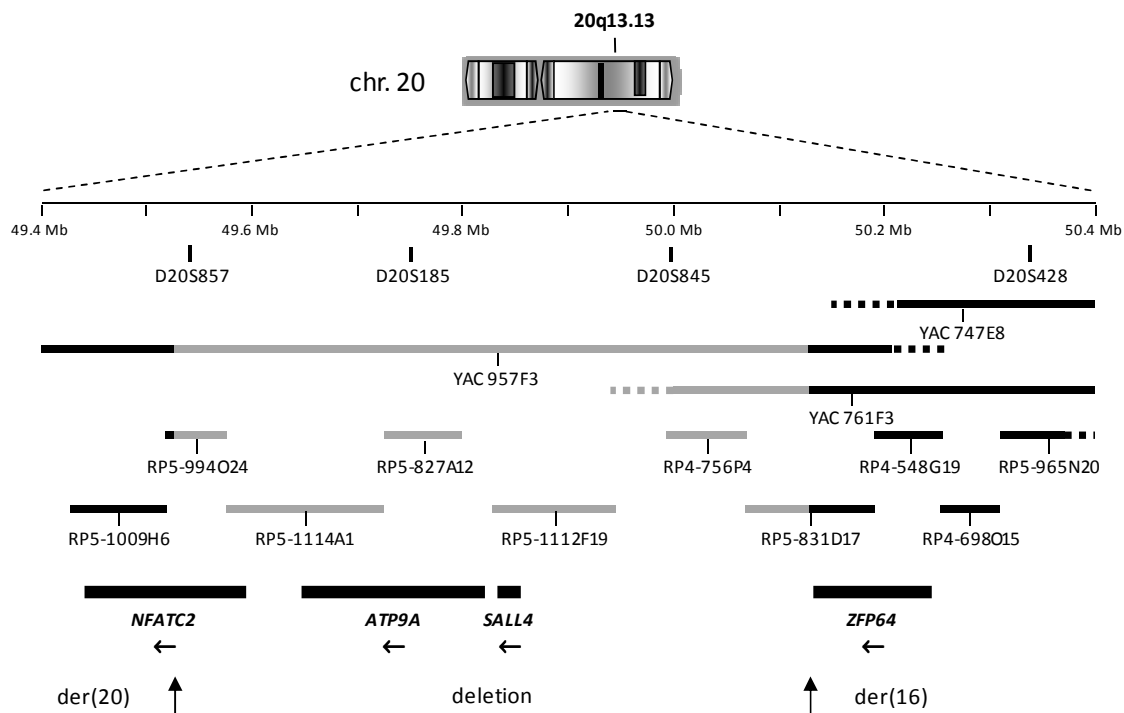


Figure 23. Schematic representation of human chromosome 20 and of an enlarged 20q13.13 region targeted by the breakpoints of a complex t(X;20;16).

The breakpoints were associated with an interstitial deletion comprising *ATP9A*, *SALL4* and the 5' side of *NFATC2*. The chromosomal region located centromeric to the proximal breakpoint remained on the der(20) chromosome whereas the region located telomeric to the distal breakpoint was translocated to chromosome 16. YAC and PAC clones used as probes in FISH experiments are represented as black or grey lines according to their inclusion outside or inside the deleted region, respectively. Clones were mapped in respect to STS markers indicated in Table VI. Dashed terminus of probes represents regions of uncertainty regarding the precise end of clones. The localization of the *NFATC2*, *ATP9A*, *SALL4* and *ZFP64* genes is shown as black boxes in the lower part of the figure. Horizontal arrows indicate the orientation of gene transcription. Physical distance is measured in Mb starting from the tip of the short arm of chromosome 20 and is scaled at 100 kb intervals according to the NCBI36 (March 2006) *Homo sapiens* sequence build. Approximate locations of molecular markers used in this study are shown below the scale.

Taken together, these results indicated that each of the D20S857, D20S185 and D20S845 *loci* was included in the 20q13.13 deletion, thus resulting in uneven proportion of each allele. Thus, the combined results of FISH and PCR established the presence of an interstitial deletion at chromosome band 20q13.13 comprising the 5' side of the *NFATC2* gene as well as the *ATP9A* and *SALL4* genes (Fig. 23).

We next performed a whole-genome array analysis of a granulocyte DNA sample of the patient as an attempt to define the proximal and distal deletion boundaries more precisely. These were found to correspond to nucleotide positions 49.508.399 and 50.121.389, respectively, of the *Homo sapiens* reference genome build NCBI36 (March 2006), indicating that the length of the deleted region was of approximately 613 kb (Fig. 24).

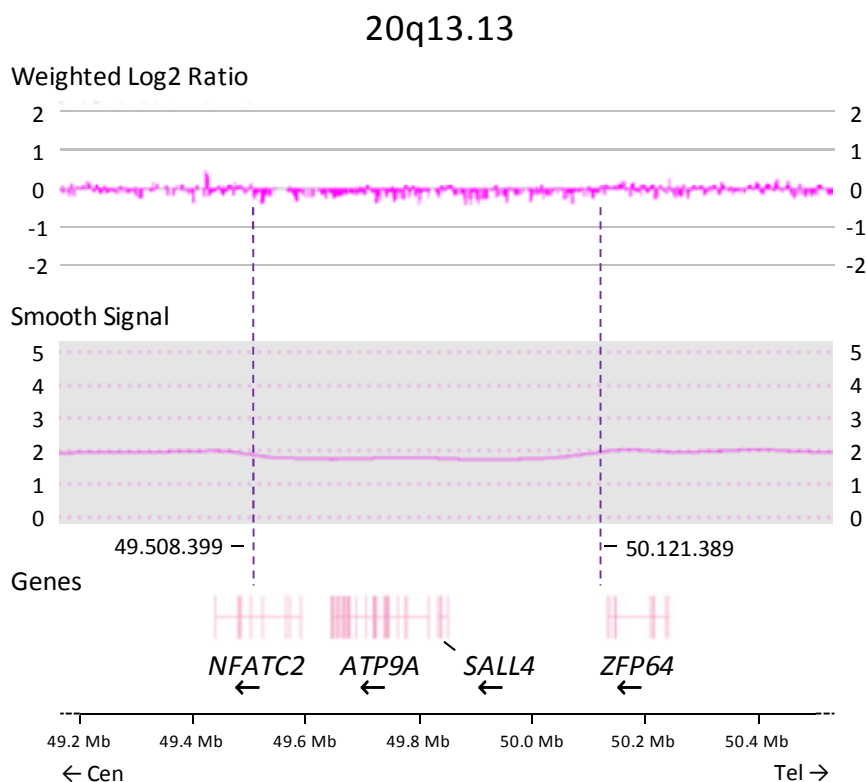


Figure 24. Results of whole-genome array analysis of chromosome region 20q13.13.

Partial graphical output of array data showing the presence of an interstitial deletion at 20q13.13. Note the deviation of the pink smooth signal line from the normal diploid level (2). The deletion was only detected at a low level of mosaicism indicating that the granulocyte sample of the patient was mostly composed of normal cells. The weighted \log_2 ratio represents a running median of a genomic region of \log_2 ratios (i.e., intensity of a marker normalized to a reference and to sample variation) which excludes outliers. The smooth signal represents the smoothed \log_2 ratio. The purple dashed vertical lines indicate the approximate locations of breakpoints of the deleted region. Numbers adjacent to deletion boundaries indicate nucleotide positions of each breakpoint (in Mb) according to the NCBI36 (March 2006) human genome sequence. Images were produced using the ChAS 1.1. software (Affymetrix). The orientation of each gene is represented by a horizontal arrow below the corresponding symbol. A scale is shown on the bottom of the figure. The directions of the centromere (cen) and telomere (tel) are indicated by arrows below the scale.

According to these results, exons 1 to 5 of *NFATC2* were contained in the deleted region, thus confirming results obtained by FISH and PCR analyses. Using RACE analysis we did not find putative fusion transcripts resulting from joining of the 3' part of *NFATC2* to chromosome X sequences in the patient sample (results not shown), suggesting that *NFATC2* was not activated by the translocation. However, because we were also unable to detect normal *NFATC2* transcripts in the same sample we cannot completely exclude the presence of a fusion gene.

Analysis of the array data for chromosome 16 also revealed the presence of an interstitial deletion at 16q23.1-16q23.2 at a similar level of mosaicism as the 20q deletion (**Fig. 25**). Because of the lack of patient material we could not confirm by FISH that the 16q23 deletion was contiguous to the chromosome 16 breakpoint involved in the t(X;20;16). However, its localization is compatible with the breakpoint position determined in WCP studies, strongly suggesting that it consisted of a breakpoint-adjacent deletion.

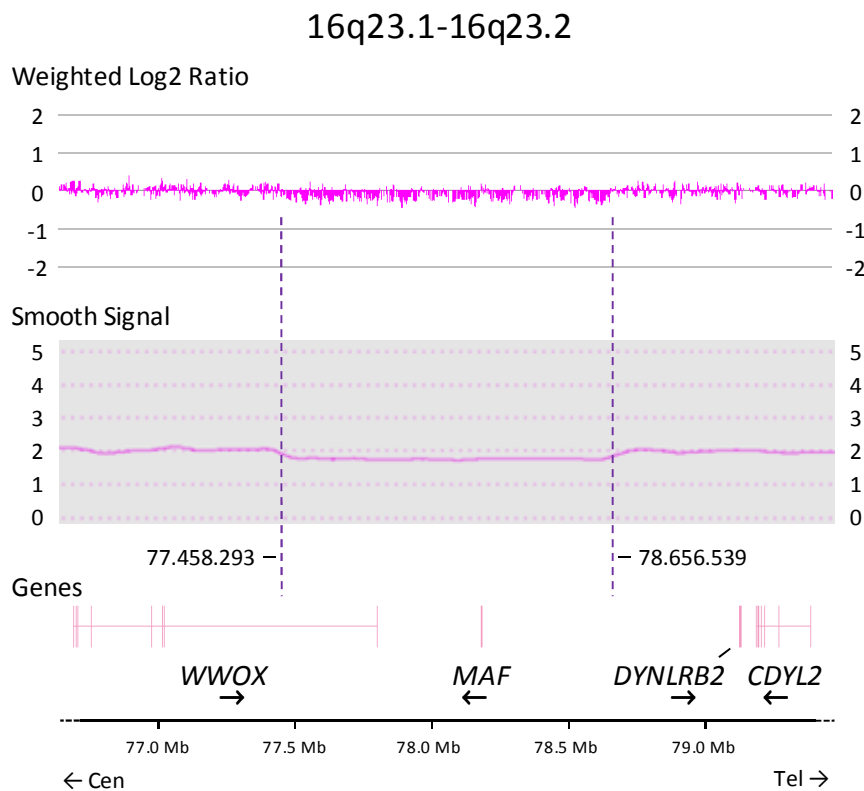


Figure 25. Results of whole-genome array analysis of chromosome region 16q23.1-16q23.2

Partial graphical output of array data showing the presence of an interstitial deletion at 16q23 involving the *MAF* gene. Note the deviation of the pink smooth signal line from the normal diploid level (2). As in the case of chromosome 20q13.13 the deletion at chromosome 16q23 was only detected at a low level of mosaicism. The weighted \log_2 ratio represents a running median of a genomic region of \log_2 ratios (i.e., intensity of a marker normalized to a reference and to sample variation) which excludes outliers. The smooth signal represents the smoothed \log_2 ratio. The purple dashed vertical lines indicate the approximate locations of breakpoints of the deleted region. Numbers adjacent to deletion boundaries indicate nucleotide positions of each breakpoint (in Mb) according to the NCBI36 (March 2006) human genome sequence. Images were produced using the ChAS 1.1. software (Affymetrix). The orientation of each gene is represented by a horizontal arrow below the corresponding symbol. A scale is shown on the bottom of the figure. The directions of the centromere (cen) and telomere (tel) are indicated by arrows below the scale.

The 16q deletion comprised a length of approximately 1.2 Mb between nucleotide positions 77.458.293 and 78.656.539 of the NCBI36 (March 2006) human genome sequence. This alteration resulted in the deletion of the v-maf musculoaponeurotic fibrosarcoma oncogene homologue (*MAF*) gene and in the truncation of the last exon of the WW domain containing oxidoreductase (*WWOX*) gene. Detailed inspection of chromosome X array data did not show the existence of a deleted segment at band Xp11, indicating that the breakpoint involved in the t(X;20;16) was not associated with an adjacent deletion (results not shown).

3.3.5.2. THE *WWOX* GENE IS NOT REARRANGED IN THE PATIENT WITH t(X;20;16)

The *WWOX* gene is located in the fragile site FRA16D region of chromosome 16 which is frequently targeted by hemizygous deletions and translocation breakpoints in breast cancer (Bednarek *et al.*, 2000). Moreover, this gene is deleted and/or is not expressed in various other tumor types including ovarian cancer, osteosarcoma and hematopoietic malignancies (Paige *et al.*, 2001; Ishii *et al.*, 2003; Kurec *et al.*, 2010; Yang *et al.*, 2010). In our case the truncated *WWOX* gene became juxtaposed to the coding sequence of *ZFP64* on the long arm of chromosome 16 following the translocation. Because these genes are oriented in opposite directions at the long arm of chromosome 16 and of chromosome 20, respectively, no *WWOX-ZFP64* fusion gene is expected to be generated. However, an abnormal *WWOX* transcript containing sequences from chromosome 20 on its 3' side could potentially be generated. To exclude this possibility we performed 3' RACE analysis of *WWOX* transcripts using mononuclear cells of the patient. We identified 3 types of alternatively-spliced *WWOX* transcripts which only contained sequences from chromosome 16, indicating that the translocation did not produced an abnormal *WWOX* transcript (**Fig. 26**). Interestingly, two of the mature transcripts included the presence of exon sequences not yet described in the transcript database of the Ensembl Genome Browser (<http://www.ensembl.org>). One of these transcript sequences did not contain a stop codon upstream of the poly-A signal, indicating that it is not functional. Despite these findings, our data indicate that rearrangement of the *WWOX* gene did not have a pathogenetic role in the patient with t(X;20;16).

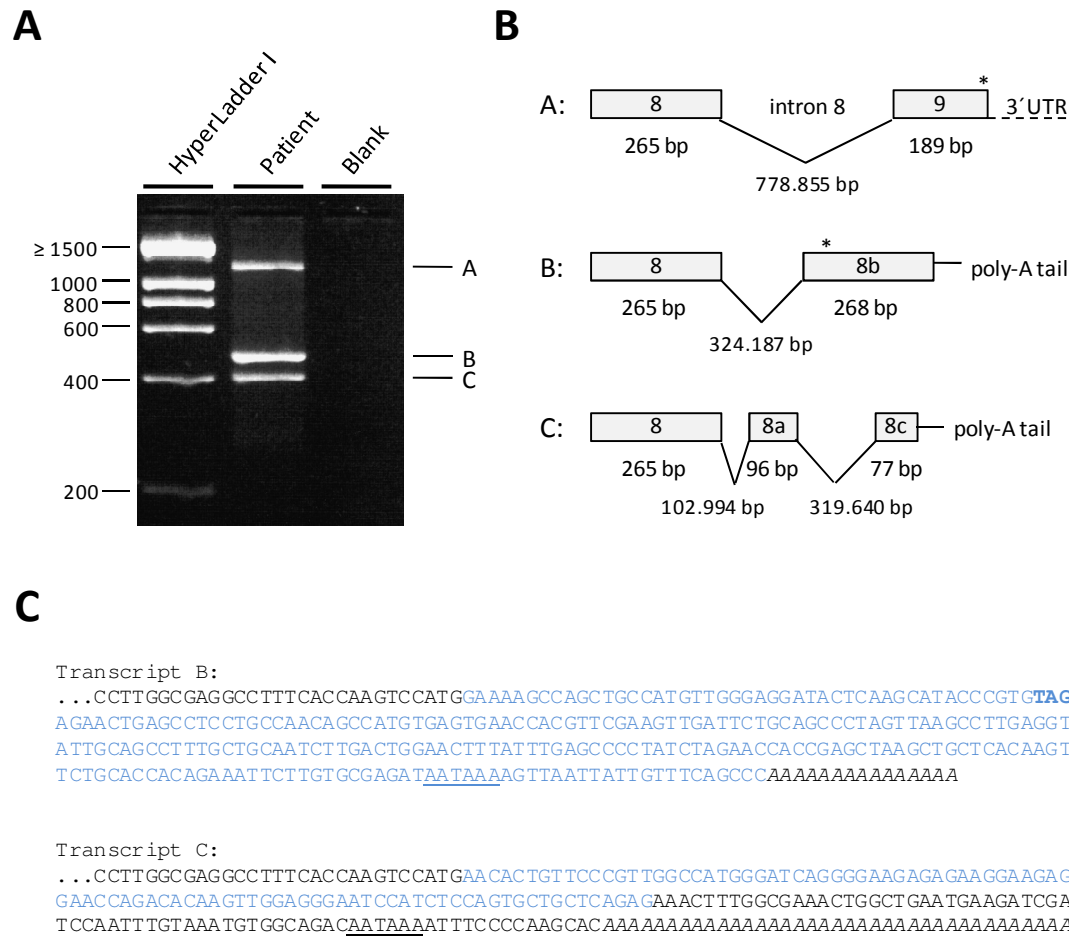


Figure 26. Results of 3' RACE analysis of *WWOX* transcripts.

(A) Agarose gel electrophoresis analysis of nested PCR products. Three bands of different sizes (A, B and C) were amplified in the patient sample. The molecular weight marker is HyperLadder I (Bioline). Sizes of representative marker bands are shown on the left side of the gel image in bp; **(B)** Schematic representation of each transcript configuration following direct sequencing of PCR products. Transcript A consists in a direct fusion of exon 8 to exon 9 of *WWOX* and is followed by a 3' untranslated region (3'UTR). Its sequence matches the sequence of the *WWOX*-206 transcript ENST00000408984 (1245 bp/414 aminoacids) in the Ensembl genome browser database (<http://www.ensembl.org>). Transcript B corresponds to a fusion of exon 8 to a novel exon sequence (here designated as 8b) located in intron 8 of *WWOX*. Transcript C contains 2 additional exon sequences (here designated as 8a and 8c) located 3' of exon 8. This transcript does not contain a stop codon before the poly-A signal and is therefore expected to be non-functional. Boxes represent exons. The numbers below the boxes and between them indicate the size of exons and introns in bp, respectively. Introns are not shown to scale. Stop codons are indicated by an asterisk (*). **(C)** Partial sequences of transcripts B and C. Exon sequences are shown in alternating black and blue colors beginning with a partial exon 8 sequence. The poly-A signal AATAAA is underlined in each of the sequences. The stop codon (TAG) located in exon 8b of transcript B is shown in bold. The poly-A tail is shown in italics. Sequences were compared to the *Homo sapiens* chromosome 16 genomic contig, genome reference consortium GRCh37 (February 2009) primary assembly (accession number NT_010498.15) following a BLAST analysis.

3.3.5.3. *NFATC2* IS UBIQUITOUSLY EXPRESSED IN NORMAL HUMAN CELLS AND BOTH ALLELES ARE PRESENT IN PERIPHERAL BLOOD LEUKOCYTES OF PATIENTS WITH ESSENTIAL THROMBOCYTHEMIA

Except for brain tissue, we detected expression of *NFATC2* in all other human tissues tested (**Fig. 27**). However, expression levels differed widely between tissues. In particular, the level of *NFATC2* expression was highest in leukocytes and spleen, which is in agreement with its role as a hematopoietic transcription factor (Hogan *et al.*, 2003).

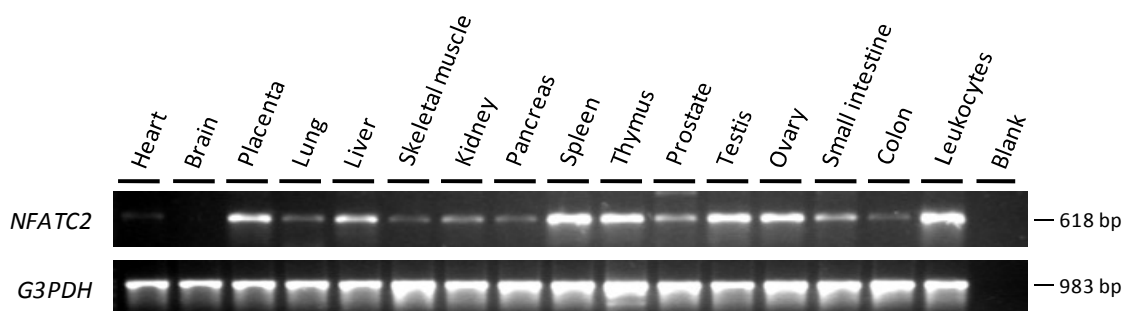


Figure 27. Expression of *NFATC2* in normal human tissues.

Gel electrophoresis analyses showing RT-PCR results of *NFATC2* and *G3PDH* expression in 16 different normal human tissues. *NFATC2* is expressed in all tissues except brain. Expression of *G3PDH* was used as a normalizer. Sizes of PCR products are shown in bp on the right side of the figure. Please note: The gel photo corresponding to *G3PDH* is the same as the one used in Fig. 15A.

We next investigated if both alleles of *NFATC2* are expressed in peripheral blood leukocytes. We hypothesized that if mono-allelic expression of *NFATC2* occurs in hematopoietic cells, deletion of chromosome 20q13.13 sequences could result in the absence of expression if the transcribed allele is located on the der(20). To test this hypothesis, we firstly identified in genomic DNA samples from different ET patients a heterozygous transcribed SNP in exon 4 of *NFATC2*. We then searched using RT-PCR and sequencing analysis for both alleles in RNA extracted from mononuclear cells. Both alleles of *NFATC2* were detected in each sample analysed, indicating that in cells with a del(20q) one copy of the gene is still expressed (**Fig. 28**). Similarly, we found that both alleles of *ATP9A* and *SALL4* are expressed in peripheral blood cells (data not shown).

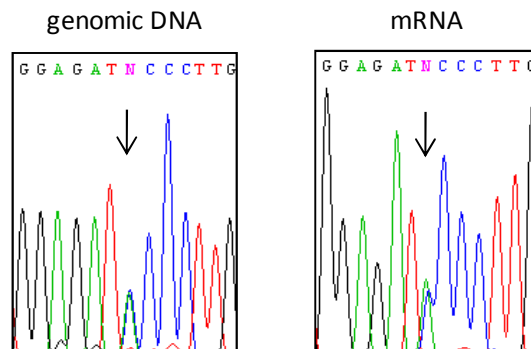


Figure 28. Expression of *NFATC2* in hematopoietic cells.

Partial sequencing traces showing the presence of a heterozygous A/C SNP in exon 4 of *NFATC2* obtained from genomic DNA (left electropherogram) and mRNA (right electropherogram) of the same ET patient. Both alleles of *NFATC2* are expressed in peripheral blood cells. Arrows indicate the nucleotide position of the SNP.

3.3.5.4. THE *NFATC2* GENE IS NOT MUTATED IN PATIENTS WITH ESSENTIAL THROMBOCYTHEMIA

We studied 20 ET patients for the presence of the *JAK2*V617F mutation by AS-PCR and *Bsa*XI digestion. Eleven of the 20 patients (55%) including the patient with t(X;20;16) showed the presence of *JAK2*V617F by both methods (**Fig. 29A**), whereas in the remaining 9 patients the mutation could not be identified using either technique. Sequencing analysis of *JAK2* exon 14 in isolated granulocytes of the patient with t(X;20;16) showed a higher burden of the mutated allele compared to the wild-type allele, indicating that the majority of clonal granulocytes were homozygous for *JAK2*V617F (**Fig. 29B**).

We next conducted a mutation screening of all *NFATC2* exons and flanking intronic regions in the 20 ET patients. However, except for several SNPs no additional alterations were found, indicating that inactivating mutations of *NFATC2* may not play a role in ET. We also could not identify mutations of *ATP9A* or *SALL4* in ET patients (results not shown). These results indicate that *NFATC2* may exert its pathogenetic role in cells with a del(20q) by a mechanism other than loss-of-function.

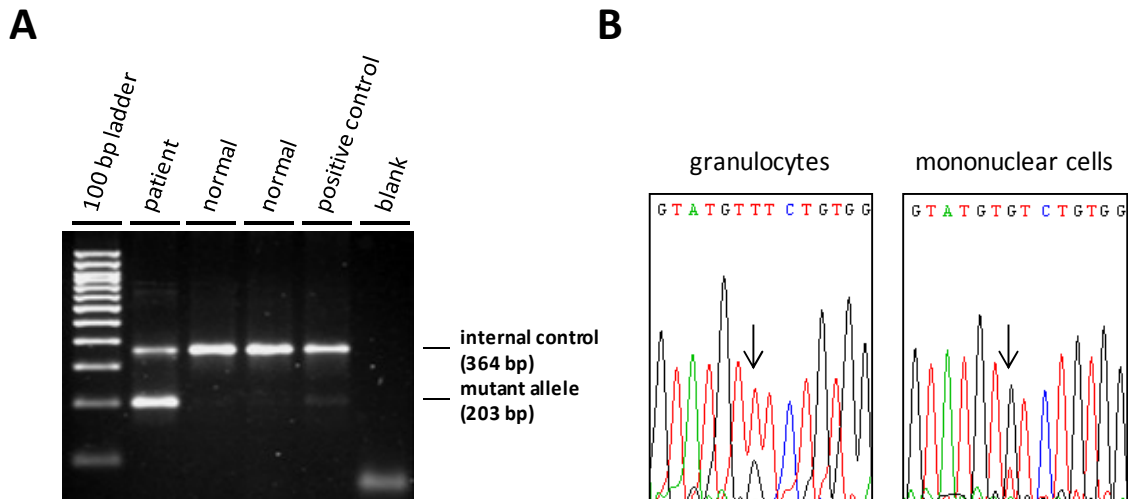


Figure 29. Analysis of *JAK2V617F* mutation in the patient with *t(X;20;16)*.

(A) Gel electrophoresis analysis of AS-PCR products showing the presence of the *JAK2V617F* mutation in the patient granulocytes. The positive control is a 1:81 dilution of a *JAK2V617F*-positive homozygous DNA into a *JAK2* wild-type DNA. PCR fragments corresponding to the internal AS-PCR control and to the mutant allele are indicated on the right side of the gel photo. **(B)** Partial sequencing traces of *JAK2* exon 14 showing the presence of a G to T mutation (arrow) corresponding to *JAK2V617F*. The mutant allele peak (T) is higher than the wild-type allele peak (G) in the granulocyte fraction, thus indicating the presence of a *JAK2V617F*-positive homozygous clone in this cell population.

3.3.5.5. *NFATC2* EXPRESSION IS DIMINISHED IN GRANULOCYTES OF PATIENTS WITH ESSENTIAL THROMBOCYTHEMIA

We used real-time Q-PCR analysis to measure the levels of *NFATC2* mRNA in granulocytes of 12 ET patients, seven (58%) of which were *JAK2V617F*-positive, and in 10 granulocyte RNA samples of normal individuals. Because the PCR efficiencies for both genes were similar we used $2^{-\Delta Ct}$ values of individual samples to compare *NFATC2* expression levels between patients and controls.

The mean $2^{-\Delta Ct}$ of ET patients was 0.92 ± 0.30 whereas that for normal individuals was 1.24 ± 0.61 ($P=0.122$, independent samples t-test), indicating a mean 1.4-fold reduction in the expression of *NFATC2* mRNA in ET patients compared to controls (**Fig. 30**). These results suggest that *NFATC2* levels in granulocytes of patients may be diminished as a consequence of mechanisms other than chromosome deletions.

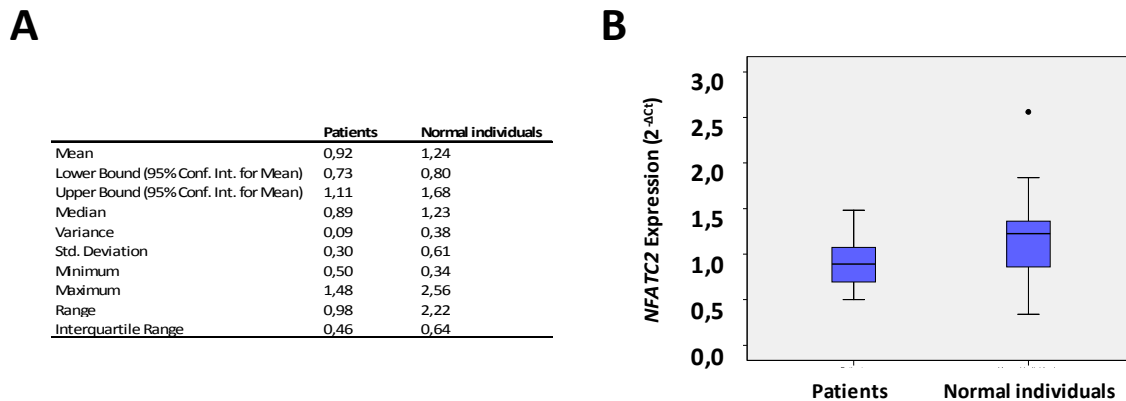


Figure 30. Comparison of *NFATC2* mRNA expression in granulocytes of ET patients and normal individuals.

The mean *NFATC2* expression is lower in ET patients but not significantly different from normal individuals (independent samples t-test, $P=0,122$). Ct values of *NFATC2* expression were normalized to Ct values of *ABL1* expression. The normalized $2^{-\Delta\text{Ct}}$ values were used for statistical analysis. **(A)** Descriptives of normalized *NFATC2* expression in patients and normal individuals. **(B)** Graphical representation of *NFATC2* expression levels between ET patients and normal individuals. The box represents the value range between the 25th and the 75th percentile. The median value corresponds to the horizontal black bold line. Bars indicate the range of values. The black dot represents an outlier value.

3.3.5.6. INHIBITION OF NFAT ACTIVATION *IN VITRO* IS ASSOCIATED WITH MEGAKARYOCYTIC PROLIFERATION

Because *NFATC2* mutations were not identified in the non-rearranged 20q allele of the patient with t(X;20;16) we hypothesized that haplo-insufficiency manifested as a reduction in the *NFATC2* protein levels could have a role in megakaryocytic growth and proliferation. To test this hypothesis, we treated SET-2 cell cultures *in vitro* with a small inhibitor peptide (VIVIT) which selectively hampers interaction between NFAT proteins and calcineurin by binding to the NFAT-docking site in calcineurin without inhibiting its phosphatase activity (Aramburu *et al.*, 1999; Roehrl *et al.*, 2004). The commercially available 11R-VIVIT inhibitor contains an 11-arginine repeat which greatly facilitates cell permeability (Noguchi *et al.*, 2004). We choose to use SET-2 cells as the cell model because these were derived from a patient with ET (Uozumi *et al.*, 2000), harbor the *JAK2V617F* mutation (results not shown) and have no deletion of the *NFATC2* gene by FISH analysis (**Fig. 31A**).

Induced dephosphorylation and nuclear translocation of NFAT proteins may be rapidly accomplished *in vitro* by stimulation of cells with the Ca^{2+} ionophore ionomycin which acts as a mobile ion carrier for Ca^{2+} (Lee, 1993; Okamura *et al.*, 2000). To test if the inhibitor was effective in blocking *NFATC2* activation in SET-2 cells, we performed semi-quantitative RT-PCR analysis of the *IL-2* gene, known to be transcriptionally regulated by *NFATC2* (Rothenberg & Ward, 1996), in

inhibitor-treated cells following ionomycin stimulation. We observed that *IL-2* mRNA levels were lower in cells treated with inhibitor compared to non-treated cells, indicating that NFATC2 was effectively blocked by the inhibitor (**Fig. 31B**). In this setting incubation for 24 hr with NFAT inhibitor alone at concentrations between 1 μM and 10 μM was associated with 1.27- and 1.76-fold increases in the number of SET-2 cells respectively, compared to untreated cells (**Fig. 31C**), whereas incubation with concentrations equal or greater than 20 μM led to an increase in cell death likely as a result of cellular toxicity. These results indicate that the calcineurin-NFAT signaling pathway contributes to proliferation control in *JAK2V617F*-positive megakaryocytes.

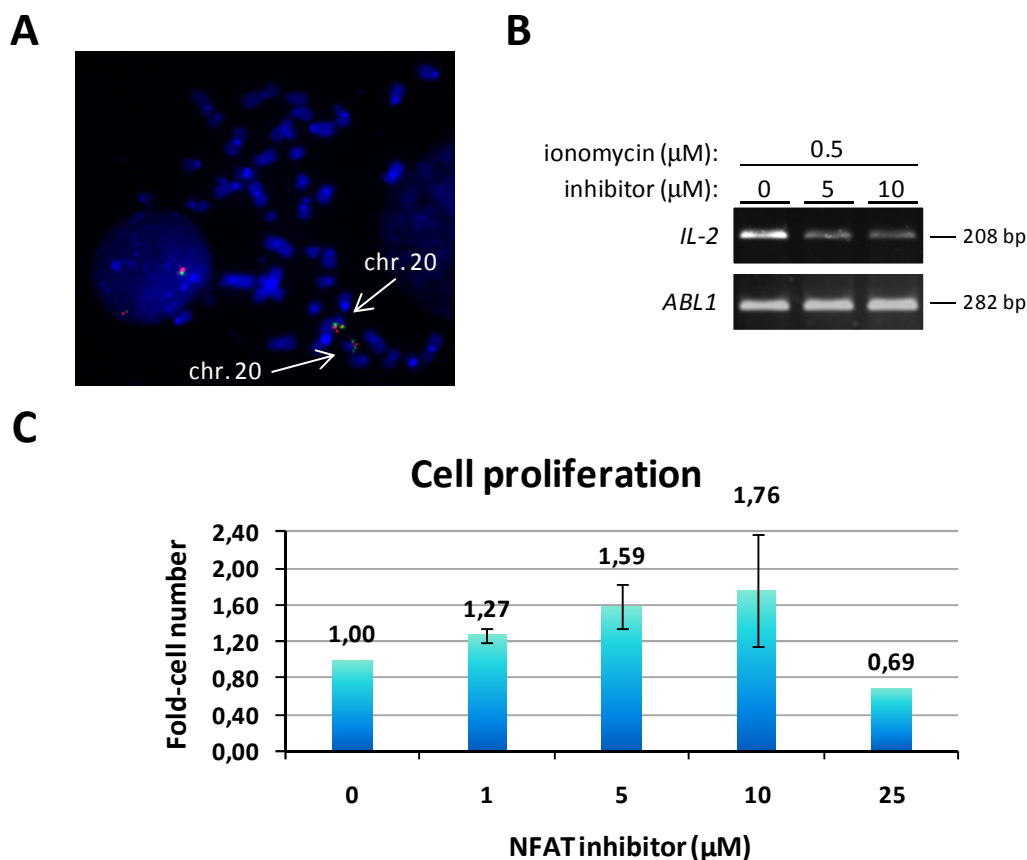


Figure 31. Inhibition of NFAT activation in SET-2 cells.

(A) FISH analysis of a SET-2 metaphase cell with PAC probes RP5-827A12 (red signal) and RP5-994024 (green signal) demonstrating the presence of the *NFATC2* gene on both chromosome 20 homologues. **(B)** Gel electrophoresis analysis of semi-quantitative RT-PCR results showing decreasing *IL-2* mRNA expression in cells treated with NFAT inhibitor comparatively to non-treated cells after stimulation with 0.5 μM ionomycin. Expression of *ABL1* was used as a loading normalizer. Sizes of PCR products are shown on the right side of the gel photos. **(C)** Graphic representation of the fold number variation of SET-2 cells treated with NFAT inhibitor normalized to the number of non-treated cells (fold cell number 1.0). Incubation for 24 h with NFAT inhibitor led to between 1.27- and 1.76-fold increases in the number of cells at concentrations of 1 μM and 10 μM , respectively. Vertical bars indicate standard deviation calculated from the results of 3 independent experiments.

3.3.5.7. SUPPRESSION OF *NFATC2* RNA PROMOTES CELL PROLIFERATION *IN VITRO*

The use of an inhibitory drug targeting calcineurin-NFAT interaction did not allow us to separate *NFATC2*-specific effects on proliferation from those occurring with other NFAT-family members which are also regulated by calcineurin (reviewed in Medyouf & Ghysdael, 2008). Therefore, to investigate an explicit role of *NFATC2* on cell proliferation we suppressed endogenous *NFATC2* expression in SET-2 cells by RNA interference. After 24 hr incubation with siRNA oligos we observed a 48.2% decrease in *NFATC2* protein levels in cells transfected with si*NFATC2* in comparison with those transfected with siControl, thus simulating haplo-insufficiency of *NFATC2* (Fig. 32).

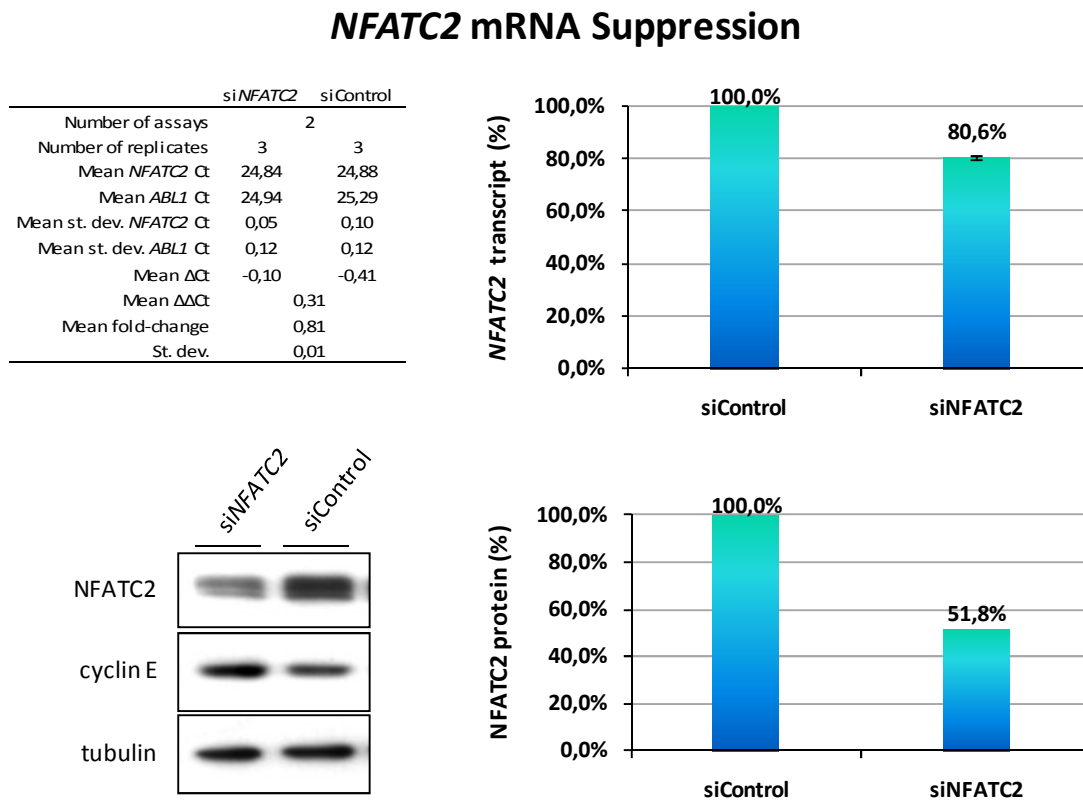


Figure 32. Suppression of *NFATC2* transcripts in SET-2 cells.

Upper left: Summary of Q-PCR data obtained for *NFATC2* and *ABL1* expression in cells transfected with si*NFATC2* and siControl. Ct, cycle threshold. Upper right: Corresponding graphic representation of Q-PCR results showing an approximately 20% reduction of *NFATC2* mRNA in cells transfected with si*NFATC2*. The percentage of *NFATC2* suppression was normalized to the level of *NFATC2* transcripts in siControl-treated cells (100%). Vertical bars indicate standard deviation calculated from 2 independent experiments. Lower left: Western-blot analysis of *NFATC2* and cyclin E in SET-2 cells transfected with si*NFATC2* and siControl. A reduction in the levels of *NFATC2* is associated with an increase in cyclin E levels. Tubulin was used as a loading normalizer. Lower right: Corresponding graphical representation of the densitometric analysis of Western-blot results showing an approximately 50% reduction of *NFATC2* protein in cells transfected with si*NFATC2*. The percentage of *NFATC2* suppression in si*NFATC2*-treated cells was normalized to the level of *NFATC2* in siControl-treated cells (100%).

The suppression level of the *NFATC2* transcript was of only 19.4% in the same sample, suggesting that maximal RNA suppression had occurred at a previous time point. Under these conditions SET-2 cells showed a mean 1.38-fold increase in cell number (paired samples t-test, $P=0,014$) (Fig. 33). Proliferation was associated with an increase in the levels of cyclin E protein, indicating that it was related to progression through the cell cycle. Moreover, cells transfected with *siNFATC2* also displayed a larger size compared to cells transfected with *siControl*, suggesting that cell growth is coupled to cell cycle progression.

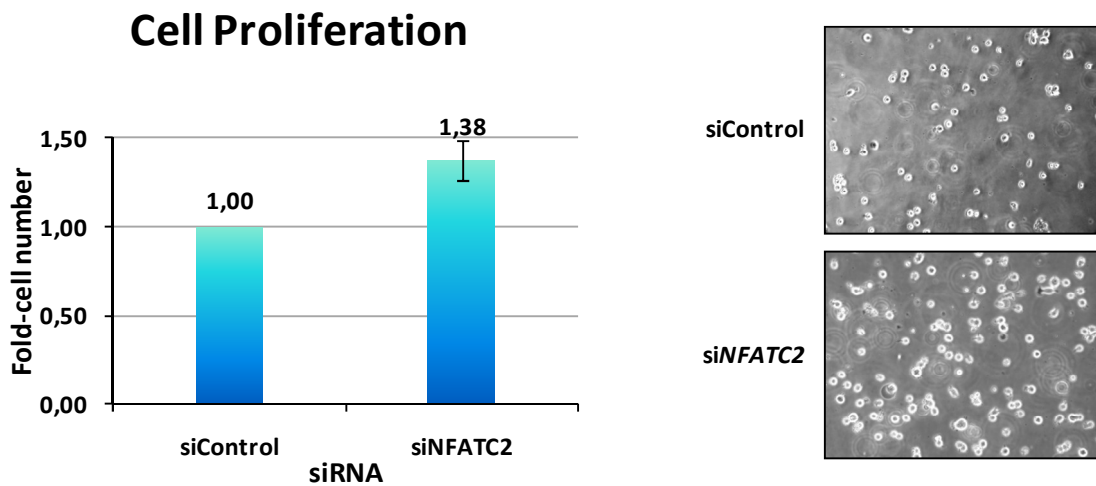


Figure 33. Effect of *NFATC2* suppression in proliferation of SET-2 cells.

Transfection with *siNFATC2* leads to a higher cellular density and increased cell size in comparison with cells transfected with *siControl*. Left: Graphic representation of the fold number variation of SET-2 cells treated with *siNFATC2* normalized to the number of *siControl*-treated cells (fold cell number 1.0). *siNFATC2*-treated cells showed a mean 1.38-fold significant increase in cell number relatively to control cells (paired samples t-test, $P=0,014$). Vertical bars indicate standard deviation obtained from 5 independent experiments. Right: Representative microscopic images of SET-2 megakaryocytes transfected with *siNFATC2* or *siControl*. Cell plates were observed using a Zeiss light microscope Axiovert 40C equipped with a Zeiss objective A-Plan (magnification 10x). Images were acquired using a Canon PowerShot G5 digital camera (magnification 4x).

3.3.5.8. REDUCED *NFATC2* EXPRESSION OR INHIBITION OF *NFATC2* ACTIVITY INCREASES *GM-CSF* EXPRESSION IN SET-2 CELLS

We next asked if proliferation of SET-2 megakaryocytes was related to a dysregulation of cytokine expression as a downstream effect of *NFATC2* protein inhibition or of *NFATC2* mRNA suppression. We choose *GM-CSF* to address the effect because this cytokine acts on the megakaryocytic cell lineage (Metcalf, 2008) and is transcriptionally regulated by *NFATC2* (Tsuboi *et al.*, 1994; Cockerill *et al.*, 1995; Luo *et al.*, 1996).

	siNFATC2	siControl
Number of assays	2	
Number of replicates	2	2
Mean <i>GM-CSF</i> Ct	36,05	37,10
Mean <i>GUS</i> Ct	23,47	23,51
Mean st. dev. <i>GM-CSF</i> Ct	0,46	0,72
Mean st. dev. <i>GUS</i> Ct	0,22	0,30
Mean Δ Ct	12,58	13,60
Mean $\Delta\Delta$ Ct	-1,02	
Mean fold-change	2,12	
St. dev.	0,91	

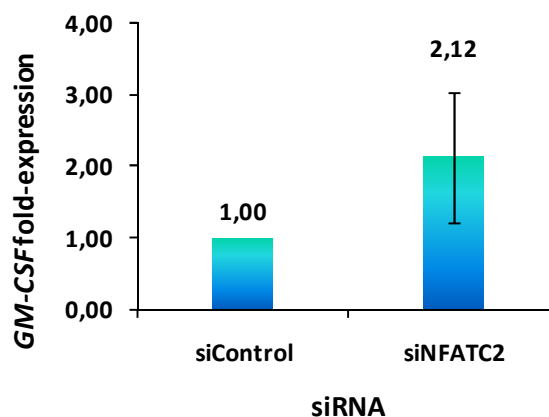


Figure 34. Partial suppression of *NFATC2* mRNA promotes *GM-CSF* expression in SET-2 cells.

Left: Summary table of Q-PCR data obtained from analysis of *GM-CSF* and *GUSB* expression in SET-2 cells treated with siNFATC2 and siControl; Quantification of *GM-CSF* expression was performed using the $\Delta\Delta$ Ct method; right: Graphical representation of the fold-expression variation in the levels of *GM-CSF* between siNFATC2- and siControl-treated cells. Vertical bar indicates the standard deviation obtained from 2 independent experiments. Mean fold-expression value of *GM-CSF* in siNFATC2-treated cells was calibrated to that of control cells (*GM-CSF* fold-expression = 1.00).

Using Q-PCR we calculated the variation in the expression levels of *GM-CSF* between cells treated with siNFATC2 or NFAT inhibitor and correspondent control cells. We observed that suppression of *NFATC2* mRNA led to an average 2.12-fold increase in the levels of *GM-CSF* transcript compared to control cells (Fig. 34). In inhibitor-treated cells a maximum of 99.2-fold increase in *GM-CSF* mRNA was observed at 10 μ M concentration of inhibitor after 2 hr incubation. Moreover, a 48.4-fold increase was observed after 24 hr incubation at 20 μ M concentration (Fig. 35). To verify if alteration of *GM-CSF* expression levels was related to a specific inhibition of NFATC2 transcriptional activity, we quantified in the same samples the levels of the *DIDO1* gene. This gene is expressed in myeloid cells from MPN patients (Fütterer *et al.*, 2005) and was not yet recognized as an NFAT target gene. We observed that the levels of *DIDO1* remained unaltered in inhibitor-treated cells after 2 or 24 hr incubation in the various concentrations of the inhibitor. Taken together, the results of the *in vitro* assays indicate that proliferation of SET-2 cells in culture was related to an increase in GM-CSF cytokine levels in the medium, which in turn was a consequence of diminished NFATC2 transcriptional activity.

A

NFATinhibitor concentration	2 hr-incubation					24 hr-incubation				
	0 μ M	1 μ M	5 μ M	10 μ M	20 μ M	0 μ M	1 μ M	5 μ M	10 μ M	20 μ M
Mean <i>GM-CSF</i> Ct	38,76	38,85	34,69	31,94	35,39	40,00*	39,29	39,24	39,61	35,83
Mean <i>DIDO1</i> Ct	24,18	23,61	23,68	24,14	24,08	24,67	24,53	24,54	24,53	25,79
Mean <i>GUS</i> Ct	25,72	26,20	26,32	25,54	26,26	25,13	25,11	24,15	24,38	26,56
St. dev. <i>GM-CSF</i> Ct	1,23	0,54	0,18	0,13	0,30	0,00	0,52	0,25	0,05	0,53
St. dev. <i>DIDO1</i> Ct	1,46	nd	nd	0,07	0,05	0,03	0,23	0,33	0,16	0,23
St. dev. <i>GUS</i> Ct	0,20	0,04	0,27	0,02	0,06	0,09	0,04	0,65	0,06	0,18
Mean Δ Ct (<i>GM-CSF</i> Ct- <i>GUS</i> Ct)	13,04	12,66	8,37	6,41	9,13	14,88	14,18	15,09	15,23	9,28
Mean Δ Ct (<i>DIDO1</i> Ct- <i>GUS</i> Ct)	-1,55	-2,59	-2,64	-1,39	-2,19	-0,45	-0,57	0,39	0,15	-0,76
Mean $\Delta\Delta$ Ct (<i>GM-CSF</i>)	-	-0,39	-4,67	-6,63	-3,91	-	-0,70	0,21	0,35	-5,60
Mean fold-change <i>GM-CSF</i>	1,00	1,3	25,4	99,2	15,0	1,00	1,62	0,86	0,78	48,39
Mean $\Delta\Delta$ Ct (<i>DIDO1</i>)	-	-1,04	-1,10	0,15	-0,64	-	-0,12	0,84	0,60	-0,31
Mean fold-change <i>DIDO1</i>	1,00	2,06	2,14	0,90	1,56	1,00	1,09	0,56	0,66	1,24

* Arbitrarily-defined Ct value; nd, not determined.

B

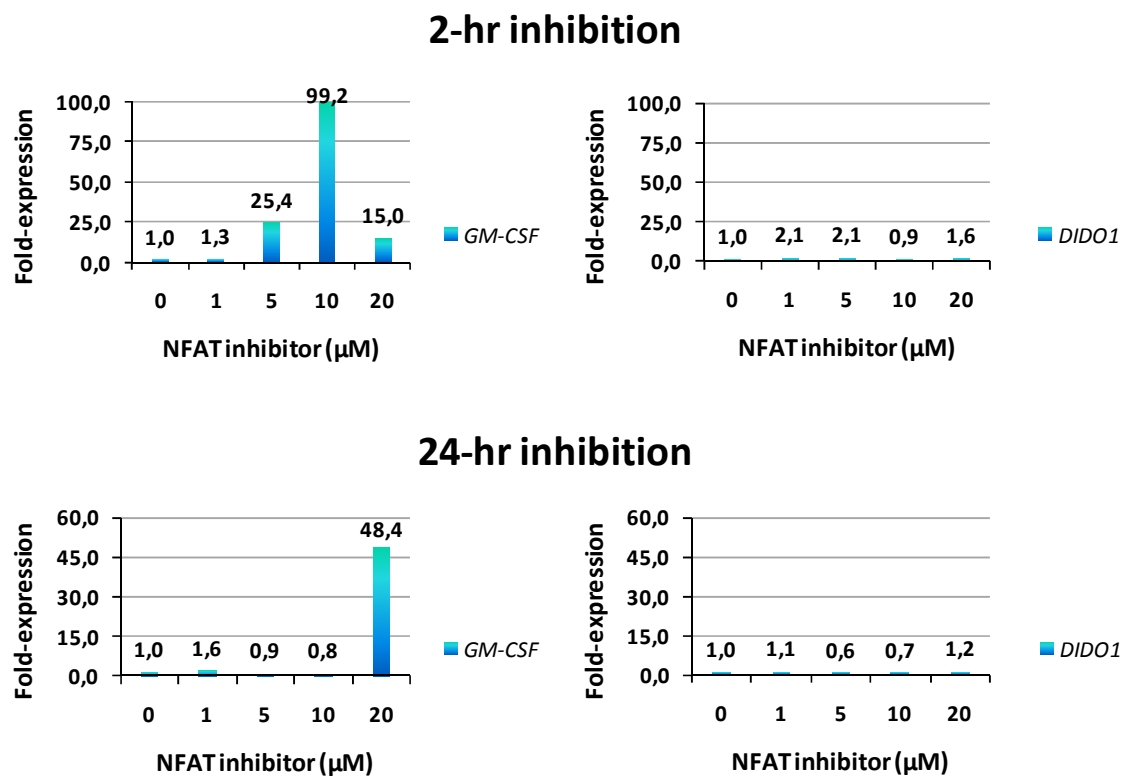


Figure 35. Inhibition of NFAT activity promotes *GM-CSF* expression in SET-2 cells.

(A) Summary table of Q-PCR data obtained from analysis of *GM-CSF*, *DIDO1* and *GUSB* expression in SET-2 cells after a 2 hr- or 24 hr-incubation in the absence or in the presence of different concentrations of NFAT inhibitor. Quantification of *GM-CSF* and *DIDO1* expression was performed using the $\Delta\Delta$ Ct method; (B) Graphical representation of the *GM-CSF* (left) and *DIDO1* (right) fold-expression variation in SET-2 cells incubated for 2 hr (upper graphs) or 24 hr (lower graphs) in the presence of different concentrations of NFAT inhibitor. Fold-expression values were calibrated relatively to cells incubated in the absence of inhibitor (*GM-CSF* fold-expression = 1.0; *DIDO1* fold-expression = 1.0).

3.3.6. DISCUSSION

In this work we describe *NFATC2* as a negative regulator of megakaryocyte proliferation and propose that abnormalities in cytokine regulation are associated with ET. Using FISH, PCR and whole-genome array techniques, we identified a 613 kb deletion at chromosome band 20q13 in a patient with ET presenting with a novel 3-way t(X;20;16)(p11.2;q13.13;q23.1). The 20q13 deletion removed the 5' region of the *NFATC2* gene and eliminated a complete copy of the *ATP9A* and *SALL4* genes. Despite the fact that 3 different genes were affected by the 20q chromosomal breakpoints, we focused our interest on *NFATC2* as a candidate gene in ET for 2 reasons.

Firstly, *NFATC2* is located at the long arm of chromosome 20, a genomic region frequently targeted by large interstitial deletions in MPN patients (Bench *et al.*, 1998a). Secondly, studies in normal myeloid cells have shown that *NFATC2* is characterized among the various NFAT-family members by its high levels of expression in CD34+ cells and megakaryocytes and low or absent expression in neutrophils, monocytes and erythrocytes (Kiani *et al.*, 2004), suggesting that *NFATC2* has a lineage-specific role within myelopoiesis. Because NFAT proteins are involved in the transcriptional regulation of myelopoietic cytokines, either as dimers or in cooperation with other transcription factors such as AP-1 (FOS/JUN) (reviewed in Rao *et al.*, 1997), we hypothesized that low levels of *NFATC2* protein in megakaryocytes could have important consequences for the regulation of cytokine expression and, as a consequence, for megakaryocyte proliferation. To test these hypotheses we simulated the loss of *NFATC2* in an ET cell line *in vitro* through the suppression of its transcript or through inhibition of protein activation with a selective peptide (Nogushi *et al.*, 2004).

We observed that the mRNA abundance of the myeloid lineage cytokine *GM-CSF* increased either in the presence of low levels of the *NFATC2* transcript or as a result of inhibition of *NFATC2* protein activation. These data indicates that *NFATC2* may play a dual role in regulating *GM-CSF* expression, either as a transcriptional repressor in megakaryocytes or as a transcriptional activator in lymphoid cells (Tsuboi *et al.*, 1994; Cockerill *et al.*, 1995; Luo *et al.*, 1996). In megakaryocytic cells of MPN patients, relieving of *NFATC2* transcriptional repression as a result of a del(20q) will promote cell growth and proliferation through increased availability of *GM-CSF*. Consistent with this hypothesis, we observed that diminished levels of *NFATC2* mRNA or protein were associated with proliferation of megakaryocytic cells *in vitro*, indicating that *NFATC2* negatively regulates megakaryocyte proliferation.

The consequences of the loss of *NFATC2* in myeloid cells have not yet been addressed *in vivo*. However, it was shown that *NFATC2*-null mice have hyperproliferation of lymphocytes (Hodge *et al.*, 1996) whereas *NFATC2/NFATC3*-double null mice develop a marked

lymphoproliferative disorder (Rengarajan *et al.*, 2002), indicating a close relationship between proliferation of lymphoid cells and absence of NFATC2. In our *in vitro* culture assays we observed that proliferation of megakaryocytes was associated with an increase in cyclin E levels, suggesting that proliferation was a consequence of cell cycle progression. Although these may be considered preliminary results which require further study, they are in line with previous data showing that hyperproliferation of *NFATC2* *-/-* lymphocytes in culture is correlated with overexpression of several cyclin proteins including cyclin E (Caetano *et al.*, 2002). Moreover, both *NFATC2*- and calcineurin A α -null mice have elevated levels of cyclin-dependent kinase 4, the catalytic partner of D-type cyclins at the G1-to-S phase transition of the cell cycle, showing that the calcineurin-NFAT signaling pathway has a negative regulatory role in cell cycle progression (Baksh *et al.*, 2002).

Constitutive activation of the calcineurin-NFAT pathway was observed in several hematological malignancies involving the lymphoid lineage. In particular, dephosphorylation of NFATC2 was documented in samples of patients with diffuse large B-cell lymphoma (DLBCL) and T-cell lymphoma whereas NFAT activation was demonstrated in cell lines derived from patients with DLBCL and T-cell ALL (reviewed in Medyouf & Ghysdael, 2008). Recently, a role for *NFATC2* as an oncogene was also demonstrated in 4 cases of Ewing sarcoma associated with the formation of a fusion gene between *NFATC2* and the *EWSR1* gene at chromosome 22 (Szuhai *et al.*, 2009). In contrast to its role as an oncogene, *NFATC2* may also act as a tumour suppressor gene in Burkitt lymphoma cells by promoting apoptosis when activated by calcineurin (Kondo *et al.*, 2003). However, there is no other study to our knowledge implicating *NFATC2* in myeloid disorders. We did not find mutations in the non-rearranged *NFATC2* allele in our patient with a t(X;20;16), suggesting that haplo-insufficiency of this gene as a result of 20q deletions is the most likely pathogenetic mechanism in ET and possibly other myeloid disorders. In 10 out of 23 patients (43%) with myeloid neoplasms and del(20q) analyzed by Huh *et al.* (2010), the extent of the 20q deletions also encompassed *NFATC2*, indicating that this gene is also haplo-insufficient in a significant proportion of patients with a del(20q). Taken together, these data indicate that different genetic mechanisms contribute to the involvement of the *NFATC2* gene in the pathogenesis of hematopoietic malignancies.

In addition to the del(20q) we also found, using array analysis, a 1.2-Mb deletion at chromosome region 16q23.1-16q23.2. The deleted region encompassed the entire *MAF* gene and the most 3' coding exon of the *WWOX* gene. *MAF* is the human homologue of the transforming gene of the avian retrovirus AS42, which encodes a transcription factor protein belonging to the bZIP protein family (Kataoka *et al.*, 1993). This family is characterized by the presence of a leucine

zipper domain and also includes as members the *NRL*, *FOS*, *JUN* and *NF-E2* genes (Swaroop *et al.*, 1992; Andrews *et al.*, 1993; Kataoka *et al.*, 1993; Kataoka *et al.*, 1994; Kerppola & Curran, 1994). Interestingly, NF-E2 is an erythroid lineage-transcription factor overexpressed in megakaryocytes, erythrocytes and granulocytic precursors within the bone marrow of PV patients (Goerttler *et al.*, 2005). NF-E2 overexpression delays erythroid maturation and, consequently, increases the number of erythroid progenitor cells (Mutschler *et al.*, 2009). Similarly, MAF operates in myeloid lineage cells by inhibiting erythroid differentiation through repression of Ets-1-mediated transactivation of the transferrin receptor (Sieweke *et al.*, 1996; Sieweke *et al.*, 1997). These data highlights a possible role of the MAF protein in erythrocyte accumulation associated with PV.

Similarly to NFAT proteins, MAF also operates as a transcription regulator of several cytokine genes. MAF inhibits *IL-12* and activates *IL-4* and *IL-10* in macrophages (Cao *et al.*, 2002; Cao *et al.*, 2005), and induces *GM-CSF* expression in T cells (Gilmour *et al.*, 2007). In addition, MAF can also form heterodimers with FOS and JUN and bind to AP-1 sites (Kerppola & Curran, 1994) which are found in a number of other cytokine genes. Thus, although the consequences of MAF deletion on cytokine expression have not been investigated in our study, our findings in the patient with t(X;20;16) suggest that haplo-insufficiency of MAF may have complemented NFATC2 deletion to disturb normal cytokine signaling in MPN cells.

In summary, characterization of the molecular abnormalities resulting from a complex 3-way t(X;20;16) in an ET patient led us to implicate the NFATC2 gene in abnormal cytokine expression and megakaryocyte proliferation. Our results further suggest that haplo-insufficiency of NFATC2 may cooperate with the JAK2V617F mutation to disturb the overall cytokine signaling circuit in hematopoietic cells. Preliminary results have shown that NFATC2 mRNA levels in granulocytes of ET patients are lower than those of normal granulocytes. These data warrants further studies to validate NFATC2 expression as a marker of megakaryocyte proliferation in ET.

4. CONCLUSIONS AND FUTURE PERSPECTIVES

It is widely accepted that cancer is a multistep phenomenon which requires alterations of several different cellular pathways in order to achieve its full transforming potential (Hanahan & Weinberg, 2000). This model of tumourigenesis has already been put in evidence in hematological malignancies, particularly in AML. The identification of major cytogenetic abnormalities as well as the detection of somatic gene mutations allowed the categorization of genetic alterations in AML patients according to a 2-hit leukemogenic model (Frankfurt *et al.*, 2007). This theory postulates that one class of mutations is responsible for the differentiation arrest of AML cells and the other for an increased and disregulated proliferative potential of the neoplastic cells. The first type is mostly typified by recurrent balanced chromosomal rearrangements such as t(8;21), inv(16), t(15;17) and 11q23/MLL translocations, which result in direct (e.g., *RUNX1*, *CBFB* or *RARA*) or indirect (e.g., *MLL*) disregulated transcription factor activity. MLL fusion oncoproteins act by disregulating the transcription of homeobox genes, which in turn modifies transcription of target genes, or by conversion of hematopoietic progenitors into leukemic stem cells expressing a self-renewal program (reviewed in Faber & Armstrong, 2007; Haferlach, 2008). The second class of mutations accounts for an increased cell proliferation as a consequence of activating mutations in genes encoding for tyrosine kinase proteins including *FLT-3*, *c-KIT* and *JAK2*, for instance. In addition to these 2 categories a third class of AML mutations has also been proposed which includes genes involved in cell cycle regulation and apoptosis (Renneville *et al.*, 2008). The typical examples include *NPM1* mutations, which constitute the most frequent genetic alterations in AML, and *TP53* deletions or mutations (Haferlach, 2008).

Therefore, fusion genes generated by recurrent chromosomal translocations in hematopoietic malignancies are just one type of alteration which contributes to the overall leukemic phenotype. One possible way to identify additional genetic lesions is through the analysis of complex chromosome translocations. The extra breakpoints involved in these rearrangements may indicate the location of genes which also can have a relevant role in the pathogenesis and that usually remain unnoticed because of their inconsistent nature and low frequency. In this perspective, we sought to identify and/or characterize the genes involved in the extra breakpoint locations of complex translocations associated with different hematological neoplasms, including a t(12;6;15), a t(9;11;19) and a t(X;20;16), and define their role in tumourigenesis.

In section 3.1 of this dissertation we have characterized by FISH analysis the breakpoints involved in different structural rearrangements detected in 2 B-cell ALL patients and in one patient with MDS/MPN, U. These rearrangements had in common the involvement of the short arm of chromosome 12. In one of the B-cell ALL cases we uncovered a 3-way translocation t(12;21;5) associated with a recurrent fusion between the *ETV6* (12p13) and the *RUNX1* (21q22)

gene on the der(21) chromosome, as observed in patients with a t(12;21)(p13;q22) (Golub *et al.*, 1995; Romana *et al.*, 1995). However, the consequences of the extra breakpoint at 5q13 to B-cell ALL pathogenesis remain to be addressed. In contrast to the B-cell ALL patient, we found that a 3-way t(12;6;15) associated with a MDS/MPN, U did not involve the formation of a fusion gene between *ETV6* and a putative partner gene at 6p24~25. Instead, we detected a 1.2-Mb interstitial deletion at chromosome band 12p13 which included *ETV6* and 8 other genes. Through an extensive mapping of the deleted region we determined that its borders were internally delimited by *ETV6* on the telomeric side and *CDKN1B* on the centromeric side.

The absence of *ETV6* in mouse embryos impairs angiogenesis within the yolk sac and leads to premature embryonic death (Wang *et al.*, 1997). Moreover, *ETV6* is absolutely required for production of erythroid, myeloid, lymphoid, mast, and megakaryocytic cells in mice bone marrow (Wang *et al.*, 1998b). In turn, *CDKN1B*, which encodes the cyclin-dependent kinase inhibitor protein P27, whose levels are elevated during quiescence, is important for blocking cell cycle progression in resting cells (Kato *et al.*, 1994; Nourse *et al.*, 1994). In this setting, the finding of a concomitant loss of a transcription factor (*ETV6*) and of a cell cycle regulator (*CDKN1B*) in the myeloid lineage cells of the patient with a t(12;6;15) parallels the 2-hit model of AML pathogenesis (Frankfurt *et al.*, 2007). Although the molecular consequences of the breakpoints at chromosomes 6 and 15 have not been addressed, these findings support the notion that different cellular pathways important for tumourigenesis may be targeted by a single complex chromosomal rearrangement.

In another B-cell ALL patient with a dicentric chromosome rearrangement dic(9;12), we also identified a large deletion which included the genomic region between band 12p13 and the telomere of the short arm of chromosome 12. In addition, this patient also presented with a major deletion of chromosome 9 sequences extending from band 9p13 to the telomere of the short arm of chromosome 9. The dic(9;12) is associated in some B-cell ALL cases with the formation of an in-frame *PAX5-ETV6* fusion (Strehl *et al.*, 2003). In our patient with a dic(9;12) we found that both genes were deleted, initially suggesting that a different pathogenic mechanism was operating in this patient. However, a more recent study has shown that *PAX5* expression levels are equally reduced in patients with dicentric chromosomes independently of the presence of a *PAX5*-derived fusion gene or of a *PAX5* deletion (An *et al.*, 2008). Moreover, the *PAX5* allele on the normal chromosome 9 may present with inactivating point mutations or intragenic deletions in some patients, indicating that *PAX5* loss-of-function is also relevant for the pathogenesis of B-cell ALL in patients with dicentric chromosomes leading to deletion of *PAX5* (An *et al.*, 2008). Significantly, the AML-related *FLT3* gene, a *PAX5*-target gene, is overexpressed in B-

cell ALL patients with *PAX5* alterations (An *et al.*, 2008). These results suggest that the inactivation of transcription factor genes (*ETV6* and *PAX5*) through chromosomal rearrangement, together with the indirect activation of proliferation genes (*FLT3*) as a result of *PAX5* alterations in B-cell ALL with dic(9;12) also agree to a double-hit model of leukemogenesis. However, the molecular consequences for tumourigenesis that may derive from the loss of other genes located at the 12p13-12pter and 9p13-9pter genomic regions remain to be further investigated.

In section 3.2 of this thesis we described the molecular rearrangements resulting from the formation of a complex 3-way t(9;11;19) associated with AML. This translocation produced an in-frame *MLL-MLLT3* fusion gene as seen in other AML patients with a t(9;11) (Iida *et al.*, 1993; Nakamura *et al.*, 1993). However, the complex translocation also resulted in the disruption of a gene previously identified as *FLJ10374* at chromosome band 19p13 (Vieira *et al.*, 2006). This gene, now referred to as *CCDC94*, was found to encode a nuclear protein which negatively controls cell cycle progression and proliferation. Because *CCDC94* was haplo-insufficient in the AML patient with *MLL-MLLT3* fusion, we hypothesize that both genetic changes concurred to disturb different cellular pathways and induce the AML phenotype. In this setting, a single complex chromosomal rearrangement may affect cell cycle regulation and normal myeloid differentiation simultaneously in accordance with the requirements of the double genetic hit model (Frankfurt *et al.*, 2007). It is not known if *CCDC94* inactivating mutations occur in other *MLL-MLLT3*-positive acute leukemias or if our findings in the patient with t(9;11;19) are exclusive. However, in view of these productive cooperating events, it constitutes an attractive hypothesis which deserves future investigation.

Disregulation of cell cycle control proteins by chromosomal breakpoints may constitute a recurrent theme in acute leukemia patients presenting with complex translocations involving formation of MLL fusion proteins. Raffini *et al.* (2002) reported that a *CDK6-MLL* fusion was generated in a *MLL-AF4*-positive B-cell ALL patient as a result of a complex t(4;11) involving an extra breakpoint at chromosome band 7q22. CDK6 is activated by any of the 3 D-type cyclin proteins during the early G1 phase of the cell cycle (Sherr & Roberts, 1999). Activated CDK6 phosphorylates and inactivates the RB1 protein, thereby releasing sequestered E2F transcription factors that lead to expression of various S-phase promoting genes (reviewed in Vieira & Gomes da Silva, 2008). The predicted configuration of the CDK6-MLL fusion protein includes the PLSTIRE aminoacid sequence and the catalytic cleft of CDK6 fused to the zinc-finger and activation domains of MLL (Raffini *et al.*, 2002). The PLSTIRE sequence motif in CDK6 functions as an interaction site for cyclins (Jeffrey *et al.*, 2000). Although Raffini *et al.* (2002) did not provide functional data for the CDK6-MLL fusion protein, it is possible that the catalytic domain of CDK6 present in the CDK6-MLL fusion was constitutively activated by the MLL moiety of the fusion protein, therefore promoting cell cycle progression of *MLL-AF4*-positive cells, similarly to our case

with t(9;11;19). Increased expression of CDK6 was also found to occur in some patients with B-cell lymphomas in association with recurrent translocations of band 7q21 (Corcoran *et al.*, 1999; Brito-Babapulle *et al.*, 2002; Hayette *et al.*, 2003).

A few other studies have provided direct or indirect evidence that genes located at the extra breakpoints involved in complex translocations of myeloid neoplasms are likely to play a role in their pathogenesis. One of the first examples in CML is the glutathione S-transferase Pi (*GSTP1*) gene, a member of the family of glutathione S-transferase enzymes involved in the detoxification of endogenous and exogenous electrophilic substrates (Strange *et al.*, 2001). The *GSTP1* gene localizes at chromosome band 11q13, a frequent hotspot of extra breakpoints in CML (De Braekeleer, 1987). The 11q13 breakpoint has been localized within the *GSTP1* sequence or at a distance of only 100-250 kb distant from the gene in 2 patients with a t(9;22;11)(q34;q11;q13) (Koduru *et al.*, 1993; Morris *et al.*, 1996). This suggests that *GSTP1* is a non-random target gene in CML patients with extra 11q13 breakpoints and reinforces the possible pathogenic role of this gene in the disease.

The *GSTP1* gene is regulated at the transcriptional level by the tumour suppressor protein P53, which binds to a specific site within intron 4 (Lo *et al.*, 2008). Interestingly, the *P53* gene, which localizes at band 17p13.1, is frequently lost in CML patients in blast crisis as a result of the formation of an isochromosome of the long arm of chromosome 17, i(17q) (Johansson *et al.*, 2002). Moreover, nucleotide mutations of the *P53* gene have been shown to occur in CML patients in blast crisis with or without the presence of i(17q), but not in chronic phase disease (Nakai *et al.*, 1992). Taken together, these observations suggest that down-regulation of the *GSTP1* gene as a result of P53 loss of function may occur frequently in advanced CML. In this context it may be hypothesized that haplo-insufficiency of *GSTP1* through physical disruption as observed in the patient with t(9;22;11) reported by Koduru *et al.* (1993) may operate similarly to the loss of the P53 protein, which is observed at later disease stages. The consequences of reduced *GSTP1* protein levels in CML cells and their putative association with disease status are yet unknown. Nevertheless, a possible role of *GSTP1* in the pathogenesis of hematological malignancies was reinforced by a more recent observation that expression of this gene is diminished in human lymphoma (Rossi *et al.*, 2004).

Perhaps the most striking example of the relevant role of additional breakpoints in hematological neoplasms was provided by the study of a 4-way t(3;9;17;22)(q26;q34;q22;q11) detected in a CML patient in blast crisis (De Weer *et al.*, 2008). In this rearrangement, juxtaposition of chromosome 17 sequences to sequences from band 3q26 led to an increased expression of the *EVI1* oncogene at 3q26 in CML cells. The *EVI1* gene is the translocation partner

of *RUNX1* in the t(3;21)(q26;q22) associated with the blast crisis phase of CML (Mitani *et al.*, 1994). The RUNX1-EVI1 fusion protein contains the entire EVI1 protein sequence fused to the N-terminal region of *RUNX1* including the runt homology domain (Mitani *et al.*, 1994). Because *EVI1* is not normally expressed in hematopoietic cells, its expression is greatly increased by the t(3;21)(q26;q22) (Ogawa *et al.*, 1996). Remarkably, over-expression of *EVI1* is also detected in CML patients in blast crisis in the absence of 3q26 abnormalities (Ogawa *et al.*, 1996). The consequences of *EVI1* over-expression in a myeloid cell line model were shown to consist in a blockage of granulocytic differentiation (Tanaka *et al.*, 1995). Although De Weer *et al.* (2008) have proposed a 2-step mechanism for the generation of t(3;9;17;22), it is highly likely that in the CML patient over-expression of *EVI1* concurred with the presence of the *BCR-ABL1* fusion gene to promote rapid progression to an acute disease phase.

Taken together, although additional breakpoints in complex translocations in leukemia target genes involved in different cellular pathways, the changes described here reinforce the concept that genetic alterations at those breakpoints may independently contribute to disease progression, particularly by mimicking specific chromosomal alterations which are usually observed in aggressive disease stages.

The double-hit model of AML pathogenesis dictates that at least 2 genetic changes affecting the pathways of differentiation, proliferation and/or cell cycle/apoptosis regulation must occur to induce the overt AML phenotype (Frankfurt *et al.*, 2007). We have provided evidence from the analysis of 2 complex translocations in myeloid disorders that genes implicated in cellular differentiation and cell cycle regulation, located at different genomic regions, may be simultaneously targeted by a single complex chromosomal rearrangement. In section 3.3 of this dissertation, we provide evidence that a complex translocation t(X;20;16) in a patient with ET affected genes with similar functions which map to different breakpoint regions. The translocation resulted in the deletion of the *NFATC2* gene at 20q13 and the *MAF* gene at 16q23, both of which encode transcription factors implicated in the regulation of cytokine genes. We showed that inhibition of *NFATC2* protein or the suppression of its mRNA sequence in a model ET cell line increases the expression of *GM-CSF*, a cytokine involved in the proliferation of various myeloid lineages (Metcalf, 2008). Although *MAF* also regulates expression of *GM-CSF*, we have not addressed the consequences of *MAF* loss-of-function in our cell line model as we did for *NFATC2*. However, given their similar functions, it is fair to hypothesize that haplo-insufficiency of both transcription factor genes in our ET patient with t(X;20;16) contributed to dysregulate the normal pattern of cytokine expression in myeloid cells.

NFATC2 protein is activated by the Ca²⁺/calmodulin-dependent calcineurin phosphatase in the cytosol as a consequence of an increase in intracellular [Ca²⁺] (Hogan *et al.*, 2003). This

dependency on Ca^{2+} ions suggests that in addition to deletion of *NFATC2*, genetic defects involving other members of cellular Ca^{2+} signaling could also contribute to an impaired *NFATC2* activity. In our patient with t(X;20;16) we found that the *ATP9A* and *SALL4* genes were also included in the deleted region at 20q13. *ATP9A* codes for a putative phospholipid-transporting (P-type) membrane ATPase involved in the transport of Ca^{2+} and other cations. Using the predicted *ATP9A* protein sequence as template, we confirmed using bioinformatics analyses that *ATP9A* shares domain-specific amino acid sequence similarities of 38-39% with the secretory pathway Ca^{2+} ATPase 1, sarco-endoplasmic reticulum Ca^{2+} ATPase 1 and plasma membrane Ca^{2+} ATPase 4b proteins (data not shown). Moreover, preliminary cellular assays indicate that *ATP9A* is an endoplasmic reticulum membrane protein (data not shown). Although no experimental data yet exists to confirm that *ATP9A* indirectly activates the calcineurin-NFAT pathway through an increase in cytosolic $[\text{Ca}^{2+}]$, it is plausible that pumping of Ca^{2+} ions from the reticulum lumen to the cytosol may activate the pathway, similarly to extracellular Ca^{2+} stimulation. Consequently, loss of both *NFATC2* and *ATP9A* through chromosomal deletion may cooperate to impair activation of the calcineurin-NFAT pathway in myeloid cells.

The interstitial 20q13 deletion in our ET patient with t(X;20;16) also encompassed the *SALL4* gene. This gene is homologous to the *spalt* gene of *Drosophila melanogaster* and encodes a zinc-finger transcription factor which modulates pluripotency of embryonic stem cells and early embryonic development (Zhang *et al.*, 2006). Germline mutations of *SALL4* are responsible for several clinical phenotypes including the Duane-radial ray syndrome and the Okihiro syndrome (OS), the acro-renal-ocular syndrome and, more rarely, the Holt-Oram syndrome (Kohlhase *et al.*, 2002; Kohlhase *et al.*, 2003). Mutations of *SALL4* are predominantly nonsense mutations or gene deletions, leading to a haplo-insufficiency of *SALL4*. In addition, a *SALL4* mutation was found in several affected individuals of a large Venezuelan family with Instituto Venezolano de Investigaciones Científicas (IVIC) syndrome (Paradisi & Arias, 2007), initially described as an autosomal dominant condition characterized mainly by upper limb malformations (Arias *et al.*, 1980). Although some of the affected individuals with IVIC displayed moderate thrombocytosis, there is no evidence for the development of hematopoietic abnormalities or of a myeloproliferative phenotype, including ET, in patients with *SALL4*-associated disorders (Kohlhase, 2008). In contrast, over-expression of *SALL4* was documented in human AML samples, indicating that it may operate as an oncogene in this disorder (Ma *et al.*, 2006).

In a few patients with OS, multigene deletions involving *SALL4* and other neighbouring genes, including *NFATC2*, have been described as an alternative mechanism to inactivating *SALL4* mutations (Borozdin *et al.*, 2004; Borozdin *et al.*, 2007). Although these OS patients presented

with additional clinical features, there was also no evidence of hematological alterations despite haplo-insufficiency of *NFATC2* in hematopoietic cells (Borozdin *et al.*, 2007). This suggests that loss of one *NFATC2* allele may only provide a proliferative advantage to a hematopoietic precursor cell if other genetic changes are also acquired, namely *JAK2V617F*. This hypothesis is supported by a study showing that the vast majority of MPN patients with del(20q) are also positive for *JAK2V617F*, as in the case of our patient, indicating that both genetic alterations are cooperating events in disease development (Campbell *et al.*, 2006). In agreement with this hypothesis, our results showing an association between inactivation of *NFATC2* and cell proliferation *in vitro* were obtained using a *JAK2V617F*-positive cell line. Taken together, the results obtained in our patient with a complex t(X;20;16) also support a 2-hit model for the pathogenesis of ET. In particular, an activating mutation (*JAK2V617F*) promoted cell proliferation whereas inactivating alterations (deletion of *NFATC2* and *MAF*) affected myeloid lineage development.

The results described in this thesis clearly highlight a fundamental role for extra breakpoint locations in the pathogenesis of hematological neoplasms. As in the case of standard 2-way translocations, extra chromosomes involved in complex translocations are neither lost nor further rearranged by other chromosomal mechanisms during clonal evolution. Moreover, the configuration of complex chromosomal rearrangements in the same patient is identical at initial diagnosis and at relapse following a period of cytogenetic remission (Huntly *et al.*, 2001), reinforcing the notion that the stability of extra rearranged chromosomes is of importance to leukemic cells throughout the course of the disease.

These clinical-cytogenetic evidences may imply that positive selection pressures are operating at the level of the leukemic clone to maintain the integrity and functionality of all rearranged chromosomes originated by a complex translocation. This apparent selection of breakpoint locations in tumour-related abnormalities is stressed by studies of mammalian chromosome evolution. Nadeau & Taylor (1984) initially proposed that there would exist approximately 180 conserved genomic blocks with preserved gene orders between man and mouse. These so-called synteny blocks, which contain at least 2 orthologous genes shared by both species, vary in length between 1 and 24 centimorgans (Nadeau & Taylor, 1984). If the frequency of the various blocks is plotted as a function of their length, the resulting histogram fits well into an exponential distribution curve where frequency diminishes as a function of block length. On this basis, a "random breakage model" was proposed, which sustained that chromosome evolution derived from the occurrence of randomly distributed breakpoints throughout the genome (Nadeau & Taylor, 1984). However, studies of human and mouse genome rearrangements have revealed that a significant number of breakpoints are located at hotspots,

implying the existence of small synteny blocks (< 1 Mb) that remained undetected in most cases even after the draft human and mouse genome sequences were published (Pevzner & Tesler, 2003a; Pevzner & Tesler, 2003b). If the length of these 190 small blocks is again plotted as a function of their frequency, the resulting histogram will show that larger blocks have a higher frequency than some of the smaller ones (Pevzner & Tesler, 2003b). This data does not fit an exponential distribution, where frequency is a function of the block length, and is therefore incompatible with the “random breakage model”. In this context, an alternative “fragile breakage model” has been proposed (Pevzner & Tesler, 2003b) which sustains that certain chromosomal regions are more prone than others to chromosomal rearrangements, and therefore are “reused” in different mammalian species during chromosome evolution (Pevzner & Tesler, 2003b; Kemkemer *et al.*, 2009). This model of breakpoint hotspots is compatible with a skewed or clustered distribution of breakpoints that are revealed by cytogenetic studies in newborns with malformations, in tumours and in families carrying constitutional translocations (Cohen *et al.*, 1996; Sankoff D *et al.*, 2002; Burrow *et al.*, 2009). Although no studies have yet been done to associate breakpoint locations of complex translocations with evolutionarily fragile breakpoint regions, the significant degree of hotspot clustering observed in some hematological malignancies, is highly suggestive that extra breakpoint locations are also under positive selection forces.

These data clearly highlights a correlation between evolutionary-related chromosome breakage and structural rearrangements in human cancer. Support for this hypothesis was provided by a molecular study of a 4-way complex $t(9;22;10;17)(q34;q11;p13;q21)$ detected in a CML patient (McKeithan *et al.*, 1992). Chromosome band 17q21 is a non-random breakpoint location in CML patients with complex rearrangements (De Braekeleer, 1987). Comparison between the 4 derivative chromosome junctions and their normal counterpart sequences showed a divergence at both the 10;17 and 17;9 chromosomal junctions. Using FISH with a probe directed to the 17q21 breakpoint region, McKeithan *et al.* (1992) also observed a signal at chromosome band 17q23 on normal hematopoietic cells. By comparing high-resolution karyotypes between humans and other primate species the authors detected that both regions on chromosome 17 corresponded to the breakpoint locations of a paracentric inversion that occurred during the evolution from an ancestral chromosome 17 to the definite human chromosome 17 (McKeithan *et al.*, 1992). In conclusion, if breakpoints at additional chromosomes involved in complex leukemia translocations are evolutionarily conserved, the molecular identification and characterization of their target genomic sequences may prove a successful means to identify novel tumour-related genes.

In summary, we undertook in this dissertation a study of 4 different complex chromosomal rearrangements including a t(12;21;5), t(12;6;15), t(9;11;19) and t(X;20;16), and of a dicentric translocation dic(9;12) associated with distinct hematological neoplasms. These studies allowed us to derive 2 main conclusions regarding the role of complex translocations in leukemia. Firstly, when complex translocations are associated with the production of recurrent fusion genes, additional breakpoint locations may target genes which obey the double-hit model of leukemogenesis; secondly, if complex translocations are recurrently associated with breakpoint-adjacent deletions and no fusion genes are present, the deletion of at least 2 genes operating in the same or in complementary cellular pathways may be necessary to promote leukemogenesis. In other words, the multi-hit stepwise model of cancer development may be obviated by simultaneous genetic hits through the occurrence of a complex translocation or of breakpoint-associated deletions, thereby avoiding the need for subsequent mutations.

5. REFERENCES

- Abe S, Minamihisamatsu M, Ishihara T, Sasaki M (1989) Chromosomal in situ hybridization and Southern blot analyses using c-abl, c-sis, or bcr probe in chronic myelogenous leukemia cells with variant Philadelphia translocations. *Cancer Genet Cytogenet* **38**: 61-74.
- Abeliovich D, Yehuda O, Krichevsky S, Nagler A, Ben-Neriah S, Werner M, Ludkovsky O, Ben-Yehuda D (1995) Reversed BCR/ABL rearrangement detected by FISH in Philadelphia negative chronic myelocytic leukemia. *Cancer Genet Cytogenet* **81**: 115-117.
- Ahmad F, Kokate P, Chheda P, Dalvi R, Das BR, Mandava S (2008) Molecular cytogenetic findings in a three-way novel variant of t(1;8;21)(p35;q22;q22): a unique relocation of the AML1/ETO fusion gene 1p35 in AML-M2. *Cancer Genet Cytogenet* **180**: 153-157.
- Albano F, Specchia G, Anelli L, Zagaria A, Storlazzi CT, Buquicchio C, Roberti MG, Liso V, Rocchi M (2003) Genomic deletions on other chromosomes involved in variant t(9;22) chronic myeloid leukemia cases. *Genes Chromosomes Cancer* **36**: 353-360.
- Alcalay M, Zangrilli D, Fagioli M, Pandolfi PP, Mencarelli A, Lo Coco F, Biondi A, Grignani F, Pelicci PG (1992) Expression pattern of the RAR α -PML fusion gene in acute promyelocytic leukemia. *Proc Natl Acad Sci USA* **89**: 4840-4844.
- Altschul SF, Madden TL, Schaffer AA, Zhang J, Zhang Z, Miller W, Lipman DJ (1997) Gapped BLAST and PSI-BLAST: A new generation of protein database search programs. *Nucleic Acids Res* **25**: 3389-3402.
- Altschul SF, Wootton JC, Gertz EM, Agarwala R, Morgulis A, Schaffer AA, and Yu Y-K (2005) Protein database searches using compositionally adjusted substitution matrices. *FEBS J* **272**: 5101-5109.
- An Q, Wright SL, Konn ZJ, Matheson E, Minto L, Moorman AV, Parker H, Griffiths M, Ross FM, Davies T, Hall AG, Harrison CJ, Irving JA, Strefford JC (2008) Variable breakpoints target PAX5 in patients with dicentric chromosomes: A model for the basis of unbalanced translocations in cancer. *Proc Natl Acad Sci U S A* **105**: 17050-17054.
- Andrews NC, Kotkow KJ, Ney PA, Erdjument-Bromage H, Tempst P, Orkin SH (1993) The ubiquitous subunit of erythroid transcription factor NF-E2 is a small basic-leucine zipper protein related to the v-maf oncogene. *Proc Natl Acad Sci U S A* **90**: 11488-11492.
- Anelli L, Albano F, Zagaria A, Liso A, Roberti MG, Rocchi M, Specchia G (2004) A chronic myelocytic leukemia case bearing deletions on the three chromosomes involved in a variant t(9;22;11). *Cancer Genet Cytogenet* **148**: 137-140.
- Aramburu J, Yaffe MB, López-Rodríguez C, Cantley LC, Hogan PG, Rao A (1999) Affinity-driven peptide selection of an NFAT inhibitor more selective than cyclosporine A. *Science* **285**: 2129-2133.
- Arellano-Rodrigo E, Alvarez-Larrán A, Reverter JC, Villamor N, Colomer D, Cervantes F (2006) Increased platelet and leukocyte activation as contributing mechanisms for thrombosis in essential thrombocythemia and correlation with the JAK2 mutational status. *Haematologica* **91**: 169-175.
- Arias S, Penchaszadeh VB, Pinto-Cisternas J, Larrauri S (1980) The IVIC syndrome: a new autosomal dominant complex pleiotropic syndrome with radial ray hypoplasia, hearing impairment, external ophthalmoplegia, and thrombocytopenia. *Am J Med Genet* **6**: 25-59.
- Arnoldus EP, Wiegant J, Noordermeer IA, Wessels JW, Beverstock GC, Grosveld GC, van der Ploeg M, Raap AK (1990) Detection of the Philadelphia chromosome in interphase nuclei. *Cytogenet Cell Genet* **54**: 108-111.
- Asimakopoulos FA, White NJ, Nacheva E, Green AR (1994) Molecular analysis of chromosome 20q deletions associated with myeloproliferative disorders and myelodysplastic syndromes. *Blood* **84**: 3086-3094.
- Atlas M, Head D, Behm F, Schmidt E, Zeleznik-Le NH, Roe BA, Burian D, Domer PH (1998) Cloning and sequence analysis of four t(9;11) therapy-related leukemia breakpoints. *Leukemia* **12**: 1895-1902.
- Axelrad AA, Eskinazi D, Correa PN, Amato D (2000) Hypersensitivity of circulating progenitor cells to megakaryocyte growth and development factor (PEG-rHu MGDF) in essential thrombocythemia. *Blood* **96**: 3310-3321.
- Ayraud N, Raynaud S, Bayle J, Dujardin P (1985) Variant translocation t(8;21;15) in an acute myeloblastic leukemia with phenotypic differential evolution. *Cancer Genet Cytogenet* **15**: 191-197.
- Ayton PM & Cleary ML (2001) Molecular mechanisms of leukemogenesis mediated by MLL fusion proteins. *Oncogene* **20**: 5695-5707.
- Baens M, Peeters P, Guo C, Aerssens J, Marynen P (1996) Genomic organization of TEL: The human ETS-variant Gene 6. *Genome Res* **6**: 404-413.
- Baksh S, Widlund HR, Frazer-Abel AA, Du J, Fosmire S, Fisher DE, DeCaprio JA, Modiano JF, Burakoff SJ (2002) NFATc2-mediated repression of cyclin-dependent kinase 4 expression. *Mol Cell* **10**: 1071-1081.
- Bartram CR, Kleihauer E, de Klein A, Grosveld G, Teyssier JR, Heisterkamp N, Groffen J (1985) c-abl and bcr are rearranged in a Ph¹-negative CML patient. *EMBO J* **4**: 683-686.

- Baxter EJ, Scott LM, Campbell PJ, East C, Fourouclas N, Swanton S, Vassiliou GS, Bench AJ, Boyd EM, Curtin N, Scott MA, Erber WN, Green AR; Cancer Genome Project (2005) Acquired mutation of the tyrosine kinase JAK2 in human myeloproliferative disorders. *Lancet* **365**: 1054-1061.
- Bednarek AK, Laffin KJ, Daniel RL, Liao Q, Hawkins KA, Aldaz CM (2000) WWOX, a novel WW domain-containing protein mapping to human chromosome 16q23.3-24.1, a region frequently affected in breast cancer. *Cancer Res* **60**: 2140-2145.
- Beillard E, Pallisgaard N, van der Velden VHJ, Bi W, Dee R, van der Schoot E, Delabesse E, Macintyre E, Gottardi E, Saglio G, Watzinger F, Lion T, van Dongen JJM, Hokland P, Gabert J (2003) Evaluation of candidate control genes for diagnosis and residual disease detection in leukemic patients using 'real-time' quantitative reverse-transcriptase polymerase chain reaction (RQ-PCR) – a Europe against cancer program. *Leukemia* **17**: 2474-2486.
- Bench AJ, Nacheva EP, Champion KM, Green AR (1998a) Molecular genetics and cytogenetics of myeloproliferative disorders. *Baillieres Clin Haematol* **11**: 819-848.
- Bench AJ, Aldred MA, Humphray SJ, Champion KM, Gilbert JG, Asimakopoulos FA, Deloukas P, Gwilliam R, Bentley DR, Green AR (1998b) A detailed physical and transcriptional map of the region of chromosome 20 that is deleted in myeloproliferative disorders and refinement of the common deleted region. *Genomics* **49**: 351-362.
- Bench AJ, Nacheva EP, Hood TL, Holden JL, French L, Swanton S, Champion KM, Li J, Whittaker P, Stavrides G, Hunt AR, Huntly BJ, Campbell LJ, Bentley DR, Deloukas P, Green AR (2000) Chromosome 20 deletions in myeloid malignancies: reduction of the common deleted region, generation of a PAC/BAC contig and identification of candidate genes. UK Cancer Cytogenetics Group (UKCCG). *Oncogene* **19**: 3902-3913.
- Bench AJ, Cross NCP, Huntly BJP, Nacheva EP, Green AR (2001) Myeloproliferative disorders. *Best Pract Res Clin Haematol* **14**: 531-551.
- Benjes SM, Millow LJ, Jeffs AR, Sowerby SJ, Reeve AE, Morris CM (1999) 3' BCR recombines with IGL locus in BCR-ABL-positive Philadelphia-negative chronic myeloid leukemia. *Genes Chromosomes Cancer* **26**: 366-371.
- Berger R, Flandrin G, Bernheim A, Le Coniat M, Vecchione D, Pacot A, Derré J, Daniel MT, Valensi F, Sigaux F, Ochoa-Noguera ME (1987) Cytogenetic studies on 519 consecutive de novo acute nonlymphocytic leukemias. *Cancer Genet Cytogenet* **29**: 9-21.
- Berger R, Derré J, Le Coniat M, Hébert J, Romana PS, Jonveaux P (1993) Inversion-associated translocations in acute myelomonocytic leukemia with eosinophilia. *Genes Chromosomes Cancer* **12**: 58-62.
- Berger R, Le Coniat M, Lacronique V, Daniel M-T, Lessard M, Berthou C, Marynen P, Bernard O (1997) Chromosome abnormalities of the short arm of chromosome 12 in hematopoietic malignancies: A report including three novel translocations involving the *TEL/ETV6* gene. *Leukemia* **11**: 1400-1403.
- Bernard P, Dachary D, Reiffers J, Marit G, Wen Z, Jonveaux P, David B, Lacombe F, Broustet A (1989) Acute nonlymphocytic leukemia with marrow eosinophilia and chromosome 16 abnormality: A report of 18 cases. *Leukemia* **3**: 740-745.
- Bernstein R, Mendelow B, Pinto MR, Morcom G, Bezwoda W (1980) Complex translocations involving chromosomes 15 and 17 in acute promyelocytic leukemia. *Br J Haematol* **46**: 311-314.
- Bernstein R, Pinto MR, Wallace C, Penfold G, Mendelow B (1984) The incidence, type, and subsequent evolution of 14 variant Ph1 translocations in 180 South African patients with Ph1-positive chronic myeloid leukemia. *Cancer Genet Cytogenet* **12**: 225-238.
- Bhambhani K, Inoue S, Tyrkus M, Gohle N (1986) Acute myelomonocytic leukemia type M4 with bone marrow eosinophilia and t(5;16)(q33;q22). *Cancer Genet Cytogenet* **20**: 187-188.
- Bitter MA, Le Beau MM, Rowley JD, Larson RA, Golomb HM, Vardiman JW (1987) Associations between morphology, karyotype, and clinical features in myeloid leukemias. *Human Pathol* **18**: 211-225.
- Bjerrum OW, Philip P, Pressler T, Tygstrup I (1987) Acute promyelocytic leukemia with t(15;17) and t(2;17;15). *Cancer Genet Cytogenet* **28**: 107-111.
- Bloomfield CD, Goldman A, Hassfeld D, de la Chapelle A (1984) Fourth international workshop on chromosomes in leukemia 1982: Clinical significance of chromosomal abnormalities in acute nonlymphoblastic leukemia. *Cancer Genet Cytogenet* **11**: 332-350.
- Bloomfield CD, Archer KJ, Mrozek K, Lillington DM, Kaneko Y, Head DR, Dal Cin P, Raimondi SC (2002) 11q23 balanced chromosome aberrations in treatment-related myelodysplastic syndromes and acute leukemia: Report from an international workshop. *Genes Chromosomes Cancer* **33**: 362-378.

- Borozdin W, Boehm D, Leipoldt M, Wilhelm C, Reardon W, Clayton-Smith J, Becker K, Muhlendyck H, Winter R, Giray O, Silan F, Kohlhase J (2004) SALL4 deletions are a common cause of Okihiro and acro-renal-ocular syndromes and confirm haploinsufficiency as the pathogenic mechanism. *J Med Genet* **41**: e113.
- Borozdin W, Graham JM Jr, Böhm D, Bamshad MJ, Spranger S, Burke L, Leipoldt M, Kohlhase J (2007) Multigene deletions on chromosome 20q13.13-q13.2 including SALL4 result in an expanded phenotype of Okihiro syndrome plus developmental delay. *Hum Mutat* **28**: 830.
- Borrow J, Goddard AD, Gibbons B, Katz F, Swirsky D, Fioretos T, Dube I, Winfield DA, Kingston J, Hagemeijer A, Rees JKH, Lister A, Solomon E (1992) Diagnosis of acute promyelocytic leukemia by RT-PCR: Detection of PML-RARA and RARA-PML fusion transcripts. *Br J Haematol* **82**: 529-540.
- Boveri T (1914) *Zur Frage der Entstehung maligner Tumoren*. Gustav Fischer. Jena, Germany. 64 pp.
- Brito-Babapulle V, Gruszka-Westwood AM, Platt G, Andersen CL, Elnenaei MO, Matutes E, Wotherspoon AC, Weston-Smith SG, Catovsky D (2002) Translocation t(2;7)(p12;q21-22) with dysregulation of the CDK6 gene mapping to 7q21-22 in a non-Hodgkin's lymphoma with leukemia. *Haematologica* **87**: 357-362.
- Burrow AA, Williams LE, Pierce LCT, Wang Y-H (2009) Over half of breakpoints in gene pairs involved in cancer-specific recurrent translocations are mapped to human chromosomal fragile sites. *BMC Genomics* **10**: 59.
- Caetano MS, Vieira-de-Abreu A, Teixeira LK, Werneck MB, Barcinski MA, Viola JP (2002) NFATC2 transcription factor regulates cell cycle progression during lymphocyte activation: Evidence of its involvement in the control of cyclin gene expression. *FASEB J* **16**: 1940-1942.
- Calabrese G, Palka G, Westbrook CA, Sheer D (1992) Complex translocation involving Ph chromosome in a patient with typical chronic myelogenous leukemia. *Cancer Genet Cytogenet* **63**: 52-55.
- Calabrese G, Stuppia L, Franchi PG, Peila R, Morizio E, Liberati AM, Spadano A, Di Lorenzo R, Donti E, Antonucci A, Palka G (1994) Complex translocations of the Ph chromosome and Ph negative CML arise from similar mechanisms, as evidenced by FISH analysis. *Cancer Genet Cytogenet* **78**: 153-159.
- Calabrese G, Min T, Stuppia L, Powles R, Swansbury JG, Morizio E, Peila R, Donti E, Fioritoni G, Palka G (1996) Complex chromosome translocations of standard t(8;21) and t(15;17) arise from a two-step mechanism as evidenced by fluorescence in situ hybridization analysis. *Cancer Genet Cytogenet* **91**: 40-45.
- Campbell PJ, Baxter EJ, Beer PA, Scott LM, Bench AJ, Huntly BJP, Erber WN, Kusec R, Larsen TS, Giraudier S, Le Bousse-Kerdile's M-C, Griesshammer M, Reilly JT, Cheung BY, Harrison CN, Green AR (2006) Mutation of *JAK2* in the myeloproliferative disorders: Timing, clonality studies, cytogenetic associations, and role in leukemic transformation. *Blood* **108**: 3548-3555.
- Cao S, Liu J, Chesi M, Bergsagel PL, Ho IC, Donnelly RP, Ma X (2002) Differential regulation of IL-12 and IL-10 gene expression in macrophages by the basic leucine zipper transcription factor c-Maf fibrosarcoma. *J Immunol* **169**: 5715-5725.
- Cao S, Liu J, Song L, Ma X (2005) The protooncogene c-Maf is an essential transcription factor for IL-10 gene expression in macrophages. *J Immunol* **174**: 3484-3492.
- Caspersson T, Gahrton G, Lindsten J, Zech L (1970) Identification of the Philadelphia chromosome as a number 22 by quinacrine mustard fluorescence analysis. *Exp Cell Res* **63**: 238-240.
- Cazzaniga G, Daniotti M, Tosi S, Giudici G, Aloisi A, Pogliani E, Kearney L, Biondi A (2001) The paired box domain gene PAX5 is fused to ETV6/TEL in an acute lymphoblastic leukemia case. *Cancer Res* **61**: 4666-4670.
- Chen GQ, Zhu J, Shi XG, Ni JH, Zhong HJ, Si GY, Jin XL, Tang W, Li XS, Xong SM, Shen ZX, Sun GL, Ma J, Zhang P, Zhang TD, Gazin C, Naoe T, Chen SJ, Wang ZY, Chen Z (1996) In vitro studies on cellular and molecular mechanisms of arsenic trioxide (As₂O₃) in the treatment of acute promyelocytic leukemia: As₂O₃ induces NB4 cell apoptosis with downregulation of Bcl-2 expression and modulation of PML-RAR alpha/PML proteins. *Blood* **88**: 1052-1061.
- Chen Z, Morgan R, Stone JF, Sandberg AA (1994) Identification of complex t(15;17) in APL by FISH (1994) *Cancer Genet Cytogenet* **72**: 73-74.
- Chissoe SL, Bodenteich A, Wang YF, Wang YP, Burian D, Clifton SW, Crabtree J, Freeman A, Lyster K, Jian L, Ma Y, McLaury H-J, Pan H-Q, Sarhan OH, Toth S, Wang Z, Zhang G, Heisterkamp N, Groffen J, Roe BA (1995) Sequence and analysis of the human ABL gene, the BCR gene, and regions involved in the Philadelphia chromosome translocation. *Genomics* **27**: 67-82.
- Cockerill PN, Shannon MF, Bert AG, Ryan GR, Vadas MA (1993) The granulocyte-macrophage colony-stimulating factor/interleukin 3 locus is regulated by an inducible cyclosporine A-sensitive enhancer. *Proc Natl Acad Sci USA* **90**: 2466-2470.

- Cockerill PN, Bert AG, Jenkins F, Ryan GR, Shannon MF, Vadas MA (1995) Human granulocyte-macrophage colony-stimulating factor enhancer function is associated with cooperative interactions between AP-1 and NFATp/c. *Mol Cell Biol* **15**: 2071-2079.
- Cohen O, Cans C, Cuillel M, Gilardi JL, Roth H, Mermet MA, Jalbert P, Demongeot J (1996) Cartographic study: Breakpoints in 1574 families carrying human reciprocal translocations. *Hum Genet* **97**: 659-667.
- Corcoran MM, Mould SJ, Orchard JA, Ibbotson RE, Chapman RM, Boright AP, Platt C, Tsui LC, Scherer SW, Oscier DG (1999) Dysregulation of cyclin dependent kinase 6 expression in splenic marginal zone lymphoma through chromosome 7q translocations. *Oncogene* **18**: 6271-6277.
- Corral J, Lavenir I, Impey H, Warren AJ, Forster A, Larson TA, Bell S, McKenzie AN, King G, Rabbitts TH (1996) An Mll-AF9 fusion gene made by homologous recombination causes acute leukemia in chimeric mice: A method to create fusion oncogenes. *Cell* **85**: 853-861.
- Corsello SM, Roti G, Ross KN, Chow KT, Galinsky I, DeAngelo DJ, Stone RM, King AL, Golub TR, Stegmaier K (2009) Identification of AML1-ETO modulators by chemical genomics. *Blood* **113**: 6193-6205.
- Cross NC, Hughes TP, Feng L, O'Shea P, Bungey J, Marks DI, Ferrant A, Martiat P, Goldman JM (1993) Minimal residual disease after allogeneic bone marrow transplantation for chronic myeloid leukaemia in first chronic phase: Correlations with acute graft-versus-host disease and relapse. *Br J Haematol* **84**: 67-74.
- Dai CH, Krantz SB, Dessypris EN, Means JR RT, Horn ST, Gilbert HS (1992) Polycythemia Vera. II. Hypersensitivity of bone marrow erythroid, granulocyte-macrophage, and megakaryocyte progenitor cells to interleukin-3 and granulocyte-macrophage colony-stimulating factor. *Blood* **80**: 891-899.
- Daley GQ, Van Etten RA, Baltimore D (1990) Induction of chronic myelogenous leukemia in mice by the P210bcr/abl gene of the Philadelphia chromosome. *Science* **247**: 824-830.
- De Braekeleer M (1987) Variant Philadelphia translocations in chronic myeloid leukemia. *Cytogenet Cell Genet* **44**: 215-222.
- de Greef GE, Hagemijer A, Morgan R, Wijsman J, Hoefsloot LH, Sandberg AA, Sacchi N (1995) Identical fusion transcript associated with different breakpoints in the AML1 gene in simple and variant t(8:21) acute myeloid leukemia. *Leukemia* **9**: 282-287.
- de Klein A, van Kessel AG, Grosveld G, Bartram CR, Hagemijer A, Bootsma D, Spurr NK, Heisterkamp N, Groffen J, Stephenson JR (1982) A cellular oncogene is translocated to the Philadelphia chromosome in chronic myelocytic leukaemia. *Nature* **300**: 765-767.
- de Klein A, van Aghoven T, Groffen C, Heisterkamp N, Groffen J, Grosveld G (1986) Molecular analysis of both translocation products of a Philadelphia-positive CML patient. *Nucleic Acids Res* **14**: 7071-7082.
- de la Chapelle A & Lahtinen R (1983) Chromosome 16 and bone-marrow eosinophilia. *N Engl J Med* **309**: 1394.
- de Thé H, Chomienne C, Lanotte M, Degos L, Dejean A (1990) The t(15;17) translocation of acute promyelocytic leukemia fuses the retinoic acid receptor alpha gene to a novel transcribed locus. *Nature* **347**: 558-561.
- de Thé H, Lavau C, Marchio A, Chomienne C, Degos L, Dejean A (1991) The PML-RAR α fusion mRNA generated by the t(15;17) translocation in acute promyelocytic leukemia encodes a functionally altered RAR. *Cell* **66**: 675-684.
- De Weer A, Poppe B, Cauwelier B, Carlier A, Dierick J, Verhasselt B, Philippe J, Van Roy N, Speleman F (2008) EVI1 activation in blast crisis CML due to juxtaposition to the rare 17q22 partner region as part of a 4-way variant translocation t(9;22). *BMC Cancer* **8**: 193.
- Delhommeau F, Pisani DF, James C, Casadevall N, Constantinescu S, Vainchenker W (2006) Oncogenic mechanisms in myeloproliferative disorders. *Cell Mol Life Sci* **63**: 2939-2953.
- Dewald GW, Schad CR, Christensen ER, Tiede AL, Zinsmeister AR, Spurbeck JL, Thibodeau SN, Jalal SM (1993) The application of fluorescent in situ hybridization to detect Mbc/abl fusion in variant Ph chromosomes in CML and ALL. *Cancer Genet Cytogenet* **71**: 7-14.
- Dierlamm J, Stul M, Vranckx H, Michaux L, Weghuis DE, Speleman F, Selleslag D, Kramer MH, Noens LA, Cassiman JJ, van den Berghe H, Hagemijer A (1998) FISH identifies inv(16)(p13q22) masked by translocations in three cases of acute myeloid leukemia. *Genes Chromosomes Cancer* **22**: 87-94.
- Djabali M, Selleri L, Parry P, Bower M, Young BD, Evans GA (1992) A trithorax-like gene is interrupted by chromosome 11q23 translocations in acute leukaemias. *Nat Genet* **2**: 113-118.

- Dobson CL, Warren AJ, Pannell R, Forster A, Lavenir I, Corral J, Smith AJ, Rabbitts TH (1999) The mll-AF9 gene fusion in mice controls myeloproliferation and specifies acute myeloid leukaemogenesis. *EMBO J* **18**: 3564-3574.
- Douet-Gilbert N, Basinko A, Morel F, Le Bris MJ, Ugo V, Morice P, Berthou C, De Braekeleer M (2008) Chromosome 20 deletions in myelodysplastic syndromes and Philadelphia-chromosome-negative myeloproliferative disorders: Characterization by molecular cytogenetics of commonly deleted and retained regions. *Ann Hematol* **87**: 537-544.
- Downing JR, Head DR, Curcio-Brint AM, Hulshof MG, Motroni TA, Raimondi SC, Carrol AJ, Drabkin HA, Willman C, Theil KS, Civin CI, Erickson P (1993) An AML1/ETO fusion transcript is consistently detected by RNA-based polymerase chain reaction in acute myelogenous leukemia containing the (8;21)(q22;q22) translocation. *Blood* **81**: 2860-2865.
- Downing JR (1999) The AML1-ETO chimeric transcription factor in acute myeloid leukemia: Biology and clinical significance. *Br J Haematol* **106**: 296-308.
- Dreazen O, Klisak I, Rassool F, Goldman JM, Sparkes RS, Gale RP (1987) Do oncogenes determine clinical features in chronic myeloid leukemia? *Lancet* **1**: 1402-1405.
- Druker BJ, Tamura S, Buchdunger E, Ohno S, Segal GM, Fanning S, Zimmermann J, Lydon NB (1996) Effects of a selective inhibitor of the Abl tyrosine kinase on the growth of Bcr-Abl positive cells. *Nat Med* **2**: 561-566.
- Durst KL, Lutterbach B, Kummalu T, Friedman AD, Hiebert SW (2003) The inv(16) fusion protein associates with corepressors via a smooth muscle myosin heavy-chain domain. *Mol Cell Biol* **23**: 607-619.
- Erickson P, Gao J, Chang K-S, Look T, Whisenant E, Raimondi S, Lasher R, Trujillo J, Rowley J, Drabkin H (1992) Identification of breakpoints in t(8;21) acute myelogenous leukemia and isolation of a fusion transcript, AML1/ETO, with similarity to Drosophila segmentation gene, runt. *Blood* **80**: 1825-1831.
- Evans RM (1988) The steroid and thyroid hormone receptor superfamily. *Science* **240**: 889-895.
- Faber J & Armstrong SA (2007) Mixed lineage leukemia translocations and a leukemia stem cell program. *Cancer Res* **67**: 8425-8428.
- Farra C, Awwad J, Valent A, Lozach F, Bernheim A (2004) Complex translocation (8;12;21): A new variant of t(8;21) in acute myeloid leukemia. *Cancer Genet Cytogenet* **155**: 138-142.
- Felix CA, Lange BJ, Hosler MR, Fertala J, Bjornsti MA (1995) Chromosome band 11q23 translocation breakpoints are DNA topoisomerase II cleavage sites. *Cancer Res* **55**: 4287-4292.
- Fisher AM, Strike P, Scott C, Moorman AV (2005) Breakpoints of variant 9;22 translocations in chronic myeloid leukemia locate preferentially in the CG-richest regions of the genome. *Genes Chromosomes Cancer* **43**: 383-389.
- Fitzgerald PH, Morris CM, Fraser GJ, Giles LM, Hamer JW, Heaton DC, Beard ME (1983) Nonrandom cytogenetic changes in New Zealand patients with acute myeloid leukemia. *Cancer Genet Cytogenet* **8**: 51-66.
- Fitzgerald PH, Beard ME, Morris CM, Heaton DC, Reeve AE (1987) Ph-negative chronic myeloid leukemia. *Br J Haematol* **66**: 311-314.
- Fitzgerald PH & Morris CM (1991) Complex chromosomal translocations in the Philadelphia chromosome leukemias. Serial translocations or a concerted genomic rearrangement? *Cancer Genet Cytogenet* **57**: 143-151.
- Frankfurt O, Licht JD, Tallman MS (2007) Molecular characterization of acute myeloid leukemia and its impact on treatment. *Curr Opin Oncol* **19**: 635-649.
- Fütterer A, Campanero MR, Leonardo E, Criado LM, Flores JM, Hernández JM, San Miguel JF, Martínez-A C (2005) Dido gene expression alterations are implicated in the induction of hematological myeloid neoplasms. *J Clin Invest* **115**: 2351-2362.
- Gabert J, Beillard E, van der Velden VHJ, Bi W, Grimwade D, Pallisgaard N, Barbany G, Cazzaniga G, Cayuela JM, Cavé H, Pane F, Aerts JLE, De Micheli D, Thirion X, Pradel V, González M, Viehmann S, Malec M, Saglio G, van Dongen JJM (2003) Standardization and quality control studies of 'real-time' quantitative reverse transcriptase polymerase chain reaction of fusion gene transcripts for residual disease detection in leukemia – A Europe Against Cancer Program. *Leukemia* **17**: 2318-2357.
- Gahrton G, Zech L, Lindsten J (1974) A new variant translocation (19q plus, 22q minus) in chronic myelocytic leukemia. *Exp Cell Res* **86**: 214-216.
- Galièni P, Marotta G, Vessichelli F, Diverio D, Minoletti F, Bucalossi A, Lo Coco F, Lauria F (1996) Variant t(1;15;17)(q23;q22;q23) in a case of acute promyelocytic leukemia. *Leukemia* **10**: 1658-1661.
- Gallego M, Carrol AJ, Gad GS, Pappo A, Head D, Behm F, Ravindranath Y, Raimondi SC (1994) Variant t(8;21) rearrangements in acute myeloblastic leukemia of childhood. *Cancer Genet Cytogenet* **75**: 139-144.

- Gamerding U, Teigler-Schlegel A, Pils S, Bruch J, Viehmann S, Keller M, Jauch A, Harbott J (2003) Cryptic chromosomal aberrations leading to an AML1/ETO rearrangement are frequently caused by small insertions. *Genes Chromosomes Cancer* **36**: 261-272.
- Giguere V, Ong ES, Segui P, Evans RM (1987) Identification of a receptor for the morphogen retinoic acid. *Nature* **330**: 624-629.
- Gilbert HS, Praloran V, Stanley ER (1989) Increased circulating CSF-1 (M-CSF) in myeloproliferative disease: Association with myeloid metaplasia and peripheral bone marrow extension. *Blood* **74**: 1231-1234.
- Gilmour J, Cousins DJ, Richards DF, Sattar Z, Lee TH, Lavender P (2007) Regulation of GM-CSF expression by the transcription factor c-Maf. *J Allergy Clin Immunol* **120**: 56-63.
- Goerttler PS, Kreutz C, Donauer J, Faller D, Maiwald T, März E, Rumberger B, Sparna T, Schmitt-Gräff A, Wilpert J, Timmer J, Walz G, Pahl HL (2005) Gene expression profiling in polycythemia vera: Overexpression of transcription factor NF-E2. *Br J Haematol* **129**: 138-150.
- Golub TR, Barker GF, Lovett M, Gilliland DG (1994) Fusion of PDGF Receptor β to a novel *ets*-like gene, *TEL*, in chronic myelomonocytic leukemia with t(5;12) chromosomal translocation. *Cell* **77**: 307-316.
- Golub TR, Barker GF, Bohlander SK, Hiebert SW, Ward DC, Bray-Ward P, Morgan E, Raimondi SC, Rowley JD, Gilliland DG (1995) Fusion of the TEL gene on 12p13 to the AML1 gene on 21q22 in acute lymphoblastic leukemia. *Proc Natl Acad Sci USA* **92**: 4917-4921.
- Grimwade D, Howe K, Langabeer S, Davies L, Oliver F, Walker H, Swirsky D, Wheatley K, Goldstone A, Burnett A, Solomon E (1996) Establishing the presence of the t(15;17) in suspected acute promyelocytic leukemia: cytogenetic, molecular and PML immunofluorescence assessment of patients entered into the M.R.C. ATRA trial. *Br J Haematol* **94**: 557-573.
- Grimwade D, Gorman P, Duprez E, Howe K, Langabeer S, Oliver F, Walker H, Culligan D, Waters J, Pomfret M, Goldstone A, Burnett A, Freemont P, Sheer D, Solomon E (1997) Characterization of cryptic rearrangements and variant translocations in acute promyelocytic leukemia. *Blood* **90**: 4876-4885.
- Grimwade D, Biondi A, Mozziconacci M-J, Hagemeyer A, Berger R, Neat M, Howe K, Dastugue N, Jansen J, Radford-Weiss I, Lo Coco F, Lessard M, Hernandez J-M, Delabesse E, Head D, Liso V, Sainy D, Flandrin G, Solomon E, Birg F, Lafage-Pochitaloff (2000) Characterization of acute promyelocytic leukemia cases lacking the classic t(15;17): Results of the European Working Party. *Blood* **96**: 1297-1308.
- Groffen J, Stephenson JR, Heisterkamp N, de Klein A, Bartram CR, Grosveld G (1984) Philadelphia chromosomal breakpoints are clustered within a limited region, bcr, on chromosome 22. *Cell* **36**: 93-99.
- Groupe Français de Cytogénétique Hématologique (1990) Acute myelogenous leukemia with an 8;21 translocation. A report on 148 cases from the Groupe Français de Cytogénétique Hématologique. *Cancer Genet Cytogenet* **44**: 169-179.
- Gu Y, Nakamura T, Alder H, Prasad R, Canaani O, Cimino G, Croce CM, Canaani E (1992) The t(4;11) chromosome translocation of human acute leukemias fuses the ALL-1 gene, related to Drosophila trithorax, to the AF-4 gene. *Cell* **71**: 701-708.
- Haferlach T (2008) Molecular genetic pathways as therapeutic targets in acute myeloid leukemia. *Hematology Am Soc Hematol Educ Program* 400-411.
- Hagemeyer A, Bartram CR, Smit EM, van Agthoven AJ, Bootsma D (1984) Is the chromosomal region 9q34 always involved in variants of the Ph1 translocation? *Cancer Genet Cytogenet* **13**: 1-16.
- Hagemeyer A, Buijs A, Smit E, Janssen B, Creemers GJ, Van der Plas D, Grosveld G (1993) Translocation of BCR to chromosome 9: A new cytogenetic variant detected by FISH in two Ph-negative, BCR-positive patients with chronic myeloid leukemia. *Genes Chromosomes Cancer* **8**: 237-245.
- Hanahan D & Weinberg RA (2000) The hallmarks of cancer. *Cell* **100**: 57-70.
- Harrison CJ & Feroni L (2002) Cytogenetics and molecular genetics of acute lymphoblastic leukemia. *Rev Clin Exp Hematol* **6**: 91-113.
- Harrison CJ, Radford-Weiss I, Ross F, Rack K, le Guyader G, Vekemans M, Macintyre E (1999) Fluorescence in situ hybridization analysis of masked (8;21)(q22;q22) translocations. *Cancer Genet Cytogenet* **112**: 15-20.
- Hayata I, Kakati S, Sandberg AA (1973) Letter: A new translocation related to the Philadelphia chromosome. *Lancet* **2**: 1385.
- Hayata I, Sakurai M, Kakati S, Sandberg AA (1975) Chromosomes and causation of human cancer and leukemia. XVI. Banding studies of chronic myelocytic leukemia, including five unusual Ph11 translocations. *Cancer* **36**: 1177-1191.

- Hayette S, Tigaud I, Callet-Bauchu E, Ffrench M, Gazzo S, Wahbi K, Callanan M, Felman P, Dumontet C, Magaud JP, Rimokh R (2003) In B-cell chronic lymphocytic leukemias, 7q21 translocations lead to overexpression of the CDK6 gene. *Blood* **102**: 1549-1550.
- Heisterkamp N, Stephenson JR, Groffen J, Hansen PF, de Klein A, Bartram CR, Grosveld G (1983) Localization of the c-ab1 oncogene adjacent to a translocation break point in chronic myelocytic leukaemia. *Nature* **306**: 239-242.
- Heisterkamp N, Stam K, Groffen J (1985) Structural organization of the bcr gene and its role in the Ph⁺ translocation. *Nature* **315**: 758-761.
- Hermouet S, Godard A, Pineau D, Corre I, Rahe S, Lippert E, Jacques Y (2002) Abnormal production of interleukin (IL)-11 and IL-8 in polycythemia vera. *Cytokine* **20**: 178-183.
- Hild F & Fonatsch C (1990) Cytogenetic peculiarities in chronic myelogenous leukemia. *Cancer Genet Cytogenet* **47**: 197-217.
- Hiorns LR, Min T, Swansbury GJ, Zelent A, Dyer MJ, Catovsky D (1994) Interstitial insertion of retinoic acid receptor-alpha gene in acute promyelocytic leukemia with normal chromosomes 15 and 17. *Blood* **83**: 2946-2951.
- Ho CL, Lasho TL, Butterfield JH, Tefferi A (2007) Global cytokine analysis in myeloproliferative disorders. *Leuk Res* **31**: 1389-1392.
- Hodge MR, Ranger AM, Charles de la Brousse F, Hoey T, Grusby MJ, Glimcher LH (1996) Hyperproliferation and dysregulation of IL-4 expression in NF-ATp-deficient mice. *Immunity* **4**: 397-405.
- Hogan PG, Chen L, Nardone J, Rao A (2003) Transcriptional regulation by calcium, calcineurin, and NFAT. *Genes Dev* **17**: 2205-2232.
- Hogge DE, Misawa S, Testa JR, Leavitt RD, Pollak A, Schiffer CA (1984) Unusual karyotypic changes and B cell involvement in a case of lymph node blast crisis of chronic myelogenous leukemia. *Blood* **64**: 123-130.
- Hollings PE (1994) Molecular heterogeneity at the breakpoints of smaller 20q deletions. *Genes Chromosomes Cancer* **11**: 21-28.
- Huang G, Shigesada K, Wee HJ, Liu PP, Osato M, Ito Y (2004) Molecular basis for a dominant inactivation of RUNX1/AML1 by the leukemogenic inversion 16 chimera. *Blood* **103**: 3200-3207.
- Huang ME, Ye YC, Chen SR, Chai JR, Lu JX, Zhao L, Gu LJ, Wang ZY (1988) Use of all-trans retinoic acid in the treatment of acute promyelocytic leukemia. *Blood* **72**: 567-572.
- Huh J, Tiu RV, Gondek LP, O'Keefe CL, Jasek M, Makishima H, Jankowska AM, Jiang Y, Verma A, Theil KS, McDevitt MA, Maciejewski JP (2010) Characterization of chromosome arm 20q abnormalities in myeloid malignancies using genome-wide single nucleotide polymorphism array analysis. *Genes Chromosomes Cancer* **49**: 390-399.
- Huntly BJP, Reid AG, Bench AJ, Campbell LJ, Telford N, Sheperd P, Szer J, Prince HM, Turner P, Grace C, Nacheva EP, Green AR (2001) Deletions of the derivative chromosome 9 occur at the time of the Philadelphia translocation and provide a powerful and independent prognostic indicator in chronic myeloid leukemia. *Blood* **98**: 1732-1738.
- Huntly BJ, Bench AJ, Delabesse E, Reid AG, Li J, Scott MA, Campbell L, Byrne J, Pinto E, Brizard A, Niedermeiser D, Nacheva EP, Guilhot F, Deininger M, Green AR (2002) Derivative chromosome 9 deletions in chronic myeloid leukemia: Poor prognosis is not associated with loss of ABL-BCR expression, elevated BCR-ABL levels, or karyotypic instability. *Blood* **99**: 4547-4553.
- Huntly BJ, Bench A, Green AR (2003) Double jeopardy from a single translocation: Deletions of the derivative chromosome 9 in chronic myeloid leukemia. *Blood* **102**: 1160-1168.
- Huret JL, Couet D, Guilhot F, Brizard A, Tanzer J (1987) A two-step t(4;der(15))t(15;17) complex translocation in an acute promyelocytic leukemia and review of the literature. *Leuk Res* **11**: 761-765.
- Huret JL (1990) Complex translocations, simple variant translocations and Ph-negative cases in chronic myelogenous leukemia. *Hum Genet* **85**: 565-568.
- Hurwitz CA, Raimondi SC, Head D, Krance R, Mirro J Jr, Kalwinsky DK, Ayers GD, Behm FG (1992) Distinctive immunophenotypic features of t(8;21)(q22;q22) acute myeloblastic leukemia in children. *Blood* **80**: 3182-3188.
- Iida S, Seto M, Yamamoto K, Komatsu H, Tojo A, Asano S, Kamada N, Ariyoshi Y, Takahashi T, Ueda R (1993) MLLT3 gene on 9p22 involved in t(9;11) leukemia encodes a serine/proline rich protein homologous to MLLT1 on 19p13. *Oncogene* **8**: 3085-3092.
- ISCN. 1995. An international system for human cytogenetic nomenclature. Mitelman F, editor. Basel, Switzerland: S. Karger.

- Ishida F, Ueno M, Tanaka H, Makishima H, Suzawa K, Hosaka S, Hidaka E, Ishikawa M, Yamauchi L, Kitano K, Kiyosawa K (2002) t(8;21)(q22;q24) is a novel variant of t(8;21) with chimeric transcripts of AML1-ETO in acute myelogenous leukemia. *Cancer Genet Cytogenet* **132**: 133-135.
- Ishii H, Vecchione A, Furukawa Y, Sutheesophon K, Han SY, Druck T, Kuroki T, Trapasso F, Nishimura M, Saito Y, Ozawa K, Croce CM, Huebner K, Furukawa Y (2003) Expression of FRA16D/WWOX and FRA3B/FHIT genes in hematopoietic malignancies. *Mol Cancer Res* **1**: 940-947.
- James C, Ugo V, Le Couédic J-P, Staerk J, Delhommeau F, Lacout C, Garçon L, Raslova H, Berger R, Bennaceur-Griscelli A, Villeval JL, Constantinescu SN, Casadevall N, Vainchenker W (2005) A unique clonal JAK2 mutation leading to constitutive signaling causes polycythemia vera. *Nature* **434**: 1144-1148.
- Jeffrey PD, Tong L, Pavletich NP (2000) Structural basis of inhibition of CDK-cyclin complexes by INK4 inhibitors. *Genes Dev* **14**: 3115-3125.
- Jeffs AR, Benjes SM, Smith TL, Sowerby SJ, Morris CM (1998) The BCR gene recombines preferentially with Alu elements in complex BCR-ABL translocations of chronic myeloid leukemia. *Hum Mol Genet* **7**: 767-776.
- Jeffs AR, Wells E, Morris CM (2001) Nonrandom distribution of interspersed repeat elements in the BCR and ABL1 genes and its relation to breakpoint cluster regions. *Genes Chromosomes Cancer* **32**: 144-154.
- Johansson B, Fioretos T, Mitelman F (2002) Cytogenetic and molecular genetic evolution of chronic myeloid leukemia. *Acta Haematol* **107**: 76-94.
- Jones AV, Kreil S, Zoi K, Waghorn K, Curtis C, Zhang L, Score J, Seear R, Chase AJ, Grand FH, White H, Zoi C, Loukopoulos D, Terpos E, Vervessou EC, Schultheis B, Emig M, Ernst T, Lengfelder E, Hehlmann R, Hochhaus A, Oscier D, Silver RT, Reiter A, Cross NC (2005) Widespread occurrence of the JAK2 V617F mutation in chronic myeloproliferative disorders. *Blood* **106**: 2162-2168.
- Kakizuka A, Miller WH Jr, Umehono K, Warrell RP Jr, Frankel SR, Murty VVVS, Dmitrovsky E, Evans RM (1991) Chromosomal translocation t(15;17) in human acute promyelocytic fuses RAR α with a novel putative transcription factor, PML. *Cell* **66**: 663-674.
- Kataoka K, Nishizawa M, Kawai S (1993) Structure-function analysis of the maf oncogene product, a member of the b-Zip protein family. *J Virol* **67**: 2133-2141.
- Kataoka K, Noda M, Nishizawa M (1994) Maf nuclear oncoprotein recognizes sequences related to an AP-1 site and forms heterodimers with both Fos and Jun. *Mol Cell Biol* **14**: 700-712.
- Kato J, Matsuoka M, Polyak K, Massague J, Sherr CJ (1994) Cyclic AMP induced G1 phase arrest mediated by an inhibitor (p27KIP1) of cyclin-dependent kinase 4 activation. *Cell* **79**: 487-496.
- Kaushansky K (2006) Hematopoietic growth factors, signaling and the chronic myeloproliferative disorders. *Cytokine Growth Factor Rev* **17**: 423-430.
- Kawakami K, Nishii K, Hyou R, Watanabe Y, Nakao M, Mitani H, Murata T, Monma F, Yamamori S, Hosokai N, Miura I (2008) A case of acute myeloblastic leukemia with a novel variant of t(8;21)(q22;q22). *Int J Hematol* **87**: 78-82.
- Kazazian Jr HH (2004) Mobile elements: Drivers of genome evolution. *Science* **303**: 1626-1632.
- Kelliher MA, McLaughlin J, Witte ON, Rosenberg N (1990) Induction of a chronic myelogenous leukemia-like syndrome in mice with v-abl and BCR/ABL. *Proc Natl Acad Sci USA* **87**: 6649-6653.
- Kemkemmer C, Kohn M, Cooper DN, Froenicke L, Hogel J, Hameister H, Kehrer-Sawatzki H (2009) Gene synteny comparisons between different vertebrates provide new insights into breakage and fusion events during mammalian karyotype evolution. *BMC Evolutionary Biol* **9**: 84.
- Kerppola TK & Curran T (1994) Maf and Nrl can bind to AP-1 sites and form heterodimers with Fos and Jun. *Oncogene* **9**: 675-684.
- Kiani A, Habermann I, Haase M, Feldmann S, Boxberger S, Sanchez-Fernandez MA, Thiede C, Bornhäuser M, Ehninger G (2004) Expression and regulation of NFAT (nuclear factors of activated T cells) in human CD34+ cells: Down-regulation upon myeloid differentiation. *J Leukoc Biol* **76**: 1057-1065.
- Koduru PR, Goh JC, Pergolizzi RG, Lichtman SM, Broome JD (1993) Molecular characterization of a variant Ph1 translocation t(9;22)(q34;q11;q13) in chronic myelogenous leukemia (CML) reveals the translocation of the 3'-part of BCR gene to the chromosome band 11q13. *Oncogene* **8**: 3239-3247.
- Kohlhase J, Heinrich M, Schubert L, Liebers M, Kispert A, Laccone F, Turnpenny P, Winter RM, Reardon W (2002) Okihiro syndrome is caused by SALL4 mutations. *Hum Mol Genet* **11**: 2979-2987.
- Kohlhase J, Schubert L, Liebers M, Rauch A, Becker K, Mohammed SN, Newbury-Ecob R, Reardon W (2003) Mutations at the SALL4 locus on chromosome 20 result in a range of clinically overlapping

- phenotypes, including Okhiro syndrome, Holt-Oram syndrome, acro-renal-ocular syndrome, and patients previously reported to represent thalidomide embryopathy. *J Med Genet* **40**: 473-478.
- Kohlhase J (2008) SALL4-related disorders. In: Pagon RA, Bird TC, Dolan CR, Stephens K, editors. GeneReviews (internet). Seattle (WA): University of Washington, Seattle.
- Kondo E, Harashima A, Takabatake T, Takahashi H, Matsuo Y, Yoshino T, Orita K, Akagi T (2003) NF-ATc2 induces apoptosis in Burkitt's lymphoma cells through signaling via the B cell antigen receptor. *Eur J Immunol* **33**: 1-11.
- Kondo K, Sasaki M, Mikuni C (1978) A complex translocation involving chromosomes 1, 8 and 21 in acute myeloblastic leukemia. *Proc Jpn Acad* **54**: 21-24.
- Konopka JB, Watanabe SM, Witte ON (1984) An alteration of the human c-abl protein in K562 leukemia cells unmasks associated tyrosine kinase activity. *Cell* **37**: 1035-1042.
- Kralovics R, Passamonti F, Buser AS, Teo SS, Tiedt R, Passweg JR, Tichelli A, Cazzola M, Skoda RC (2005) A gain-of-function mutation of JAK2 in myeloproliferative disorders. *N Engl J Med* **352**: 1779-1790.
- Kreil S, Pfirrmann M, Haferlach C, Waghorn K, Chase A, Hehlmann R, Reiter A, Hochhaus A, Cross NC; German Chronic Myelogenous Leukemia (CML) Study Group (2007) Heterogeneous prognostic impact of derivative chromosome 9 deletions in chronic myelogenous leukemia. *Blood* **110**: 1283-1290.
- Kurec KC, Del Mare S, Salah Z, Abdeen S, Sadiq H, Lee SH, Gaudio E, Zanesi N, Jones KB, DeYoung B, Amir G, Gebhardt M, Warman M, Stein GS, Stein JL, Lian JB, Aqeilan RI (2010) Frequent attenuation of the WWOX tumor suppressor in osteosarcoma is associated with increased tumorigenicity and aberrant RUNX2 expression. *Cancer Res* **70**: 5577-5586.
- Kurzrock R, Blick MB, Talpaz M, Velasquez WS, Trujillo JM, Kouttab NM, Kloetzer WS, Arlinghaus RB, Gutterman JU (1986) Rearrangement in the breakpoint cluster region and the clinical course in Philadelphia-negative chronic myelogenous leukemia. *Ann Intern Med* **105**: 673-679.
- La Starza R, Stella M, Testoni N, Di Bona E, Ciolli S, Marynen P, Martelli MF, Mandelli F, Mecucci C (1999) Characterization of 12p molecular events outside *ETV6* in complex karyotypes of acute myeloid malignancies. *Br J Haematol* **107**: 340-346.
- Langer T, Metzler M, Reinhardt D, Viehmann S, Borkhardt A, Reichel M, Stanulla M, Schrappe M, Creutzig U, Ritter J, Leis T, Jacobs U, Harbott J, Beck JD, Rascher W, Repp R (2003) Analysis of t(9;11) chromosomal breakpoint sequences in childhood acute leukemia: Almost identical MLL breakpoints in therapy-related AML after treatment without etoposides. *Genes Chromosomes Cancer* **36**: 393-401.
- Lavau C, Szilvassy SJ, Slany R, Cleary ML (1997) immortalization and leukemic transformation of a myelomonocytic precursor by retrovirally transduced HRX-ENL. *EMBO J* **16**: 4226-4237.
- Lavau C, Luo RT, Du C, Thirman MJ (2000) Retrovirus-mediated gene transfer of MLL-ELL transforms primary myeloid progenitors and causes acute myeloid leukemias in mice. *Proc Natl Acad Sci U S A* **97**: 10984-10989.
- Lazaridou A, Chase A, Melo J, Garicochea B, Diamond J, Goldman J (1994) Lack of reciprocal translocation in BCR-ABL positive Ph-negative chronic myeloid leukemia. *Leukemia* **8**: 454-457.
- Le Beau MM, Larson RA, Bitter MA, Vardiman JW, Golomb HM, Rowley JD (1983) Association of an inversion of chromosome 16 with abnormal marrow eosinophils in acute myelomonocytic leukemia. A unique cytogenetic-clinicopathological association. *N Engl J Med* **309**: 630-636.
- Lee DS, Lee YS, Yun YS, Kim YR, Jeong SS, Lee YK, She CJ, Yoon SS, Shin HR, Kim Y, Cho HI (2003) A study on the incidence of ABL gene deletion on derivative chromosome 9 in chronic myelogenous leukemia by interphase fluorescence in situ hybridization and its association with disease progression. *Genes Chromosomes Cancer* **37**: 291-299.
- Lee HC (1993) Potentiation of calcium- and caffeine-induced calcium release by cyclic ADP-ribose. *J Biol Chem* **268**: 293-299.
- Lee YK, Kim YR, Min HC, Oh BR, Kim TY, Kim YS, Cho HI, Kim HC, Lee YS, Lee DS (2006) Deletion of any part of the BCR and ABL gene on the derivative chromosome 9 is a poor prognostic marker in chronic myelogenous leukemia. *Cancer Genet Cytogenet* **166**: 65-73.
- Lessard M & Le Prisé P-Y (1982) Cytogenetic studies in 56 cases with Ph¹-positive hematologic disorders. *Cancer Genet Cytogenet* **5**: 37-49.
- Li J, Bench AJ, Vassiliou GS, Fourouclas N, Ferguson-Smith AC, Green AR (2004) Imprinting of the human L3MBTL gene, a polycomb family member located in a region of chromosome 20 deleted in human myeloid malignancies. *Proc Natl Acad Sci U S A* **101**: 7341-7346.

- Li S, Couzi RJ, Thomas GH, Friedman AD, Borowitz MJ (2001) A novel variant three-way translocation of inversion 16 in a case of AML-M4eo following low dose methotrexate therapy. *Cancer Genet Cytogenet* **125**: 74-77.
- Lin RJ, Sternsdorf T, Tini M, Evans RM (2001) Transcriptional regulation in acute promyelocytic leukemia. *Oncogene* **20**: 7204-7215.
- Lindgren V & Rowley JD (1977) Comparable complex rearrangements involving 8;21 and 9;22 translocations in leukemia. *Nature* **266**: 744-745.
- Liu P, Tarlé SA, Hajra A, Claxton DF, Marlton P, Freedman M, Siciliano MJ, Collins FS (1993) Fusion between transcription factor CBF β /PEBP2 β and a myosin heavy chain in acute myeloid leukemia. *Science* **261**: 1041-1044.
- Liu PP, Hajra A, Wijmenga C, Collins FS (1995) Molecular pathogenesis of the chromosome 16 inversion in the M4Eo subtype of acute myeloid leukemia. *Blood* **85**: 2289-2302.
- Lo HW, Stephenson L, Cao X, Milas M, Pollock R, Ali-Osman F (2008) Identification and functional characterization of the human glutathione S-transferase P1 gene as a novel transcriptional target of the p53 tumor suppressor gene. *Mol Cancer Res* **6**: 843-850.
- Lovett BD, Lo Nigro L, Rappaport EF, Blair IA, Osheroff N, Zheng N, Megonigal MD, Williams WR, Nowell PC, Feliz CA (2001) Near-precise interchromosomal recombination and functional DNA topoisomerase II cleavage sites at MLL and AF-4 genomic breakpoints in treatment-related acute lymphoblastic leukemia with t(4;11) translocation. *Proc Natl Acad Sci U S A* **98**: 9802-9807.
- Lugo TG, Pendergast AM, Muller AJ, Witte ON (1990) Tyrosine kinase activity and transformation potency of bcr-abl oncogene products. *Science* **247**: 1079-1082.
- Luo C, Burgeon E, Carew JA, McCaffrey PG, Badalian TM, Lane WS, Hogan PG, Rao A (1996) Recombinant NFAT1 (NFATp) is regulated by calcineurin in T cells and mediates transcription of several cytokine genes. *Mol Cell Biol* **16**: 3955-3966.
- Ma Y, Cui W, Yang J, Qu J, Di C, Amin HM, Lai R, Ritz J, Krause DS, Chai L (2006) SALL4, a novel oncogene, is constitutively expressed in human acute myeloid leukemia (AML) and induces AML in transgenic mice. *Blood* **108**: 2726-2735.
- MacGrogan D, Alvarez S, DeBlassio T, Jhanwar SC, Nimer SD (2001) Identification of candidate genes on chromosome band 20q12 by physical mapping of translocation breakpoints found in myeloid leukemia cell lines. *Oncogene* **20**: 4150-4160.
- Martin ES, Joseph A, Ahmad MA, Borgaonkar DS, Martin SE (1997) Complex chromosome 4, 9, and 22 rearrangement in a patient presenting with AML-FAB M2. *Cancer Genet Cytogenet* **93**: 119-124.
- Martinez-Climent JA, Thirman MJ, Espinosa R 3rd, Le Beau MM, Rowley JD (1995) Detection of 11q23/MLL rearrangements in infant leukemias with fluorescence in situ hybridization and molecular analysis. *Leukemia* **9**: 1299-1304.
- Martinez-Climent JA, Comes AM, Vizcarra E, Reshmi S, Benet I, Marugan I, Tormo M, Terol MJ, Solano C, Arbona C, Prosper F, Barragan E, Bolufer P, Rowley JD, García-Conde J (1999) Variant three-way translocation of inversion 16 in AML-M4Eo confirmed by fluorescence in situ hybridization analysis. *Cancer Genet Cytogenet* **110**: 111-114.
- Maseki N, Miyoshi H, Shimizu K, Homma C, Ohki M, Sakurai M, Kaneko Y (1993) The 8;21 chromosome translocation in acute myeloid leukemia is always detectable by molecular analysis using AML1. *Blood* **81**: 1573-1579.
- Mathew S, Shurtleff SA, Raimondi SC (2001) Novel cryptic, complex rearrangements involving *ETV6-CBFA2 (TEL-AML1)* genes identified by fluorescence in situ hybridisation in pediatric patients with acute lymphoblastic leukemia. *Genes Chromosomes Cancer* **32**: 188-193.
- Mathew S, Shurtleff S, Ribeiro RC, Behm FG, Raimondi SC (2003) A complex variant t(8;21) involving chromosome 3 in a child with acute myeloblastic leukemia with eosinophilia (AML M4Eo). *Leuk Lymphoma* **44**: 183-187.
- Matos P, Skaug J, Marques B, Beck S, Veríssimo F, Gespach C, Boavida MG, Scherer SW, Jordan P (2000) Small GTPase *RAC1*: Structure, localization and expression of the human gene. *Biochem Biophys Res Commun* **277**: 741-751.
- Matos P, Collard JG, Jordan P (2003) Tumor-related alternatively spliced Rac1b is not regulated by Rho-GDP dissociation inhibitors and exhibits selective downstream signaling. *J Biol Chem* **278**: 50442-50448.
- Matos P & Jordan P (2005) Expression of Rac1b stimulates NF-kappaB-mediated cell survival and G1/S progression. *Exp Cell Res* **305**: 292-299.

- Mattarucchi E, Guerini V, Rambaldi A, Campiotti L, Venco A, Pasquali F, Lo Curto F, Porta G (2008) Microhomologies and interspersed repeat elements at genomic breakpoints in chronic myeloid leukemia. *Genes Chromosomes Cancer* **47**: 625-632.
- McKeithan TW, Warshawsky L, Espinosa III R, LeBeau MM (1992) Molecular cloning of the breakpoints of a complex Philadelphia chromosome translocation: Identification of a repeated region on chromosome 17. *Proc Natl Acad Sci USA* **89**: 4923-4927.
- McKinney CD, Golden WL, Gemma NW, Swerdlow SH, Williams ME (1994) RARA and PML gene rearrangements in acute promyelocytic leukemia with complex translocations and atypical features. *Genes Chromosomes Cancer* **9**: 49-56.
- Medyouf H & Ghysdael J (2008) The calcineurin/NFAT signaling pathway. A novel therapeutic target in leukemia and solid tumours. *Cell Cycle* **7**: 1-7.
- Megonigal MD, Rappaport EF, Jones DH, Kim CS, Nowell PC, Lange BJ, Felix CA (1997) Panhandle PCR strategy to amplify MLL genomic breakpoints in treatment-related leukemias. *Proc Natl Acad Sci USA* **94**: 11583-11588.
- Megonigal MD, Rappaport EF, Wilson RB, Jones DH, Whitlock JZ, Ortega JA, Slater DJ, Nowell PC, Felix CA (2000) Panhandle PCR for cDNA: A rapid method for isolation of MLL fusion transcripts involving unknown partner genes. *Proc Natl Acad Sci U S A* **97**: 9597-9602.
- Melo JV, Gordon DE, Cross NC, Goldman JM (1993) The ABL-BCR fusion gene is expressed in chronic myeloid leukemia. *Blood* **81**: 158-165.
- Melo JV (1997) BCR-ABL gene variants. *Baillieres Clin Haematol* **10**: 203-222.
- Metcalf D (2008) Hematopoietic cytokines. *Blood* **111**: 485-491.
- Michiels JJ & Thiele J (2002) Clinical and pathological criteria for the diagnosis of essential thrombocythemia, polycythemia vera, and idiopathic myelofibrosis (agnogenic myeloid metaplasia). *Int J Hematol* **76**: 133-145.
- Mikkola I, Heavey B, Horcher M, Busslinger M (2002) Reversion of B cell commitment upon loss of Pax5 expression. *Science* **297**: 110-113.
- Minamihisamatsu M & Ishihara T (1988) Translocation (8;21) and its variants in acute nonlymphocytic leukemia. The relative importance of chromosomes 8 and 21 to the genesis of the disease. *Cancer Genet Cytogenet* **33**: 161-173.
- Misawa S, Lee E, Schiffer CA, Liu Z, Testa JR (1986) Association of the translocation (15;17) with malignant proliferation of promyelocytes in acute leukemia and chronic myelogenous leukemia at blastic crisis. *Blood* **67**: 270-274.
- Mitani K, Ogawa S, Tanaka T, Miyoshi H, Kurokawa M, Mano H, Yazaki Y, Ohki M, Hirai H (1994) Generation of the AML1-EVI-1 fusion gene in the t(3;21)(q26;q22) causes blastic crisis in chronic myelocytic leukemia. *EMBO J* **13**: 504-510.
- Mitelman Database of Chromosome Aberrations in Cancer. Available at: <http://cgap.nci.nih.gov/Chromosomes/Mitelman>. Accessed June 3, 2004.
- Mitelman F (1993) The cytogenetic scenario of chronic myeloid leukemia. *Leuk Lymphoma* **11** (Suppl 1): 11-15.
- Miyagi J, Kakazu N, Masuda M, Miyagi T, Toyohama T, Nakazato T, Tomoyose T, Shinjyo T, Nagasaki A, Taira N, Ohki M, Abe T, Takasu N (2002) Acute myeloid leukemia (FAB-M2) with a masked type of t(8;21) translocation revealed by spectral karyotyping. *Int J Hematol* **76**: 338-343.
- Miyoshi H, Shimizu K, Kozu T, Maseki N, Kaneko Y, Ohki M (1991) t(8;21) breakpoints on chromosome 21 in acute myeloid leukemia are clustered within a limited region of a single gene, AML1. *Proc Natl Acad Sci U S A* **88**: 10431-10434.
- Miyoshi H, Kozu T, Shimizu K, Enomoto K, Maseki N, Kaneko Y, Kamada N, Ohki M (1993) The t(8;21) translocation in acute myeloid leukemia results in production of an AML1-MTG8 fusion transcript. *EMBO J* **12**: 2715-2721.
- Morel F, Herry A, Le Bris M-J, Morice P, Bouquard P, Abgrall J-F, Berthou C, De Braekeleer M (2003) Contribution of fluorescence in situ hybridization analyses to the characterization of masked and complex Philadelphia chromosome translocations in chronic myelocytic leukemia. *Cancer Genet Cytogenet* **147**: 115-120.
- Morris CM, Reeve AE, Fitzgerald PH, Hollings PE, Beard ME, Heaton DC (1986) Genomic diversity correlates with clinical variation in Ph⁻-negative chronic myeloid leukemia. *Nature* **320**: 281-283.
- Morris CM & Fitzgerald PH (1987) Complexity of an apparently simple variant Ph translocation in chronic myeloid leukemia. *Leuk Res* **11**: 163-169.

- Morris CM, Rosman I, Archer SA, Cochrane JM, Fitzgerald PH (1988) A cytogenetic and molecular analysis of five variant Philadelphia translocations in chronic myeloid leukemia. *Cancer Genet Cytogenet* **35**: 179-197.
- Morris CM, Heisterkamp N, Kennedy MA, Fitzgerald PH, Groffen J (1990) Ph-negative chronic myeloid leukemia: Molecular analysis of ABL insertion into M-BCR on chromosome 22. *Blood* **76**: 1812-1818.
- Morris C, Kennedy M, Heisterkamp N, Columbano-Green L, Romeril K, Groffen J, Fitzgerald P (1991) A complex chromosome rearrangement forms the BCR-ABL fusion gene in leukemic cells with a normal karyotype. *Genes Chromosomes Cancer* **3**: 263-271.
- Morris C, Jeffs A, Smith T, McDonald M, Board P, Kennedy M, Fitzgerald P (1996) BCR gene recombines with genomically distinct sites on band 11q13 in complex BCR-ABL translocations of chronic myeloid leukemia. *Oncogene* **12**: 677-685.
- Murray PJ (2007) The JAK-STAT signaling pathway: Input and output Integration. *J Immunol* **178**: 2623-2629.
- Mutschler M, Magin AS, Buerge M, Roelz R, Schanne DH, Will B, Pilz IH, Migliaccio AR, Pahl HL (2009) NF-E2 overexpression delays erythroid maturation and increases erythrocyte production. *Br J Haematol* **146**: 203-217.
- Nacheva E, Holloway T, Brown K, Bloxham D, Green AR (1994) Philadelphia-negative chronic myeloid leukemia: Detection by FISH of BCR-ABL fusion gene localized either to chromosome 9 or chromosome 22. *Br J Haematol* **87**: 409-412.
- Nacheva E, Holloway T, Carter N, Grace C, White N, Green AR (1995) Characterization of 20q deletions in patients with myeloproliferative disorders or myelodysplastic syndromes. *Cancer Genet Cytogenet* **80**: 87-94.
- Nadeau JH & Taylor BA (1984) Lengths of chromosomal segments conserved since divergence of man and mouse. *Proc Natl Acad Sci U S A* **81**: 814-818.
- Nakai H, Misawa S, Togushida J, Yandell DW, Ishizaki K (1992) Frequent p53 gene mutations in blast crisis of chronic myelogenous leukemia, especially in myeloid crisis harboring loss of a chromosome 17p. *Cancer Res* **52**: 6588-6593.
- Nakamura T, Alder H, Gu Y, Prasad R, Canaani O, Kamada N, Gale RP, Lange B, Crist WM, Nowell PC, Croce CM, Canaani E (1993) Genes on chromosomes 4, 9 and 19 involved in 11q23 abnormalities in acute leukemia share sequence homology and/or common motifs. *Proc Natl Acad Sci U S A* **90**: 4631-4635.
- Negrini M, Felix CA, Martin C, Lange BJ, Nakamura T, Canaani E, Croce CM (1993) Potential topoisomerase II DNA-binding sites at the breakpoints of a t(9;11) chromosome translocation in acute myeloid leukemia. *Cancer Res* **53**: 4489-4492.
- Nishigaki H, Misawa S, Inazawa J, Abe T (1992) Absence in Ph-negative, M-BCR rearrangement-positive chronic myelogenous leukemia of linkage between 5' ABL and 3' M-BCR sequences in Philadelphia translocation. *Leukemia* **6**: 385-392.
- Nisson PE, Watkins PC, Sacchi N (1992) Transcriptionally active chimeric gene derived from the fusion of the AML1 gene and a novel gene on chromosome 8 in t(8;21) leukemic cells. *Cancer Genet Cytogenet* **63**: 81-88.
- Noguchi H, Matsushita M, Okitsu T, Moriwaki A, Tomizawa K, Kang S, Li S-T, Kobayashi N, Matsumoto S, Tanaka K, Tanaka N, Matsui H (2004) A new cell-permeable peptide allows successful allogeneic islet transplantation in mice. *Nature Med* **10**: 305-309.
- Nourse J, Firpo E, Flanagan WM, Coats S, Polyak K, Lee MH, Massague J, Crabtree GR, Roberts JM (1994) Interleukin-2-mediated elimination of the p27Kip1 cyclin-dependent kinase inhibitor prevented by rapamycin. *Nature* **372**: 570-573.
- Nowell P & Hungerford D (1960) *Science* **132**: 1497 (abstract)
- Nowell PC & Hungerford DA (1961) Chromosome studies in human leukemia. II. Chronic granulocytic leukemia. *J Natl Cancer Inst* **27**: 1013-1035.
- Nucifora G & Rowley JD (1995) AML1 and the 8;21 and 3;21 translocations in acute and chronic myeloid leukemia. *Blood* **86**: 1-14.
- Nutt SL, Vambrie S, Steinlein P, Kozmik Z, Rolink A, Weith A, Busslinger M (1999) Independent regulation of the two PAX5 alleles during B-cell development. *Nat Genet* **21**: 390-395.
- O'Brien S, Thall PF, Siciliano MJ (1997) Cytogenetics of chronic myelogenous leukemia. *Baillieres Clin Haematol* **10**: 259-276.
- O'Brien SG, Guilhot F, Larson RA, Gathmann I, Baccarani M, Cervantes F, Cornelissen JJ, Fisher T, Hochhaus A, Hughes T, Lechner K, Nielsen JL, Rousselot P, Reiffers J, Saglio G, Shepherd J, Simonsson B, Gratwohl A, Goldman JM, Kantarjian H, Taylor K, Verhoef G, Bolton AE, Capdeville R, Druker BJ, IRIS

- Investigators (2003) Imatinib compared with interferon and low-dose cytarabine for newly diagnosed chronic-phase chronic myeloid leukemia. *N Engl J Med* **348**: 994-1004.
- Odero MD, Zeleznik-Le NJ, Chinwalla V, Rowley JD (2000) Cytogenetic and molecular analysis of the acute monocytic leukemia cell line THP-1 with an MLL-AF9 translocation. *Genes Chromosomes Cancer* **29**: 333-338.
- Odero MD, Carlson K, Calasanz MJ, Lahortiga I, Chinwalla V, Rowley JD (2001) Identification of new translocations involving *ETV6* in hematologic malignancies by fluorescence in situ hybridisation and spectral karyotyping. *Genes Chromosomes Cancer* **31**: 134-142.
- Odero MD, Vizmanos JL, Román JP, Lahortiga I, Panizo C, Calasanz MJ, Zeleznik-Le NJ, Rowley JD, Novo FJ (2002) A novel gene, *MDS2*, is fused to *ETV6/TEL* in a t(1;12)(p36.1;p13) in a patient with myelodysplastic syndrome. *Genes Chromosomes Cancer* **35**: 11-19.
- Odero MD, Carlson K, Lahortiga I, Calasanz MJ, Rowley JD (2003) Molecular cytogenetic characterization of breakpoints in 19 patients with hematologic malignancies and 12p unbalanced translocations. *Cancer Genet Cytogenet* **142**: 115-119.
- Ogawa E, Maruyama M, Kagoshima H, Inuzuka M, Lu J, Satake M, Shigesada K, Ito Y (1993) PEBP2/PEA2 represents a family of transcription factors homologous to the products of the Drosophila runt gene and the human AML1 gene. *Proc Natl Acad Sci U S A* **90**: 6859-6863.
- Ogawa S, Kurokawa M, Tanaka T, Tanaka K, Hangaishi A, Mitani K, Kamada N, Yazaki Y, Hirai H (1996) Increased Evi-1 expression is frequently observed in blastic crisis of chronic myelocytic leukemia. *Leukemia* **10**: 788-794.
- Oguma N, Misawa S, Testa JR (1983) A variant 8;21 translocation in acute myeloblastic leukemia. *Am J Hematol* **15**: 391-396.
- Ohi MD, Link AJ, Ren L, Jennings JL, McDonald WH, Gould KL (2002) Proteomics analysis reveals stable multiprotein complexes in both fission and budding yeasts containing Myb-related Cdc5p/Cef1p, novel pre-mRNA splicing factors, and snRNAs. *Mol Cell Biol* **22**: 2011-2024.
- Ohsaka A, Otsubo K, Yokota H, Hisa T, Saito H, Kozaki T (2008) Spectral karyotyping and fluorescence in situ hybridization analyses identified a novel three-way translocation involving inversion 16 in therapy-related acute myeloid leukemia M4eo. *Cancer Genet Cytogenet* **184**: 113-118.
- Ohyashiki JH, Ohyashiki K, Ito H, Toyama K (1988) Molecular and clinical investigations in Philadelphia chromosome-negative chronic myelogenous leukemia. *Cancer Genet Cytogenet* **33**: 119-126.
- Ohyashiki K, Ohyashiki JH, Kinniburgh AJ, Rowe J, Miller KB, Raza A, Preisler HD, Sandberg AA (1987) Transposition of breakpoint cluster region (3' bcr) in CML cells with variant Philadelphia translocations. *Cancer Genet Cytogenet* **26**: 105-115.
- Okamura H, Aramburu J, García-Rodríguez C, Viola JPB, Raghavan A, Tahiliani M, Zhang X, Qin J, Hogan PG, Rao A (2000) Concerted dephosphorylation of the transcription factor NFAT1 induces a conformational switch that regulates transcriptional activity. *Mol Cell* **6**: 539-550.
- Osella P, Wyandt H, Vosburgh E, Milunsky A (1991) Report of a variant t(1;15;17)(p36;q22;q21.1) in a patient with acute promyelocytic leukemia. *Cancer Genet Cytogenet* **57**: 201-207.
- Oshimura M, Ohyashiki K, Terada M, Takaku F, Tonomura A (1982) Variant Ph1 translocations in CML and their incidence, including two cases with sequential lymphoid and myeloid crises. *Cancer Genet Cytogenet* **5**: 187-201.
- Paige AJ, Taylor KJ, Taylor C, Hillier SG, Farrington S, Scott D, Porteous DJ, Smyth JF, Gabra H, Watson JE (2001) WWOX: A candidate tumor suppressor gene involved in multiple tumor types. *Proc Natl Acad Sci U S A* **98**: 11417-11422.
- Pan G, Bauer JH, Haridas V, Wang S, Liu D, Yu G, Vincenz C, Aggarwal BB, Ni J, Dixit VM (1998) Identification and functional characterization of DR6, a novel death domain-containing TNF receptor. *FEBS Letters* **431**: 351-356.
- Paradisi I & Arias S (2007) IVIC syndrome is caused by a c.2607delA mutation in the SALL4 locus. *Am J Med Genet* **143**: 326-332.
- Pardanani AD, Levine RL, Lasho T, Pikman Y, Mesa RA, Wadleigh M, Steensma DP, Elliott MA, Wolanskyj AP, Hogan WJ, McClure RF, Litzow MR, Gilliland DG, Tefferi A (2006) MPL515 mutations in myeloproliferative and other myeloid disorders: A study of 1182 patients. *Blood* **108**: 3472-3476.
- Parganas E, Wang D, Stravopodis D, Topham DJ, Marine JC, Teglund S, Vanin EF, Bodner S, Colamonici OR, van Deursen JM, Grosveld G, Ihle JN (1998) Jak2 is essential for signaling through a variety of cytokine receptors. *Cell* **93**: 385-395.
- Pasquali F, Casalone R, Francesconi D, Peretti D, Fraccaro M, Bernasconi C, Lazzarino M (1979) Transposition of 9q34 and 22 (q11toqter) regions has a specific role in chronic myelocytic leukemia. *Hum Genet* **52**: 55-67.

- Pederson B (1984) Coexistence of cells with unmasked and masked Ph1 in a case of chronic myeloid leukemia in blastic phase. *Cancer Genet Cytogenet* **12**: 129-137.
- Penas EM, Cools J, Algenstaedt P, Hinz K, Seeger D, Schafhausen P, Schilling G, Marynen P, Hossfeld DK, Dierlamm J (2003) A novel cryptic translocation t(12;17)(p13;p12-p13) in a secondary acute myeloid leukemia results in a fusion of the *ETV6* gene and the antisense strand of the *PER1* gene. *Genes Chromosomes Cancer* **37**: 79-83.
- Petkovich M, Brand NJ, Krust A, Chambon P (1987) A human retinoic acid receptor which belongs to the family of nuclear receptors. *Nature* **330**: 444-450.
- Pevzner P & Tesler G (2003a) Genome rearrangements in mammalian evolution: Lessons from human and mouse genomes. *Genome Res* **13**: 37-45.
- Pevzner P & Tesler G (2003b) Human and mouse genomic sequences reveal extensive breakpoint reuse in mammalian evolution. *Proc Natl Acad Sci U S A* **100**: 7672-7677.
- Pikman Y, Lee BH, Mercher T, McDowell E, Ebert BL, Gozo M, Cuker A, Wernig G, Moore S, Galinsky I, DeAngelo DJ, Clark JJ, Lee SJ, Golub TR, Wadleigh M, Gilliland DG, Levine RL (2006) MPLW515L is a novel somatic activating mutation in myelofibrosis with myeloid metaplasia. *PLoS Med* **3**: e270.
- Potter AM, Watmore AE, Cooke P, Lilleyman JS, Sokol RJ (1981) Significance of non-standard Philadelphia chromosomes in chronic granulocytic leukemia. *Br J Cancer* **44**: 51-54.
- Prchal JF & Axelrad AA (1974) Letter: Bone-marrow responses in polycythemia vera. *N Engl J Med* **290**: 1382.
- Przeziorka D & Thomas ED (1988) Prognostic significance of cytogenetic abnormalities in patients with chronic myelogenous leukemia. *Bone Marrow Transplant* **3**: 113-119.
- Qiao Y, Ogawa S, Hangaishi A, Yuji K, Izutsu K, Kunisato A, Imai Y, Wang L, Hosoya N, Nannya Y, Sato Y, Maki K, Mitani K, Hirai H (2003) Identification of a novel fusion gene, *TTL*, fused to *ETV6* in acute lymphoblastic leukemia with t(12;13)(p13;q14), and its implication in leukemogenesis. *Leukemia* **17**: 1112-1120.
- Raffini LJ, Slater DJ, Rappaport EF, Lo Nigro L, Cheung NV, Biegel JA, Nowell PC, Lange BJ, Felix CA (2002) Panhandle and reverse-panhandle PCR enable cloning of der(11) and der(other) genomic breakpoint junctions of MLL translocations and identify complex translocation of MLL, AF-4, and CDK6. *Proc Natl Acad Sci U S A* **99**: 4568-4573.
- Rao A, Luo C, Hogan PG (1997) Transcription factors of the NFAT family: Regulation and function. *Annu Rev Immunol* **15**: 707-747.
- Rassool F, Martiat P, Taj A, Klisak I, Goldman J (1990) Interstitial insertion of varying amounts of ABL-containing genetic material into chromosome 22 in Ph-negative CML. *Leukemia* **4**: 273-277.
- Rengarajan J, Tang B, Glimcher LH (2002) NFATc2 and NFATc3 regulate T(H)2 differentiation and modulate TCR-responsiveness of naïve T(H) cells. *Nat Immunol* **3**: 48-54.
- Renneville A, Roumier C, Biggio V, Nibourel O, Boissel N, Fenaux P, Preudhomme C (2008) Cooperating gene mutations in acute myeloid leukemia: A review of the literature. *Leukemia* **22**: 915-931.
- Roehrl MH, Kang S, Aramburu J, Wagner G, Rao A, Hogan PG (2004) Selective inhibition of calcineurin-NFAT signaling by blocking protein-protein interaction with small organic molecules. *Proc Natl Acad Sci U S A* **101**: 7554-7559.
- Romana SP, Mauchauffé M, Le Coniat M, Chumakov I, Le Paslier D, Berger R, Bernard OA (1995) The t(12;21) of acute lymphoblastic leukemia results in a *TEL-AML1* gene fusion. *Blood* **85**: 3662-3670.
- Rossi D, Capello D, Gloghini A, Franceschetti S, Paulli M, Bhatia K, Saglio G, Vitolo U, Pileri SA, Esteller M, Carbone A, Gaidano G (2004) Aberrant promoter methylation of multiple genes throughout the clinico-pathologic spectrum of B-cell neoplasia. *Haematologica* **89**: 154-164.
- Rothenberg EV & Ward SB (1996) A dynamic assembly of diverse transcription factors integrates activation and cell-type information for interleukin 2 gene regulation. *Proc Natl Acad Sci U S A* **93**: 9358-9365.
- Roulston D, Espinosa R III, Stoffel M, Bell GI, Le Beau MM (1993) Molecular genetics of myeloid leukemia: Identification of the commonly deleted segment of chromosome 20. *Blood* **82**: 3424-3429.
- Rowley JD (1973a) A new consistent chromosomal abnormality in chronic myelogenous leukemia identified by quinacrine fluorescence and giemsa staining. *Nature* **243**: 290-293.
- Rowley JD (1973b) Identification of a translocation with quinacrine fluorescence in a patient with acute leukemia. *Ann Genet* **16**: 109-112.
- Rowley JD, Golomb HM, Dougherty C (1977) 15/17 translocation, a consistent chromosomal change in acute promyelocytic leukemia. *Lancet* **1**: 549-550.
- Rowley JD (2001) Chromosome translocations: Dangerous liaisons revisited. *Nat Rev Cancer* **1**: 245-250.

- Rozen S & Skaletsky HJ (2000) Primer3 on the WWW for general users and for biologist programmers. In: Krawetz S, Misener S, editors. *Bioinformatics Methods and Protocols: Methods in Molecular Biology*. Totowa: Humana Press. p 365-386.
- Saitoh K, Miura I, Kobayashi Y, Kume M, Utsumi S, Takahashi N, Hatano Y, Nimura T, Hashimoto K, Takahashi S, Miura AB (1998) A new variant translocation of t(15;17) in a patient with acute promyelocytic leukemia (M3): t(15;19;17)(q22;p13;q12). *Cancer Genet Cytogenet* **102**: 15-18.
- Sandberg AA (1980) Chromosomes and causation of human cancer and leukemia: XL. The Ph1 and other translocations in CML. *Cancer* **46**: 2221-2226.
- Sankoff D, Deneault M, Turbis P, Allen C (2002) Chromosomal distributions of breakpoints in cancer, infertility and evolution. *Theor Popul Biol* **61**: 497-501.
- Sato Y, Bohlander SK, Kobayashi H, Reshmi S, Suto Y, Davis EM, Espinosa III R, Hoopes R, Montgomery KT, Kucherlapati RS, Le Beau MM, Rowley JD (1997) Heterogeneity in the breakpoints in balanced rearrangements involving band 12p13 in hematologic malignancies identified by fluorescence in situ hybridisation: TEL (ETV6) is involved in only one half. *Blood* **90**: 4886-4893.
- Sawyers CL (1997) Signal transduction pathways involved in BCR-ABL transformation. *Baillieres Clin Haematol* **10**: 223-231.
- Schaub FX, Jäger R, Looser R, Hao-Shen H, Hermouet S, Girodon F, Tichelli A, Gisslinger H, Kralovics R, Skoda RC (2009) Clonal analysis of deletions on chromosome 20q and JAK2-V617F in MPD suggests that del20q acts independently and is not one of the predisposing mutations for JAK2-V617F. *Blood* **113**: 2022-2027.
- Scheres JM, Hustinx TW, de Vaan GA, Rutten FJ (1978) 15/17 translocation in acute promyelocytic leukemia. *Hum Genet* **43**: 115-117.
- Schmittgen TD & Livak KJ (2008) Analyzing real-time PCR data by the comparative C_T method. *Nat Protoc* **3**: 1101-1108.
- Sherbenou DW & Druker BJ (2007) Applying the discovery of the Philadelphia chromosome. *J Clin Invest* **117**: 2067-2074.
- Sherr CJ & Roberts JM (1999) CDK inhibitors: Positive and negative regulators of G1-phase progression. *Genes Dev* **13**: 1501-1512.
- Shinagawa A, Komatsu T, Ninomiya H (1999) Complex translocation (6;21;8), a variant of t(8;21), with trisomy 4 in a patient with acute myelogenous leukemia (M2). *Cancer Genet Cytogenet* **109**: 72-75.
- Shtivelman E, Lifshitz B, Gale RP, Canaani E (1985) Fused transcript of abl and bcr genes in chronic myelogenous leukemia. *Nature* **315**: 550-554.
- Sieweke MH, Tekotte H, Frampton J, Graf T (1996) MafB is an interaction partner and repressor of Ets-1 that inhibits erythroid differentiation. *Cell* **85**: 49-60.
- Sieweke MH, Tekotte H, Frampton J, Graf T (1997) MafB represses erythroid genes and differentiation through direct interaction with c-Ets-1. *Leukemia* **11** Suppl 3: 486-488.
- Sinclair PB, Nacheva EP, Leversha M, Telford N, Chang J, Reid A, Bench A, Champion K, Huntly B, Green AR (2000) Large deletions at the t(9;22) breakpoint are common and may identify a poor-prognosis subgroup of patients with chronic myeloid leukemia. *Blood* **95**: 738-743.
- Slater RM, Behrendt H, de Waal FC (1983) Chromosome studies on acute nonlymphocytic leukemia in children. *Pediatr Res* **17**: 398-405.
- So CW, Caldas C, Liu M, Chen S, Huang Q, Gu L, Sham M, Wiedemann L, Chan L (1997) EEN encodes for a member of a new family of proteins containing an Src homology 3 domain and is the third gene located on chromosome 19p13 that fuses to MLL in human leukemia. *Proc Natl Acad Sci U S A* **94**: 2563-2568.
- Sonta SI & Sandberg AA (1977) Chromosomes and causation of human cancer and leukemia. XXIV. Unusual and complex Ph¹ translocations and their clinical significance. *Blood* **50**: 691-697.
- Sorensen PH, Chen CS, Smith FO, Arthur DC, Domer PH, Bernstein ID, Korsmeyer SJ, Hammond GD, Kersey JH (1994) Molecular rearrangements of the MLL gene are present in most cases of infant acute myeloid leukemia and are strongly correlated with monocytic or myelomonocytic phenotypes. *J Clin Invest* **93**: 429-437.
- Sowerby SJ, Kennedy MA, Fitzgerald PH, Morris CM (1993) DNA sequence analysis of the major breakpoint cluster region of the BCR gene rearranged in Philadelphia-positive human leukemias. *Oncogene* **8**: 1679-1683.
- Spector LG, Xie Y, Robison LL, Heerema NA, Hilden JM, Lange B, Felix CA, Davies SM, Slavin J, Potter JD, Blair CK, Reaman GH, Ross JA (2005) Maternal diet and infant leukemia: The DNA topoisomerase II inhibitor hypothesis: A report from the children's oncology group. *Cancer Epidemiol Biomarkers Prev* **14**: 651-655.

- Spivak JL (2004) The chronic myeloproliferative disorders: clonality and clinical heterogeneity. *Semin Hematol* **41** (Suppl 3): 1-5.
- Starza RL, Matteucci C, Crescenzi B, Perla G, Carotenuto M, Martelli MF, Hagemeyer A, Mecucci C (1997) Identification of chromosome changes in acute myeloid leukemia (AML-M2) by molecular cytogenetics. *Cancer Genet Cytogenet* **95**: 148-152.
- Stegmaier K, Takeuchi S, Golub TR, Bohlander SK, Bartram CR, Koeffler HP, Gilliland DG (1996) Mutational analysis of the candidate tumor suppressor genes TEL and KIP1 in childhood acute lymphoblastic leukemia. *Cancer Res* **56**: 1413-1417.
- Strange RC, Spiteri MA, Ramachandran S, Fryer AA (2001) Glutathione-S-transferase family of enzymes. *Mutat Res* **482**: 21-26.
- Strehl S, König M, Dworzak MN, Kalwak K, Haas AO (2003) PAX5/ETV6 fusion defines cytogenetic entity dic(9;12)(p13;p13). *Leukemia* **17**: 1121-1123.
- Strissel PL, Strick R, Tomek RJ, Roe BA, Rowley JD, Zeleznik-Le NJ (2000) DNA structural properties of AF9 are similar to MLL and could act as recombinant hot spots resulting in MLL/AF9 translocations and leukemogenesis. *Hum Mol Genet* **9**: 1671-1679.
- Su XY, Busson M, Della Valle V, Ballerini P, Dastugue N, Talmant P, Ferrando AA, Baudry-Bluteau D, Romana S, Berger R, Bernard OA (2004) Various types of rearrangements target TLX3 locus in T-cell acute lymphoblastic leukemia. *Genes Chromosomes Cancer* **41**: 243-249.
- Sundareshan TS, Augustus M, Yasha T, Shailaja SN, Lalitha N (1992) Variant complex translocation t(8;15;21) in acute myeloblastic leukemia (M2) associated with bilateral chloroma. *Cancer Genet Cytogenet* **64**: 35-37.
- Super HG, Strissel PL, Sobulo OM, Burian D, Reshmi SC, Roe B, Zeleznik-Le NJ, Diaz MO, Rowley JD (1997) Identification of complex genomic breakpoint junctions in the t(9;11) MLL-AF9 fusion gene in acute leukemia. *Genes Chromosomes Cancer* **20**: 185-195.
- Swaroop A, Xu JZ, Pawar H, Jackson A, Skolnick C, Agarwal N (1992) A conserved retina-specific gene encodes a basic motif/leucine zipper domain. *Proc Natl Acad Sci U S A* **89**: 266-270.
- Szuhai K, Iiszenga M, de Jong D, Karseladze A, Tanke HJ, Hogendoorn PCW (2009) The NFATc2 gene is involved in a novel cloned translocation in a ewing sarcoma variant that couples its function in immunology to oncology. *Clin Cancer Res* **15**: 2259-2268.
- Tagushi H, Kitagawa T, Yamashita M, Kubonishi I, Miyoshi I (1986) New variant translocation (1;8;21) in a case of acute myeloblastic leukemia (M2). *Cancer Genet Cytogenet* **23**: 219-223.
- Tanaka T, Mitani K, Kurokawa M, Ogawa S, Tanaka K, Nishida J, Yazaki Y, Shibata Y, Hirai H (1995) Dual functions of the AML1/Evi-1 chimeric protein in the mechanisms of leukemogenesis in t(3;21) leukemias. *Mol Cell Biol* **15**: 2383-2392.
- Testa JR, Golomb HM, Rowley JD, Vardiman JW, Sweet DL Jr (1978) Hypergranular promyelocytic leukemia (APL): Cytogenetic and ultrastructural specificity. *Blood* **52**: 272-280.
- Testa JR, Misawa S, Oguma N, van Sloten K, Wiernik PH (1985) Chromosomal alterations in acute leukemia patients studied with improved culture methods. *Cancer Res* **45**: 430-434.
- Thompson PW, Lucas GS, Davies MF, Whittaker JA (1991) Variant translocation (3;inv(16)) in acute myelomonocytic leukemia with eosinophilia. *Cancer Genet Cytogenet* **55**: 269-271.
- Tirado CA, Chena W, Valdez FJ, Henderson S, Smart RL, Doolittle J, Garcia R, Patel S, Holdridge S, Chastain C, Auchus M, Collins RH (2009) A cryptic t(1;21;8)(p36;q22;q22) in a case of acute myeloid leukemia with maturation. *J Assoc Genet Technol* **35**: 88-92.
- Tkachuk DC, Westbrook CA, Andreeff M, Donlon TA, Cleary ML, Suryanarayan K, Homge M, Redner A, Gray J, Pinkel D (1990) Detection of bcr-abl fusion in chronic myelogenous leukemia by in situ hybridization. *Science* **250**: 559-562.
- Tkachuk DC, Kohler S, Cleary ML (1992) Involvement of homolog of Drosophila trithorax by 11q23 chromosomal translocations in acute leukemias. *Cell* **71**: 691-700.
- Tosi S, Giudici G, Mosna G, Harbott J, Specchia G, Grosveld G, Privitera E, Kearney L, Biondi A, Cazzaniga G (1998) Identification of new partner chromosomes involved in fusions with the ETV6 (TEL) gene in hematologic malignancies. *Genes Chromosomes Cancer* **21**: 223-229.
- Tough IM, Court Brown WM, Baikie AG, Buckton KE, Harnden DG, Jacobs PA, King MJ, McBride JA (1961) Cytogenetic studies in chronic myeloid leukaemia and acute leukaemia associated with monogolism. *Lancet* **1**: 411-417.

- Tsuboi A, Masuda ES, Naito Y, Tokumitsu H, Arai K, Arai N (1994) Calcineurin potentiates activation of the granulocyte-macrophage colony-stimulating factor gene in T cells: Involvement of the conserved lymphokine element 0. *Mol Cell Biol* **5**: 119-128.
- Uchida H, Ohyashiki K, Toyama K, Kondo M, Ito H, Oshumi A (1988) Variant t(8;18;21) translocation in acute myeloid leukemia. *Cancer Genet Cytogenet* **36**: 231-232.
- Udayakumar AM, Alkindi S, Pathare AV, Raeburn JA (2008) Complex t(8;13;21)(q22;q14;q22)-a novel variant of t(8;21) in a patient with acute myeloid leukemia (AML-M2). *Arch Med Res* **39**: 252-256.
- Uozumi K, Otsuka M, Ohno N, Moriyama T, Suzuki S, Shimotakahara S, Matsumura I, Hanada S, Arima T (2000) Establishment and characterization of a new human megakaryoblastic cell line (SET-2) that spontaneously matures to megakaryocytes and produces platelet-like particles. *Leukemia* **14**: 142-152.
- van der Plas DC, Grosveld G, Hagemeijer A (1991) Review of clinical, cytogenetic, and molecular aspects of Ph-negative CML. *Cancer Genet Cytogenet* **52**: 143-156.
- van der Reijden BA, Lombardo M, Dauwerse HG, Giles RH, Mühlematter D, Bellomo MJ, Wessels HW, Beverstock GC, van Ommen G-JB, Hagemeijer A, Breuning MH (1995) RT-PCR diagnosis of patients with acute nonlymphocytic leukemia and inv(16)(p13q22) and identification of new alternative splicing in CFBF-MYH11 transcripts. *Blood* **86**: 277-282.
- van Dongen JJM, Macintyre EA, Gabert JA, Delabesse E, Rossi V, Saglio G, Gottardi E, Rambaldi A, Dotti G, Griesinger F, Parreira A, Gameiro P, González Díáz M, Malec M, Langerak AW, San Miguel JF, Biondi A (1999). Standardized RT-PCR analysis of fusion gene transcripts from chromosome aberrations in acute leukemia for detection of minimal residual disease. *Leukemia* **13**: 1901-1928.
- Vieira L, Alves AC, Marques B, Reis I, Jorge G, Ambrósio AP, de Sousa AB, Boavida MG (1999) Insertion of the 5' part of BCR within the ABL gene at 9q34 in a Philadelphia-negative chronic myeloid leukemia. *Cancer Genet Cytogenet* **114**: 17-21.
- Vieira L, Oliveira V, Ambrósio AP, Marques B, Pereira AM, Hagemeijer A, Boavida MG (2001) Translocation t(8;17;15;21)(q22;q23;q15;q22) in acute myeloid leukemia (M2): A four-way variant of t(8;21). *Cancer Genet Cytogenet* **28**: 104-107.
- Vieira L, Marques B, Cavaleiro C, Ambrósio AP, Jorge M, Neto A, Costa JM, Júnior EC, Boavida MG (2005) Molecular cytogenetic characterization of rearrangements involving 12p in leukemia. *Cancer Genet Cytogenet* **157**: 134-139.
- Vieira L, Sousa AC, Matos P, Marques B, Alaiz H, Ribeiro MJ, Braga P, da Silva MG, Jordan P (2006) Three-way translocation involves *MLL*, *MLLT3* and a novel cell cycle control gene, *FLJ10374*, in the pathogenesis of acute myeloid leukemia with t(9;11;19)(p22;q23;p13.3). *Genes Chromosomes Cancer* **45**: 455-469.
- Vieira L & Gomes da Silva M (2008) The role of cell cycle control genes in the pathogenesis of human hematological neoplasms. In: *Cell Cycle Control: New Research* (Eds. Nathan H. Leroy e Noah T. Fournier). Nova Publishers, Nova Iorque.
- Von Hansemann D (1890) Ueber asymmetrische Zelltheilung in Epithelkrebsen und deren biologische bedeutung. *Virchows Arch A Pathol Anat* **119**: 299-326.
- Vundinti BR, Kerketta L, Madkaikar M, Jijina F, Ghosh K (2008) Three way translocation in a new variant of t(8;21) acute myeloid leukemia involving Xp22. *Indian J Cancer* **45**: 30-32.
- Wan TSK, Chim CS, So CK, Chan LC, Ma SK (1999) Complex variant 15;17 translocations in acute promyelocytic leukemia. *Cancer Genet Cytogenet* **111**: 139-143.
- Wang LC, Kuo F, Fujiwara Y, Gilliland DG, Golub TR, Orkin SH (1997) Yolk sac angiogenic defect and intra-embryonic apoptosis in mice lacking the Ets-related factor TEL. *EMBO J* **16**: 4374-4383.
- Wang LC, Swat W, Fujiwara Y, Davidson L, Visvader J, Kuo F, Alt FW, Gilliland DG, Golub TR, Orkin SH (1998b) The TEL/ETV6 gene is required specifically for hematopoiesis in the bone marrow. *Genes Dev* **12**: 2392-2402.
- Wang PW, Iannantuoni K, Davis EM, Espinosa R 3rd, Stoffel M, Le Beau MM (1998a) Refinement of the commonly deleted segment in myeloid leukemias with a del(20q). *Genes Chromosomes Cancer* **21**: 75-81.
- Wang PW, Eisenbart JD, Espinosa R 3rd, Davies EM, Larson RA, Le Beau MM (2000) Refinement of the smallest commonly deleted segment of chromosome 20 in malignant myeloid diseases and development of a PAC-based physical and transcription map. *Genomics* **67**: 28-39.
- Whitmarsh RJ, Saginario C, Zhuo Y, Hilgenfeld E, Rappaport EF, Megonigal MD, Carrol M, Liu M, Osherof N, Cheung NV, Slater DJ, Ried T, Knutsen T, Blair IA, Felix CA (2003) Reciprocal DNA topoisomerase II cleavage events at 5'-TATTA-3' sequences in *MLL* and *AF-9* create homologous single-stranded

- overhangs that anneal to form der(11) and der(9) genomic breakpoint junctions in treatment-related AML without further processing. *Oncogene* **22**: 8448-8459.
- Wiemels JL, Alexander FE, Cazzaniga G, Biondi A, Mayer SP, Greaves M (2000) Microclustering of *TEL-AML1* translocation breakpoints in childhood acute lymphoblastic leukemia. *Genes Chromosomes Cancer* **29**: 219-228.
- Willis TG, Jadayel DM, Coignet LJA, Abdul-Rauf M, Treleaven JG, Catovsky D, Dyer MJS (1997) Rapid molecular cloning of rearrangements of the IGJH locus using long distance inverse polymerase chain reaction. *Blood* **90**: 2456-2464.
- Wlodarska I, Marynen P, La Starza R, Mecucci C, Van den Berghe H (1996) The *ETV6*, *CDKN1B* and D12S178 loci are involved in a segment commonly deleted in various 12p aberrations in different hematological malignancies. *Cytogenet Cell Genet* **72**: 229-235.
- Wlodarska I, La Starza R, Baens M, Dierlamm J, Uyttebroeck A, Selleslag D, Francine A, Mecucci C, Hagemeijer A, Van den Berghe H, Marynen P (1998) Fluorescence in situ hybridisation characterization of new translocations involving *TEL (ETV6)* in a wide spectrum of hematologic malignancies. *Blood* **91**: 1399-1406.
- Wolanskyj AP, Schwager SM, McClure RF, Larson DR, Tefferi A (2006) Essential thrombocythemia beyond the first decade: Life expectancy, long-term complication rates, and prognostic factors. *Mayo Clin Proc* **81**: 159-166.
- Wong KF, Kwong YL, So CC (1998) Translocation(8;20;21)(q22;q13;q22) in acute myeloblastic leukemia with maturation: A variant form of t(8;21). *Cancer Genet Cytogenet* **101**: 39-41.
- Xue Y, Xu L, Chen S, Fu J, Guo Y, Li J, Wu Y, Pan J, Lu D (2001) t(8;21;8)(p23;q22;q22): A new variant form of t(8;21) translocation in acute myeloblastic leukemia with maturation. *Leuk Lymphoma* **42**: 533-537.
- Yagasaki F, Wakao D, Yokoyama Y, Uchida Y, Murohashi I, Kayano H, Taniwaki M, Matsuda A, Bessho M (2001) Fusion of *ETV6* to fibroblast growth factor receptor 3 in peripheral T-cell lymphoma with a t(4;12)(p16;p13) chromosomal translocation. *Cancer Res* **61**: 8371-8374.
- Yamamoto K, Seto M, Iida S, Komatsu H, Kamada N, Kojima S, Koderia Y, Nakazawa S, Saito H, Takahashi T, Ueda R (1994) A reverse transcriptase-polymerase chain reaction detects heterogeneous chimeric mRNAs in leukemias with 11q23 abnormalities. *Blood* **83**: 2912-2921.
- Yamamoto K, Hamaguchi H, Nagata K, Kobayashi M, Takashima T, Taniwaki M (1998) A new complex translocation (15;20;17)(q22;p13;q21) in acute promyelocytic leukemia. *Cancer Genet Cytogenet* **101**: 89-94.
- Yang J, Cogdell D, Yang D, Hu L, Li H, Zheng H, Du X, Pang Y, Trent J, Chen K, Zhang W (2010) Deletion of the *WWOX* gene and frequent loss of its protein expression in human osteosarcoma. *Cancer Lett* **291**: 31-38.
- Yip MY, Sharma P, White L (1991) Acute myelomonocytic leukemia with bone marrow eosinophilia and inv(16)(p13q22),t(1;16)(q32;q22). *Cancer Genet Cytogenet* **51**: 235-238.
- Zaccaria A, Testoni N, Tassinari A, Celso B, Rassool F, Saglio G, Guerrasio A, Rosti G, Tura S (1989) Cytogenetic and molecular studies in patients with chronic myeloid leukemia and variant Philadelphia translocations. *Cancer Genet Cytogenet* **42**: 191-201.
- Zhang J, Tam WL, Tong GQ, Wu Q, Chan HY, Soh BS, Lou Y, Yang J, Ma Y, Chai L, Ng HH, Lufkin T, Robson P, Lim B (2006) *Sall4* modulates embryonic stem cell pluripotency and early embryonic development by the transcriptional regulation of *Pou5f1*. *Nat Cell Biol* **8**: 1114-1123.
- Zhang JG, Goldman JM, Cross NC (1995) Characterization of genomic BCR-ABL breakpoints in chronic myeloid leukemia by PCR. *Br J Haematol* **90**: 138-146.
- Zhong S, Salomoni P, Pandolfi PP (2000) The transcriptional role of PML and the nuclear body. *Nat Cell Biol* **2**: E85-E90.
- Ziemin-van Der Poel S, McCabe NR, Gill HJ, Espinosa R 3rd, Patel Y, Harden A, Rubinelli P, Smith SD, LeBeau MM, Rowley JD, Diaz MO (1991) Identification of a gene, *MLL*, that spans the breakpoint in 11q23 translocations associated with human leukemias. *Proc Natl Acad Sci U S A* **88**: 10735-10739.